



**US Army Corps
of Engineers®**
Engineer Research and
Development Center

ERDC
INNOVATIVE SOLUTIONS
for a safer, better world

The Biology of Bioavailability: The Role of Functional Ecology in Exposure Processes

SERDP ER-1750

Todd S. Bridges, Alan J. Kennedy, Guilherme R. Lotufo,
Jessica G. Coleman, Carlos E. Ruiz, James H. Lindsay,
Jeffery A. Steevens, Allyson Wooley, Gerald Matisoff,
Peter McCall, Eliza Kaltenberg, Robert M. Burgess,
and Loretta A. Fernandez

January 2017



The U.S. Army Engineer Research and Development Center (ERDC) solves the nation's toughest engineering and environmental challenges. ERDC develops innovative solutions in civil and military engineering, geospatial sciences, water resources, and environmental sciences for the Army, the Department of Defense, civilian agencies, and our nation's public good. Find out more at www.erdclibrary.usace.army.mil.

To search for other technical reports published by ERDC, visit the ERDC online library at <http://acwc.sdp.sirsi.net/client/default>.

The Biology of Bioavailability: The Role of Functional Ecology in Exposure Processes

SERDP ER-1750

Todd S. Bridges, Alan J. Kennedy, Guilherme R. Lotufo,
Jessica G. Coleman, Carlos E. Ruiz, James H. Lindsay,
Allyson Wooley, and Jeffery A. Steevens

*Environmental Laboratory
U.S. Army Engineer Research and Development Center
3909 Halls Ferry Road
Vicksburg, MS 39180-6199*

Gerald Matisoff, Peter McCall, and Eliza Kaltenberg,

*Case Western Reserve University
Crawford Hall
10900 Euclid Avenue
Cleveland, OH 44106-7068*

Robert M. Burgess

*U.S. Environmental Protection Agency
USEPA Environmental Effects Research Laboratory
Atlantic Ecology Division / ORD
27 Tarzwell Drive
Narragansett, RI 02882*

Loretta A. Fernandez

*Northeastern University
473 Snell Engineering
360 Huntington Avenue
Boston, MA 02115*

Final report

Approved for public release; distribution is unlimited.

Prepared for Strategic Environmental Research and Development Program (SERDP)

Under "The Biology of Bioavailability: The Role of Functional Ecology in Exposure Processes," Project ER-1750

Abstract

The research objective was to improve accuracy of sediment exposure assessments by considering the functional ecology of benthic organisms and different exposure routes (sediment particles, pore water, overlying water). Laboratory experiments were conducted using four marine invertebrates (a worm, two amphipods, and a clam). Organisms were exposed to two different contaminated sediments within mesocosms designed to assess polychlorinated biphenyl (PCB) exposure from overlying water and whole sediment using pathway isolation chambers. The impacts of two sediment remediation methods were also tested: (1) a 2 cm sand cap; and (2) activated carbon (AC) that was not aggressively mixed with sediment prior to organism testing to simulate a field deployment. Porewater concentrations were assessed using polyethylene devices (PEDs) and provided a reasonable indicator of organism exposure but did not account for organisms with connections to the overlying water and direct particle ingestion. The sand cap significantly reduced PCB exposure for all the species except the clam while non-equilibrated AC did not result in significant reductions in bioaccumulation. These results can be used to design functional bioavailability assessments and provide basis for future guidance. Data were used to enhance the capability and predictive reliability of an existing modeling framework (RECOVERY).

DISCLAIMER: The contents of this report are not to be used for advertising, publication, or promotional purposes. Citation of trade names does not constitute an official endorsement or approval of the use of such commercial products. All product names and trademarks cited are the property of their respective owners. The findings of this report are not to be construed as an official Department of the Army position unless so designated by other authorized documents.

DESTROY THIS REPORT WHEN NO LONGER NEEDED. DO NOT RETURN IT TO THE ORIGINATOR.

Contents

Abstract	ii
Figures and Tables.....	vii
Preface.....	xiii
Unit Conversion Factors	xiv
Acronyms	xv
1 Introduction.....	1
1.1 Objective	1
1.2 Technical approach	1
1.3 Results	2
1.4 Benefits.....	3
2 Project Objective.....	4
3 Background.....	6
4 Materials and Methods.....	13
4.1 Technical approach	13
4.1.1 Task description	13
5 TASK 1A: Selection of test organisms and sediments	15
5.1 Introduction.....	15
5.2 Materials and methods	16
5.2.1 Sediment selection	16
5.2.2 Organism selection	17
5.3 Results and discussion	18
5.3.1 Sediment selection	18
5.3.2 Organism selection	20
6 TASK 1B: Development of the flow through exposure system.....	25
6.1 Exposure and Recirculation System	25
6.2 Tracer study.....	27
6.3 Passive dosing for the recirculation system.....	28
7 TASK 1B: Development of membrane equipped isolation chambers for characterization of infaunal invertebrate exposure to PCBs via sediment pore water	30
7.1 Introduction.....	30
7.2 Materials and methods	31
7.2.1 Membranes	31
7.2.2 Porewater analysis.....	32

7.2.3	Passive diffusion of radio-labeled contaminant in water.....	32
7.2.4	Diffusion of radio-labeled contaminants from a continuous source.....	33
7.2.5	Passive diffusion of humic acids through membranes.....	33
7.2.6	Passive diffusion of cold contaminant from sediment to Prototype PICs.....	34
7.3	Results and discussion	34
7.3.1	Passive diffusion of radio-labeled contaminant	34
7.3.2	Diffusion of radio-labeled contaminants from a continuous source.....	35
7.3.3	Passive diffusion of humic acids through membranes.....	36
7.3.4	Passive diffusion of cold contaminant from sediment to prototype PICs	37
7.4	Discussion.....	37
8	TASK 1C: Passive sampler evaluation and selection.....	40
8.1	Introduction.....	40
8.2	Methods	41
8.3	Results and discussion	43
9	TASK 1C: Bioaccumulation kinetics of PCBs to four marine benthic invertebrates.....	46
9.1	Background.....	46
9.2	Objectives.....	46
9.3	Material and Methods	47
9.3.1	Field-collected PCB-contaminated sediments.....	47
9.3.2	Experimental species.....	47
9.3.3	Uptake and elimination kinetics exposures.....	47
9.3.4	Modeling.....	49
9.4	Results and discussion	50
9.4.1	Total lipids content.....	50
9.4.2	Uptake kinetics.....	51
9.4.3	Elimination kinetics – New Bedford Harbor sediment.....	62
9.4.4	Uptake and elimination kinetics – Bremerton sediment.....	67
9.4.5	Comparison of predicted with observed bioaccumulation	70
9.4.6	Species-specific bioaccumulation of PCBs.....	73
10	Task 2a: Importance of exposure pathways for determining bioaccumulation in four functionally different benthic macroinvertebrates.....	75
10.1	Introduction.....	75
10.2	Materials and methods	78
10.2.1	Test sediments and chemicals.....	78
10.2.2	Exposure system	78
10.2.3	Passive dosing of unique PCB congeners into overlying water	80
10.2.4	Study organisms.....	81
10.2.5	Bioaccumulation exposures.....	82
10.2.6	Passive sampler exposures	83
10.2.7	Analytical	83
10.2.8	Data analysis.....	84
10.3	Results and discussion	84
10.3.1	Exposure condition summary.....	84
10.3.2	Bioaccumulation	89

10.3.3	Bioaccumulation of sediment-associated congeners.....	90
10.3.4	Bioaccumulation of overlying water (OW) congeners	101
10.3.5	Conclusion	108
11	Task 2B: Model Development using RECOVERY	111
11.1	Introduction.....	111
11.2	Materials and methods	113
11.2.1	First approach	113
11.2.2	Second approach	114
11.2.3	Exposure system	115
11.3	Results and discussion	115
11.4	Conclusion	132
12	TASK 3A: Experiments using management scenarios: impact of functional feeding group on efficacy.....	133
12.1	Introduction.....	133
12.2	Materials and methods	133
12.2.1	Test sediments and chemicals.....	133
12.2.2	Benthic test organisms.....	134
12.2.3	Organism chambers.....	134
12.2.4	Exposure system	134
12.2.5	Sediment treatments	135
12.2.6	Bioaccumulation exposures	136
12.2.7	Passive sampler exposures	137
12.2.8	Analytical	139
12.2.9	Data analysis.....	139
12.3	Results and discussion	139
12.3.1	PCB congeners in sediment	139
12.3.2	Tissue recovery and residues	141
12.3.3	Overlying water congeners concentrations and tissue residues.....	143
12.3.4	Polyethylene device (PED) estimates of dissolved concentrations	147
12.3.5	Bioaccumulation of sediment associated congeners in tissue.....	150
12.3.6	Conclusion	156
13	Sediment particle and solute mixing.....	158
13.1	Objective	158
13.2	Background.....	158
13.3	Materials and methods	159
13.3.1	Materials.....	159
13.3.2	Organisms	159
13.3.3	Sediments.....	160
13.3.4	Experimental setup	160
13.3.5	Mixing parameters	162
13.3.6	3-D burrow model of dissolved oxygen	164
13.4	Results and discussion	165
13.4.1	<i>L. plumulosus</i>	165
13.4.2	<i>M. mercenaria</i>	174

13.4.3 3-D burrow model of solute flux	178
14 Comparison of fluorescent and radioactive particle tracers	182
14.1 Objective	182
14.2 Background	182
14.3 Materials and methods	183
14.3.1 Materials.....	183
14.3.2 Organisms and sediment.....	184
14.3.3 Experimental setup.....	184
14.3.4 Data processing	185
14.4 Results and Discussion	185
15 Conclusions and implications for future research/implementation.....	190
References	192
Appendix A: Supporting Data	206
Report Documentation Page	

Figures and Tables

Figures

Figure 1. Exposure pathways.....	7
Figure 2. Changes in faunal composition over time after a singular physical disturbance, such as will occur as a part of contaminated sediment remedy implementation.....	10
Figure 3. Types of pathway isolation chambers.	14
Figure 4. Polychlorinated biphenyl (PCB) concentrations across congeners for sediments of interest.	21
Figure 5. Polychlorinated biphenyl (PCB) congeners from sediments containing concentrations high enough to meet project objectives.....	21
Figure 6. Test organism survival in fine and coarse grain sediment.	22
Figure 7. Selected test organisms.....	23
Figure 8. Diagrammatic representation of the exposure system.	26
Figure 9. Prototype exposure system	26
Figure 10. Top view of mixed reactors of the prototype exposure system.....	27
Figure 11. Salt tracer concentration in the beta prototype exposure system.....	28
Figure 12. Experimental setup for SPMD-based passive dosing system.....	29
Figure 13. Diffusion of ¹⁴ C radio-labeled DDT across various membrane materials into test vials.....	35
Figure 14. Comparative equilibrium of ¹⁴ C radio-labeled DDT in Teflon 1.0 µm membrane vial relative to surrounding supply water.....	35
Figure 15. Comparison of [¹⁴ C] DDT DPMs in SPME within Teflon/ Polytetrafluoroethylene (PTFE) 1.0 µm vial relative to DPMs of 0.5mL water samples taken from within vial.	36
Figure 16. Diffusion of humic acid across the 0.1 µm Teflon (TFE) membranes vs. a control vial with no membrane.....	37
Figure 17. Prototype Pathway Isolation Chamber (PIC) performance.	38
Figure 18. SPME and PE generated pore water concentrations (ng/L) for all detected PCB congeners following the 28-day exposure to New Bedford Harbor sediment.	44
Figure 19. Bioaccumulation of total PCBs over time in five infaunal invertebrates exposed to New Bedford Harbor sediment.	53
Figure 20. Bioaccumulation of PCB homolog groups over time in five infaunal invertebrates exposed to New Bedford Harbor sediment.	57
Figure 21. Uptake rate constants (g/g/day) for five infaunal invertebrates exposed to New Bedford Harbor sediment determined for individual homolog groups and for total PCBs.....	59
Figure 22. Biota-to-sediment accumulation factors (BSAFs) for five infaunal invertebrates exposed to NBH sediment determined for individual homolog groups and for total PCBs.	60
Figure 23. PCB homolog groups as a percent of total PCBs in tissues of five infaunal invertebrates exposed to New Bedford Harbor sediment at single or multiple times.	61
Figure 24. Elimination of total PCBs over time in five infaunal invertebrates exposed to New Bedford Harbor sediment.....	64

Figure 25. Elimination of PCB homolog groups over time in five infaunal invertebrates exposed to New Bedford Harbor sediment.....	65
Figure 26. Elimination rate constants (day ⁻¹) and time to steady state predictions for five infaunal invertebrates exposed to New Bedford Harbor sediment determined for individual homolog groups and for total PCBs.	67
Figure 27. Bioaccumulation of PCBs homolog groups over time in <i>L. plumulosus</i> exposed to BNC sediment.	68
Figure 28. Uptake rate constants (g/g/day; top graph), elimination rate constants (day ⁻¹ , middle graph), and biota-to-sediment accumulation factors (BSAFs bottom graph) for <i>L. plumulosus</i> exposed to New Bedford Harbor (NBH) and BNC sediments determined for individual homolog groups and for total PCBs.	69
Figure 29. Bioaccumulation of total PCBs over time for <i>L. plumulosus</i> exposed to NBH sediment in a study conducted in 2009 (left graph, Lotufo, unpublished) and bioaccumulation of total DDTs over time for <i>L. plumulosus</i> exposed to spiked sediment (right graph, Lotufo, unpublished).....	71
Figure 30. Diagram of exposure system and Pathway Isolation Chamber (PIC) design. Panel (a) provides an overview of the exposure system.	79
Figure 31. Dissolved concentrations predicted from analysis of polyethylene devices (PEDs).	86
Figure 32. Sum PCB congeners in organism tissue exposure in different pathway isolation chambers.	90
Figure 33. Summary of bioaccumulation factors for animals exposed to whole sediment.	93
Figure 34. Lipid normalized tissue residues by homolog group for organisms exposed in the whole sediment pathway isolation chambers (PICs).....	94
Figure 35. Lipid normalized tissue residues by homolog group for organisms exposed in the overlying water and pore water pathway isolation chambers (PICs).	99
Figure 36. Bioconcentration factors (BCFs) for study organisms standardized by lipid content and polyethylene devices (PEDs) predicted pore water concentration for select congeners.....	102
Figure 37. Overlying water congeners (PCB24/104) in organisms exposed to New Bedford Harbor Sediment.	104
Figure 38. Overlying water congeners (PCB24/104) in organisms exposed to the Bremerton Navy Complex sediment.....	107
Figure 39. Importance of overlying water exposure to the test organisms living in whole sediment.	108
Figure 40. Schematic of the Sediment-Water System as Modeled in RECOVERY.	112
Figure 41. Simulated PCB Congeners 24 and 104 Concentrations in Reactor Water.	117
Figure 42. Simulated PCB Congeners 24 and 104 Concentrations in Reactor Water and New Bedford Sediment.	117
Figure 43. Simulated PCB Congeners 24 and 104 Concentrations in Reactor Water and Bremerton Sediment.	118
Figure 44. Simulated and Measured Total PCBs Concentrations in Exposure System with New Bedford Sediment.	118
Figure 45. Simulated Total PCBs Concentrations in PICs Exposed to New Bedford Sediment.	121
Figure 46. Simulated and Measured Total PCBs Concentration in PICs Exposed to New Bedford Sediment.	121

Figure 47. Simulated and Measured Total PCBs Concentrations in Exposure System with Bremerton Harbor sediment.	122
Figure 48. Simulated Total PCBs Concentrations in PICs Exposed to Bremerton Harbor Sediment.	123
Figure 49. Three-year simulation of Total PCBs Concentrations in PICs Exposed to Bremerton Harbor Sediment.	124
Figure 50. Four-year simulation of PCB 24 Congener Concentration in PICs Exposed to New Bedford Sediment.	125
Figure 51. Simulation of PCB 24 Congener Concentration in PICs Exposed to New Bedford Sediment.	126
Figure 52. Four-year simulation of PCB 104 Congener Concentration in PICs Exposed to New Bedford Sediment.	126
Figure 53. Simulation of PCB104 Congener Concentration in PICs Exposed to New Bedford Sediment.	127
Figure 54. Four-year simulation of PCB 24 Congener Concentration in PICs Exposed to Bremerton Harbor Sediment.	128
Figure 55. Simulation of PCB 24 Congener Concentration in PICs Exposed to Bremerton Harbor Sediment.	128
Figure 56. Four-year simulation of PCB 104 Congener Concentration in PICs Exposed to Bremerton Harbor Sediment.	129
Figure 57. Simulation of PCB 104 Congener Concentration in PICs Exposed to Bremerton Harbor Sediment.	130
Figure 58. Sum of PCBs Congeners <i>Leptocheirus plumulosus</i> Tissue Concentrations in PICs Exposed to New Bedford Sediment.	131
Figure 59. PCB 24 Congener <i>Leptocheirus plumulosus</i> Tissue Concentration in PICs Exposed to New Bedford Sediment.	131
Figure 60. Diagram of exposure system: including position of sediment treatments, organisms, and polyethylene devices.	136
Figure 61. Diagram of polyethylene device (PED) position in the Pathway Isolation Chambers (PICs).	138
Figure 62. Photographs of the exposure system.	140
Figure 63. Distribution of PCB congeners in the Bremerton Naval Complex (BNC) sediment used in this exposure.	141
Figure 64. Concentrations of PCB 24 and 104 in the overlying water.	144
Figure 65. Concentrations of (a) PCB 24 and (b) PCB 104 in tissue.	145
Figure 66. PED estimates of (a) PCB 24 and (b) PCB 104 in the sediment pore water in the animal exposure chambers.	148
Figure 67. PED estimates of dissolved concentrations in the animal exposure chambers at 1 cm and 3 cm below the surface.	150
Figure 68. Tissue residues for sum PCB congeners sourced from the sediment.	151
Figure 69. Sketch of the experimental gamma scan system.	162
Figure 70. A Gaussian is fit to each scan for each cell to obtain the peak position and the spread of the peak.	163
Figure 71. Obtaining burial rate and particle biodiffusion coefficient from the scanner data.	165

Figure 72. Tracer burial velocity (average from three replicates, one standard deviation error bar).....	167
Figure 73. Depth of the tracer layer at the end of the experiment.....	167
Figure 74. Particle biodiffusion enhancement factors.....	169
Figure 75. Vertical profiles of the ^{22}Na activity obtained over four days from one of the microcosms.....	171
Figure 76. Mean solute biodiffusion enhancement factors with one standard deviation error bars.....	172
Figure 77. Peak's position and peak's spread change in time. After very little change from day 10 to day 28, a sudden increase in both measurements was observed.....	175
Figure 78. Change of peak position with time for clean (left hand side panel) and contaminated (right hand side panel) sediments.....	175
Figure 79. Squared peak's spread (σ) vs. $2 \times$ time plots used for particle biodiffusion coefficient determination.....	176
Figure 80. Solute diffusion enhancement factors for <i>M. mercenaria</i>	177
Figure 81. A color contour plot of a 2-D cross section through the center of the burrow of the steady state model.....	179
Figure 82. Increase in solute flux (oxygen) as a function of burrow density.....	180
Figure 83. Comparisons of models of solute transport by <i>Y. limatula</i>	180
Figure 84. System used for luminophores position measurements.....	185
Figure 85. Progression of fluorescent particles redistribution for one of the experimental cells. Undisturbed layer of luminophores (day 0), luminophore layer partly mixed (day 6), and surficial layer of luminophores completely redistributed (day 22).	186
Figure 86. Comparison of two sides of the same cell. Each division on the scale bar on the left hand side of the pictures is 1 cm.....	187
Figure 87. Fluorescent intensity profiles for the front (30a) and back (30b) of cell 30 (left panel). Averaged fluorescence intensity $(30a+30b)/2$ profile for cell 30 with corresponding ^{137}Cs data for the same cell.....	187
Figure 88. Comparison of ^{137}Cs (black line) and luminophore (grey line) profiles. The blue dotted line indicates the position of sediment-water interface.....	189
Figure S1. Pre-exposure confirmation of PCB diffusion into the pore water PICs using SPME fibers in the NBH experiment.....	215
Figure S2. Photograph of in-use exposure system. Panel (a) exposure system. The reactor, which contains the solid phase membrane device (SPMD), is the silver box shown in the lower right-hand image. Panel (b) PICs.....	216
Figure S3. Summary of PCB congener distribution for the two test sediments. Congeners not shown were below analytical reporting limits ($< 2 \mu\text{g/kg}$).....	217
Figure S4. Overlying water concentrations of PCB congeners 24 and 104 in a preliminary water-only experiment (a) and during the NBH (b) and BNC (c) sediment exposures.....	222
Figure S5. Estimated dissolved concentrations in the Bremerton sediment exposure using polyethylene devices (PEDs) for (a) PCB24 and (b) PCB104.....	223
Figure S6. Bioaccumulated PCB homolog groups in test organisms exposed to the NBH sediment in PICs.....	224
Figure S7. Bioaccumulated PCB homolog groups in test organisms exposed to the BNC sediment in PICs.....	225

Tables

Table 1. List of candidate organisms, functional attributes, and taxonomic groups initially considered to test the project hypothesis.	15
Table 2. Preliminary test conditions.	16
Table 3. Initial list of potential sources of contaminated sediments.	17
Table 4. Summary of sediment characteristics and PCB concentrations.	19
Table 5. Collection information for the project sediments. All sediment was stored in the dark at 4 ± 2 °C.	19
Table 6. Selected test organisms for Tasks 1c, 2, and 3.	23
Table 7. Summary of membranes tested in an effort to be used in prototype pathway isolation chambers (PICs).	32
Table 8. Freely dissolved pore water concentrations (C_w , ng/L) of PCBs in test sediment that were generated using the PE sampling method.	45
Table 9. Sampling time for the uptake, the elimination exposures, and organisms loading per replicate.	48
Table 10. Total lipids content for the experimental organisms from uptake exposure, ND = not determined.	50
Table 11. Percent of experimental organisms alive at termination of the uptake exposures.	52
Table 12. Temporal trend of bioaccumulation for five infaunal invertebrates exposed to New Bedford Harbor sediment and time to approach steady state per ASTM (2010).	53
Table 13. Uptake rate constants (g/g/day) for five infaunal invertebrates exposed to New Bedford Harbor sediment determined for individual homolog groups and for total PCBs.	54
Table 14. Biota-to-sediment accumulation factors (BSAFs) for five infaunal invertebrates exposed to New Bedford Harbor sediment determined for individual homolog groups and for total PCBs.	60
Table 15. PCB homolog groups as a percent of total PCBs in tissues of five infaunal invertebrates exposed to New Bedford Harbor sediment at single or multiple times.	61
Table 16. Experimentally measured elimination rate constants (day^{-1}) and time to steady state predictions for five infaunal invertebrates exposed to New Bedford Harbor sediment determined for individual homolog groups and for total PCBs.	62
Table 17. Uptake rate constants (g/g/day), elimination rate constants (day^{-1}) and time to steady state predictions, and biota-to-sediment accumulation factors (BSAFs) for <i>L. plumulosus</i> exposed to BNC sediment determined for individual homolog groups and for total PCBs.	70
Table 18. Maximum body residues (kinetically derived and measured) and BSAF (kinetically derived and measured) in five infaunal invertebrates exposed to NBH and BNC sediments.	72
Table 19. Summary of the relative importance of different exposure pathways for the study organisms.	95
Table 20. Summary of sediment chemistry and characteristics.	96
Table 21. Values used in the New Bedford Sediment Experiment.	119
Table 22. Efficacy of different sediment treatments based on organism or functional feeding strategy.	142
Table 23. Summary of percent animals and tissue mass recovered.	142

Table 24. Experimental duration	161
Table 25. Measured particle biodiffusion coefficients and average particle biodiffusion enhancement factors.	170
Table 26. Solute diffusion coefficients for bioturbated cells and corresponding control cells.	172
Table S1. Summary of analytical methods used.	206
Table S2. Summary of initial laboratory observational experiments in control sediment.	210
Table S3. Organism field and extrapolated maximum loading densities for exposure chambers.	212
Table S4. Organism field and extrapolated maximum loading densities for exposure chambers.	214
Table S5. List of PCB congeners and concentrations ($\mu\text{g}/\text{kg}$) in the project sediments.....	217
Table S6. Survival of <i>Eohaustorius estuarius</i> at termination of the uptake exposure.	221

Preface

This study was conducted for the Strategic Environmental Research and Development Program under “The Biology of Bioavailability: The Role of Functional Ecology in Exposure Processes”; Project ER-1750 under Statement of Need ERSON-10-4 (Improved Fundamental Understanding of Contaminant Bioavailability in Aquatic Sediments). The technical monitor¹ was Dr. Andrea Leeson, deputy Director and Environmental Restoration Program Manager (SERDP & ESTCP).

The work was performed by the Environmental Processes and Risk Branch of the Environmental Processes Division (CEERD-EPR), U.S. Army Engineer Research and Development Center, Environmental Laboratory (ERDC-EL). At the time of publication, Buddy Goatcher was Chief, CEERD-EPR; Warren Lorentz was Chief, CEERD-EP; and Dr. Elizabeth Ferguson, CEERD-EMJ was the Technical Director for Military Environmental Quality and Installations. The Deputy Director of ERDC-EL was Dr. Jack Davis and the Director was Dr. Beth Fleming.

The authors would like to thank Scott Lemmons, Nick Melby, and Lauren Rabalais for laboratory support. The authors would also like to thank Dr. David Gent for significant contributions building the exposure system.

The Commander of ERDC was COL Bryan S. Green and the Director was Dr. Jeffery P. Holland.

¹ This descriptor refers to the technical POC and approver for the sponsoring organization. The person may be referred to as a technical monitor, program manager, point of contact, or other descriptor that is customary for the sponsoring organization.

Unit Conversion Factors

Multiply	By	To Obtain
cubic yards	0.7645549	cubic meters
degrees Fahrenheit	$(F-32)/1.8$	degrees Celsius
feet	0.3048	meters
gallons (U.S. liquid)	3.785412 E-03	cubic meters
inches	0.0254	meters
microns	1.0 E-06	meters
miles (U.S. statute)	1,609.347	meters
mils	0.0254	millimeters
ounces (U.S. fluid)	2.957353 E-05	cubic meters

Acronyms

2-D	Two-dimensional
3-D	Three-dimensional
σ	Peak spread
AC	Activated Carbon
ARO	Aquatic Research Organisms
ASTM	American Society for Testing and Materials
BAF	Bioaccumulation Factor
BNC	Bremerton Navy Complex
BSAFs	Biota-Sediment-Accumulation Factors
°C	Degrees Celsius
^{14}C	Carbon 14
^{137}Cs	Cesium 137
C_b	Concentration of chemical in benthos
C_D	Dissolved concentrations of chemical in sediment porewaters
Cm	Centimeter
cm^2	Centimeter Squared
C_i	Activity of the tracer
C_o	Overlying water activity of the tracer
C_{ps}	Passive sampler concentration
CsCl	Cesium Chloride
$C_{t_{\text{issue}}}$	Contaminant concentration in tissue
C_s	Contaminant concentration in the sediment
$C_{t=0}$	Initial chemical concentration in the invertebrates at the initiation of the elimination experiment
$C_{t-\text{max}}$	Maximum or equilibrium concentration within the organism

C_p	Particulate concentration
CSU	California State University
C_w	Freely-dissolved porewater concentrations
D_b	Biodiffusion
D_e	Enhanced diffusion coefficient
d	Mixed zone thickness
DDT	Dichlorodiphenyltrichloroethane
D_d	Route of elimination to water through defecation
D_i	Dichlorobiphenyls
DMDCS	Dimethyldichlorosilane
D_m	Route of elimination to water through metabolism
DOC	Dissolved Organic Carbon
DoD	Department of Defense
DPM	Disintegrations per Minute
EqP	Equilibrium Partitioning
ERDC	Engineer Research and Development Center
ε	Uptake efficiency
FLA	Fluoranthene
f_{BC}	Fraction of black carbon in the sediment
f_{oc}	Fraction of organic carbon in the sediment
g	Gram
GAC	Granular activated carbon
g/cm ³	Gram /Cubic Centimeter
gal	Gallon
GC-ECD	Gas Chromatograph Equipped with an Electron Capture Detector
h	Hour
Hg	Mercury
HPLC	High-performance Liquid Chromatography
indiv/m ²	Number of burrows/square meter

K_{abs}	Gill or tissue exchange rate
kBq	Kilobecquerel
K_d	Measure of sorption of contaminants
K_{dep}	Depuration rate
keV	Kiloelectron Volt
K_{oc}	Organic Carbon Partition Coefficient
K_{ow}	Exposure rates as a function of contaminant
K_{inj}	Ingestion rate
K_{ps}	Passive sampler partition coefficient
K_{BC}	Black carbon normalized partition coefficient
Kg	Kilogram
k_s	Uptake rate constant from sediment to the organism
k_2	Elimination rate constant from the organism
$k_{e(m)}$	Experimentally measured elimination rate
k_u	Uptake clearance
L	Liter
LDPE	Low-Density Polyethylene
LSC	Liquid Scintillation Counter
m	Meter
M	Molar
m^2	Square Meters
MeV	Megaelectron Volt
mg	Milligram
mg/kg	Milligram per Kilogram
mg/L	Milligram per Liter
min	Minute
ml	Milliliter
mm	Millimeter
^{22}Na	Sodium 22

MWF	Monday, Wednesday, Friday
NA	Not applicable
NBH	New Bedford Harbor
ND	not detected (not determined; Section 9 only)
ng/L	Nano Grams per Liter
nm	Nanometers
NWAS	Northwest Aquatic Science
O ₂	Oxygen
OVL	Overlying
OW	Overlying Water
OW-PIC	Overlying Water Pathway Isolation Chamber
PAH	Polycyclic Aromatic Hydrocarbons
PC	Polycarbonate
PCB	Polychlorinated Biphenyl
PDMS	Polydimethylsiloxane
PE	Polyethylsulfone
PED	Polyethylene Devices
PICs	Pathway Isolation Chambers
ppm	Parts per Million
ppt	Parts per Thousand
PRCs	Performance Reference Compounds
PTFE	Polytetrafluoroethylene
PW	Pore water
PW-BCF	Pore water Bioconcentration Factor
PW-PIC	Pore water Pathway Isolation Chamber
QA-QC	Quality Assurance-Quality Control
OC	Organochlorine
Penta	Pentachlorobiphenyls
R	Elimination to water from respiration

rpms	Revolutions per Minute
RT	Reasonable time
SD	Standard Deviation
Sec	Second
SOD	Sediment Oxygen Demand
SPMD	Solid Phase Membrane Device
SPME	Solid-Phase Micro Extraction
Suppl.	Supplemental
^3H	Tritium
Hexa	Hexachlorobiphenyls
Hepta-Nona	Sum of hepta-, octa-, and nonachlorobiphenyls
Hg	Mercury
Tetra	Tetrachlorobiphenyls
TBP	Theoretical Bioaccumulation Potential
TFE	Teflon
TOC	Total Organic Carbon
Tri	Trichlorobiphenyls
TSS	Time to steady state at 95%
μCi	Micro Curies
μg	Microgram
μL	Microliter
μm	Micrometer
Unk.	Unknown
U_w	Chemical intake from water
U_{food}	Chemical intake from food
UV	Ultra Violet
USEPA	United States Environmental Protection Agency
ω	Sediment ingestion rate
WS	Whole Sediment

WS-PIC	Whole Sediment Pathway Isolation Chamber
Wt	Weight
Yr	Year

1 Introduction

1.1 Objective

The objective of the proposed research was to provide the basis for improving the accuracy of sediment exposure assessments by including explicit consideration of the functional ecology of benthic receptors, which determines the nature of their interactions with sediment particles, pore water, and overlying water. Much of the uncertainty that currently plagues sediment risk assessments, remedy selection, and design is due to limitations associated with characterizing exposure processes in sediment. The lack of consideration given to biological variation in feeding strategies, uptake responses, and physiology among benthos produces significant uncertainty, preventing accurate assessment of bioavailability and risk. The research conducted in this project was in response to SERDP (Strategic Environmental Research and Development Program) Statement of Need (SON), ERSON-10-04, *Improved Fundamental Understanding of Contaminant Bioavailability in Aquatic Sediments*. The overarching hypothesis used to inform experimental design and analyses within the study was that *functional attributes of benthic organisms explain differences in observed exposure, uptake, and bioaccumulation among benthic functional groups*.

1.2 Technical approach

A series of laboratory experiments was conducted to test the hypothesis that the functional attributes of benthic organisms can explain differences in the organism's exposure, measured in terms of bioaccumulation, to different contaminant compartments within sediment. Four benthic invertebrates (a polychaete, two functionally distinct amphipods, and a bivalve) with differing functional attributes were exposed, through manipulative experiments, to a series of conditions that were designed to assess the relative contribution to exposure made by contaminants in overlying water, pore water, and sediment particles using pathway isolation chambers (PICs). Two polychlorinated biphenyl (PCB) contaminated sediments (from New Bedford Harbor (NBH), MA and the Bremerton Navy Complex (BNC), WA) were used in the experiments, in addition to uncontaminated control sediments. Experiments were performed to define the bioaccumulation kinetics for the four organisms.

These experiments were complemented with tests that evaluated how organism behavior impacts the movement of sediment particles and solutes using radioactive and fluorescent tracers. Finally, organism exposure was evaluated under two remediation scenarios (application of a thin sand cap and activated carbon (AC)). Measurements of PCB bioaccumulation were related to bulk PCB concentrations in overlying water and sediment, as well as dissolved contaminant concentrations in overlying water and sediments that were estimated using polyethylene devices (PED). Data collected during experiments were used to enhance the capability and predictive reliability of an existing modeling framework (RECOVERY) for assessing exposure processes in contaminated sediment.

1.3 Results

The evaluation of bioaccumulation kinetics in NBH sediment revealed significant differences among the benthic invertebrates. Lipid-normalized net body residues varied greatly among the species investigated, consequently, so did biota-sediment accumulation factor (BSAF) values. The measured BSAF was highest for *L. plumulosus* (5.4), intermediate for *Y. limatula* (2.9) and *E. estuarius* (2.4), and lowest for the polychaete *N. arenaceodentata* (2.0). The manipulative experiments using PICs resulted in a number of observations. As expected, exposures to whole sediment produced the greatest bioaccumulation for all four species. The amphipod, *L. plumulosus*, bioaccumulated more PCBs than the other organisms (particularly high log K_{ow} homolog groups), whereas *M. mercenaria* generally accumulated lower concentrations of PCBs. While overlying water exposure had some importance to the amphipod *L. plumulosus*, which comes to the substrate surface often, pore water exposure and direct sediment particle exposure were by far more important factors for determining overall *L. plumulosus* tissue residues. The overlying water had lower importance for *E. estuarius* and was virtually irrelevant for the worm *N. arenaceodentata*. Exposure to PCBs sourced from the overlying water was clearly more important for the filter-feeding clam, *M. mercenaria*. The 2 cm sand cap significantly reduced PCB exposure by 78–95 percent for all the species except *M. mercenaria*. However, the use of *in situ* placement of AC in the top 2 cm did not result in significant reductions in bioaccumulation. PED estimations of pore water concentrations were a vast improvement over bulk sediment concentration for predicting bioavailability, but could not account for divergent animal behavior between species and substrate types.

1.4 Benefits

Contaminant bioaccumulation from benthos to fish, wildlife, and humans is the exposure pathway responsible for the risks driving most contaminated sediments cleanup decisions. Risk assessments that have been performed at sediment cleanup sites to date have primarily relied on bulk sediment chemistry and a number of simplifying assumptions in order to model exposure processes and risk. However, the results of the present study document the complexity of exposure processes for benthic organisms. Because current risk assessment and performance monitoring practice does not generally consider the role of functional differences among benthic organisms, these assessments can produce inaccurate risk estimates, as well as inaccurate projections of the risk reduction benefits associated with proposed remedies. The combined use of passive sampling techniques, information about the functional ecology and physiology of the target receptors, and site-specific bioaccumulation data for the functional receptors of concern will lead to more accurate projections of risk and remedy performance. The results of the present study can be used to help design functional bioavailability assessments at contaminated sediment sites as well as provide the basis for development of future guidance.

2 Project Objective

This final report for SERDP Project ER-1750 describes research conducted in response to SERDP Statement of Need ERSON-10-04, Improved Fundamental Understanding of Contaminant Bioavailability in Aquatic Sediments. The large level of uncertainty involved in characterizing contaminant exposure (i.e., bioavailability) in sediments hinders efforts to develop optimal remediation strategies and increases cleanup costs. Large uncertainties contribute to conservative estimates of risk, very low cleanup levels, and unnecessarily high remediation costs.

The objective of ER-1750 was to substantially increase the accuracy of bioavailability assessments for contaminated sediment by developing a more comprehensive understanding of exposure variation among benthic species due to functional attributes that determine how organisms interact with sediment particles, pore water, and overlying water. Benthic organisms vary in terms of their position within the sediment column (e.g., epibenthic vs. infaunal), their relationship to sediment particles and pore water (e.g., tube building vs. free burrowing), and feeding behavior (filter feeding vs. deposit feeding), all of which contribute to differences in exposure to contaminants and bioavailability. Manipulative experiments conducted in this project relate the functional ecology of a receptor with its realized exposure. The resulting understanding enables improved exposure models, which will provide for more credible risk assessments and better predictions about remedy performance.

The experimental design for studies conducted during this project was based upon the following overarching hypothesis:

Differences in exposure rates (as measured by bioaccumulation into tissues) among benthic species is explained by differences in the functional attributes of those species.

The understanding gained through this research will reduce the uncertainty associated with current exposure assessments and predictions that are used in remedy selection and design. This outcome will reduce the need for using conservative safety factors in calculating exposure point estimates, as well as provide a mechanistic basis for designing *in situ*

remedies that are targeted to reduce exposures to benthos and fish that consume benthos. Incorporating the predictive algorithms within RECOVERY (Ruiz, 2001), which has been (and is being) used to evaluate *in situ* remedies, will greatly facilitate technology infusion.

Transition and implementation of the project's results will be accomplished through coordination with other research programs/efforts and through support to ongoing remedial projects. Project results will affect the direction and scope of ongoing and future contaminated sediment research in the Dredging Operations Environmental Research (DOER) Program and research supporting the United States Environmental Protection Agency's (USEPA) Superfund program. The results will be applicable to numerous ongoing remedial projects supported by the Principal Investigators. The modeling algorithms developed during the project will be incorporated and distributed as part of an enhanced version of modeling software currently in use at contaminated sediment sites.

3 Background

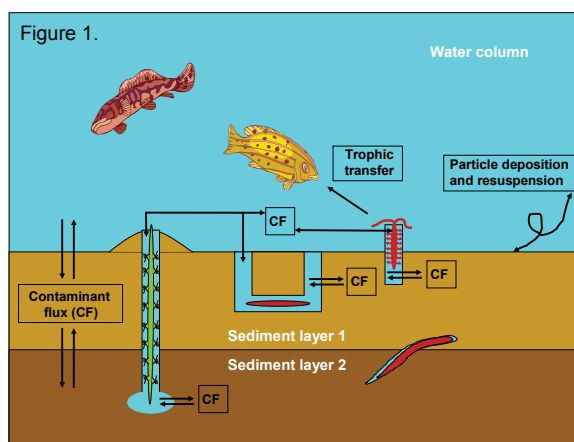
The total estimated cost for remediating 200 Navy sediment sites is \$1 billion. While no quantitative analysis has been conducted to scope the magnitude of the sediment problem at Army and Air Force sites, contaminated sediments are certain to be present when contaminants are evident in soils, surface waters, and effluents. Contaminant bioaccumulation through benthos to fish, wildlife, and humans is the exposure pathway responsible for the risks driving most cleanup decisions for contaminated sediments. Improved approaches for quantifying contaminant bioavailability and exposures within the sediment bed is key to reducing uncertainties in descriptions of risks to benthos and fish that feed on benthos. More accurate exposure characterizations are also necessary to support the challenges of designing, implementing, and monitoring the performance of cost-effective, *in situ* remedies for contaminated sediments. Approaches that explicitly consider the functional ecology of the diverse array of species comprising benthos will produce more accurate and certain exposure assessments and predictions for remedial decision-making. Research focused on these approaches will support a critical research need in the area of “improved approaches for biological assessments of bioavailability” (SERDP 2008).

The objective of the proposed research is to improve the accuracy of exposure assessments by including explicit consideration of the functional ecology of benthic receptors, which determines the nature of their interactions with sediment particles, pore water, and overlying water. Much of the uncertainty that currently plagues sediment risk assessments and remedy selection and design is due to limitations associated with characterizing exposure processes in sediment (National Research Council (NRC) 2003). The lack of consideration in current chemistry-focused assessment approaches that is given to biological variation in feeding strategies, uptake responses, and physiology among benthos produces significant uncertainty, preventing accurate assessment of bioavailability and risk (SERDP 2008).

Contaminant bioaccumulation into sediment-dwelling organisms is the first step in the most significant exposure pathway producing risks at upper trophic levels (Figure 1). Risks to upper trophic levels (e.g., fish, wildlife,

and humans) are the primary decision drivers at the majority of contaminated sediment sites (SERDP 2004, 2008). Researchers can address a significant source of uncertainty in bioaccumulation processes by developing a more complete understanding of exposure variation among benthic species caused by functional differences in how organisms interact with sediment particles, pore water, and overlying water. Benthic species vary in terms of their position within the sediment column (e.g., shallow vs. deep), their relation to sediment particles, pore water (e.g., tube building vs. free burrowing), and feeding behavior (filter feeding vs. deposit feeding) (Figure 1), all of which contribute to differences in contaminant exposure and the notion of contaminant bioavailability. Experiments conducted during the course of this project provided insight relating the functional ecology of a receptor with its realized exposure. This understanding enables improved exposure models, which will provide for more credible risk assessments and better predictions about remedy performance.

Figure 1. Exposure pathways.



A large and varied collection of *bioavailability* definitions and methodological approaches has been employed in contaminated sediments research (see review in NRC 2003). In response to this conceptual diversity, NRC (2003) proposed the following definition for *bioavailability processes*: “The individual physical, chemical, and biological interactions that determine exposure of organisms to chemicals associated with soils and sediments...” This definition illustrates two important points: 1) a variety of processes (i.e., physical, chemical, and biological) contributes to bioavailability and 2) the objective of bioavailability assessments is the quantification of exposure to organisms.

For contaminated sediments, assessing risks and designing risk-reducing remedies require the use of tools to quantitatively measure and predict exposure of benthic organisms. For many years, considerable attention in bioavailability research has focused on chemical partitioning behavior and the use of dissolved contaminant concentrations in pore water as a surrogate measure for bioavailability (Di Toro et al 1991). It must be understood that benthic organisms will be exposed to contaminants associated with multiple phases or compartments in addition to that portion which is present in dissolved form within pore water (this is discussed in more detail below). However, the fraction of contaminant dissolved in pore water has been used as an indicator of chemical fugacity or activity in order to estimate the potential for exposure and toxicity (e.g., Meyer et al 2000; Lohmann et al 2004, Vinturella et al 2004; You et al 2007; Hawthorne et al 2007; Kreitinger, et al, 2007; Witt et al, 2009). Based on this construct, much research has been conducted to define the means to directly measure or indirectly predict pore water concentrations of contaminants. Relative to predicting these concentrations, the equilibrium partitioning (EqP) model was applied to estimate the dissolved concentrations of chemical in sediment pore waters (C_D) based on the particulate concentration (C_P) and fraction of organic carbon (f_{OC}) in the sediment (Di Toro et al 1991). This approach assumes that the majority of contaminants partition to the sediment organic carbon, while a small fraction occur in the dissolved phase. This approach has successfully predicted pore water concentrations of several contaminants, especially in very contaminated sediments (Swartz et al 1990, DeWitt et al 1992, Hoke et al 1994, Swartz et al 1995, Ozretich et al 2000). However, the approach sometimes over-estimates bioavailability. This over-estimation is likely due to the presence of other partitioning phases in sediments (e.g., black carbon) that sequester contaminants; to address this, EqP models are still under development (Cornelissen et al 2005). Accardi-Dey and Gschwend (2002) proposed the following EqP model to explain dissolved concentrations affected by natural organic carbon and black carbon:

$$C_D = \frac{C_P}{f_{OC}K_{OC} + f_{BC}K_{BC}C_D^n} \quad (1)$$

where K_{OC} is the organic carbon partition coefficient, f_{BC} is the fraction black carbon in the sediment, K_{BC} is the black carbon normalized partition coefficient, and n is the Freundlich nonlinear sorption coefficient. This model has also been successful at predicting pore water concentrations,

but considerable uncertainty still exists around the measurement of f_{BC} and values for K_{BC} and n . These sources of uncertainty limit the confident application of this model in risk assessment and management.

As with the use of the EqP model to indirectly predict dissolved concentrations of contaminants, directly measuring the dissolved concentrations of contaminants in pore water poses uncertainties and challenges. For example, distinguishing the dissolved concentrations of contaminants from dissolved organic carbon (DOC)-bound contaminants in pore waters represents an analytical challenge. For pore water obtained by separation methods (e.g., centrifugation and filtration), concentrations are determined for “whole” pore water based on solvent extraction followed by analytical quantitation. Predictive three-phase distribution models can be applied to estimate C_D using measured DOC and estimated partition coefficients (K_{DOC}) (McGroddy and Farrington, 1995; Mitra et al, 1999; Burkhard 2000, Persson et al, 2002; Accardi-Dey and Gschwend, 2003), but, as noted above, uncertainties exist. In the past, substantial effort was devoted to developing analytical methods that distinguished between dissolved, particulate, and DOC phases. For example, dialysis (Escher and Schwarzenbach, 1996), solubility enhancement (Chiou et al, 1986), and fluorescence quenching (Backhus and Gschwend, 1990) methods are available, but have their own limitations. More recently, techniques have been developed based on passive sampling devices (discussed below), which collect chemicals directly from the dissolved phase, providing a great deal of improvement over predictive methods.

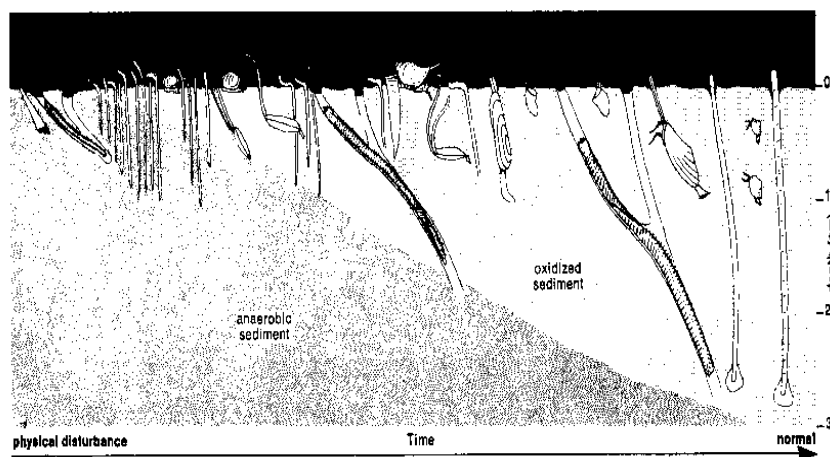
Despite the amount of attention that chemical processes have received in bioavailability research over the last 15 years, large uncertainties continue to plague attempts to translate information about chemical processes into quantitative descriptions of exposure for use in risk assessment and management (SERDP 2008). One of the most significant sources of uncertainty in characterizing bioavailability is the contribution of biological processes to the measurement of bioavailability and exposure.

Benthic communities comprise hundreds of individual species. Ecological and physiological differences among the numerous species inhabiting or associated with sediments will influence how organisms encounter contaminants, the rate and duration of that encounter, and the kinetics of contaminant uptake into the tissues of organisms. The organisms relevant to risks posed by contaminated sediments include microbes, meiofauna

inhabiting pore spaces within sediment, and bioturbating macrofauna that build structures within the sediment fabric.

The division of benthic communities into groups of organisms that share similar functional attributes (i.e., functional groups) has proved itself useful as an approach for describing the structure of benthic communities and for predicting recovery and successional processes following disturbance (McCall, 1977; Rhoads et al, 1978; Pearson and Rosenberg, 1978). In general, small tube-dwelling surface deposit-feeders that first colonize disturbed bottom sediments in large numbers are in time replaced by much larger, but less abundant deep-dwelling deposit and suspension feeders whose activities structure the seafloor (Figure 2). In sediments where large bioturbating infauna dominate, they re-engineer the biologically active zone to prevent the invasion of other functional groups, while fostering others (Lohrer et al, 2008). Overtime, this model has found broad applicability to both natural and anthropogenically disturbed systems in Atlantic, Gulf of Mexico, Pacific, and European coastal marine bottoms (Nichols, 1979; Rhoads and Germano, 1986; Scott, 1989; Germano et al, 1994; Gaston et al., 1998; SFEI, 1999; Pearson, 2001; Fredette and French, 2004; Norkko et al, 2006; Lohrer et al, 2008). The model has proven useful in describing benthic dynamics in large freshwater lakes (Soster and McCall, 1990) and in describing the sequential development of changes in the chemistry of the pore waters in freshwater sediments (Soster et al, 2001). Through the research described herein, the authors extend the use of this functional ecology paradigm to explain observed variation in contaminant exposure rates experienced by benthic species.

Figure 2. Changes in faunal composition over time after a singular physical disturbance, such as will occur as a part of contaminated sediment remedy implementation (Graphic is from Rhoads et al (1978)).



Trophic functional groups among macrofauna inhabiting soft-sediment environments include surface deposit feeders, subsurface deposit feeders, suspension feeders, scavengers, and predators (Pearson 2001). Some organisms mix sediment particles in a random or diffusive manner, others recycle or advect sediment solids in a directed manner by feeding at depth and defecating at the sediment-water interface, while others pump oxygenated surface water into reduced sediments by irrigating burrows or by direct injection into the pore fluids. Infaunal macrobenthos can: alter the early chemical diagenesis of sediments, modify the exchange of solutes across the sediment-water interface, alter sedimentary fabric, texture, porosity, and compaction, bind sediment particles and fabricate burrows that are sometimes maintained with semi-permeable linings, mix sediment particles, selectively feed on certain sizes or classes of sediment, secrete mucus and excrete metabolites, recycle buried contaminants, alter oxidation/reduction conditions, and affect the chemical exchange between sediments and overlying water. The variation in feeding mechanisms will govern how organisms encounter sediment particles, pore water, and other phases associated with contaminants. The relative motility of benthic organisms and the ways in which organisms manipulate the sediment fabric to accommodate their functional attributes (e.g., construction of burrows, permanent tubes, etc.) will similarly influence the rates at which they are directly exposed to sediment particles with varying contaminant loads, pore water, and overlying water. The mucopolysaccharide/protein tube linings of late successional infauna can inhibit the diffusion of organic and inorganic pore water solutes by factors of 3–8x relative to free solution, where this hindrance to diffusion has been found to be a function of both solute charge and size (Aller, 1983; Hannides et al, 2005). Infaunal suspension feeding bivalves, which possess thick shells and relatively impermeable siphons, may experience much less exposure to sediment pore water than other less protected species.

The current approach to assessing benthic exposure processes in contaminated sediment is simple and ostensibly ignores the biological and functional diversity present in benthic communities. The approach is based on (1) defining, for the site in question, the “biologically active zone,” which is the sediment horizon containing most of the biological activity (application of this ambiguous concept has proven to be very difficult to accomplish, in practice), (2) characterizing the bulk sediment and/or pore water contaminant concentration within this zone, and (3) comparing the sediment and/or pore water concentration to the measured

or predicted benthic tissue concentration in one or two standard laboratory bioaccumulation test organisms, or in some cases, to a composite of field-collected organisms containing multiple, often unidentified, species. This approach has proven itself to be an overly simplistic method that results in considerable uncertainty in exposure rate estimates and provides little mechanistic insight regarding the processes governing exposure and risk. Published reports abound which describe differences in contaminant exposure and bioaccumulation by a variety of companion filter feeders and deposit feeders in similar sedimentary environments (for examples, consult Meador et al, 1997; Kaag et al, 1997; Burgess and McKinney, 1999; Millward et al, 2001; Lohmann et al, 2004; Cho et al, 2007).

Contaminant bioaccumulation through benthos to fish, wildlife, and humans is the exposure pathway responsible for the risks driving most cleanup decisions for contaminated sediments at DOD sites. Improved approaches for quantifying contaminant bioavailability and exposures within the sediment bed is key to reducing uncertainties in descriptions of risks to benthos and fish that feed on benthos. More accurate exposure characterizations are also necessary to support the challenges of designing, implementing, and monitoring the performance of cost-effective *in situ* remedies for contaminated sediments. Approaches that explicitly consider the functional ecology of the diverse array of species comprising benthos will produce more accurate and certain exposure assessments and predictions for remedial decision-making.

4 Materials and Methods

The remainder of the report is organized into discrete chapters associated with the tasks laid out in the proposal and as described in Section 7.1.1. Thus, the pertinent methods, results, and discussions are available within each of the report's chapters.

4.1 Technical approach

4.1.1 Task description

The research tasks for the project are briefly summarized here; additional information on these tasks is presented in the project proposal. The research activities for the project are associated with three major task groupings.

4.1.1.1 Task 1. Preliminary Activities.

- Task 1a: Suitability of Candidate Species. Five candidate species representing different functional groups were selected based on the criteria discussed in the next section. The suitability of the candidate species for representing their target functional attributes were determined within the specialized observation chambers described in Task 1b (below), which allow for continuous visualization of organism interactions with the sediment. The selected species were used in follow-on experimentation (Tasks 1c, 2, 3). This task is addressed in Section 5 of this report. Five species were evaluated in Task 1c. Four of the five species were also evaluated in Task 2.
- Task 1b: Construction of Experimental Chambers. Replicate exposure chambers used in these experiments (Task 2) were constructed from glass that was silanized. This task is addressed in Sections 6, 7, and 10.
- Task 1c. Kinetics for Candidate Species. Five candidate test species representing different functional attributes were exposed to gain basic uptake kinetics information, including estimates of steady-state tissue concentrations. This task is addressed in Section 8.

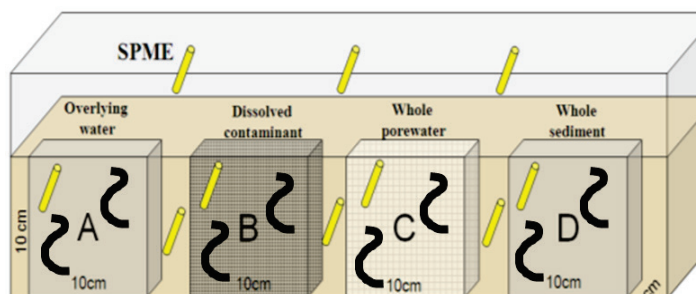
4.1.1.2 Task 2. Exposure Processes and Model Development.

The authors' overarching hypothesis was experimentally evaluated by examining contaminant uptake into the tissue of experimental organisms

exposed to combinations of overlying water, sediment pore water, sediment particulate matter, and living biomass. Exposures will be assessed and modeled in relation to these compartments and exchange across these compartments.

- **Task 2a.** Exposure Experiments. The research proposal discussed use of exposure manipulations using four PICs incorporated into an exposure system graphically summarized in Figure 3 (note: preliminary experimental findings resulted in eliminating the “dissolved contaminant” pathway isolation chamber from the experimental system design). Data collected from these experiments were used to develop an exposure model for the experimental organisms and their functional attributes (Task 2b). This task is addressed in Section 10 of this report.
- **Task 2b.** Model Development: The data collected during Tasks 1c and 2a was used as inputs to developing algorithms to describe exposure to benthic organisms having different functional attributes. These algorithms enhance the capability of RECOVERY, an existing model framework for assessing contaminant processes in sediment systems.

Figure 3. Types of pathway isolation chambers.



4.1.1.3 Task 3. Model Verification and Proving.

- **Task 3a.** Experiments Using Management Scenarios. The exposure model developed in Task 2b was verified in the laboratory system through manipulative experiments. Experimental exposures with the same organisms used in Task 2a was conducted with a novel field-collected, contaminated sediment.
- **Task 3b.** Model Verification. The algorithms developed and the enhanced RECOVERY framework produced in Task 2b was used to simulate the exposure and contaminant uptake by benthic organisms tested in the experiments conducted in Task 3a.

5 TASK 1A: Selection of test organisms and sediments

5.1 Introduction

Recent work conducted at the U.S. Army Engineer Research and Development Center (ERDC) has demonstrated that the use of different test sediment characteristics and functionally different test organisms (e.g., marine polychaetes versus clams) can lead to very different bioaccumulation kinetics, steady state concentrations, and biota-to-sediment accumulation factors (Kennedy et al 2010). However, the relative importance of organism functional ecology (including feeding strategy) versus exposure vector (e.g., overlying water, pore water, whole sediment, and dietary) is not well understood. Thus, candidate organisms were selected to represent diversity in both phylogeny and functional feeding strategies to consider the implications on the bioavailability of sediment-borne contaminants (Table 1, Table 2).

Table 1. List of candidate organisms, functional attributes, and taxonomic groups initially considered to test the project hypothesis.

Functional group	Taxonomic group	Organism	Comment
Surface deposit feeders	Arthropod	<i>Leptocheirus plumulosus</i> *	Burrows
	Arthropod	<i>Ampelisca abdita</i> *	Tube dwellers
	Annelid	<i>Steblospio benedicti</i> *	
	Mollusc (clam)	<i>Macoma baltica</i> *, <i>Mulinia lateralis</i>	Siphons
Infaunal deposit feeders	Mollusc (clam)	<i>Yoldia limatula</i> *	
	Arthropod	<i>Eohaustorius estuarius</i> *	Free living
	Annelid	<i>Arenicola marina</i> , <i>Clymenalla torquata</i>	
Suspension feeders	Mollusc (clam)	<i>Mercenaria mercenaria</i> *, <i>Ensis directu</i> , <i>Mya arenaria</i>	
Various	Annelid	<i>Neanthes areanaceodentata</i> *	Free burrowing
*Asterisks indicate organisms acquired and tested in the laboratory.			

Table 2. Preliminary test conditions.

Organism	Source	Salinity	Sediment	Temp.	1 L beaker		Ant farm		
					Date	Number added	Date	Type	Number added
<i>Eohaustorius estuarius</i>	NWAS	20	Field Y. limatula	15	17 March 10	10	20 March 2010	Small	4
<i>Yoldia limatula</i>	MBL	30	Field Y. limatula	15	17 March 10	5	20 March 2010	Small	4
<i>Ampelisca abdita</i>	ARO	30	ARO	20	20 March 2010	20	20 March 2010	Small	20
<i>Mercenaria mercenaria</i>	ARO	30	ARO	20	20 March 2010	5	20 March 2010	Large	5
<i>Neanthes arenaceodentata</i>	ERDC	30	ARO	20	24 March 2010	5	24 March 2010	Small	5
<i>Streblospio benedicti</i>	CSU	30	ARO	20	1 April	10	31 March	Small	5

NWAS = Northwest Aquatic Science, Newport, OR; MBL = Marine Biology Laboratory, Woods Hole, MA; ARO = Aquatic Research Organisms, Hampton, NH; ERDC = Engineer Research and Development Center, Vicksburg, MS; CSU = California State University, Long Beach, CA

Further, work has suggested that sediment characteristics (e.g., grain size, total organic carbon (TOC), etc.) can also significantly impact bioaccumulation kinetics between sediments and species (e.g., Kennedy et al 2010). Thus, it was important to employ several different representative sediments to test the hypothesis. Marine/estuarine sediments were selected to be applicable to both Navy and Army sites, though the methodology developed in this work could easily be applied to freshwater sites. While logistically more complicated and costly, it was important to use field-collected sediments for both conceptual (i.e., direct field, DOD relevance) and technical (it is known that contaminants are more bioavailable in laboratory spiked sediments) (Kukkonen and Landrum 1998) reasons.

5.2 Materials and methods

5.2.1 Sediment selection

An initial effort was made to identify PCB-contaminated sediment sites. Adequate sediment volumes for analytical chemistry were collected from three DOD (Fort Eustis, VA; Navy Station Newport at Gould Island, RI; BNC, WA) and three non-DOD (Mare Island, CA; Stege Marsh, CA; NBH, MA) sites (Table 3). Sediments were analyzed for PCBs, metals, pesticides, total organic carbon, and grain size characteristics as in Section 10.3.6. This

analysis determined the adequacy of the candidate sediments for grain size compatibility with the organisms (U.S. EPA, 1994; U.S. EPA/ACE, 2001; Emery et al, 1997; Kennedy et al 2009; Postma et al, 2002) and the theoretical bioaccumulation potential (TBP) of the PCBs in the sediment to partition into organism tissue based on total concentrations, lipid content, and TOC (USEPA / USACE 1998). Sediments were submitted to the ERDC Environmental Chemistry Branch for analysis of PCB congeners and TOC. Analytical determinations were as described in Appendix A: Supporting Data (Table S1).

Table 3. Initial list of potential sources of contaminated sediments.

Site and Service	Chemicals
Alameda Air Naval Station, Sea Plane Lagoon, Alameda, CA	PCB, Cd, Pb, Radiological
Fort Eustis, VA	PCB, PAH
Hunter's Point Naval Shipyard, San Francisco, CA, Navy	PCB, Hg
Inner Apra Harbor, Naval Berthing Facility, Guam	PCB
Mare Island Naval Shipyard, Outfall into bay, San Francisco Bay, San Francisco, CA	PCB, Hg
Naval Weapons Station, Concord, CA	OC Pesticides, Metals
Pearl Harbor Naval Complex, Dry Dock, Pearl Harbor, HI	PAH, Metals

5.2.2 Organism selection

As previously discussed, candidate organisms were selected based on their ecological role and functional attributes, organism compatibility with experimental / laboratory conditions, geographical distribution, availability, and previous use in routine bioaccumulation testing. A full list of candidate organisms initially considered is provided in Table 1. Live specimens from a smaller list of representative organisms (indicated by asterisks in Table 1) were acquired for further examination of experimental suitability. Survival in both fine-grained sediment (collected from Sequim Bay, WA; described in Kennedy et al 2009) and less than 60 μm grained sand was measured for 10 days in 1 liter glass beakers using previously described methods (Kennedy et al 2009). Tests were conducted to meet optimum ranges for each organism (Table 2) using artificial seawater (Crystal Sea Marine Mix® (Enterprises International, Baltimore, MD, USA)). Surviving organisms were enumerated by sieving (500 μm) substrate at termination. No external food was supplied during the short duration exposures (10 days). In addition, the burrowing behavior of each organism in the sediment and sand was assessed in plexiglass ant farms for four days. Finally, calculations

were made to relate the density of organisms in the experimental apparatus (determined to satisfy analytical tissue requirements) to naturally occurring densities.

It was observed that the suspension feeding *Mercenaria mercenaria* ceased filtering after approximately three to four days in laboratory test conditions. Thus, a flow through experiment was conducted utilizing metering pumps to determine what cell densities of *Isochrysis*/diatom mix (Aquatic Research Organisms, Hampton, NH) and commercially available Phytoplex® (Kent Marine, Franklin, WI) would maintain consistent filtering activity for a 28-day period. The amphipod *Eohaustorius estuarius* was also tested in this system to determine if the algae blend would support them for 28 days. Algae concentrations were determined over time by measuring 10 µL water samples and enumerating cells (cells/ml) on a hemacytometer.

5.3 Results and discussion

5.3.1 Sediment selection

Sixteen sediments were initially obtained for analysis of physical characteristics, total organic carbon concentrations, and PCB concentrations. DOD relevant sediments were collected and analyzed from two locations at Fort Eustis, VA six locations in Gould Island, RI, and one location at BNC, WA. Sediments were also collected and analyzed from three locations in Mare Island, CA and Stege Marsh, CA and one location in NBH, MA. General results and observations are summarized in Table 4. Samples from Fort Eustis were not selected due to frequent freshwater intrusion, which has questionable relevance to the marine-focused study. Sediments from Mare Island were not selected as PCB concentrations were too low to meet project objectives based on theoretical bioaccumulation potential. While Gould Island is a relevant sediment site with measured PCB concentrations at the low end of the desired range of 5 to 30 mg/kg, these sediments were not used in Tasks 1 and 2 because the coarse grain size of the sediments would challenge the tolerance range of some of the selected model organisms. Ultimately, the NBH sediment was selected for Tasks 1c and 2a, and BNC sediment (DOD site) was selected for a second Task 2a experiment due to its grain size characteristics, PCB concentrations, and DOD relevance. A bulk collection of both the NBH sediment and the Bremerton sediment used in Tasks 2 and 3 was made and collection information is provided in Table 5. Sediments from Gould Island and Hunters Point, CA (DOD site in the south

basin of San Francisco Bay) were considered for use in Task 3 experiments. The authors previously showed that Hunters Point sediments consist of adequate grain size and PCB concentrations for bioaccumulation testing (Millward et al 2005; Cho et al 2007, 2009). All sediments were stored in a cold room in the dark at 4 ± 1 °C.

Table 4. Summary of sediment characteristics and PCB concentrations.

Site	DoD	Sites	Sum PCB congeners (mg/kg) ^a	TOC ^b (%)	Solids (%)	Grain Size ^c	Selected for Project	Comment
Mare Island, CA	N	3	< 0.1	NA	NA	Fine-grained	N	PCBs too low
Stege Marsh, CA	N	3	1.7 to 18.6	NA	NA	Fine-grained; debris	N	Non-DOD Cost (potential Task 3)
New Bedford, MA	N	1	33.7	6.4	58	Fine-grained	Y	High PCBs
Fort Eustis, VA Bailey Creek Lake Eustis	Y	2	NA	NA	NA	Low PW salinity	N	Freshwater / estuarine
Gould Island, RI	Y	6	2.1 to 4.5	0.5 – 0.9	NA	Coarse grained	N	Low PCBs Coarse grains (potential Task 3)
Bremerton Navy Complex, WA	Y	1	3.9, 16.6	1.0%	46%	Fine-grained	Y	DOD High PCBs

a = U.S. EPA 846 method 8082

b = U.S. EPA 846 method 9060

c = ASTM Method D422

Table 5. Collection information for the project sediments. All sediment was stored in the dark at 4 ± 2 °C.

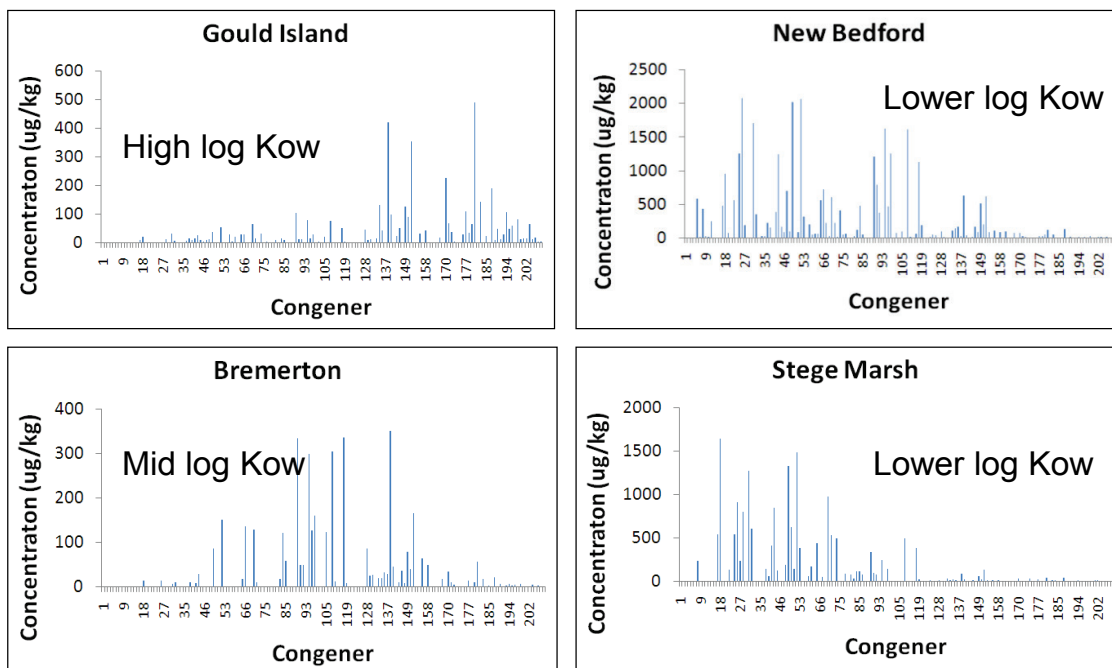
	New Bedford	Bremerton
Collection coordinates	41.658509 °N 70.913572 °W	47.558780 °N 122.628896 °W
Collection date	30 March 2009 to 8 April 2009	15 June 2011
Collection volume	110 gallons	110 gallons
Storage time (Task 1C experiments)	27 months	10 months
Storage time (Task 2A experiments)	38 months	15 months
Storage time (Task 3A experiments)	Not applicable	27 months

In addition, all sediments submitted to the ERDC Environmental Chemistry Branch were analyzed for all PCB congeners and results were summarized in Figure 4 and Figure 5. The objective was to select sediment(s) with a full range of high and low log K_{ow} congeners that would be representative of sediment sites contaminated with PCBs. Further, all congeners were assessed to identify two congeners that were not detected in sediments (i.e., below analytical reporting limits of 0.8 µg/kg) so that these congeners could be passively dosed into the water column as a unique source in order to separate the importance of the overlying water pathway from the other pathways. Based on this analysis (Figure 5), congeners 24 and 104 were selected for passive dosing into the overlying water.

5.3.2 Organism selection

From a large field of potential organisms, eight candidate organisms (*Leptocheirus plumulosus*, *Ampelisca abdita*, *Streblospio benedicti*, *Macoma nasuta*, *Yoldia limatula*, *Eohaustorius estuarius*, *Mercenaria mercenaria*, and *Neanthes arenaceodentata*) were acquired and evaluated in relation to the experimental system. As a part of the selection process, the authors considered taxonomic diversity, functional feeding strategies, geographical distribution, interactions with the sediment (i.e., infaunal vs. epibenthic), current availability, suitability for laboratory handling, and frequency of use in sediment evaluations as selection criteria. The capacity of the candidate organisms to metabolize contaminants was also considered (Rust et al 2004). The authors also assessed the 28-day laboratory survival of the candidate organisms in both fine and coarse grained sediment, in addition to monitoring changes in lipid content, burrowing and feeding behavior within the experimental system and constructed exposure chambers. Survival of all test organisms in both sediment and sand was relatively high after 10 days (>80%), with the exception of *L. plumulosus* (72%) in sand and *E. estuarius* (53%) in the fine-grained sediment (Figure 6). The low tolerance of *L. plumulosus* in sand (Emery et al 1997, Kennedy et al 2009) and *E. estuarius* in fine-grained sediment (U.S. EPA 1994) has been previously documented.

Figure 4. Polychlorinated biphenyl (PCB) concentrations across congeners for sediments of interest.



Note: low log Kow congeners expected to be more available in porewater

Figure 5. Polychlorinated biphenyl (PCB) congeners from sediments containing concentrations high enough to meet project objectives. (This overlay was used to determine unique congeners (not in any sediment) to passively dose into the water column.)

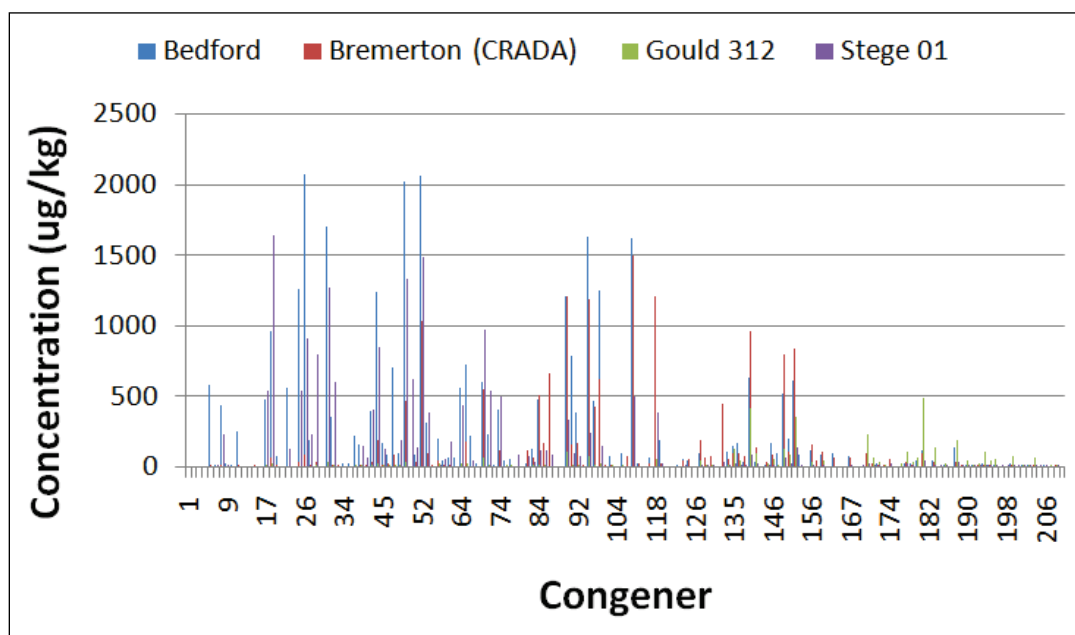
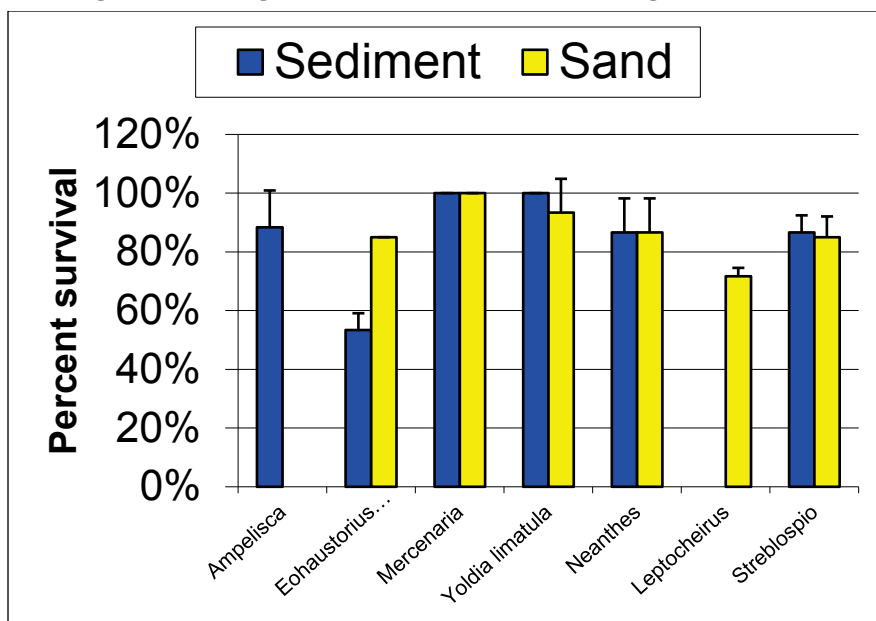


Figure 6. Test organism survival in fine and coarse grain sediment.



In addition to candidate organism tolerance to grain size and handling, a general assessment of burrowing depths, tissue mass available for analytical chemistry, lipid content, and information on natural field densities related to laboratory conditions was performed (Table S2, Table S3, Table S4). Certain candidate organisms were eliminated based on low availability and tissue mass for analytical chemistry (e.g., *S. benedicti*).

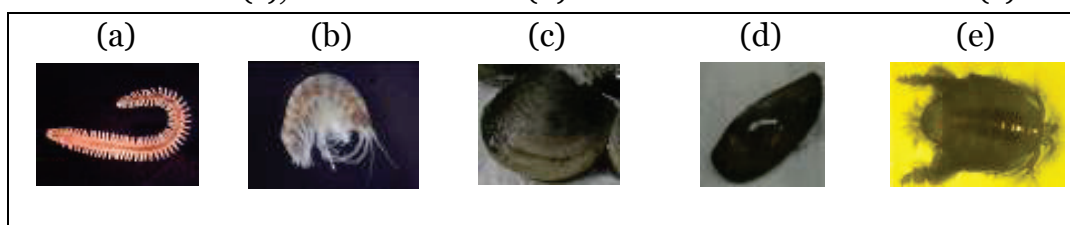
Based on these parameters, four organisms were selected for use in this project. The selections (Table 6; Figure 7) provided a balance between taxonomic diversity and functional feeding strategies. Unfortunately, while the sub-surface deposit feeding clam *Y. limatula* was initially selected and kinetics information was obtained as part of Task 1c (Section 8), the supplier (Marine Biology Laboratory, Woods Hole, MA) informed us that adequate field numbers were no longer available for collection after Task 1c was complete, but before initiation of Task 2a. Consequently, the authors selected an alternative sub-surface deposit feeder, *E. estuarius*, based on information that this amphipod remains below the surface of the sediment more than the amphipod *L. plumulosus* (ASTM 2008). An effort was made to retroactively gain Task 1c kinetic bioaccumulation information for this organism (Section 8). A short description of each of the final four selected species follows (Table 6).

Table 6. Selected test organisms for Tasks 1c, 2, and 3.

Functional feeding group	Common name	Scientific name
Surface deposit feeder	Amphipod	<i>Leptocheirus plumulosus</i>
Suspension feeder	Clam	<i>Mercenaria mercenaria</i>
Infaunal / surface feeder	Polychaete	<i>Neanthes arenaceodentata</i>
Infaunal deposit feeder (original selection)	Clam	<i>Yoldia limatula</i> ²
Infaunal deposit feeder (alternative selection)	Amphipod	<i>Eohaustorius estuarius</i>

Figure 7. Selected test organisms.

Neanthes arenaceodentata (a), *Leptocheirus plumulosus* (b), *Mercenaria mercenaria* (c), *Yoldia limatula* (d) and *Eohaustorius estuarius* (e).



Leptocheirus plumulosus (Figure 7) is an amphipod in the phylum Arthropoda (Class Crustacea) that surface deposit feeds in estuarine/marine silty, fine-grained sediments predominately on the eastern coast of the United States. *Leptocheirus plumulosus* typically burrows from 0 – 3 cm, and its natural density range is 190 to 29,217 m² (Table S4). Mature individuals used in testing weigh approximately 2 mg (2% lipid content). Testing 35 individuals in the PICs (Section 10) would not exceed relevant density thresholds (Table S4).

Mercenaria mercenaria (Figure 7) is a clam in the phylum Mollusca (Class Bivalvia) that filter feeds and burrows in sandy marine sediments predominately on the eastern coast of the United States. Research observations showed that the *Mercenaria mercenaria* burrowed from 0 – 3 cm, and its natural density range is 100 to 1200 m² (Table S4). Mature individuals used in testing weigh approximately 396 mg (1.1% lipid content). Testing 3 to 5 individuals in the PICs (Section 10) would not exceed relevant density thresholds (Table S4).

Neanthes arenaceodentata (Figure 7) is a polychaete worm in the phylum Annelida (Class Polychaeta) that surface and sub-surface deposit feeds in marine sediments throughout the world. *Neanthes arenaceodentata*

² Not selected for Task 2 due to a decline in availability

typically burrows from 0 – >8 cm and its natural density range is 350 to 1059 m² (Table S4). Mature individuals used in testing weigh approximately 2 to 10 mg (2.6% lipid content). Testing five individuals in the PICs (Section 10) would not exceed relevant density thresholds (Table S4).

Eohaustorius estuarius (Figure 7) is an amphipod in the phylum Arthropoda (Class Crustacea) that sub-surface deposit feeds in marine silty-sandy grained sediments predominately on the west coast of the United States. *Eohaustorius estuarius* typically burrows from 0 – 3 cm and its natural density is reported to be 35,000 m² (Table S4). Mature individuals used in testing weigh approximately 3.6 mg (2.8% lipid content). Testing 35 individuals in the PICs (Section 10) would not exceed relevant density thresholds (Table S4).

For some of the organisms listed above (i.e., *L. plumulosus*, *E. estuarius*, *N. areanaceodentata*), standard EPA or American Society for Testing and Materials (ASTM) toxicity test protocols exist with ranges in temperature from 15 to 20 °C and 20 to 30 ‰ in salinity (Kennedy et al 2009). Since the temperature used during testing can influence uptake kinetics (Kennedy et al 2010), universal temperatures and salinities of 20 °C and 25 ‰ were selected for Tasks 1c, 2a and 3 after it was confirmed in the laboratory that all the above organisms could tolerate these conditions.

Since the authors observed that the suspension-feeding clam *M. mercenaria* did not actively siphon water in the exposure chambers in the absence of a food source in the overlying water, a series of experiments was conducted with two different algae (Phytoplex® and *Isochrysis*). It was determined that a modest concentration of Phytoplex® (8667 ± 2735 cells/ml), a commercially available product (Kent Marine, Franklin, WI), was suitable for stimulating active siphoning by *M. mercenaria* for 28 days while minimizing organic carbon input. This ration also succeeded in maintaining *E. estuarius* in sand (devoid of other nutrients) for 28 days. Thus, it was determined that a universal supplemental feeding ration of this food should be applied to all organism exposures to maintain consistent experimental conditions.

6 TASK 1B: Development of the flow through exposure system

6.1 Exposure and Recirculation System

A recirculating exposure system was designed and built for use in Tasks 2 and 3. A depiction of the system is presented in Figure 8. The prototype system (Figure 9 and Figure 10) was used for Task 2 and was modified for Task 3 experiments. The system consists of four, 5-gallon silanized glass aquaria each containing 12 PICs (described in detail in Section 10.2.3) housing the experimental organisms and a dual-chamber dosing and equilibration reactor. The PICs were surrounded by field-collected, contaminated sediment that was consolidated against the membrane by gentle agitation on a shaker table. Fine-grained sand was added to the overlying water and pore water pathway PICs to provide the experimental organisms a substrate that would provide minimal binding capacity for organic contaminants. Five to ten cm of overlying seawater (flow-through) was added on top of the sediment and partially buried PICs; the system was allowed to equilibrate for approximately three months, based upon preliminary experimentation (Section 7). The equilibration period was to allow diffusion of contaminants through the membrane into the chambers containing the fine-grained sand. Following the equilibration period, unique PCB congeners (PCB₂₄ and 104), not present in the sediment, were added to the overlying water of the flow-through system (Figure 9).

The flow-through system consisted of two, 19.7 L completely mixed reactors separated by a plug-flow baffle to ensure uniform distribution of the PCB congener in the water column (Figure 9). The first reactor of the flow system incorporated a serpentine-like passive dosing system, described below (Section 6.3), to achieve the desired water column PCB congener concentration. Total LDPE SPMD tubing length was a function of the desired water column residence time and the mass transfer rate of the SPMD for the selected PCB congener (see Section 10.3.4.2). One PCB congener was added to the overlying water (PCB₂₄); a second PCB congener (PCB₁₀₄) with significantly different hydrophobicity was also included to establish exposure rates as a function of contaminant K_{ow} . Flow rates (1–4 ml/min) resulted in water column residence time (RT) over the PICs of 1–4 days. Actual flow rates for the four aquaria ranged

from 2.93 – 3.13 ml/min resulting in an overall system (tanks and reactors) retention time of 4.6 – 5.8 days and an individual reactor detention time of 2.2 to 3.7 days.

Figure 8. Diagrammatic representation of the exposure system.

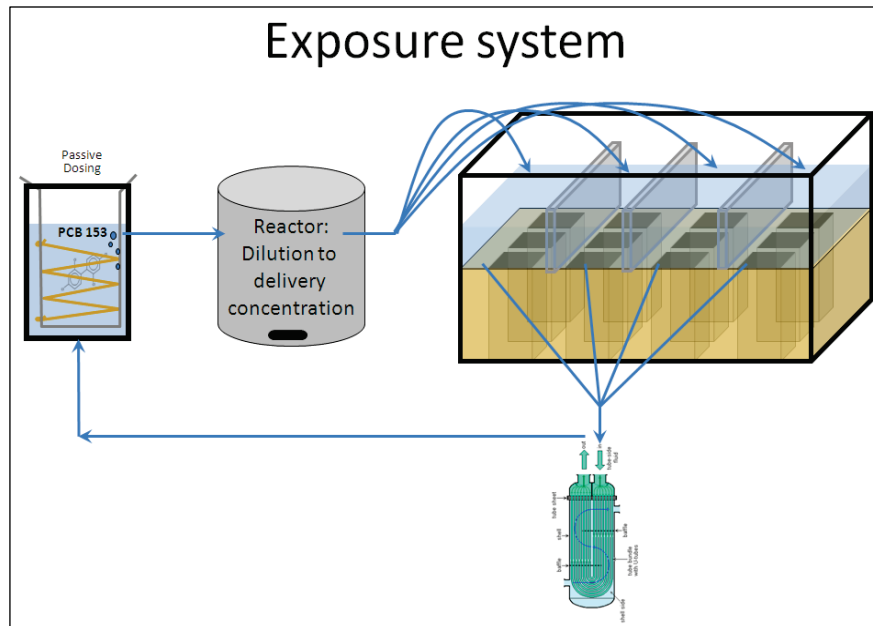


Figure 9. Prototype exposure system.

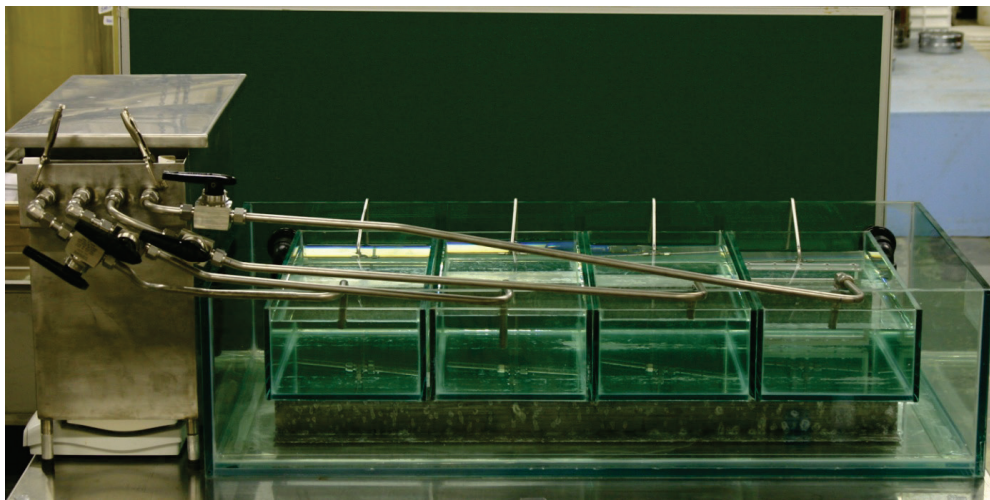
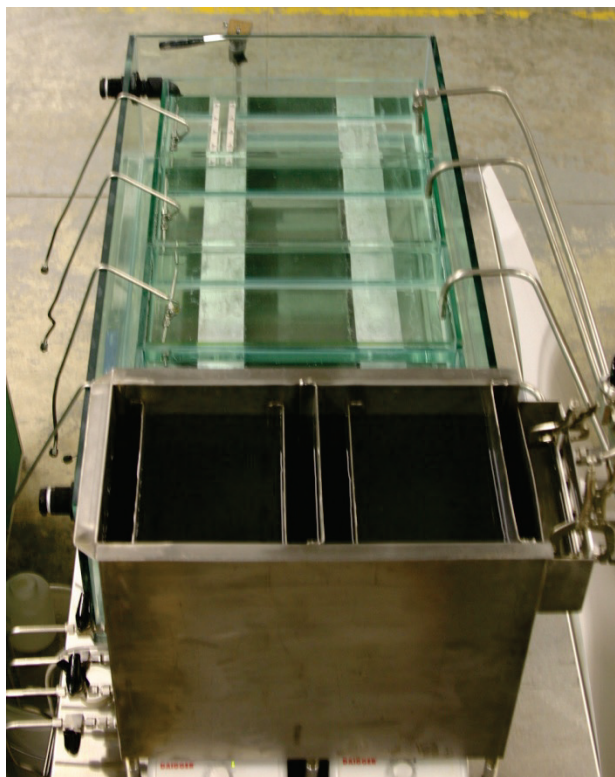


Figure 10. Top view of mixed reactors of the prototype exposure system.



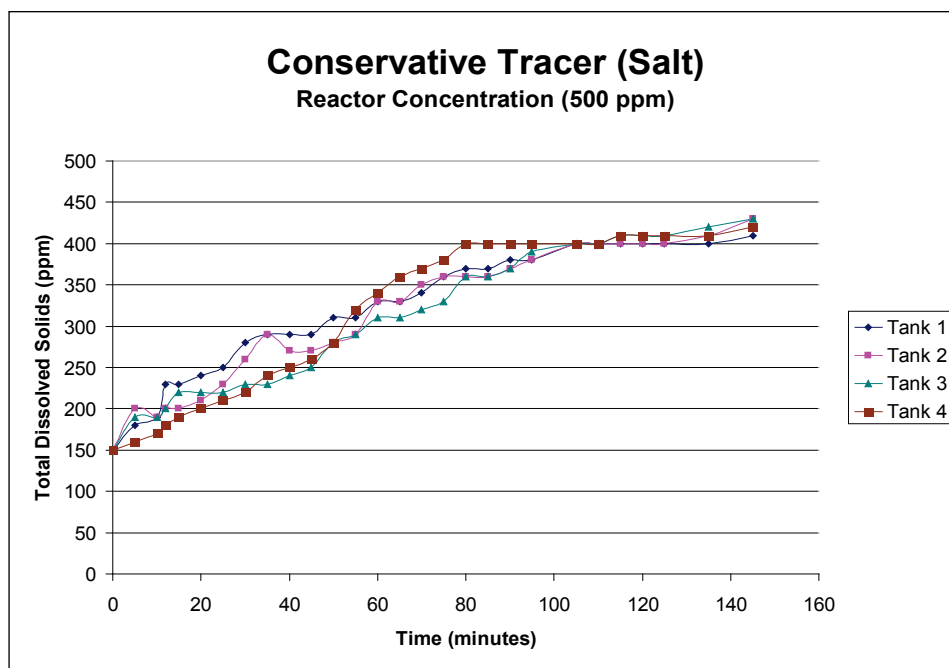
The system is easily modified to include a support system (see Figure 6-1, green biofilter) to assimilate organic matter generated within the system. The exposures were conducted for a duration determined by the results of the kinetics experiments conducted in Task 1c (Section 9). No significant accumulation of organic matter or decrease in dissolved oxygen was measured throughout the experiments, thus the support system was not needed. Decreases in dissolved oxygen were due to sediment oxygen demand and were corrected by aeration in the tanks and reactor. Temperature was maintained within the water bath using a recirculating REMCOR unit (REMCOR Products Company, Glendale Heights, IL).

6.2 Tracer study

A tracer study was performed on the beta prototype of the exposure system to test the system's ability to achieve a target water column concentration in a reasonable time (RT). The beta prototype reactor was loaded with a salt concentration of 500 mg/L and the initial concentration in each of the four exposure tanks was 150 mg/L. The exposure tanks were filled with sand to account for the typical volume of sediment that will be placed in the tanks. The salt concentration was measured over time and the results are shown

on Figure 11. All of the tanks approached the reactor concentration (500 mg/l) in less than three hours. The prototype in Figure 9 had better flow control, so that all four glass tanks showed a tighter response than that of Figure 11.

Figure 11. Salt tracer concentration in the beta prototype exposure system.



The next step in testing the prototype exposure system was to load the serpentine-like passive dosing system in the reactor with PCB congeners 24 and 104, as described in Section 10.4.1.2. The exposure system was loaded to estimate the time to achieve a uniform concentration in the reactors and the exposure tanks. This test was performed without sediment, but with the same total water column volume; thus there was no need to account for sorption losses to the sediment. This test verified tubing length required to achieve a desired congener concentration in the overall system and the system's response to changes in concentration. Potential changes in concentration that could affect the systems response are sediment sorption, losses due to optional treatment, and volatilization.

6.3 Passive dosing for the recirculation system

A solid phase membrane device (SPMD) was used to deliver PCB into the water in basic accordance with previous guidance (Smith et al 2007; USEPA 2007). A preliminary experimental set-up is illustrated in Figure 12. Briefly, 10 mg of PCB 153 was dissolved in hexane, reduced to around 100 μ l total

volume and added to 0.5 g of glyceryl trioleate (triolein) for each SPMD. The PCB and triolein were vortexed to ensure a homogenous mixture and then added to 10 cm sections of LDPE SPMD tubing. The SPMD sections were heat sealed and placed in a silanized 1 L glass beaker containing dechlorinated tap water. The water was continuously mixed through light aeration. After 7 days, PCB 153 levels in the water reached 0.058 ± 0.039 $\mu\text{g/L}$ ($n=7$). This system was then placed with the proper PCBs congeners into the first reactor where the water was continuously mixed with a magnetic stirrer. Experimentation and results are described more specifically in Sections 10.3 and 10.4.

Figure 12. Experimental setup for SPMD-based passive dosing system.



7 TASK 1B: Development of membrane equipped isolation chambers for characterization of infaunal invertebrate exposure to PCBs via sediment pore water

7.1 Introduction

The PICs used in Task 2 called for allowing the movement of pore water, containing dissolved contaminants, while holding back particulate-associated contaminant. The present study assessed the efficacy of various membranes to allow diffusion of dissolved chlorinated hydrocarbons (e.g., chlorinated pesticides, *polychlorinated biphenyls*) through a membrane while excluding fine sediment particles and dissolved organic carbon (DOC). Commercially available membranes were purchased and initially tested utilizing a glass diffusion test vial, followed by a membrane equipped prototype PIC. The membranes were tested in a variety of exposure designs ranging in complexity. Exposures included both diffusion of radio-labeled and non-labeled contaminants across membranes from an aqueous, sediment slurry, and whole sediment source. Data generated from the exposures was ultimately utilized to select the best candidate membrane for use in the large-scale exposures.

Traditional methods for measuring dissolved chlorinated hydrocarbons in sediment pore water are not always effective or efficient, and often involve sediment manipulation through centrifugation prior to chemical analysis. While passive sampling devices such as solid-phase micro extraction (SPME) and semi-permeable membrane devices (SPMDs) can provide more accurate measurements and uptake predictions of dissolved contaminants in aquatic organisms (Bao et al 2011), they are most effective when used in conjunction with whole organism exposures to generate adequate information to predict risk. Currently, there are no published methods for conducting real-time organism exposure to dissolved contaminants available in pore water alone. The present set of exposures sought to incorporate passive sampler technology with membrane diffusion potentials to create a PIC for dissolved chlorinated hydrocarbons exposures.

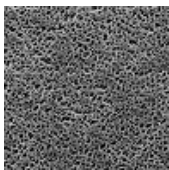
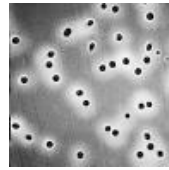
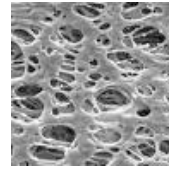
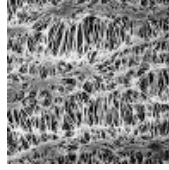
Membranes can significantly differ in their interaction with contaminants based on their structural properties, pore size, material composition, and coatings. For example, the hydrophobic properties of some polyethylene material makes it useful in SPMDs as passive samplers to sorb PCBs (Alvarez et al 2010). Alternatively, porous Teflon membranes have been utilized *in situ* peepers to assess dissolved solutes in the surrounding water (Murdoch and MacKnight, 1991). The authors compared hydrophilic membranes made of nylon, polycarbonate, and polyethylsulfone with a polytetrafluoroethylene hydrophobic membrane covered with a hydrophilic coating in aquatic assays utilizing both radio-labeled and non-labeled chlorinated hydrocarbons for their ability to allow the passage of dissolved chlorinated hydrocarbons while excluding dissolved organic carbons and sediment. Ultimately, extensive testing resulted in the selection of the Teflon membrane for use in the final system, although exclusion of dissolved organic carbon was not possible.

7.2 Materials and methods

7.2.1 Membranes

Various commercially available membranes for the hydrophobic contaminant studies were selected and purchased for testing. The membranes selected were 0.1 and 1.2 μm nylon, 0.01 and 1.0 μm polycarbonate (PC), 0.1 and 1.2 μm polyethylsulfone (PE) (Sterlitech Corp., Kent, WA, USA), and 0.1 and 1.0 μm polytetrafluoroethylene (Teflon) (Millipore, Billerica, MA, USA) with a hydrophilic coating (Table 7). Additionally, a stainless steel screen (1.0 μm) was also tested as a positive control for comparative diffusion potential. Forty mL vials (27.5 x 95 mm) were utilized to test the membranes and screens in exposures. The vials were cut with two, 3 inch x 1 inch holes; both holes were fitted with either a membrane or screen mesh utilizing silicone caulk and filled with clean seawater. All glassware was silanized using dimethyldichlorosilane in toluene (5% DMDCS, Cat. No. 33065-U, Supelco, Sylon, CT, USA) and allowed to dry overnight to reduce the affinity of hydrophobic compounds to sorb to the glass surfaces prior to testing.

Table 7. Summary of membranes tested in an effort to be used in prototype pathway isolation chambers (PICs).

Membrane	Size	Supplier	Image
Nylon	1.2	Sterlitech	
	0.1	Sterlitech	
Polycarbonate (PC)	1.0	Sterlitech	
	0.01	Sterlitech	
Polyethylsulfone (PE)	0.1	Sterlitech	
	1.2	Sterlitech	
Hydrophilic Polytetrafluoroethylene (Teflon)	0.1	Millipore	
	1.0	Millipore	

7.2.2 Porewater analysis

Solid phase micro-extraction fibers (SPME) 210/230 (Fiberguide, Caldwell, ID, USA) were also utilized to assess PCB contaminant availability in pore water. Two, 2.5 centimeter SPME fibers were placed in stainless steel mesh envelopes to create the sample devices. The SPMEs utilized in radio-label exposures were analyzed using a Perkin Elmer Liquid Scintillation Counter (LSC) 3110 (Waltham, MA, USA) and reported as disintegrations per minute (DPM). The SPMEs in cold contaminant exposures were analyzed at the ERDC Environmental Chemistry Branch (Vicksburg, MS) following the USEPA 846 methodology. Specific methods include a modification of 3630 for pesticides and 3665 for PCBs. All samples were reported as total congeners.

7.2.3 Passive diffusion of radio-labeled contaminant in water

A passive diffusion system was designed to compare ^{14}C dichlorodiphenyltrichloroethane (C-DDT) diffusion potential across the

different membranes. A 40 mL glass test vial was equipped with either a Teflon (1.0 μm), Nylon (1.2 μm), PE (1.0 μm), or PC (0.1 μm) membrane, filled with clean seawater, and placed in the center of a 1L beaker (n=1 per membrane). The beaker was then filled with seawater to surround the vial, spiked with ^{14}C -DDT (DDT, Perkin Elmer), and mixed briefly. A vial with a stainless steel screen covering was tested as a positive control. Samples were taken from the spiked water surrounding the vial and inside the vial (0.5 mL, n=1) after 2, 24, 48, 72, and 96 hours. Samples were reported as DPMs.

7.2.4 Diffusion of radio-labeled contaminants from a continuous source

In an effort to test an exposure system with a continuous PCB supply, a sediment slurry exposure was conducted. The slurry included 100 grams of clean sediment (Sequim Bay, WA, USA) in 1.5 L of seawater that was spiked with ^{14}C -DDT and ^3H Fluoranthene (FLA, Perkin Elmer) within a 2 L beaker on a magnetic stir plate overnight. The next day, the slurry mixture was separated into two, 1L beakers and placed on a rotating shaker table (Bench-top Open Platform Shaker table, VWR, Radnor, PA, USA) set to 60 rpms. A diffusion test vial was fitted with the Teflon 1.0 μm membrane, filled with seawater and placed into the beaker. The test chamber contained four SPME envelopes inside and outside of the diffusion vial. An SPME envelope and a 0.5 mL aqueous sample were taken from inside and outside of the vial at day 2, 7, 14, and 35.

7.2.5 Passive diffusion of humic acids through membranes

A diffusion study was conducted to determine if a membrane that allowed chlorinated hydrocarbons to pass through could exclude dissolved organic carbon (DOC). Seawater was spiked with 50 mg/L humic acid (International Humic Substance Society, Atlanta, GA, USA), magnetically stirred overnight, and distributed in two, 1 L glass beakers. A diffusion test vial was fitted with the smaller Teflon 0.1 μm membrane and compared with a control (no membrane) vial and placed in the center of each beaker. Samples were taken from the outer spiked water and inside the vial (0.5 mL) at 0, 2, 8, and 24 hours for chemical analysis.

7.2.6 Passive diffusion of cold contaminant from sediment to Prototype PICs

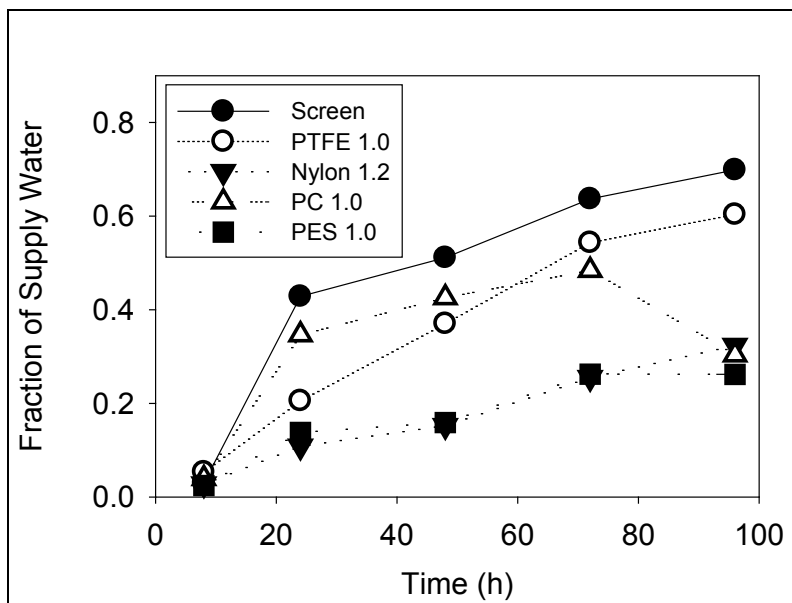
All glass, silanized prototype PICs were constructed with the dimensions of 9 x 9 x 2 cm, with one side of the chamber remaining open and covered with a membrane and a 2 cm glass strip at the top to support the membrane. The prototype PICs (n=4) were fitted with Teflon 1.0 μm membranes and filled with clean seawater. The experimental system utilized 2 L beakers filled with PCB contaminated New Bedford sediment. The prototype PICs containing clean seawater were placed within the New Bedford sediment. Multiple SPMEs were placed directly into the sediment and within the prototype PIC. The SPME collection time points were 28, 42, 56, and 70 days within the prototype PICs and 7, 21, 28, and 56 days in the surrounding sediment. SPME collection time-points varied due to previous determinations that the fibers in the sediment would come to steady state more rapidly than fibers in the prototype PIC. The day 70 collection time-point within the prototype PIC and day 28 collection time-point from the surrounding sediment were both n=3, all other SPME time-points were n=1 to reduce costs of chemical analysis. The internal water within the prototype PIC was observed daily for any intrusion of the sediment.

7.3 Results and discussion

7.3.1 Passive diffusion of radio-labeled contaminant

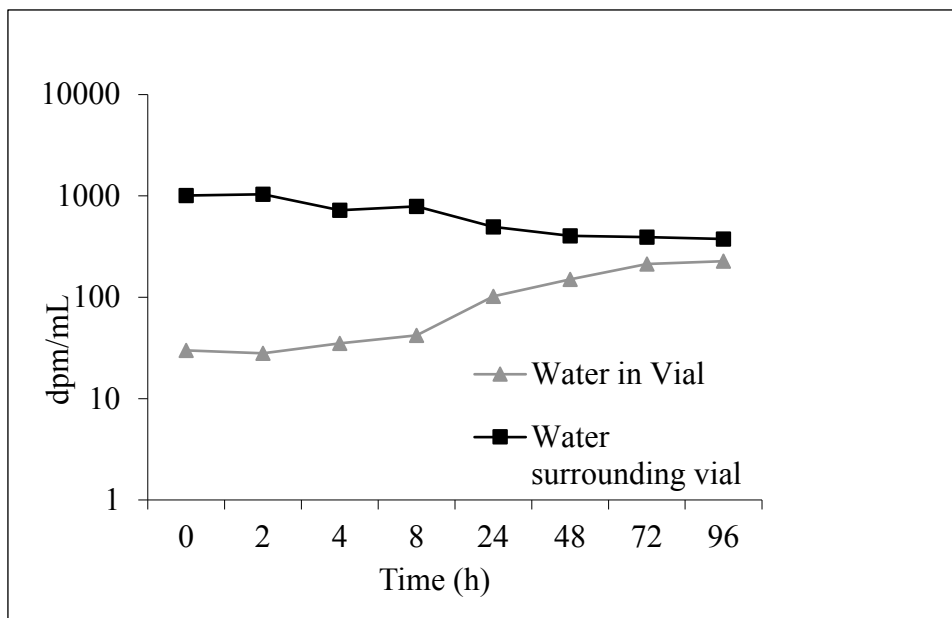
The comparative DPM counts inside and outside of the diffusion test vial were reported as a fraction of supply water in (Figure 13), which divided the total number of DPMs inside the vial at each time-point by the DPMs of the supply water outside of the vial after the initial spiking. The LSC analysis of water within the vials resulted in the stainless steel mesh having the highest DPM counts, followed by the Teflon 1.0 μm membrane. Further analysis of the same 1.0 μm Teflon membrane resulted in DPM counts inside the test vial reaching near that of the supply water outside of the vial (Figure 14). Overall, it was determined that the Teflon Millipore membrane performed best, based upon highest diffusion of DDT.

Figure 13. Diffusion of ^{14}C radio-labeled DDT across various membrane materials into test vials.



The stainless steel screen was employed as a positive control to demonstrate uninhibited passive transport of DDT.

Figure 14. Comparative equilibrium of ^{14}C radio-labeled DDT in Teflon 1.0 μm membrane vial relative to surrounding supply water.

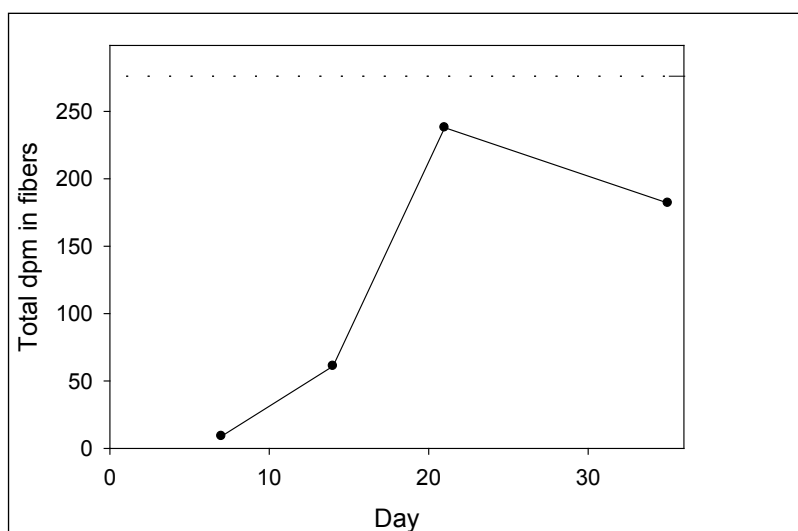


7.3.2 Diffusion of radio-labeled contaminants from a continuous source

Since experiments involving spiking of ^{14}C -DDT directly into water resulted in gradual reduction in concentration over time, an experiment was

conducted utilizing a continuous source of radio-labeled hydrocarbons (^3H -FLA and ^{14}C -DDT) from a sediment slurry. The LSC SPME measurements from within and outside of the Teflon 1.0 μm vial showed a steady increase of ^3H -FLA over the course of 35 days in samples (Figure 15). In addition to an increase, the SPME concentration within the vial was near the SPME concentration in the sediment slurry at day 35 (Figure 15). Water within the vial remained visibly clear over the course of the exposure, indicating the ability of the Teflon membrane to exclude sediment particles from a system while allowing passage of the contaminants. From the data generated, it was determined that the Teflon membrane allowed contaminant passage while proving to be very durable for testing.

Figure 15. Comparison of [^{14}C] DDT DPMs in SPME within Teflon/ Polytetrafluoroethylene (PTFE) 1.0 μm vial relative to DPMs of 0.5mL water samples taken from within vial.

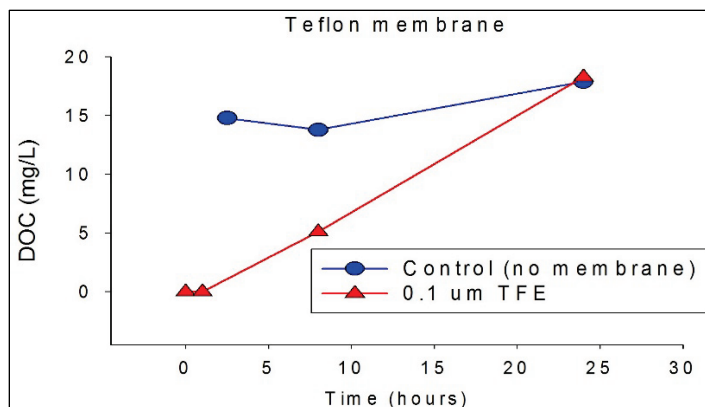


Upper horizontal line represents DPMS in SPME within surrounding slurry at day 35.

7.3.3 Passive diffusion of humic acids through membranes

One experimental component of the project was to determine if a membrane could exclude DOC while allowing the passage of PCBs. The smaller pore-size, 0.1 μm membrane did not effectively exclude the diffusion of suspended/dissolved humic matter (Figure 16). The Teflon 0.1 μm allowed a gradual increase in DOC concentration, but was near equilibrium at 24 hours compared to the control DOC. Results indicate that while the Teflon membrane was effective at allowing PCB diffusion, it was not able to exclude DOC in the present test system.

Figure 16. Diffusion of humic acid across the 0.1 μm Teflon (TFE) membranes vs. a control vial with no membrane.



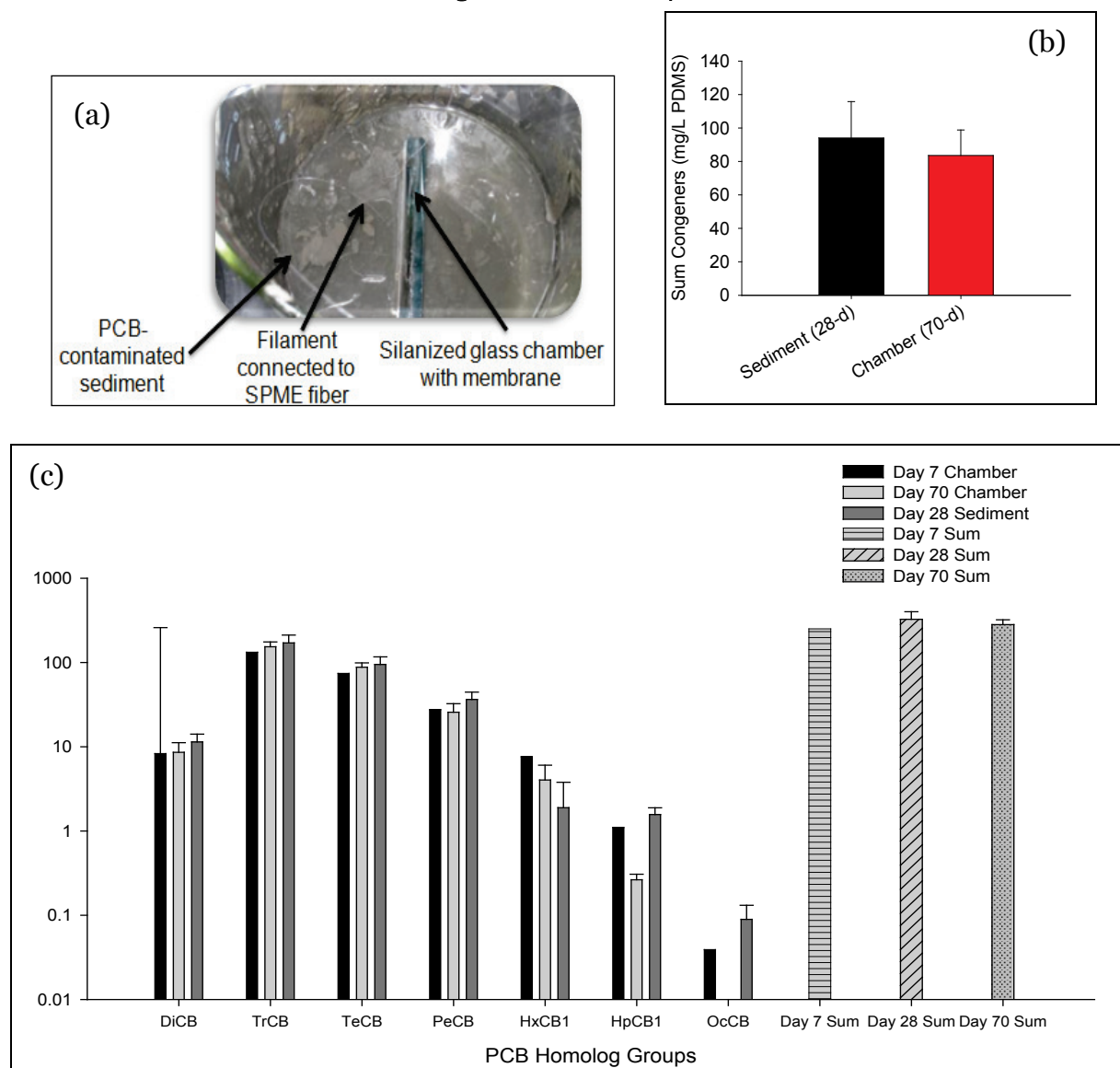
7.3.4 Passive diffusion of cold contaminant from sediment to prototype PICs

Following tests in the slurry experiment, prototype PICs ($n=4$) were constructed with the Teflon 1.0 μm membrane and tested in PCB contaminated whole sediment to study the membrane effectiveness in a system similar to the larger exposure (Section 10). Chemical analysis of the SPMEs showed the Teflon membrane to be effective in allowing passage of PCBs into the prototype PICs while minimally sorbing the chlorinated hydrocarbons. SPMEs within the prototype PIC took much longer to reach steady state than SPMEs in the surrounding sediment due to the increased amount of time it took for PCBs to cross the membrane. Therefore, SPMEs in the sediment at day 28 were comparatively assessed to SPMEs in the prototype PICs at day 70. When compared with the 28 day SPME PCB sediment samples, the SPMEs inside the prototype PIC (Figure 17a) were at 89% of the total PCB concentration of the sediment at day 70 (Figure 17b). Water within the prototype PIC remained visibly clear over the course of the exposure, indicating the ability of the Teflon membrane to exclude sediment particles from a system while allowing passage of PCBs.

7.4 Discussion

The Teflon 1.0 μm membrane was selected for the larger test system due to its durability and highest allowance of hydrocarbon passive diffusion (Section 10). The early observations of these characteristics were quantified in the passive diffusion exposures with ^{14}C -DDT; therefore, additional experiments were focused on the Teflon (TFE) membrane. The membrane's construction of a hydrophobic base with a hydrophilic coating is thought to be the main property that allowed movement of PCBs across the membrane while excluding sediment particles.

Figure 17. Prototype Pathway Isolation Chamber (PIC) performance. (a) Photograph of a prototype PIC equipped with a membrane in sediment (b) and comparison of total PCB congeners inside and outside of the chamber (c) Chemical analysis of the PCB congeners in the SPME fibers within the PIC (Day 7 and Day 70) relative to the SPME in the surrounding sediment (Day 28). Data represents homolog groups and sum congeners at each time point.



Sediment slurry exposures provided a continuous PCB source and resulted in a near steady state equilibrium between the diffusion test vial and outer slurry concentrations in analysis with the LSC. These exposures provided a logical foundation for the testing of the final passive diffusion of cold contaminant from sediment in PICs to mimic the larger exposure system design (Section 10). The SPME analysis of samples collected from inside and outside of the PICs resulted in a steady trend of PCB uptake in both sets of fibers. At exposure termination, the near equilibrium concentration

of PCBs within the PIC indicated the membrane's ability to allow contaminants through while excluding sediment particles. These results were a key factor in the final Teflon membrane selection.

The effects of pH, calcium, and ionic strength are known to play a role in the interaction of humic matter in aqueous solutions. Changes in these variables can increase or decrease the hydrophobicity of the humics and alter their affinity for chlorinated hydrocarbons (Carter and Suffet 1982). Although sediment particles were excluded, it was determined that the Teflon membrane selected for the exposures was unable to exclude dissolved organic matter while allowing passage of chlorinated hydrocarbons regardless of pore size.

8 TASK 1C: Passive sampler evaluation and selection

8.1 Introduction

Freely dissolved pore water concentrations of hydrophobic, organic contaminants like PCBs have been determined to be useful indicators of bioavailability (e.g., You et al 2006; Lu et al 2011). Several techniques have been developed to facilitate and improve the quantification of the freely dissolved pore water concentrations of hydrophobic contaminants in sediment pore water, including the use of passive samplers (Gschwend et al 2011; Gschwend et al 2012a,b). Among the available passive samplers, two were selected for evaluation for use in Task 2 of this study.

Polydimethylsiloxane (PDMS) coated solid-phase microextraction (SPME) fibers were selected because their configuration, consisting of a thin annular layer of sorbent coating on a small-diameter silica core, provides a high surface area to volume ratio in a format that can be inserted easily into sediments during bioaccumulation and toxicity studies. Solid-phase microextraction is a partition-based, solvent-free, negligible-depletion extraction technique used to measure freely dissolved organic chemicals (Mayer et al 2000). Application of the SPME technique included direct insertion into the sediment to allow equilibration with the sediment–pore water system (e.g., Mayer et al 2000; Conder et al 2003; You et al 2007; Lu et al 2011). In this application, SPMEs are used to estimate freely-dissolved contaminant concentrations in pore water and provide a measure of chemical activity in the whole-sediment phase as altered by the various modifying factors affecting bioavailability, and hence, bioaccumulation and toxicity, in exposures to whole sediments from the NBH Superfund site.

Polyethylene is a sorbent that has been used widely to measure dissolved PAHs, PCBs, and a variety of other organic contaminants in aquatic environments (Adams et al 2007; Bao et al 2012). Sampling devices using polyethylene have been selected over others because they are biomimetic, inexpensive, and convenient for field deployment (Lohmann et al 2010). Like SPME, polyethylene devices (PEDs) have been used as passive samplers in a wide range of matrices, such as in sediment pore water, the

water column, and atmosphere, as well as to assess the activity gradients across sediment-water and water-air interfaces (Fernandez et al 2012, Lohmann 2012). Polyethylene devices have most often been used in the field (Adams et al 2007; Anderson et al 2008; Allan et al 2009), but have been shown to be suitable for laboratory applications as well (Pablo and Hyne 2009; Vinturella et al 2004, Friedman et al 2009; Gschwend et al 2011). Polyethylene devices can be deployed for times that are too short to attain environment-sampler equilibrium by impregnating performance reference compounds (PRCs) into the sampler before deployment. The concentration of the reference compound in the sampler after it is retrieved can then be used to extrapolate the measured contaminant concentrations to their equilibrium values.

Solid-phase micro-extraction fibers and PEDs were placed within each exposure chamber to measure dissolved contaminant concentrations in relation to specific media (e.g., overlying water and sediment pore water) and sampled at the four time points described above in tandem with tissues. These findings are important for determining the best exposure conditions for experiments in Task 2. This experiment was used to compare SPME and PEDs and to select the passive sampling device to be used in Tasks 2 and 3.

8.2 Methods

The SPME fibers consisting of a glass core (230 μm diameter) with a 10 μm thick PDMS coating (Model SPC210/230R) were purchased from Fiberguide Industries (www.fiberguide.com). Fibers were cut into 2.5 cm pieces using a double-bladed, stainless steel razor blade apparatus. Two pieces (5 cm total length) of SPME fiber were placed in a protective, 5 cm x 4 cm, 100 μm , stainless steel mesh envelope (Model 165 Mesh T316 Stainless from TWP Inc., www.twpinc.com) and inserted into the sediment using mesh envelopes containing SPMEs according to Conder et al 2003. The use of a mesh envelope provided a means to safely handle the fragile fibers when deploying into and retrieving from sediment.

Preparation of the PEDs was performed at the Parsons Laboratory (Massachusetts Institute of Technology, Cambridge, MA). Polyethylene devices were 1 cm x 1 cm and 25 μm thick plastic squares that were pre-loaded with performance reference compounds. The PE (ACE Hardware Corp., Oak Brook, Illinois) was cleaned by soaking twice, for 24 hours, in dichloromethane, followed by soaking twice, for 24 hours, in methanol,

and finally, rinsing and soaking in ultrapure water. After cutting to 1 cm², each square was placed in an 125 mL amber bottle containing an aqueous solution of PRCs (4-chlorobiphenyl (PCB₃), 3,5-dichlorobiphenyl (PCB₁₄), 3,3',4-trichlorobiphenyl (PCB₃₅), and 2,3',4,5-tetrachlorobiphenyl (PCB₆₇) at 0.24 to 0.48 µg/L each) and allowed to equilibrate with PRC solution, agitating occasionally, for 30 days. Once prepared and equilibrated, PE squares were shipped to ERDC on ice and stored in the freezer until use.

To assess the uptake of PCBs in the passive samplers, 180 mL of New Bedford sediment was added to 1 L glass test chambers. Artificial seawater (25‰ Instant Ocean seawater, Mentor, OH, USA) was gently added over the sediment using a turbulence reducer, and the system was allowed to equilibrate overnight. After 24 hours, samplers were added to separate exposure beakers, midway into the sediment column, one per replicate. Two beakers were sampled following 3, 7, 14, 21 and 28 days of exposure.

At the termination of each exposure, mesh envelopes containing the SPME fibers were removed from the sediment, rinsed with distilled or ultrapure water, and opened for the removal of fibers. Fibers were carefully removed from the envelope using plastic forceps, rinsed with ultrapure water, and placed on lint-free paper for blotting. The dry fibers were transferred to a 0.1 ml conical glass insert placed inside an HPLC auto-sampling vial and capped tightly with a Teflon-lined screw cap. PE samplers were rinsed with ultrapure water, placed on lint-free paper for blotting, and stored in a 20 ml vial with a foil-lined cap.

The SPME were analyzed by adding 100 µL of ultrapure hexane to 0.1 ml conical glass insert placed inside a HPLC auto-sampling vial. PE squares were extracted three times by soaking in 15 mL of dichloromethane overnight. The combined extracts were concentrated to approximately 0.5 mL under a gentle stream of ultrapure grade nitrogen. SPME fiber and PE extracts were analyzed for PCBs by a gas chromatograph equipped with an electron capture detector (GC-ECD) following EPA method 8082. Analyses of PCBs were performed with an Agilent 6890 series GCECD and HP-5-type 30 m capillary column (internal diameter 0.32 mm and film thickness 0.25 µm). Polychlorinated biphenyl congeners were identified based on the retention times of the corresponding peaks in the standard. A second column was used to confirm individual congeners. Analytical

determinations were as described in Appendix A: Supporting Data (Supporting Data).

8.3 Results and discussion

While SPME were assumed to equilibrate with sediment pore water quickly (less than one week), PRCs were used to determine the fractional equilibration of PE samplers at each sampling time. The PCB congeners used as PRCs were selected based on non-detects in extracts of the test sediment. A range of degree of chlorination was also desired. The lightest PRC, PCB₃, was not detected in samplers at any time step, indicating that PE and sediment pore water were equilibrated for the smallest PCBs in all exposures. As expected, the concentrations of larger PRCs (PCBs 14 and 35) decreased with exposure time. The largest PRC, PCB₆₇, could not be used because it co-eluted with another compound present in the test sediment.

Freely dissolved pore water concentrations, C_w , were calculated from the mass of target compound in the equilibrated sampler (N),

$$C_w = N / (K_{pw} V_p) \quad (2)$$

where K_{pw} is the polymer water partition coefficient (Appendix 19.1.1), and V_p is the polymer volume. The fractional loss of PRCs in PE (f_{eq}) were used to calculate what the mass of target compound in PE would be if allowed to fully equilibrate with the sediments and pore water,

$$N = N_{(t)} / f_{eq} \quad (3)$$

where $N_{(t)}$ is the mass of target chemical in the PE after a given exposure time.

In general, SPME and PE generated similar freely dissolved pore water concentrations at each sampling point for all detected PCBs congeners. Pore water concentrations, calculated using the two methods after the 28 day deployment, matched within a factor of five for all congeners with detectable masses in the sampler extracts (except for CB₆₀) (Figure 18). Although PE squares required additional preparation steps in order to add PRCs, the ease with which they can be deployed in the test-sediment beds (i.e., no mesh envelopes were needed) make them more applicable to the current work. A one-dimensional, Fickian diffusion model was used to

estimate the fractional equilibration of larger PCB congeners (Fernandez et al 2009), and pore water concentrations for PCB with up to seven chlorines were estimated from the mass of compound taken up by PE samplers after 28 days (Table 8).

Figure 18. SPME and PE generated pore water concentrations (ng/L) for all detected PCB congeners following the 28-day exposure to New Bedford Harbor sediment. PE generated Cw (ng/L) = $0.64 * \text{SPME generated Cw (ng/L)} + 6.2$ ($r^2 = 0.88$). Note that concentrations are expressed on a log-scale.

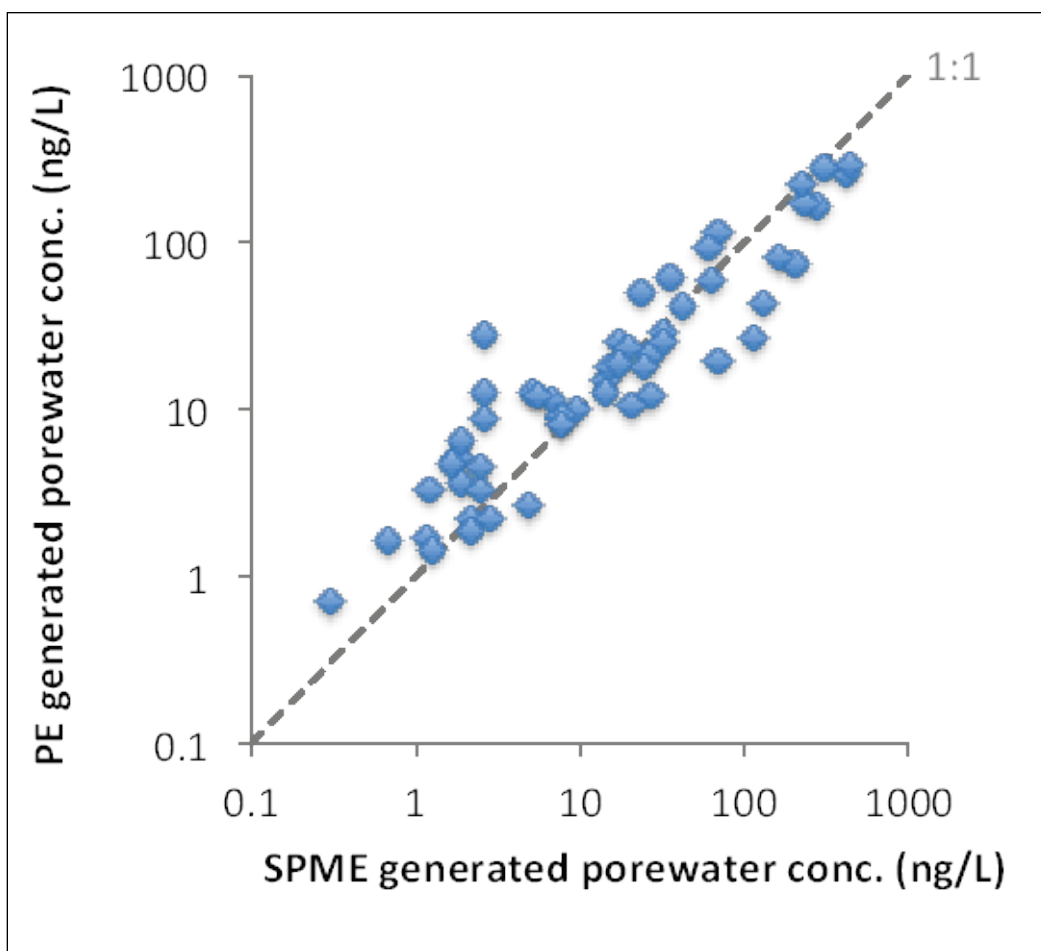


Table 8. Freely dissolved pore water concentrations (C_w , ng/L) of PCBs in test sediment that were generated using the PE sampling method.

PCB congener	C_w	PCB congener	C_w	PCB congener	C_w
PCB6	71	PCB63	2.2	PCB132	1.6
PCB8	26	PCB66	25	PCB134	2.4
PCB12/13	29	PCB70	18	PCB135	4.7
PCB15	42	PCB74	12	PCB136	3.3
PCB17	78	PCB77	2.2	PCB137	0.45
PCB18	160	PCB82	1.1	PCB138/163	8.7
PCB22	59	PCB83	5.0	PCB141	0.68
PCB25	170	PCB84	25	PCB144	0.57
PCB26	250	PCB85	1.8	PCB146	4.2
PCB27	12	PCB87	3.5	PCB147	2.4
PCB28/31	280	PCB90/101	49	PCB149	21
PCB32	19	PCB91	18	PCB151	6.2
PCB33	10	PCB92	7.9	PCB153	12
PCB34	2.7	PCB95	41	PCB154	1.8
PCB35	30	PCB97	11	PCB156	0.48
PCB40/71	13	PCB99	23	PCB157	0.14
PCB42	59	PCB100	12	PCB158	0.72
PCB44	110	PCB103	3.3	PCB164	1.0
PCB45	15	PCB107	1.7	PCB167	0.43
PCB46	8.7	PCB117	1.8	PCB170	0.40
PCB47	88	PCB118	18	PCB171	0.14
PCB48	8.8	PCB119	4.4	PCB174	0.23
PCB49	220	PCB122	0.38	PCB178	0.11
PCB51	10	PCB123/131	0.92	PCB179	0.61
PCB52	270	PCB124	1.4	PCB180	0.48
PCB53	21	PCB128	1.0	PCB183	0.25
PCB56	9.1	PCB130	0.43	PCB190	0.06
PCB60	28	PCB131	0.50		

9 TASK 1C: Bioaccumulation kinetics of PCBs to four marine benthic invertebrates

9.1 Background

The processes of uptake, biotransformation, and elimination, also called toxicokinetics, modify the concentration of organic chemicals in organisms. Kinetic rate constant models of these processes are used to quantify the temporal pattern of the internal concentrations of a chemical (Landrum et al 1992). Contaminant uptake, biotransformation and elimination are key factors modifying net bioaccumulation and consequently toxicity (Mackay et al. 2000).

Contaminant bioaccumulation into sediment-dwelling organisms is the first step in the most significant exposure pathway producing risks at upper trophic levels. Benthic species vary in terms of their position within the sediment column, their relation to sediment particles and pore water (e.g., tube building vs. free burrowing), and feeding behavior (e.g., filter feeding vs. deposit feeding), all of which contribute to differences in contaminant exposure and the notion of contaminant bioavailability.

9.2 Objectives

The first objective of the sediment toxicokinetics experiments was to estimate the time required to achieve steady state concentrations in tissues and to establish the exposure duration used in Tasks 2 and 3. Steady state is achieved when the flux of contaminant into the organism comes into equilibrium with the flux of contaminant out of the organism (Landrum et al. 1992).

The second objective of this experiment was to derive and BSAFs among four benthic species with differing traits that were expected to produce differences in exposure and therefore bioaccumulation of sediment-associated PCBs. The EqP model assumes that BSAFs should be constant and independent of chemical, sediment, and organism properties (U.S.EPA 2000). The BSAFs outside of the theoretical range of 1 to 4

(U.S.EPA 2000) may result from chemical disequilibrium, or processes related to organism-specific factors, such as biotransformation or differential uptake and elimination rates. Those same factors are expected to, at least partly, explain differences in BSAFs observed among infaunal invertebrates exposed to the same sediment, under identical conditions.

9.3 Material and Methods

9.3.1 Field-collected PCB-contaminated sediments

Sediment exposures were conducted using sediments selected for Task 2a (see Section 8). NBH sediment had total organic carbon content of 6.4% and a total concentration of PCB (sum of detected congeners) of 33.7 mg/kg dry wt. or 527 mg/kg-organic carbon. The BNC sediment had total organic carbon content of 1% and total concentration of PCB (sum of detected congeners) of 16.6 mg/kg dry wt. or 1,660 mg/kg-organic carbon.

9.3.2 Experimental species

Invertebrates selected for the toxicokinetics evaluation were the polychaete *Neanthes arenaceodentata* (21day old males), the amphipods *Leptocheirus plumulosus* (mature amphipods) and *Eohaustorius estuarius* (mature amphipods), and the clams *Mercenaria mercenaria* (juveniles with shell length between 15–20 cm) and *Yoldia limatula* (shell length between 8 – 15 cm).

9.3.3 Uptake and elimination kinetics exposures

To determine uptake and elimination kinetics of PCBs in invertebrate tissue, NBH or BNC sediment (3 cm layer) was added to 1 L glass test chambers. Artificial seawater (25‰ Instant Ocean seawater, from Mentor, OH, USA) was gently added over the sediment using a turbulence reducer, and the system was allowed to equilibrate overnight. After 24 hours, each test species was added to separate chambers.

The organisms were exposed to the test sediment and sampled after increasing exposure durations in triplicate chambers. Each test beaker contained at least 100 mg wet mass to allow the use of the micro analytical method (Jones et al. 2006). The time series sampling regimes and organism loading per replicate are presented in Table 9. All four experimental species were exposed to NBH sediment. Only *L. plumulosus* was exposed to the BNC sediment.

Table 9. Sampling time for the uptake, the elimination exposures, and organisms loading per replicate.

Species	Uptake Sampling times	Elimination Sampling times	Organisms per replicate
<i>L. plumulosus</i>	2, 5, 9, 14 days	2, 7, and 21 days	35
<i>E. estuarius</i>	4, 7, 9, 11, and 14 days	2, 7, and 14 days	35
<i>N. arenaceodentata</i>	3, 7, 14, 21 and 28 days	3, 7, and 21 days	3
<i>Y. limatula</i>	3, 7, 14 and 21 days	3, 14 and 21 days	3‡
<i>M. mercenaria</i>	2, 7, 14, 21 and 28 days	3, 7, and 21 days	3
<i>L. plumulosus</i> (BNC sediment)	0.5, 1, 2, 3, 8 days	1, 4, and 10 days	35

‡ While all *Y. limatula* exposure replicates contained three clams, due to poor survival (and resulting low tissue recovery) for the 21 day time-point, three additional clams from three extra replicates that were exposed for the same time duration were pooled to obtain sufficient tissue mass to meet the analytical requirement.

A second group of organisms were also exposed to the NBH sediment (for 28 days for *N. arenaceodentata* and *M. mercenaria*, and *Y. limatula*, but only 14 days for *L. plumulosus*, and 9 days for *E. estuarius*) and then transferred to 1 L chambers containing 200 mL of clean sediment from Sequin Bay (WA) for direct determination of elimination rates.

Leptocheirus plumulosus was also exposed to BNC sediment for 8 days. The organisms transferred to clean sediment were sampled after increasing exposure durations in triplicate chambers (Table 9). Organism loading per replicate was the same as that used in the uptake kinetics exposure.

For both, the uptake and the elimination kinetics experiments, 70% overlying water exchanges were performed three times per week. Supplemental feeding was provided to *L. plumulosus* (14mg of Tetramin beaker twice weekly), *N. arenaceodentata* (20 mg of Tetramin twice weekly), and to *M. mercenaria* (Phytoplex, Kent Marine, Franklin, WI).

At each exposure time-point sampling, sediments were gently sieved at 500 µm, organisms were collected and placed in clean water for purging of gut content. To minimize excessive depuration of chemicals from tissues during placement in clean water, the 6 hour gut-purging period, recommended by Mount et al. (1999) for *Lumbriculus variegatus*, was employed for *L. plumulosus*, *N. arenaceodentata*, and *E. estuarius*. Excess sediment in the gut of *N. arenaceodentata* following the purging period was pushed out using a soft bristle paintbrush. The clams *Y. limatula* and *M. mercenaria* were dissected and gut contents were removed and rinsed with deionized water. Organisms from each replicate were homogenized, and separate aliquots were analyzed for lipid content (uptake exposure only) or

submitted to the ERDC Environmental Chemistry Branch for determination of tissue residues. Analytical determinations were as described in Appendix A: Supporting Data Table S1 (Supporting Data).

9.3.4 Modeling

The kinetics of contaminant uptake in organisms was estimated using the following models (Landrum et al. 1992):

$$C_{tissue} = \left(\frac{k_s * C_s}{k_e} \right) (1 - e^{-k_e * t}) \quad TSS_{95\%} = \frac{Ln\left(\frac{1}{1-0.95}\right)}{k_2} = \frac{3}{k_2}$$

where k_s = uptake rate constant from sediment to the organism (g/g/d), k_2 = elimination rate constant from the organism (1/t), C_s = contaminant concentration in the sediment and t = time in days.

Estimation of k_u was also derived from the slope of tissue residues vs. time linear regression (Landrum et al. 1992) using data from the earliest exposure time point. The slope was calculated as the average body residue divided by the exposure period.

The experimentally measured elimination rate ($k_{e(m)}$) was determined by fitting the data from the depuration experiments to the first-order decay (Landrum et al. 1992):

$$C_{tissue} = C_{t=0} \bullet e^{-k_{e(m)} \bullet time(days)}$$

where $C_{t=0}$ is the initial chemical concentration in the invertebrates at the initiation of the elimination experiment.

The maximum or equilibrium concentration within the organism (C_{t-max}) was estimated as

$$C_{t-max} = C_s \bullet (k_s / k_{e(m)})$$

9.4 Results and discussion

9.4.1 Total lipids content

The lipid content of the experimental organisms expressed as average, and one standard deviation using individual values determined for each exposure period for the uptake exposure are presented in Table 10. The lipid content of *Y. limatula* used in the uptake exposure was not determined, and the average lipid content ($1.3 \pm 0.2\%$) determined for two specimens used in preliminary experiments was used for lipid normalization of uptake data and calculation of BSAF values. Lipid content for *N. areanaceodontata* was highly variable and considered inaccurate when compared to previous data (Lotufo et al, 2000; Millward et al. 2005). The average lipid content reported in Lotufo et al. (2000) for males (1.5%) was used for lipid normalization of uptake data and calculation of BSAF values.

Table 10. Total lipids content for the experimental organisms from uptake exposure, ND = not determined.

Species	Day	Average	SD	<i>n</i>
<i>L. plumulosus</i>	2	2.3	0.4	3
	5	1.6	0.5	3
	9	1.4	0.6	3
	14	1.3	0.1	3
	21	1.2	0.4	3
<i>E. estuarius</i>	4	1.1	0.04	2
	7	1.1	0.4	3
	9	1.1	0.4	3
	11	1.1	0	3
	14	1.1	0	2
	2	1.2	0.1	3
<i>M. mercenaria</i>	7	0.9	0.1	3
	14	1	0.2	3
	21	1.1	0.1	3
	28	1.1	0.2	3
<i>L. plumulosus</i> (BNC Sediment)	0.5	2.3	0.4	3
	1	1.9	0.05	3
	2	1.3	0.2	3
	3	1.6	0.4	3
	8	ND		

9.4.2 Uptake kinetics

9.4.2.1 Survival

The average survival at exposure termination was 78% or higher for *L. plumulosus*, *N. arenaceodentata*, and *M. mercenaria* exposed to NBH sediment (Table 11). In addition to physiological impairment caused by exposure to PCBs, poor survival of *Y. limatula* (39% survival at day 21) was also likely attributed to the apparent poor health of field-collected organisms (as indicated by the vendor at the time of collection). As excellent survival in NBH sediment was observed in a preliminary experiment of similar duration, the overall low survival of *E. estuarius* was also likely attributed to prolonged exposure to fine-grained sediment. Somewhat low average survival at exposure termination was also observed for *L. plumulosus* exposed to BNC sediment, likely due to stress caused by the predominantly sandy nature of that sediment.

9.4.2.2 Total PCBs

Markedly different temporal patterns of bioaccumulation were observed among the five species investigated (Figure 19 and Table 12). The body residue of total PCBs remained relatively constant over time for the amphipod species, with an average for all exposure periods of 2841 and 1064 mg/kg-lipids for *L. plumulosus* and *E. estuarius*, respectively. Analysis of Variance (ANOVA) followed by Fisher's Least Significant Difference (LSD) Pairwise Multiple Comparison Procedure revealed no significant differences (i.e., $p < 0.05$) among exposure time points, but when isolated, body residue at day 14 was significantly higher than that at day 2 for *L. plumulosus*. For the polychaete *N. arenaceodentata*, an increasing trend of body residue over time was observed, with the average body residue increasing from 115 mg/kg-lipids at day 3 to 404 mg/kg-lipids at day 28, but ANOVA revealed no significant differences among exposure time points. For the clam *M. mercenaria*, an increasing trend of body residue over time was observed, with body residues reaching a plateau after approximately 7 to 14 days of exposure (no significant increase from day 7 to 28); the average body residue increased from 48 mg/kg-lipids at day 2 to 135 mg/kg-lipids at day 28. For the clam *Y. limatula*, body residue increased linearly over the first 14 days of exposure, but appeared to approach steady state between days 7 and 21 (no significant increase from day 7 to 28); the average body residue increased from 295 mg/kg-lipids at day 3 to 1987 mg/kg-lipids at day 21. Uptake rate constants (Table 13) were lower than for

N. arenaceodentata (0.11 g/g/day) and *M. mercenaria* (0.05 g/g/day) than for *E. estuarius* (1.17 g/g/day, $p = 0.14$) and *Y. limatula* (0.20 g/g/day). Rate of uptake for *L. plumulosus* could not be determined by the non-linear model because of the lack of increasing trend within the sampling period, but were estimated using linear regression (2.1 g/g/day).

Table 11. Percent of experimental organisms alive at termination of the uptake exposures.

Species	Day	Average	SD
<i>L. plumulosus</i>	2	94	5
	5	96	2
	9	90	7
	14	80	3
<i>E. estuarius</i>	4	89	5
	7	60	6
	9	47	7
	11	50	13
	14	59	26
<i>N. arenaceodentata</i>	3	100	0
	7	100	0
	14	89	19
	21	89	19
	28	78	58
<i>Y. limatula</i>	3	100	0
	7	100	0
	14	89	19
	21	39	10
<i>M. mercenaria</i>	2	100	0
	7	100	0
	14	100	0
	21	89	19
	28	100	0
<i>L. plumulosus</i> (BNC sediment)	0.5	91	3
	1	70	7
	2	53	9
	3	58	22
	8	69	27

Figure 19. Bioaccumulation of total PCBs over time in five infaunal invertebrates exposed to New Bedford Harbor sediment. The lines represent the prediction from the one-compartment model.

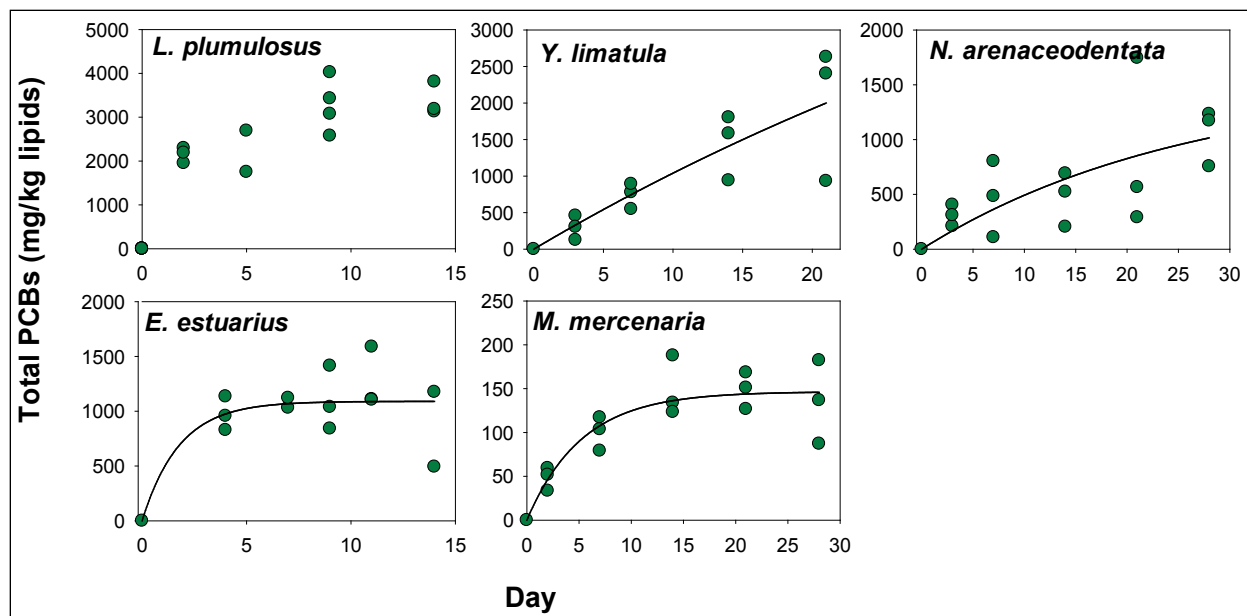


Table 12. Temporal trend of bioaccumulation for five infaunal invertebrates exposed to New Bedford Harbor sediment and time to approach steady state per ASTM (2010).

Species	Uptake temporal trend	Time to approach steady-state (d)
<i>E. estuarius</i>	No significant change from day 4 to 14.	4
<i>L. plumulosus</i>	No significant increase from day 2 to 14.	2
<i>N. arenaceodentata</i>	No significant change from day 3 to 28.	3
<i>Y. limatula</i>	No significant change from day 14 to 21, significant increase from day 7 to 21.	ND, but likely 14 or 21
<i>M. mercenaria</i>	No significant change from day 7–28.	7

Table 13. Uptake rate constants (g/g/day) for five infaunal invertebrates exposed to New Bedford Harbor sediment determined for individual homolog groups and for total PCBs.

PCBs	<i>E. estuarius</i>			
	Non- linear Regression			Linear Regression
	Estimate	SD	p	Estimate
Di	ND			0.35
Tri	2.85	7.33	0.70	0.73
Tetra	1.29	0.99	0.22	0.49
Penta	0.71	0.36	0.07	0.31
Hexa	0.51	0.16	0.01	0.29
Hepta-Nona	0.39	0.13	0.06	0.22
Total	1.17	0.75	0.14	0.47
<i>L. plumulosus</i>				
Di	ND			1.7
Tri	ND			3.0
Tetra	2.24	0.47	<0.01	1.9
Penta	1.60	0.31	<0.01	1.7
Hexa	1.95	0.33	<0.01	1.7
Hepta-Nona	1.79	0.77	0.04	1.0
Total	ND			2.1
<i>N. arenaceodentata</i>				
Di	ND			0.09
Tri	ND			0.30
Tetra	0.08	0.05	0.15	0.13
Penta	0.14	0.09	0.12	0.19
Hexa	0.10	0.06	0.13	0.24
Hepta-Nona	0.05	0.03	0.07	0.11
Total	0.11	0.06	0.08	0.20
<i>Y. limatula</i>				
Di	0.20	0.08	0.04	ND
Tri	0.29	0.12	0.03	ND
Tetra	0.21	0.09	0.04	ND
Penta	0.16	0.02	<0.01	ND
Hexa	0.21	0.08	0.03	ND
Hepta-Nona	0.28	0.07	<0.01	ND
Total	0.22	0.08	0.03	ND

PCBs	<i>E. estuarius</i>			
	Non- linear Regression			Linear Regression
	Estimate	SD	p	Estimate
<i>M. mercenaria</i>				
Di	0.17	0.06	0.02	ND
Tri	0.09	0.02	<0.01	ND
Tetra	0.05	0.01	<0.01	ND
Penta	0.03	0.01	<0.01	ND
Hexa	0.02	0.01	0.01	ND
Hepta-Nona	0.0020	0.0004	<0.01	ND
Total	0.05	0.01	<0.01	ND

Di = dichlorobiphenyls, Tri = trichlorobiphenyls, Tetra = tetrachlorobiphenyls, Penta = pentachlorobiphenyls, Hexa = hexachlorobiphenyls, Hepta-Nona = sum of hepta-, octa-, and nonachlorobiphenyls.

Using the operational definition of state-state (ASTM 2010) as “steady-state is defined operationally as the absence of any significant difference (ANOVA, $\alpha = 0.05$) among tissue residues taken at three consecutive sampling intervals,” time to approach steady state are presented in Table 12.

Survival during sediment exposures were within the range (> 80%) expected in long term exposures (USEPA 2001), except for *Y. limatula*, for which survival was only 39% after 21 days and *E. estuarius* for which survival was as low as 47% after 7 days. Even when the overall rate of survival was high, experimental organisms were likely physiologically impaired by the bioaccumulation of PCBs and other contaminants present in the experimental sediments. The rate of uptake of contaminants from sediment by benthic invertebrates is influenced by the health of the test organisms (ASTM 2010). Physiologically impaired organisms, such as those experiencing general narcosis, have been reported to bioaccumulate hydrophobic, organic contaminants at a lower rate compared to non-impaired organisms (Kukkonen et al. 1994; Driscoll et al. 1998; Lotufo et al. 2001). Therefore, rates of uptake derived in this study may represent an underestimate of the rates of uptake in less contaminated NBH and BNC sediments, especially for *E. estuarius* and *Y. limatula* for which mortality increased over time during the uptake exposure.

9.4.2.3 PCB homolog groups

The temporal pattern of bioaccumulation was examined for different homolog groups for the five species investigated (Figure 20). For *E. estuarius*, body residue remained relatively constant over time for all PCB homolog groups, with peak average concentrations observed at day 11. Average body residues at day 11 were significantly higher than at day 3 for pentachlorobiphenyls, hexachlorobiphenyls and sum of hepta-, octa-, and nonachlorobiphenyls (hepta-nonachlorobiphenyls). For *L. plumulosus*, body residue also remained relatively constant over time for all PCB homolog groups, but a significant increase in body residue was observed between days 2 and either day 9 or 14 for all homolog groups except di- and trichlorobiphenyls. For *N. arenaceodentata* an increasing trend from day 3 to 28 was observed for all homolog groups except di- and trichlorobiphenyls. For *Y. limatula*, an increasing trend from day 3 to 21 was observed for all homolog groups. For *M. mercenaria*, a similar temporal trend of change in body residues was observed across homolog groups, with body residues overall increasing between days 7 and 14 and remaining relatively unchanged thereafter.

Uptake rate constants were derived for different homolog groups (Table 13 and Figure 21). Estimates for uptake rates for di- and trichlorobiphenyls for *E. estuarius*, *L. plumulosus*, and *N. arenaceodentata* (dichlorobiphenyl only for *L. plumulosus*) could not be determined by the non-linear model because of the lack of increasing trend within the sampling period. Moreover, high variability in replicate data and unclear temporal trends resulted in unreliable estimates of rates of uptake (i.e., when p value > 0.1). For those species, estimates of k_u were also derived from the slope of the linear regression of body residues vs. time using data from the earliest exposure time point (Table 13) to improve comparisons across homolog groups and species. Those values should be considered underestimates as they were calculated using body residue data beyond the linear portion of the theoretical uptake curve (i.e., the rate was derived by dividing the average body residue by too large of a value for exposure time).

Figure 21 allows comparison of uptake rate constants across homolog groups and species. Values for *E. estuarius*, *L. plumulosus*, and *N. arenaceodentata* were derived using the linear regression approach. Rates of uptake were substantially higher for *L. plumulosus* than for the other species investigated. Rates of uptake were lowest for *M. mercenaria*. No overall decreasing trend in the rate of uptake from low to highly chlorinated PCB homolog groups was observed for any species, except for *M. mercenaria*.

Figure 20. Bioaccumulation of PCB homolog groups over time in five infaunal invertebrates exposed to New Bedford Harbor sediment. The lines represent the prediction from the one-compartment model. Black = dichlorobiphenyls, red = trichlorobiphenyls, green = tetrachlorobiphenyls, yellow = pentachlorobiphenyls, blue = hexachlorobiphenyls, pink = sum of hepta-, octa-, and nonachlorobiphenyls. (continued)

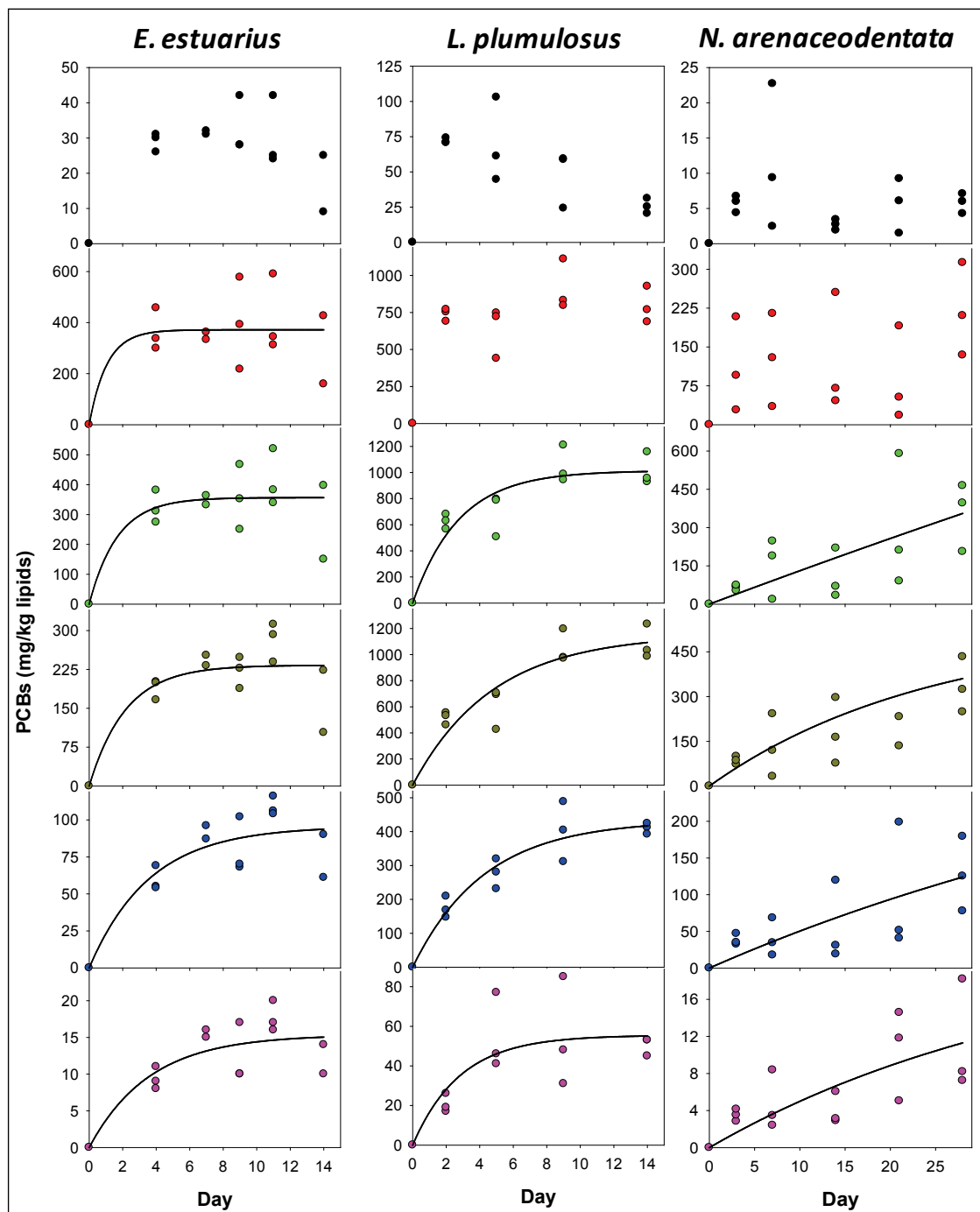


Figure 20. (concluded)

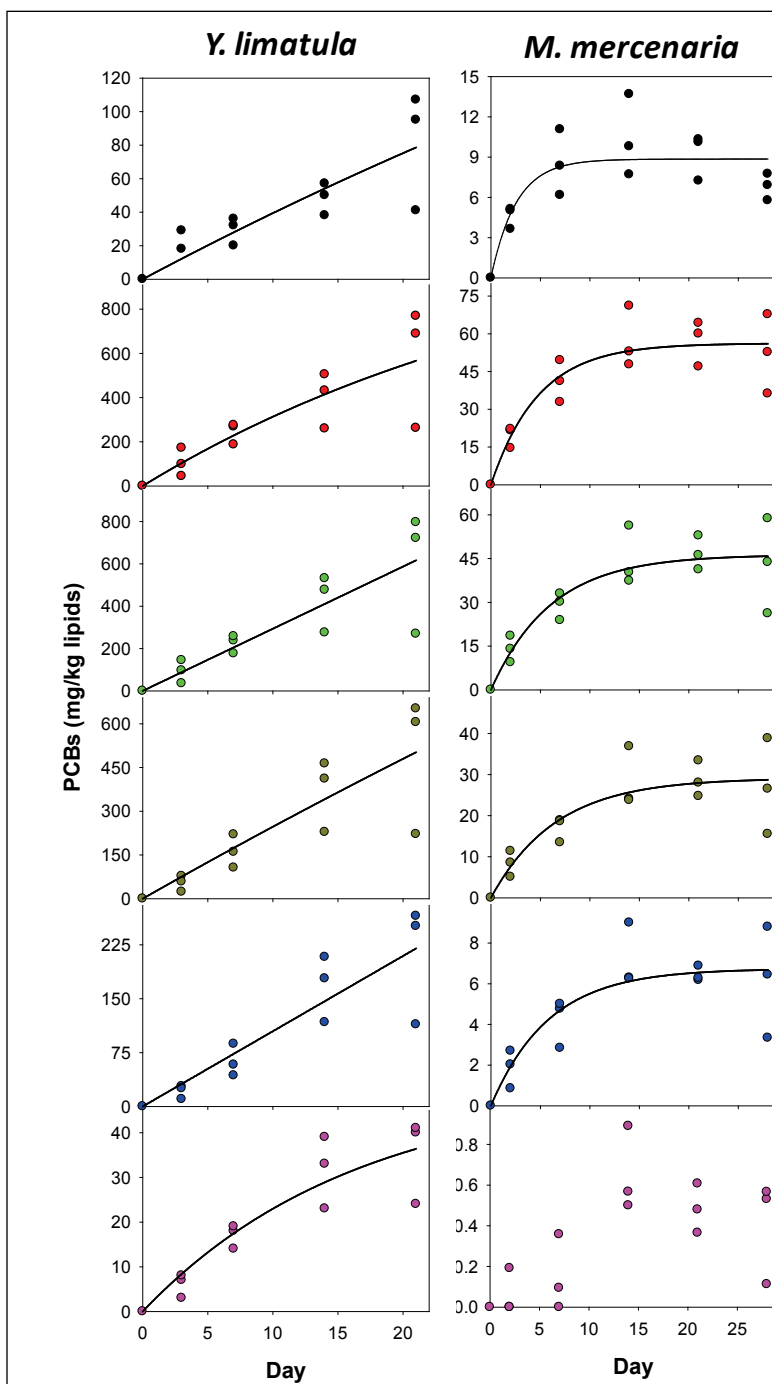
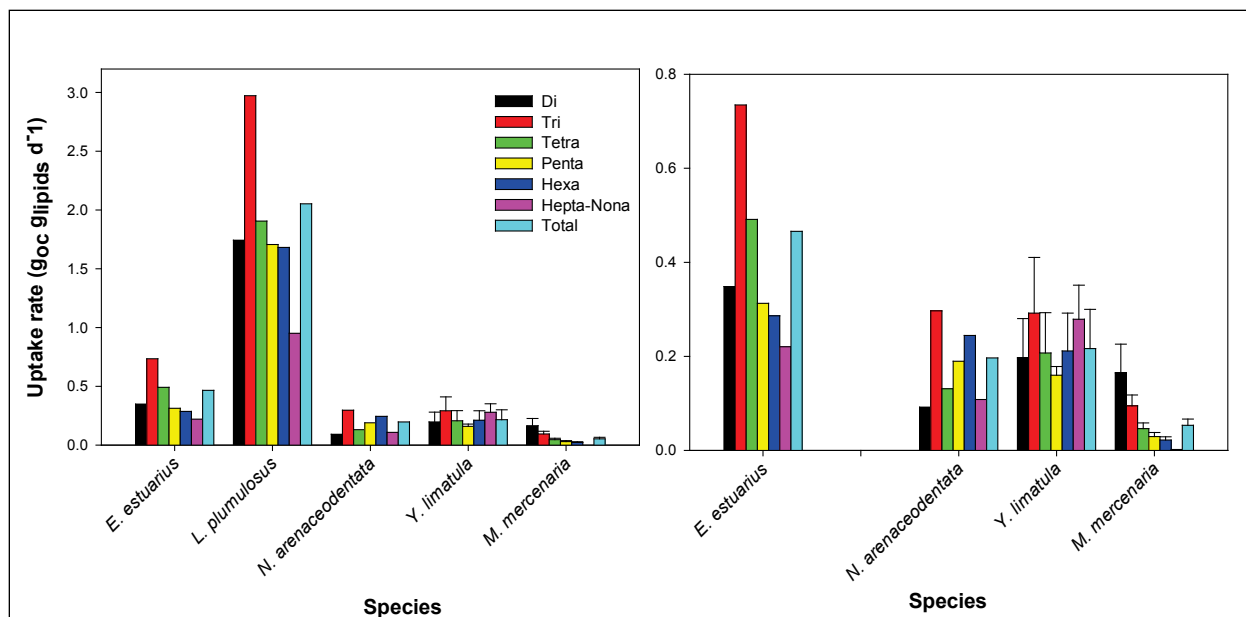


Figure 21. Uptake rate constants (g/g/day) for five infaunal invertebrates exposed to New Bedford Harbor sediment determined for individual homolog groups and for total PCBs. The data for *L. plumulosus* was omitted from the right graph and the y-axis scale adjusted accordingly. Di = dichlorobiphenyls, Tri = trichlorobiphenyls, Tetra = tetrachlorobiphenyls, Penta = pentachlorobiphenyls, Hexa = hexachlorobiphenyls, Hepta-Nona = sum of hepta-, octa-, and nonachlorobiphenyls



9.4.2.4 Biota-sediment bioaccumulation factors (BSAFs)

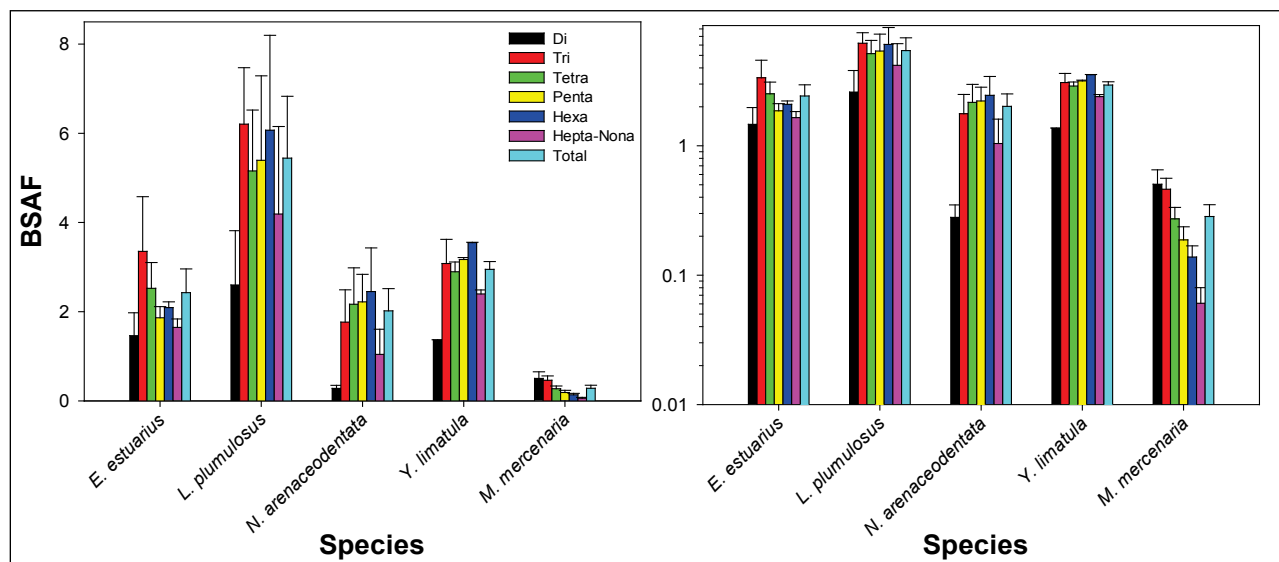
Lipid-normalized body residues of five infaunal invertebrates exposed to NBH sediment were highly variable, with average highest tissue concentration for each species ranging from (*M. mercenaria*) 149 to (*L. plumulosus*) 3,509 mg/kg-lipids, and lipid-normalized values decreased in the following order for the various species: *L. plumulosus* > *Y. limatula* > *E. estuarius* > *N. arenaceodentata* > *M. mercenaria*. Because all exposures were to the same sediment, BSAF values (Table 14 and Figure 22) varied in the same proportion as lipid-normalized body residues. For *M. mercenaria*, average BSAFs had a decreasing trend from di- to hepta-nonachlorobiphenyl. For the other species investigated, BSAFs were lower for dichlorobiphenyl, and overall similar for the other homolog groups.

Table 14. Biota-to-sediment accumulation factors (BSAFs) for five infaunal invertebrates exposed to New Bedford Harbor sediment determined for individual homolog groups and for total PCBs.

PCBs	<i>E. estuarius</i>		<i>L. plumulosus</i>		<i>N. arenaceodentata</i>		<i>Y. limatula</i>		<i>M. mercenaria</i>	
	Day 11		Days 1-14		Day 28		Day 21		Day 14	
	Avg	SD	Avg	SD	Avg	SD	Avg	SD	Avg	SD
Di	1.5	0.5	2.6	1.2	0.3	0.1	1.4	1.2	0.50	0.15
Tri	3.4	1.2	6.2	1.3	1.8	0.7	3.1	2.7	0.46	0.10
Tetra	2.5	0.6	5.2	1.4	2.2	0.8	2.9	2.0	0.27	0.06
Penta	1.9	0.3	5.4	1.9	2.2	0.6	3.2	1.9	0.19	0.05
Hexa	2.1	0.1	6.1	2.1	2.5	1.0	3.6	2.2	0.14	0.03
Hepta-Nona	1.6	0.2	4.2	2.0	1.0	0.6	2.4	1.6	0.06	0.02
Total	2.4	0.5	5.4	1.4	2.0	0.5	2.9	2.2	0.28	0.07

Di = dichlorobiphenyls, Tri = trichlorobiphenyls, Tetra = tetrachlorobiphenyls, Penta = pentachlorobiphenyls, Hexa = hexachlorobiphenyls, Hepta-Nona = sum of hepta-, octa-, and nonachlorobiphenyls.

Figure 22. Biota-to-sediment accumulation factors (BSAFs) for five infaunal invertebrates exposed to NBH sediment determined for individual homolog groups and for total PCBs. Note the logarithmic scale for the y-axis of the right graph.



9.4.2.5 Homolog group distribution

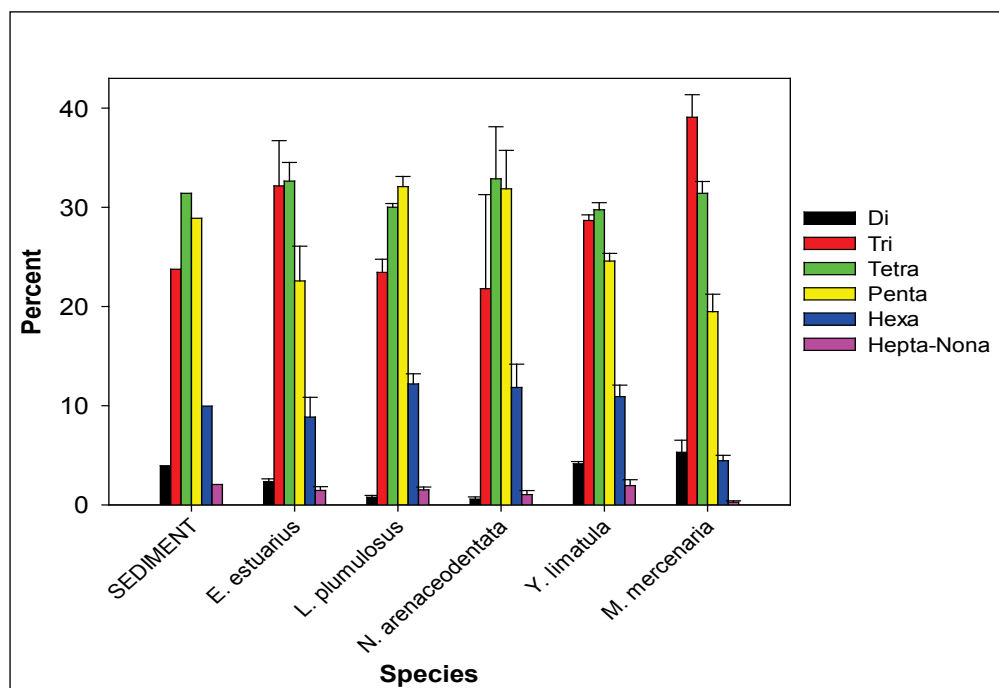
The relative proportion of PCB homolog groups in tissues was overall similar among the five benthic invertebrates used in this study (Table 15 and Figure 23) with tri-, tetra-, and pentachlorobiphenyl dominating among homolog groups. The fraction of the total corresponding to dichlorobiphenyl was lowest for *N. arenaceodentata* (0.6%) and highest for *M. mercenaria* (5%). The sum concentration of hexa-, hepta-, octa-, and nonachlorobiphenyl was highest in *L. plumulosus* (13.5%) and lowest in *M. mercenaria* (4.3%).

Table 15. PCB homolog groups as a percent of total PCBs in tissues of five infaunal invertebrates exposed to New Bedford Harbor sediment at single or multiple times.

PCBs	Sediment	<i>E. estuarius</i>		<i>L. plumulosus</i>		
		Day 11		Days 1–14		
		Avg	SD	Avg	SD	
Di	4	2	0.3	0.8	0.2	
Tri	24	32	4.6	23	1.3	
Tetra	31	33	1.9	30	0.4	
Penta	29	23	3.5	32	1.0	
Hexa	10	9	2.0	12	1.0	
Hepta-Nona	2	1.5	0.4	1.5	0.3	
PCBs	<i>N. arenaceodentata</i>		<i>Y. limatula</i>		<i>M. mercenaria</i>	
	Day 28		Day 21		Day 14	
	Avg	SD	Avg	SD	Avg	SD
Di	0.6	0.2	4	0.2	5	1.2
Tri	22	9.5	29	0.6	39	2.3
Tetra	33	5.2	30	0.7	31	1.2
Penta	32	3.9	25	0.8	19	1.7
Hexa	12	2.4	11	1.2	4	0.5
Hepta-Nona	1.0	0.4	1.9	0.6	0.3	0.1

Di = dichlorobiphenyls, Tri = trichlorobiphenyls, Tetra = tetrachlorobiphenyls, Penta = pentachlorobiphenyls, Hexa = hexachlorobiphenyls, Hepta-Nona = sum of hepta-, octa-, and nonachlorobiphenyls

Figure 23. PCB homolog groups as a percent of total PCBs in tissues of five infaunal invertebrates exposed to New Bedford Harbor sediment at single or multiple times.



9.4.3 Elimination kinetics – New Bedford Harbor sediment

Upon transfer to clean sediment following exposure to NBH sediment, a decreasing trend of total PCB body residues was observed for all Table 16 species, except *M. mercenaria* (Figure 24). The estimated rate of elimination (Table 15), experimentally measured for all species except *M. mercenaria*, was fastest for *L. plumulosus* (0.20 d^{-1}), followed by *E. estuarius* (0.13 d^{-1}), *N. arenaceodentata* (0.09 d^{-1}), and *Y. limatula* (0.07 d^{-1}). Elimination rates were used to calculate the theoretical time for PCBs to approach steady state in the organisms, which was fastest for *L. plumulosus* (15 d). For *M. mercenaria*, average body residue at day 21 (1307 mg/kg) was virtually unchanged relative to the initial residue (1565 mg/kg), suggesting that bioaccumulation of PCBs would approach steady state well beyond 21 days. As discussed above, physiologically impaired organisms, such as those experiencing general narcosis, may bioaccumulate hydrophobic, organic contaminants at a lower rate compared to non-impaired organisms (Kukkonen et al. 1994; Driscoll et al. 1998; Lotufo et al. 2001). However, in those studies, elimination did not change in a dose-dependent manner. Therefore, rates of elimination derived in this study, following exposure to the highly contaminated NBH, likely represent rates of elimination in less contaminated sediments.

Elimination rate constants were derived for different homolog groups (Table 16 and Figure 26). An overall decreasing trend with increasing chlorination was observed for *L. plumulosus*, but not for other species.

Table 16. Experimentally measured elimination rate constants (day^{-1}) and time to steady state predictions for five infaunal invertebrates exposed to New Bedford Harbor sediment determined for individual homolog groups and for total PCBs.

PCBs	<i>E. estuarius</i>			
	Estimate	SD	p	Time to Steady State
Di	0.21	0.11	0.11	14
Tri	0.17	0.09	0.10	18
Tetra	0.15	0.07	0.07	19
Penta	0.10	0.02	<0.01	31
Hexa	0.07	0.01	<0.01	41
Hepta-Nona	0.10	0.01	<0.01	30
Total	0.13	0.04	0.02	24

PCBs	<i>E. estuarius</i>			
	Estimate	SD	p	Time to Steady State
<i>L. plumulosus</i>				
Di	0.15	0.06	0.04	20
Tri	0.21	0.06	0.01	14
Tetra	0.20	0.04	<0.01	15
Penta	0.20	0.04	<0.01	15
Hexa	0.17	0.03	<0.01	17
Hepta-Nona	0.22	0.04	<0.01	14
Total	0.20	0.04	<0.01	15
<i>N. arenaceodentata</i>				
Di	0.18	0.08	0.05	17
Tri	0.08	0.05	0.14	38
Tetra	0.15	0.09	0.15	20
Penta	0.10	0.04	0.04	30
Hexa	0.07	0.05	0.19	41
Hepta-Nona	0.07	0.07	0.35	45
Total	0.09	0.04	0.07	32
<i>Y. limatula</i>				
Di	0.05	0.06	0.44	60
Tri	0.06	0.06	0.35	50
Tetra	0.07	0.05	0.17	40
Penta	0.08	0.04	0.09	37
Hexa	0.08	0.03	0.04	36
Hepta-Nona	0.06	0.02	0.04	48
Total	0.07	0.04	0.14	40
<i>M. mercenaria</i>				
Di	0.05	0.02	0.09	65
Tri	0.01	0.01	0.33	203
Tetra	ND			
Penta	ND			
Hexa	ND			
Hepta-Nona	ND			
Total	ND			

Figure 24. Elimination of total PCBs over time in five infaunal invertebrates exposed to New Bedford Harbor sediment. The lines represent the prediction from the exponential decay model

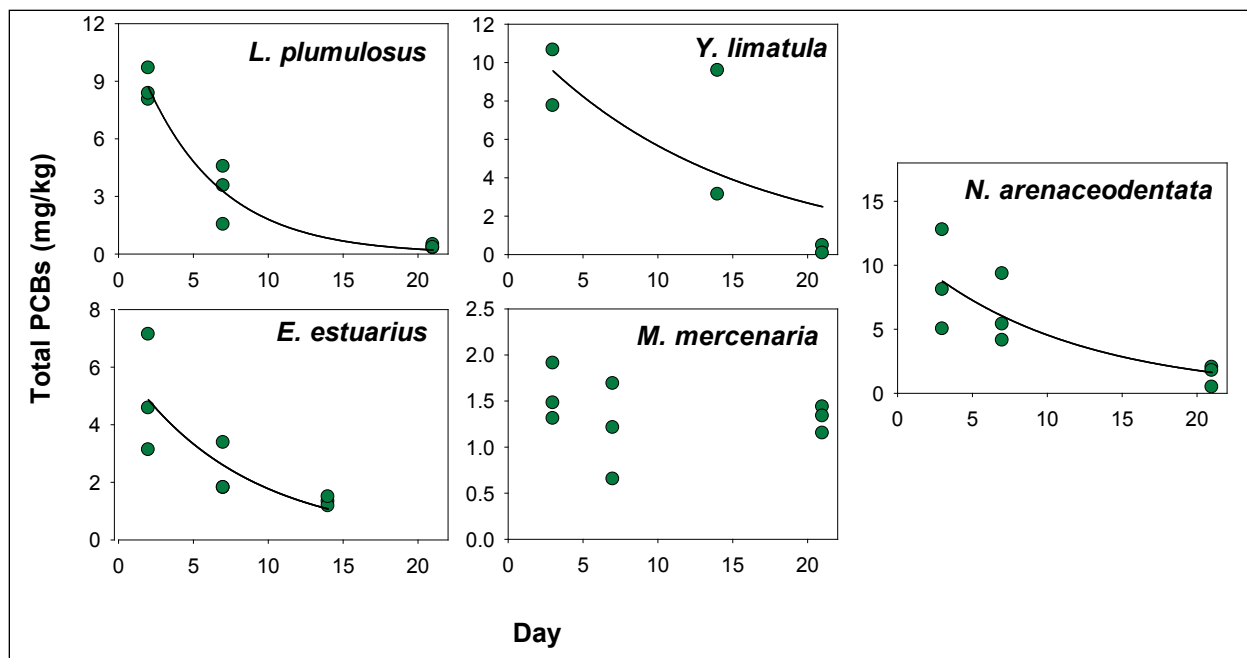


Figure 25. Elimination of PCB homolog groups over time in five infaunal invertebrates exposed to New Bedford Harbor sediment. The lines represent the prediction from the one-compartment model. Black = dichlorobiphenyl, red = trichlorobiphenyl, green = tetrachlorobiphenyl, yellow = pentachlorobiphenyl, blue = hexachlorobiphenyl, pink = sum of hepta-, octa-, and nonachlorobiphenyl. (continued)

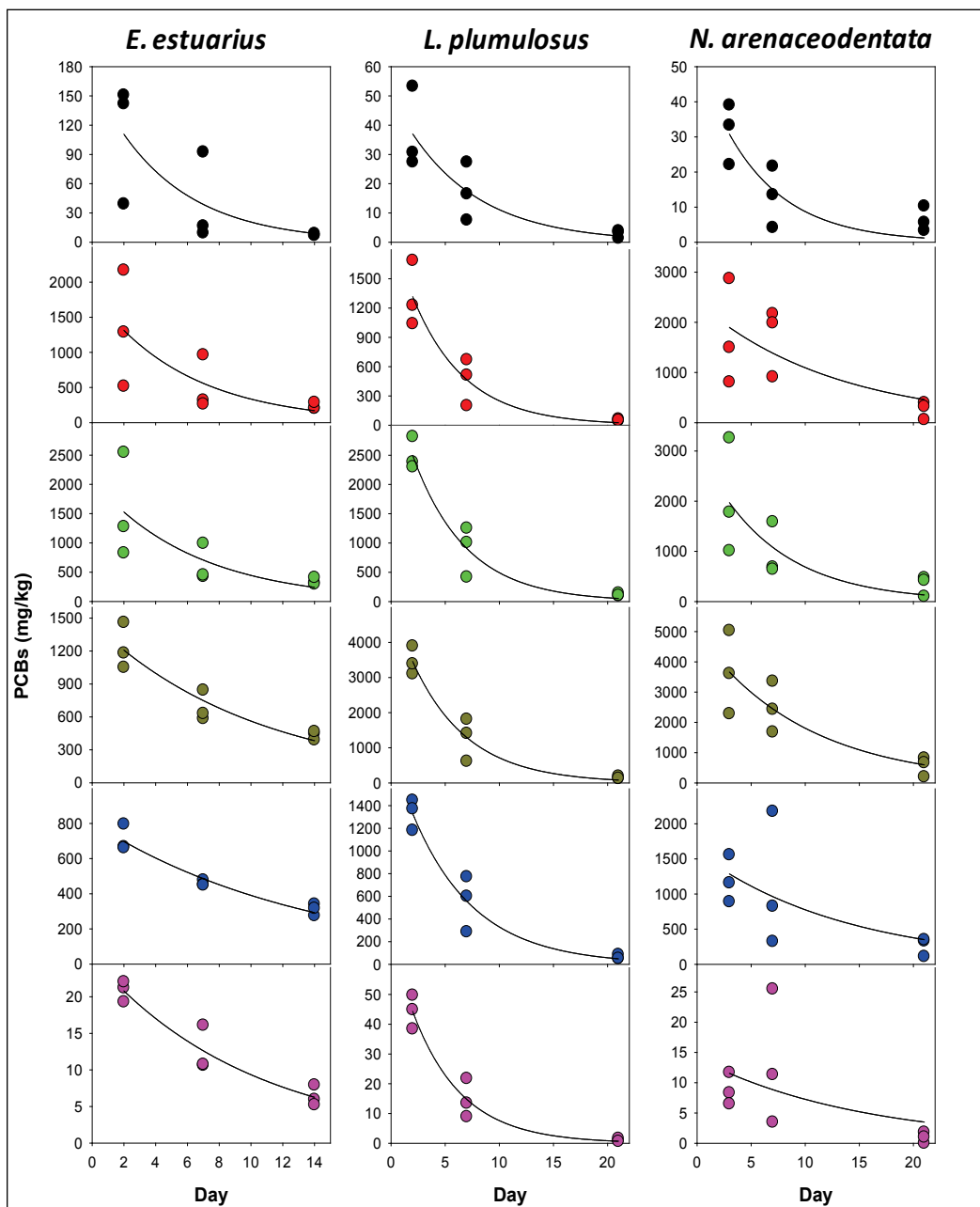


Figure 25. (concluded)

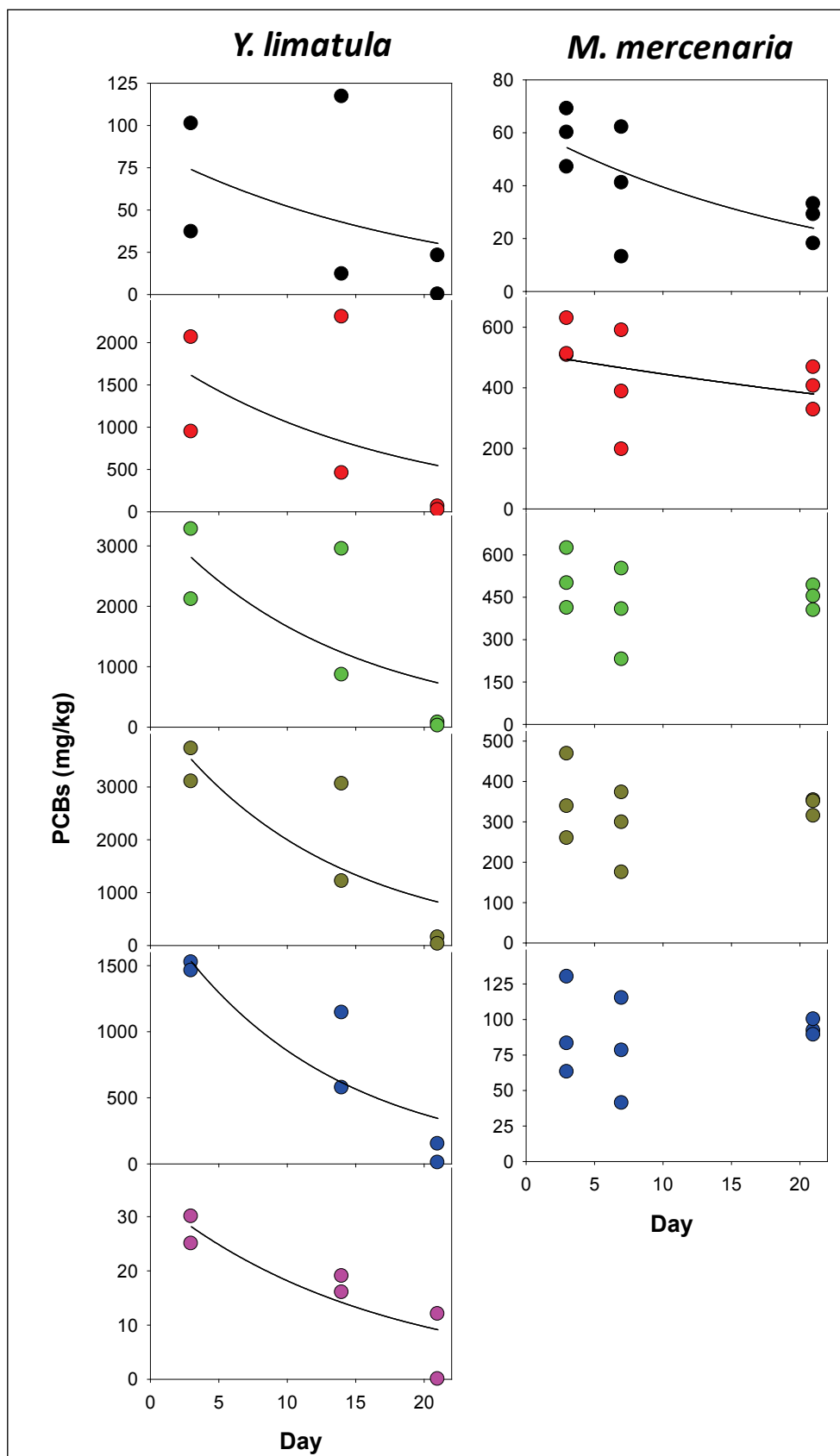
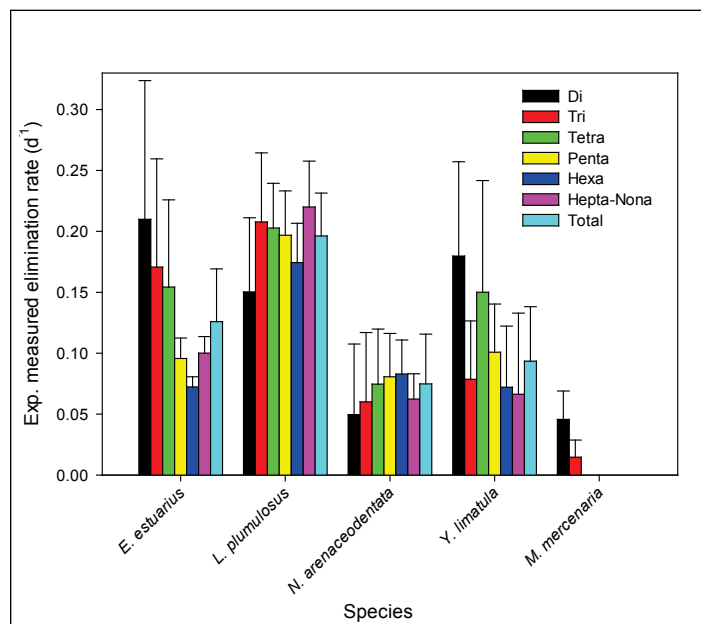


Figure 26. Elimination rate constants (day⁻¹) and time to steady state predictions for five infaunal invertebrates exposed to New Bedford Harbor sediment determined for individual homolog groups and for total PCBs.



9.4.4 Uptake and elimination kinetics – Bremerton sediment

Only *L. plumulosus* was exposed to BNC sediment for the evaluation of the toxicokinetics of sediment-associated PCBs. The body residue of total PCBs remained relatively constant over time for total PCBs and homolog groups (Figure 27), and steady state was approached within 0.5 days. Uptake rate constants seemed best represented by linear regression estimates using the earliest time point (0.5 days), similar to observed for the NBH sediment. Those estimates were overall similar to those estimated using the best fit of the non-linear model (Table 16). The rate of uptake increased with increasing degree of chlorination and that trend contrasts with the lack of trend observed for the NBH sediment (Figure 28). As explained above, estimates derived for NBH are expected to be underestimates because the body residues were beyond the phase of linear increase by the earliest sampling time point (day 2).

Experimentally measured elimination rate constants were derived for total PCBs and for different homolog groups (Table 17 Figure 28 and Figure 28). Rates of elimination were highest for dichlorobiphenyl and overall similar for other homolog groups. As expected, rates of elimination for total PCBs and PCB homolog groups were similar following exposure to both sediments (Figure 28).

Figure 27. Bioaccumulation of PCBs homolog groups over time in *L. plumulosus* exposed to BNC sediment. The lines represent the prediction from the one-compartment model. Black = dichlorobiphenyls, red = trichlorobiphenyls, green = tetrachlorobiphenyls, yellow = pentachlorobiphenyls, blue = hexachlorobiphenyls, pink = sum of hepta-, octa-, and nonachlorobiphenyls, gray = total PCBs.

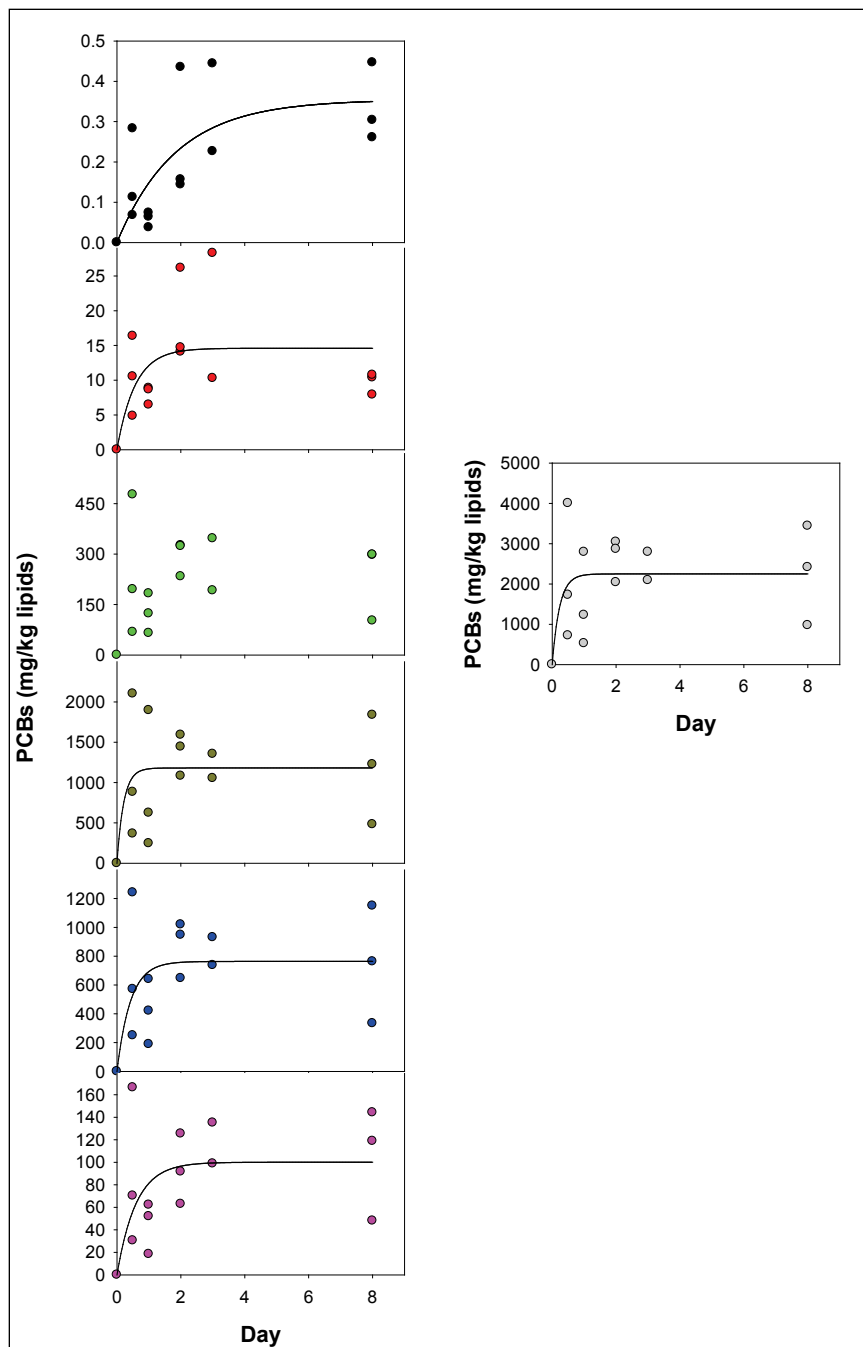


Figure 28. Uptake rate constants (g/g/day ; top graph), elimination rate constants (day^{-1} , middle graph), and biota-to-sediment accumulation factors (BSAFs bottom graph) for *L. plumulosus* exposed to New Bedford Harbor (NBH) and BNC sediments determined for individual homolog groups and for total PCBs. Di = dichlorobiphenyls, Tri = trichlorobiphenyls, Tetra = tetrachlorobiphenyls, Penta = pentachlorobiphenyls, Hexa = hexachlorobiphenyls, Hepta-Nona = sum of hepta-, octa-, and nonachlorobiphenyls.

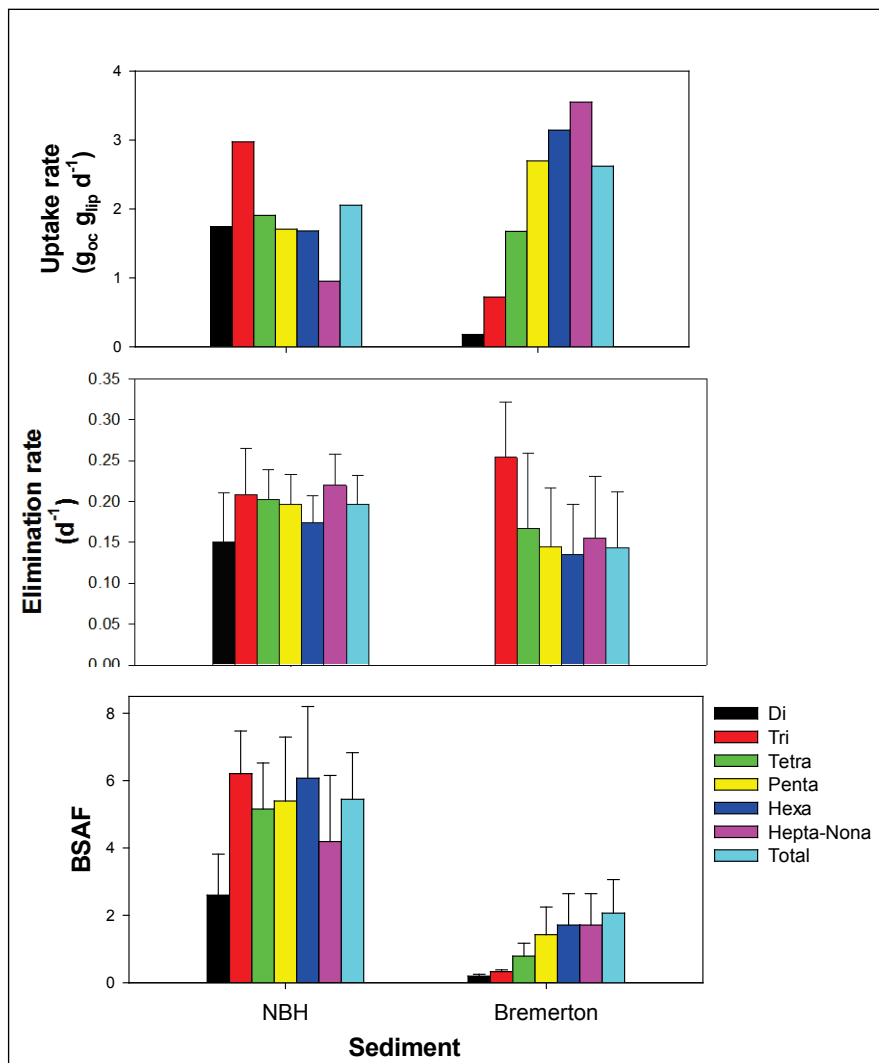


Table 17. Uptake rate constants (g/g/day), elimination rate constants (day⁻¹) and time to steady state predictions, and biota-to-sediment accumulation factors (BSAFs) for *L. plumulosus* exposed to BNC sediment determined for individual homolog groups and for total PCBs.

PCBs	Uptake				Elimination				BSAF	
	Non- linear Regression			Linear Regression						
	Estimate	SD	p	Estimate	Estimate	SD	p	TSS	Avg	SD
Di	0.10	0.03	0.01	0.18	ND			ND	0.20	0.06
Tri	0.89	0.52	0.11	0.72	0.25	0.07	0.01	12	0.33	0.05
Tetra	ND			1.67	0.17	0.09	0.11	18	0.79	0.38
Penta	6.75	0.72	0.49	2.70	0.14	0.07	0.09	21	1.43	0.82
Hexa	4.17	2.65	0.14	3.14	0.13	0.06	0.07	22	1.71	0.93
Hepta-Nona	3.36	1.95	0.11	3.55	0.16	0.08	0.08	19	1.71	0.93
Total	5.91	6.80	0.40	2.62	0.14	0.07	0.07	21	2.07	0.99

Di = dichlorobiphenyls, Tri = trichlorobiphenyls, Tetra = tetrachlorobiphenyls, Penta = pentachlorobiphenyls, Hexa = hexachlorobiphenyls, Hepta-Nona = sum of hepta-, octa-, and nonachlorobiphenyls.

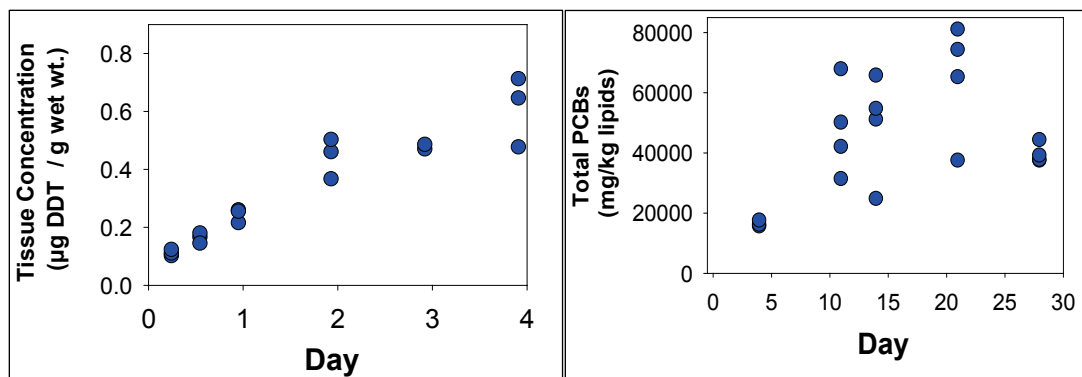
BSAF values for the BNC (Table 17) sediment were substantially lower than for the NBH sediment (Figure 28). BSAF values were lowest for dichlorobiphenyl (0.20) and increased with degree of chlorination, but remained relatively constant for pentachlorobiphenyl and higher homolog groups (1.43 – 1.71). Because hydrophobicity increases with increasing chlorination (Hawker and Connell 1988), this increasing trend indicates that the bioaccumulation potential increased with increasing hydrophobicity from di- to pentachlorobiphenyls for *L. plumulosus* exposed to BNC sediment. Landrum et al. (2001) also reported a strong relation between increase in PCB hydrophobicity and BSAF for PCBs in the amphipods *Diporeia* spp. collected in Lake Michigan sediment. According to Landrum et al. (2001), a strong relation between BSAF values and hydrophobicity suggest that the mechanism for accumulation is not simply passive partitioning as suggested by the equilibrium partitioning theory.

9.4.5 Comparison of predicted with observed bioaccumulation

In this study, body residues of PCBs in the amphipods *L. plumulosus* and *E. estuarius* approached maximum levels very quickly after exposure periods as short as 12 hours (*L. plumulosus* exposed to BNC sediment). Similar findings were observed in similar experiments conducted in 2009 using NBH sediment collected from a different location than that sampled for this study (Lotufo, unpublished). However, in contrast from the

present experiment, body residue at day four in the 2009 study was only approximately one-third the average body residue representing the apparent steady state (Figure 29). A study of the uptake of DDTs (sum of DDT, DDD, and DDE) in *L. plumulosus* exposed to spiked sediment (Lotufo, unpublished) also showed body residue approaching apparent steady state within two days (Figure 29). In addition to exposing aquatic organisms to contaminated media for increasing time periods to investigate the temporal pattern of bioaccumulation, the time to approach steady state tissue residues can be estimated using elimination rate constants. Using the elimination rate derived for *L. plumulosus* in the NBH elimination experiment of this study (0.20 d^{-1}), steady state body residues are predicted after 15 days of exposure. For DDTs, the elimination rate measured for *L. plumulosus* (0.29 d^{-1}) is associated with an estimated time to steady state of 10 days.

Figure 29. Bioaccumulation of total PCBs over time for *L. plumulosus* exposed to NBH sediment in a study conducted in 2009 (left graph, Lotufo, unpublished) and bioaccumulation of total DDTs over time for *L. plumulosus* exposed to spiked sediment (right graph, Lotufo, unpublished).



Two methods can be used to estimate steady state bioaccumulation and time to approach steady state (ASTM 2010). The kinetic-based method uses direct measurements of chemical uptake and estimates of elimination rates. The operational method simply applies statistical comparisons of tissue residues over time. Time to approach steady state using the operational method was 0.5 days for *L. plumulosus* that was exposed to BNC sediment; in addition, it ranged from 2 to 14 days for invertebrates exposed to New Bedford sediment (Table 12). The maximum or equilibrium body residue estimated using uptake and elimination kinetics are compared to maximum average concentrations during the uptake exposure are shown in Table 18. Measured body residues were higher than predicted maximum body residues for *N. arenaceodentata* and *Y. limatula*, but were much lower for amphipods, especially *L. plumulosus*.

exposed to BNC sediment. Elimination rates measured for amphipods suggest that body residues should continue to increase steadily for 15 days and beyond. Table 18 also shows kinetically derived ($k_s/k_{e(m)}$) BSAF values, which were much higher than BSAF values calculated using measured body residues for amphipods, but were lower for *N. arenaceodentata* and *Y. limatula*. Kinetically derived maximum body residue and BSAF for total PCBs could not be accurately calculated for *M. mercenaria* because measured elimination rate could not be measured in this study. If the rate of elimination estimated for trichlorobiphenyls (0.01 d^{-1}) is used as the estimated elimination rate for total PCBs in the calculations, it becomes evident that the measured bioaccumulation and BSAF were much lower than the kinetically predicted values.

Table 18. Maximum body residues (kinetically derived and measured) and BSAF (kinetically derived and measured) in five infaunal invertebrates exposed to NBH and BNC sediments.

Species	Body Residue (mg/kg lipids)			BSAF	
	Kinetically derived maximum body residue	Measured highest average	Measured/Predicted	$k_s / k_{e(m)}$	Measured
<i>E. estuarius</i>	4713	1267	0.27	9.0	2.4
<i>L. plumulosus</i> NBH	5480	3509	0.64	10.5	5.4
<i>L. plumulosus</i> BNC sediment	21746	2648	0.12	13.1	2.1
<i>N. arenaceodentata</i>	638	1053	1.65	1.2	2
<i>Y. limatula</i>	1640	1987	1.21	3.1	2.9
<i>M. mercenaria</i>	2609	149	0.06	5.0	0.3

The kinetics model assumes that the sediment concentration and kinetic coefficients are invariant. Depletion of the sediment concentrations in the vicinity of the organism would invalidate the model (ASTM 2010) and would lead to observed body residues lower than kinetically predicted for *M. mercenaria* and amphipods. The faster than expected approach of steady state for *M. mercenaria* in the sediment exposure may have resulted from a gradual decrease in uptake rate over time, which is likely explained by the expected limited dermal contact of the clam with the sediment and limited uptake from sediment particles via filter-feeding for this species.

Based on the results from the toxicokinetics experiments, seven-day sediment exposures appear adequate for achieving maximal body residues

in amphipods, while 28-day exposures are recommended for polychaete and clam species.

9.4.6 Species-specific bioaccumulation of PCBs

Lipid-normalized net body residues varied greatly among the five species investigated, and because all species were exposed to the same sediment, BSAF values varied in the same proportion. Among invertebrates known to feed on sediment particles, measured BSAF was highest for *L. plumulosus* (5.4), intermediate for *Y. limatula* (2.9) and *E. estuarius* (2.4), and lowest for the polychaete *N. arenaceodentata* (2.0). Using a different batch of NBH (Lotufo, unpublished) BSAF values were highest for *L. plumulosus* (4.0), intermediate for the clam *M. nasuta* (1.4), and lowest for polychaete *Nereis virens* (0.5). In this study, the BSAF for the filter-feeding, bivalve *M. mercenaria* was substantially lower than for the other species investigated, which was likely because of minimal dermal and dietary exposure to sediment by that species. As discussed above, physiologically impaired organisms, such as those experiencing general narcosis, have been reported to bioaccumulate hydrophobic, organic contaminants at a lower rate. Therefore, BSAF values derived in this study may represent an underestimate of those associated with less contaminated sediments, especially for *E. estuarius* and *Y. limatula* for which mortality increased over time during the uptake exposure.

In addition to uptake and elimination kinetics, factors known to influence the net bioaccumulation of contaminants from sediment are growth dilution (Landrum et al. 1992), biotransformation potential (Goerke and Weber 2001; Rust et al. 2004), and feeding ecology (Means and McElroy 1997; Sormunen et al. 2006; Thorsson et al. 2008).

The elimination kinetics experiment showed that the rate of elimination measured for total PCBs were relatively high for all species, except for *M. mercenaria*. Therefore, except for the low net bioaccumulation of PCBs in *M. mercenaria*, differences in elimination rate likely had limited influence on the differences in PCB bioaccumulation observed in this study. Since the sediment was the only source of PCBs in this study, differences in the interaction between the organisms and the sediment, including differences in the role of sediment particles as a food source, likely explained the differences in BSAF observed in this study. Although PCBs are generally recognized as being recalcitrant and poorly metabolized in aquatic invertebrates (Buckman et al. 2006), species-specific differences in

metabolic capacity likely play a role in large interspecific differences in the bioaccumulation of PCBs, which were found in benthic invertebrates according to Magnusson et al. (2006). Therefore, differences in biotransformation efficiency along with feeding strategy influenced the differences in PCB bioaccumulation observed in this study.

10 Task 2a: Importance of exposure pathways for determining bioaccumulation in four functionally different benthic macroinvertebrates

10.1 Introduction

Contaminated sediments are evaluated for toxicity and bioaccumulation potential to inform management decisions. Bioaccumulation potential is often the driver for how contaminated sediment sites are managed. Data generation for and interpretation of bioaccumulation potential is costly and carries a large amount of uncertainty. The uncertainty is driven by complexities such as understanding bioavailability to benthic macroinvertebrates, multiple exposure pathways, estimating contaminant uptake and elimination rates in organisms, determining the ecological significance of elevated tissue residues, and estimating trophic transfer from benthic organisms to higher level receptors of concern (e.g., fish, birds of prey, and humans). Predictive models were developed to estimate sediment bioaccumulation potential; the most commonly used models are theoretical or empirical BSAFs and EqP (Di Toro et al 2001). The BSAF approach is relatively simple and requires knowledge of contaminant concentration in sediment, sediment TOC, contaminant concentration in organism tissue, and tissue lipid content as inputs. While it is understood that hydrophobic contaminants such as PCBs associate predominately in the solid phase (e.g., bedded sediment, particulates, and organic matter), the much lower dissolved concentrations in sediment pore water are considered more bioavailable to benthic organisms, and thus most predictive of bioaccumulation (Adams et al 1997, Di Toro et al 2001). The EqP approach estimates bioaccumulation from predicted sediment pore water concentrations based on whole sediment chemistry and organic carbon concentrations (Di Toro et al 2001); this method has shown efficacy in published investigations (e.g., Swartz et al 1990, DeWitt et al 1992, Hoke et al 1994, Swartz et al 1995, Ozretich et al 2000).

Uncertainty may be reduced by direct measurement, rather than theoretical estimation, of sediment pore water concentrations. Recent advancements in passive sampler technologies (Gschwend et al 2011; Lu et al 2011; Friedman

et al 2009) have made direct measurements of pore water concentrations feasible. However, pore water-based models derived from passive sampler generated data have under-predicted bioaccumulation (Barthe et al 2008; Burkhard et al 2013). Factors other than sediment TOC can impact bioavailability, and differences between organisms other than lipid content can impact contaminant uptake. Studies have shown correlation between bioaccumulation and the whole sediment, particulate or overlying water concentrations (Lores et al 1993, Harkey et al 1994, Burgess and McKinney 1999; Lohmann 2004). These exposure pathways can be additive contributors to bulk tissue residues that are not directly considered in EqP (Kaag et al 1997; Lohmann 2004). Unfortunately, it has so far been difficult to make robust conclusions regarding the relative contribution of pore water, overlying water, and sediment exposure vectors in contributing to tissue residues due to high levels of correlation between these phases (Burgess and McKinney 1999). Thus, bioaccumulation complexities are yet to be resolved by existing advanced techniques and models even after the pore water compartment is well characterized. These persistent knowledge and site-specific data gaps result in large assumptions about the extent of biological exposure, which ultimately increases uncertainty. Such uncertainty and the desire to err on the side of conservatism (precautionary principle) leads to overly protective management decisions that drive high costs for contaminated-sediment management and remediation.

A better understanding of how biotic factors may influence bioaccumulation potential may provide an avenue for uncertainty reduction rather than relying exclusively on the abiotic factors of exposure. Benthic macroinvertebrates represent the initial point of uptake of sediment contaminants that drive food chain risk management and site remediation decisions. However, “benthic macroinvertebrate” is an over generalized term that does not represent an easily definable group. Benthic organisms are both phylogenetically (e.g., soft bodied worms, crustaceans with exoskeletons, hard-shelled clams) and functionally diverse in terms of their natural history (e.g., pelagic, epibenthic, infaunal, tube-building, free-living), trophic level (e.g., predator, detritivore, omnivore, scavenger), and feeding strategy (e.g., suspension feeder, sediment surface deposit feeder, subsurface deposit feeder) (Pearson 2001). Thus, it is unlikely that a hard shelled clam that is shielded it from direct sediment contact and that filter-feeds from the overlying water will bioaccumulate sediment-borne contaminants to the same degree as a soft bodied infaunal organism that directly deposit feeds below the surface of

the sediment. Burrowing activity leads to bioturbation, sediment and contaminant advection, and an influx of overlying water into sediment by tube dwellers (Francois et al 1997). Likewise, it can oxidize and generally alter sediment structure, which can lead to dramatically different contaminant exposure conditions.

Bioaccumulation potential is also impacted by body size, life span, metabolism (Magnussen et al 2006; Rust et al 2004; Goerke and Weber 2001), and species-specific differences (feeding rate, body permeability) even within the same feeding group (Mearns and McElroy 1997). While it is known within the research community that different benthic invertebrates have distinct contaminant bioaccumulation potentials, the relative importance of different exposure pathways (e.g., whole sediment, pore water, and overlying water) for functionally different organisms is not well quantified. While others have investigated the role of three phases of uptake (i.e., sediment, colloid, and interstitial water) in a deposit versus filter-feeding clam, co-variation in bioavailability between phases restricted quantification (Burgess and McKinney 1999). Despite providing simplistic expediency, models should not assume all benthic macroinvertebrates are exposed to different contaminant pathways equally. There is a substantial amount of published evidence concerning species-specific PCB elimination rates and feeding habits within the same sediment exposure (Burgess and McKinney 1999, Cho et al 2007, Lake et al 1990, Kaag et al 1997, Hickey et al 1995, Kennedy et al 2010; Lohmann et al 2004, Lotufo et al, in prep, Meador et al 1997, Millward et al 2005; Ruus 2005). Failing to consider the functional ecology of the benthic macroinvertebrates present at a contaminated sediment site (community composition can vary drastically between sites) will reduce the accuracy of risk assessments.

An improved understanding of how benthic organisms bioaccumulate contaminants should reduce uncertainty and costs associated with overly conservative risk management. The authors hypothesized that the functional attributes of benthic organisms will explain a substantial portion of observed variation in contaminant exposure and bioaccumulation among species. The objective of this experimentation was to investigate the relative importance of whole sediment, pore water, and overlying water bioaccumulation exposure pathways of PCBs to four phylogenetically and functionally distinct benthic macroinvertebrates by compartmentalizing their exposure using specially designed bio-boxes, hereafter referred to as PICs. Passive sampling devices (e.g., Polyethylene Devices, or PEDs) were

deployed simultaneously with study organisms to provide additional interpretative information on pore water exposure. PEDs were previously shown to provide good estimates of sediment pore water concentration of hydrophobic organic contaminants in both field (Adams et al 2007, Anderson et al 2008; Fernandez et al. 2009; Oen et al. 2011; Allan et al, 2012) and laboratory (e.g., Vinurella et al 2004; Gschwend et al. 2011; Charasse et al. 2014) investigations.

10.2 Materials and methods

10.2.1 Test sediments and chemicals

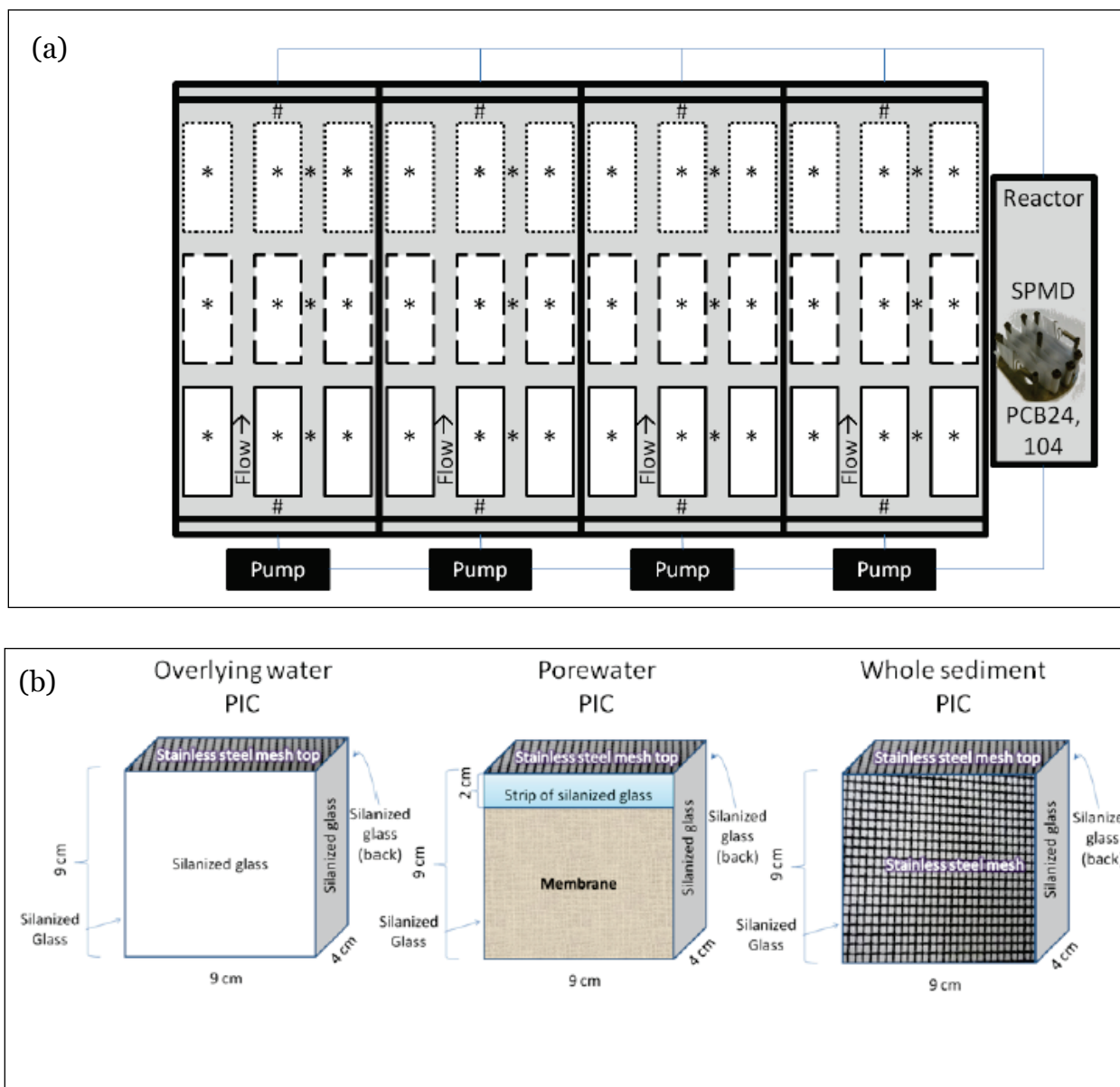
Sediment was collected from a tidal estuary in NBH in Massachusetts (Management Unit 29; 41.658509 °N; 70.913572 °W) and BNC in Washington State (Pier 7; 47.558780 °N; 122.628896 °W). The sediment tested was from a single, bulk collection and the entire amount of sediment was rehomogenized prior to each use. Both locations were listed as superfund sites due to high PCB concentrations. PCB congeners 24 (2,3,6-trichlorobiphenyl) and 104 (2,2',4,6,6'-pentachlorobiphenyl) were obtained from a commercial source (BZ#24, BZ#104 UltraScientific, N. Kingstown, RI, USA) for passive dosing into the overlying water. All analytical determinations were as described in Appendix A: Supporting Data (Table S1).

10.2.2 Exposure system

A recirculating exposure system was designed to contain experimental sediments and PICs that housed experimental organisms (Figure 30a). The system included four, five-gallon glass tanks that were silanized (5% dimethyldichlorosilane, Cat. No. 33065-U, Supelco, Sylon, CT) to reduce PCB sorption. Test sediment was carefully layered around PICs, taking care not to contaminate within the PIC chamber. Overlying seawater (25 ppt, Crystal Sea Marine Mix®, Enterprises International, Baltimore, MD, USA) was slowly added to a depth of five cm to avoid sediment suspension and recirculated at 3 ml/min through TFE tubing by piston pumps (Fluid Metering, Inc.). Recirculation included a divided 19.7 L ionized aluminum reactor box within which PCBs were passively dosed (described below). The system was equilibrated for approximately 90 days based on previously determined passive diffusion through a hydrophilic-coated TFE membrane that demonstrated the best available passive diffusion of hydrophobic-chlorinated compounds (Coleman et al, 2014). The exposure was

maintained at 20 ± 1 °C using a recirculating REMCOR heating/cooling unit (REMCOR Products Company, Glendale Heights, IL) with continuous fluorescent light to promote burrowing (as in USEPA 1994).

Figure 30. Diagram of exposure system and Pathway Isolation Chamber (PIC) design. Panel (a) provides an overview of the exposure system. The flow direction is indicated, with whole sediment (dotted border) PICs located downstream of pore water (dashed border) and overlying water (solid border) PICs to prevent contamination. Asterisks and number signs indicate positioning of polyethylene samplers in the sediment and overlying water, respectively. The solid phase membrane device (SPMD), which is the dosing device, is shown in the reactor to the right. A photograph of the in-use system is supplied in the SI (Figure S2). Panel (b) illustrates the individual PIC designs.



To isolate three different PCB exposure pathways from test sediments (overlying water, pore water, whole sediment), three types of PICs were designed. The PICs were 9 x 9 x 4 cm boxes (Figure 30b) constructed from 0.4 cm silanized glass panels sealed together with marine grade caulk (Starbrite, Montgomery, AL). Overlying water-pathway isolation chambers (OW-PICs) consisted of all glass sides with only the top open to exchange. Pore water pathway isolation chambers (PW-PICs) were equipped with a 9 x 9 cm hydrophilic-coated TFE membrane (1.0 μm , pore size, Millipore®, JAWP, P09025) caulked to one side in place of the glass, with other sides constructed of silanized glass. Since it is notoriously difficult to maintain PCB concentrations in water or pore water simulations (Alvarez 2010, Burgess and McKinney 1999, Carter and Suffet 1982), this PW-PIC design was intended to allow a continuous source of PCBs by maintaining equilibrium with the surrounding sediment through this previously validated membrane, which allowed the movement of DOC (Coleman et al, 2014). The OW and PW PICs were not only filled with low organic carbon content, <60 μm sand, to allow test organisms to burrow, but to also provide relatively low sorption potential for PCBs. SPME fibers placed into PW-PICs confirmed movement of PCBs from the surrounding sediment into the PIC compartment prior to addition of test organisms (supporting information (SI)). Finally, whole sediment pathway isolation chambers (WS-PICs) were filled with test sediment and equipped with a stainless steel mesh back, instead of glass, to allow exchange with the surrounding sediment. All PICs were covered with a stainless steel mesh screen tops and secured with marine grade, non-toxic caulk to contain test organisms. A TFE gasket was attached to the mesh top to hold a glass tube that extended through the mesh into the chamber and above the water surface, which was used for organism addition. The mesh top screen size was reduced from 1 mm to 0.5 mm for the BNC exposures since some *L. plumulosus* escaped from PICs during the NBH exposure (despite being retained on a 1 mm sieve). A photograph of the exposure system is provided in (Figure S2) located in the Supporting Information (SI) section of Appendix A.

10.2.3 Passive dosing of unique PCB congeners into overlying water

Two PCB congeners (24, 104) not detected in either test sediment were dosed into the overlying water to quantify the extent to which the OW-PIC contributed to overall contaminant exposure and tissue residues. Although still hydrophobic, these congeners represent relatively low to moderate log K_{ow} PCBs (5.35 and 5.81, respectively). A semi-permeable membrane device (SPMD) was used to passively dose PCB 24 and 104 into the water in basic

accordance with previous guidance (USEPA 2007). Briefly, 10 mg of PCB 24 and 104 were dissolved in hexane, which was reduced to approximately 1 ml with a stream of high purity nitrogen gas. This 1 ml of hexane containing PCBs was then layered on top of 1.0 g of glyceryl trioleate (triolein, Sigma-Aldrich Chemical Company, St. Louis, MO USA) in a glass vial. The hexane was then further evaporated using a stream of nitrogen gas. Just prior to complete evaporation of the hexane, the triolein and hexane was homogenized using a vortex mixer at high speed for three minutes. Then, a stream of nitrogen gas was used to completely evaporate the hexane in the hexane/triolein mixture, allowing the PCBs to partition into the triolein. The PCB and triolein were vortexed again to ensure homogenous mixture, and then evenly distributed within 100 cm sections of low-density polyethylene (LDPE) SPMD tubing (2.5 cm width, 100 µm wall thickness, Environmental Sampling Technologies, Inc., Mo., USA). The SPMD sections were heat sealed at each end and wrapped around a stainless steel rack, which was placed within the reactor (Figure 30, Figure S2). Water samples (120 ml) were taken from the system periodically and analyzed to confirm successful passive dosing of both congeners.

10.2.4 Study organisms

Four benthic macroinvertebrates were selected to represent a diversity of phyla (e.g., arthropods, annelids, and molluscs) and functional feeding strategies (e.g., surface deposit feeders, infaunal deposit feeders, and suspension feeders) while considering compatibility with experimental conditions, availability, and routine use in bioaccumulation assessments. The east coast amphipod *Leptocheirus plumulosus* (in-house laboratory cultures; 1.0 – 1.7 mm) was selected as a tube building, surface deposit feeder (USEPA 1994; ASTM 2010). It is routinely used in acute and chronic sediment toxicity assessments (USEPA 1994, USEPA/USACE 2001). In addition, the west coast amphipod *Eohaustorius estuarius* (field-collected by Northwest Aquatic Sciences, Newport, OR; 3 – 5 mm) was selected as a free burrowing, subsurface deposit feeder that is also used routinely in acute toxicity assessments (USEPA 1994; ASTM 2010). The east coast clam *Mercenaria mercenaria* (field collected; Aquatic Research Organisms, Hampton, NH; shell length of 15 – 20 mm) was selected as a suspension feeder that is partially removed from sediment porewater exposure due to its shell. This clam is used abundantly in aquaculture, and thus has direct human consumption relevance. Finally, the ubiquitous polychaete worm *Neanthes arenaceodentata* (laboratory cultured; Aquatic Toxicology Support, BNC, WA; 11–12 week old males)

was selected as a deep burrowing (0 to > 8 cm) and mucoid tube building, generalist deposit feeder (ASTM 2010; Millward et al 2005) that typically deposit feeds in the laboratory. Its soft body is directly exposed to the pore water. Male worms were selected to reduce lipid variability associated with female reproductive maturity. Relatively small animal sizes were chosen to allow loading into the exposure system and provide relatively rapid bioaccumulation (steady state).

10.2.5 Bioaccumulation exposures

Following the equilibration period, each of the four test organisms was added to nine PICs (3 OW, 3 PW, and 3 WS) held separately in the four glass tanks (Figure 30, Figure S2, SI). Plastic transfer pipettes were used to add 35 *L. plumulosus*, 35 *E. estuarius*, 5 *M. mercenaria* or 5 *N. arenaceodentata* to the equilibrated, in-place PICs using the previously described glass tubes for all species except *M. mercenaria*. Exposure durations were four days for amphipods and 28 days for worms and clams in accordance with steady state estimates for these organisms in NBH sediment (see section 12). Since preliminary observations revealed that *M. mercenaria* ceased siphoning after 3 to 5 days when food was absent, approximately 6,000 cells/ml of phytoplankton mixture (Phytoplex, Kent Marine, Franklin, WI) was added to the test system to maintain filter feeding. The exposures were conducted in basic accordance with ASTM (2010).

At the termination of each exposure, PICs were removed, and substrate within the boxes was sieved (0.6 mm stainless steel mesh) to recover organisms. Amphipods and worms were purged for six hours in 1 L beakers containing clean seawater. Soft bristle paintbrushes were used to push remaining undigested sediment from worm guts. Clams were dissected to remove undigested material and homogenized using a hand held tissue grinder made by Omni, which is located in Kennesaw, GA, USA. All tissue was thoroughly rinsed with deionized water, blotted, and frozen in 20 ml glass scintillation vials with TFE lid liners for analytical determination.

Despite aeration of the water, the 90-day equilibration period resulted in anoxic sediment in the NBH exposure that induced *L. plumulosus* to escape from whole sediment PICs (excluding overlying water PICs where there was no sediment exposure). *Eohaustorius estuarius* were too large to escape and died. Thus, to acquire tissue data, *L. plumulosus* and *E. estuarius* were

added to clam and worm PICs, respectively 4 days prior to the breakdown of those 28-day exposures. Anoxia was counteracted during the remainder of the NBH exposure and throughout the BNC exposure by inserting airlines with Pasteur pipettes to aerate directly over the PICs.

10.2.6 Passive sampler exposures

PED samplers, were constructed from commercially available polyethylene sheets (ACE Hardware Corp., Oak Brook, IL), and were cut down to 1x1 cm squares. PEDs were cleaned by soaking first in dichloromethane for 24 hours and then in methanol for 24 hours. The samplers were spiked with congeners 3, 14, 35, 69, and 88 (0.24 to 0.48 µg/L) in a 125 mL amber bottle for 30 days at the Massachusetts Institute of Technology, Parsons Laboratory (Cambridge, MA) and frozen until use. For both sediment experiments, PEDs were inserted < 1 cm into the substrate within the 36 PICs. In addition, each of the four tanks included PEDs placed outside of the PICs in the sediment (n = 3) and the overlying water (n = 2), as illustrated in Figure 30a. The PEDs were sampled from the exposure system at the same time as organism recovery, rinsed thoroughly with deionized water, and frozen in 20 ml glass scintillation vials with TFE lid liners for analytical determination. Data were generated as ng PCB/ mg PED, but expressed as ng/L to represent the freely dissolved fraction in the overlying water or pore water. No data were presented for PEDs in the *E. estuarius* chamber in the NBH experiment due to failure to obtain analytical data. PW concentrations in the *E. estuarius* chamber are expected to be similar to those in the *L. plumulosus* chamber.

10.2.7 Analytical

Sediment, passive samplers, water, and tissue samples were analyzed at the ERDC Environmental Chemistry Branch (Vicksburg, MS) for PCBs congeners following USEPA 846 methodology (method 3665). Tissue samples were analyzed for organics by a micro-analytical technique, described in Jones et al (2006). Lipid analysis was conducted using a colorimetric method (Van Handel 1985). This method was applied due to the small body size and mass of the study organisms, especially the amphipods, where only 10 mg or less was available for lipid determinations. The colorimetric method by Van Handel (1985) has been used routinely in bioavailability and bioaccumulation studies with aquatic invertebrates (e.g., Landrum et al. 2002, Beckingham et al. 2010; Ding et al 2013). No significant difference was found in lipid determination when lipid content

was measured using colorimetric method and compared to results obtained using a macro-gravimetric method (Inouye and Lotufo 2006; Cheng et al. 2011). Since tissue recovery was insufficient to perform lipid analysis, lipid content for *N. arenaceodentata* was from Lotufo et al (2000).

10.2.8 Data analysis

All statistical comparisons and determinations of data normality (Kolmogorov-Smirnov test) and homogeneity (Levene's test) were performed using SigmaStat v3.5 software (SSPS, Chicago, IL, USA). One-way, two-way (factors: organism vs. exposure pathway), and three-way (PED location vs. PED exposure tank vs. exposure pathway) ANOVAs were performed to determine statistically significant differences ($\alpha = 0.05$). If data failed normality or homogeneity tests, \log_{10} or square root transformations were performed. The Holm-Sidak method was employed as an all-pairwise multiple comparison procedure to determine statistical significance in bioaccumulation between different organisms and exposure pathways. Bioaccumulation factors (BAFs) and biota-to-sediment accumulation factors (BSAFs) were calculated as described in ASTM (2010). Lipid normalized concentrations were determined by dividing bulk tissue concentration by the organism sample-specific fraction lipid content (data were expressed as mg PCB/kg lipid). Pore water Bioconcentration Factors (PW-BCFs) were determined by dividing tissue concentration for a single congener by the PED-estimated PW concentration for that same congener.

10.3 Results and discussion

10.3.1 Exposure condition summary

This investigation considered how three different exposure pathways (i.e., whole sediment, pore water, and overlying water) impacted bioaccumulation of PCBs into the tissues of four phylogenetically and functionally different benthic organisms. To aid interpretation of the tissue bioaccumulation data relative to the exposure pathways, information on the measured exposure conditions is presented first. Whole sediment characteristics, whole sediment congener concentrations, PED estimates of dissolved congener concentrations in pore water provide relevant information to the WS and PW pathways. In addition, total measured and PED-determined dissolved concentrations of PCB 24/104 in the water are provided for interpretation of the OW exposure pathway.

10.3.1.1 Sediment chemistry and characteristics

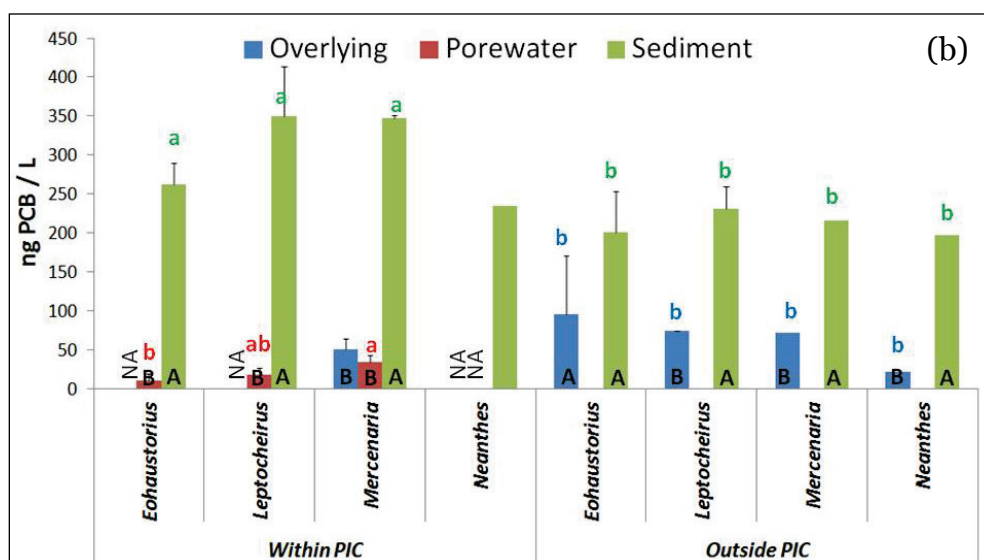
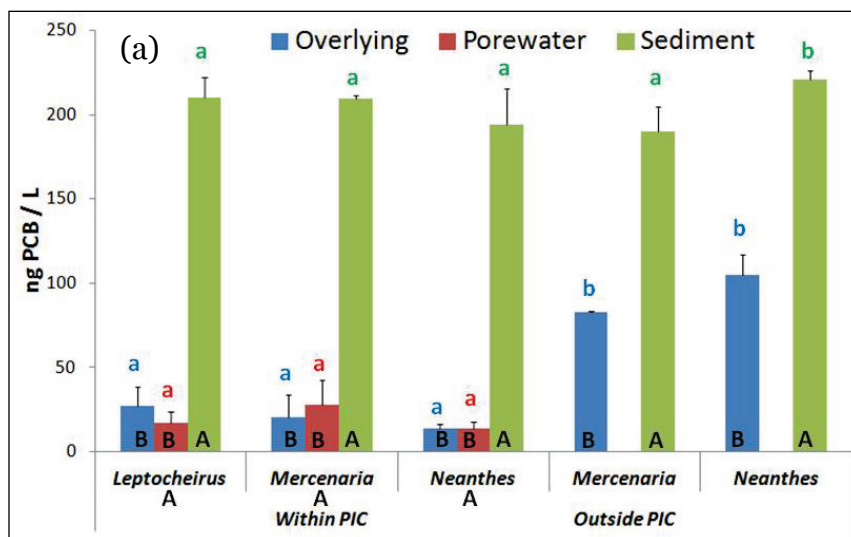
Generally, the NBH sediment contained higher PCB concentrations and more, lower log K_{ow} congeners. Sum PCB congener (Σ PCB) concentrations of the NBH and BNC sediments were 33.7 and 16.6 mg/kg, respectively. However, the TOC of NBH (6.4%) was considerably higher than BNC (1.0%), suggesting lower bioavailability potential of sediment-associated PCBs. In the NBH sediment, mono- to tri-, tetra- to penta-, and hexa- to nona-chlorinated congeners made up 28, 61, and 12%, respectively, of all congeners. The BNC sediment generally contained a larger proportion of higher, log K_{ow} congeners, with mono- to tri-, tetra- to penta-, and hexa- to nona-chlorinated congeners which make up 2, 68, and 30%, respectively, of all congeners. The BNC sediment (3% gravel, 70% sand, 16% silt, and 11% clay) contained more coarse material than the NBH sediment (1% gravel, 42% sand, 50% silt, and 7% clay). Greater sand content has implications on burrowing behavior and health of certain organisms (Emery et al 1997) and infiltration of OW (discussed below). A detailed summary of sediment characteristics (Table 20) and full congener distributions and concentrations (Figure S3, SI) are available.

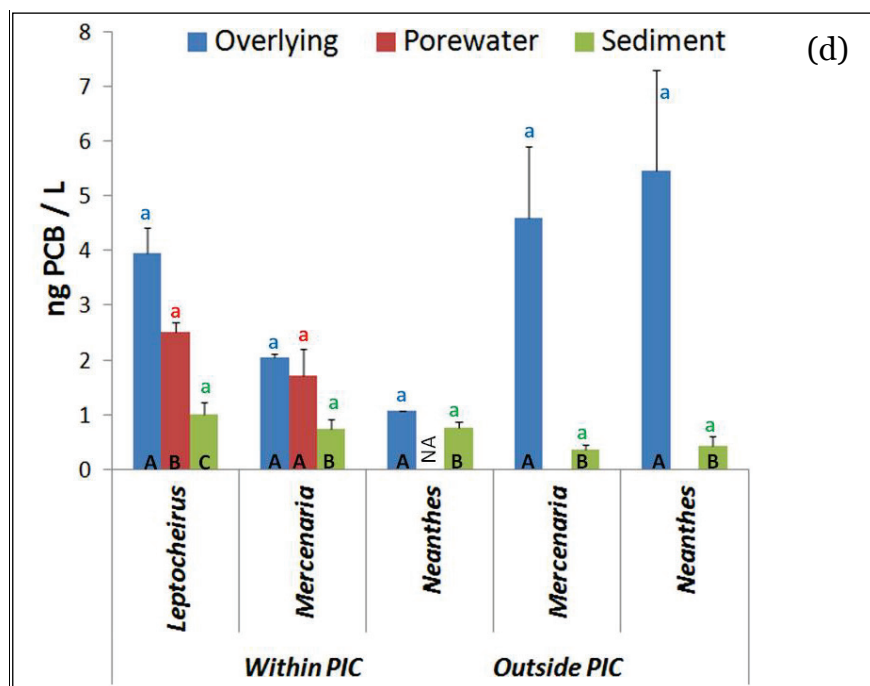
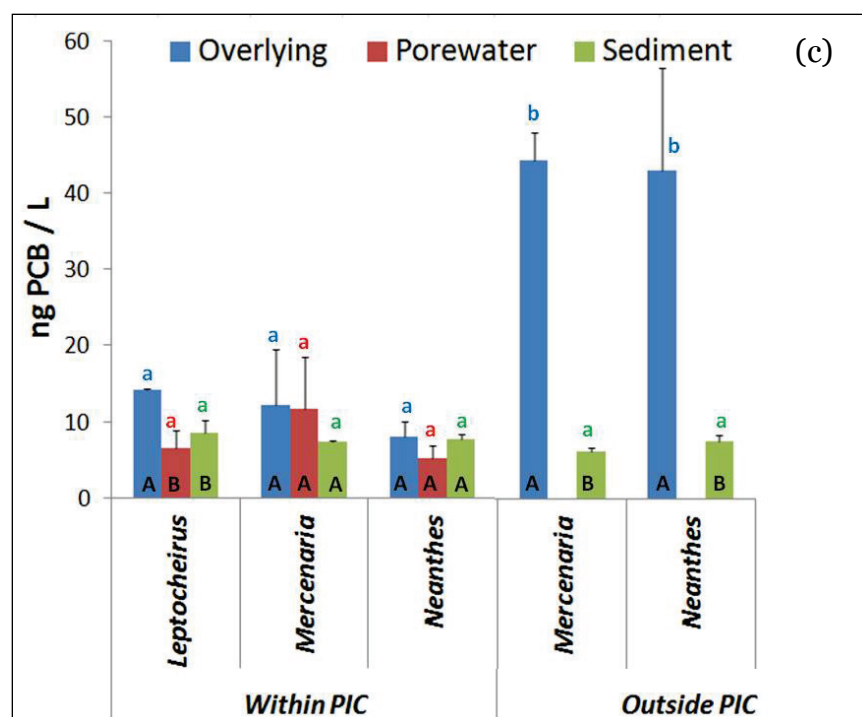
10.3.1.2 Estimated pore water exposure

PEDs were deployed as in Figure 30, analyzed and used to estimate dissolved congener concentrations within the three PIC types. PED-estimated concentrations of Σ PCB in PW were statistically significantly higher in the WS-PICs, relative to the PW-PICs and OW-PICs for both the NBH sediment (Figure 31a) and the BNC (Figure 31b) sediment exposures. The PW concentrations of Σ PCB in the BNC WS-PICs (range: 234 – 350 ng/L) were higher than in the NBH WS-PICs (range: 194 – 210), despite higher Σ PCB in the NBH sediment. This is likely related to six-fold higher TOC in the NBH sediment and suggests relatively greater potential for biological uptake from exposure to the BNC sediment. PW concentrations were statistically similar (two-way ANOVA; PIC type X organism) within each PIC type between the four tanks organisms were exposed in, suggesting that the different test organisms were exposed to similar PW conditions. PW concentrations in the WS did not differ in the NBH exposure between the WS-PICs and the sediment surrounding the PICs; however, PW concentrations in the BNC within the WS-PICs were slightly but significantly higher than in the surrounding sediment. Comparison between organisms exposed in the WS-PICs is valid since PW conditions were statistically similar within the PICs for both sediment exposures (Figure 31a,b).

Figure 31. Dissolved concentrations predicted from analysis of polyethylene devices (PEDs). Results are separated on the X-axis by PEDs placed inside the pathway isolations chambers (within PIC) and PEDs placed outside the PICs in the sediment or in the overlying water (outside PIC). Results are presented as (a) NBH sediment sum congeners, (b) BNC sediment sum congeners, (c) NBH PCB 24, (d) NBH PCB104.

PCB24/104 were delivered to the overlying water. Bars with the same letter designation were not statistically significant. Black capital letters represent statistical comparisons within each organism tank. Lower case letters represent statistical comparisons of the same pathway (designated by color) across organism tanks.





In addition to the PED-mediated estimates of PW concentrations, an attempt was made to create a unique exposure where organisms were directly exposed to PW with sediment particles excluded; thus, the PW-PICs equipped with TFE membrane were intended to create a combined PW and OW exposure. Deployment and temporal sampling of SPME fibers (placed 1 cm into the sand) during the 90 d equilibration of the PW-PICs

in the NBH sediment provided initial validation of a gradual increase of select congeners in the PW-PICs (Figure S1, SI). Higher concentrations of lower log K_{ow} congeners were observed in the PW-PICs, as expected due to greater mobility (Burgess and McKinney 1999). Previous supportive work provided evidence that passive diffusion of chlorinated hydrocarbons, including molecules associated with DOC, though the TFE membrane occurred in both water and sand systems (Coleman et al 2014). However, comparison of the PED estimates of PW congener concentrations of the OW-PICs and the PW-PICs showed that they were statistically similar for both the NBH sediment (Figure 31a) and the BNC sediment (Figure 31b). These PED data suggest the PW-PICs did not create a unique PW exposure for test organisms. This may be explained by the requirement to increase the size of the PICs relative to what was used in Coleman et al (2014) to support organism life in this study; smaller chambers lead to high 10 day *L. plumulosus* mortality (SERDP ER-1750, unpublished data). Since congeners other than PCB24 and 104 were also observed in PEs placed in the OW-PICs (all glass sides), the temporal increases in congener concentrations in the pre-exposure SPME fibers were likely related to congener movement from the sediment through the OW pathway (via the mesh lids). Estimated overlying water exposure

A preliminary experiment performed in the exposure system without sediment confirmed successful dosing of PCB 24 and 104 into seawater, which also showed a gradual increase in concentrations to equilibrium observed over time (Table S5). The concentrations of PCB24/104 were approximately 70 to 80% lower in the organism exposures that included NBH or BNC sediment (Table S5). This is not surprising due to sorption with the surficial sediment that was not in the preliminary water-only validation study. Also as expected, concentrations of the less hydrophobic (lower log K_{ow}) PCB24 were 7.4-fold (NBH) to 6.8-fold (BNC) higher than PCB104 in the water. Similarly, Burgess and McKinney (1999) reported that only low and some medium molecular weight congeners were maintained and measured in OW. Concentrations of PCB24/104 were generally comparable between the NBH and BNC experiments, though more variable in the BNC experiment.

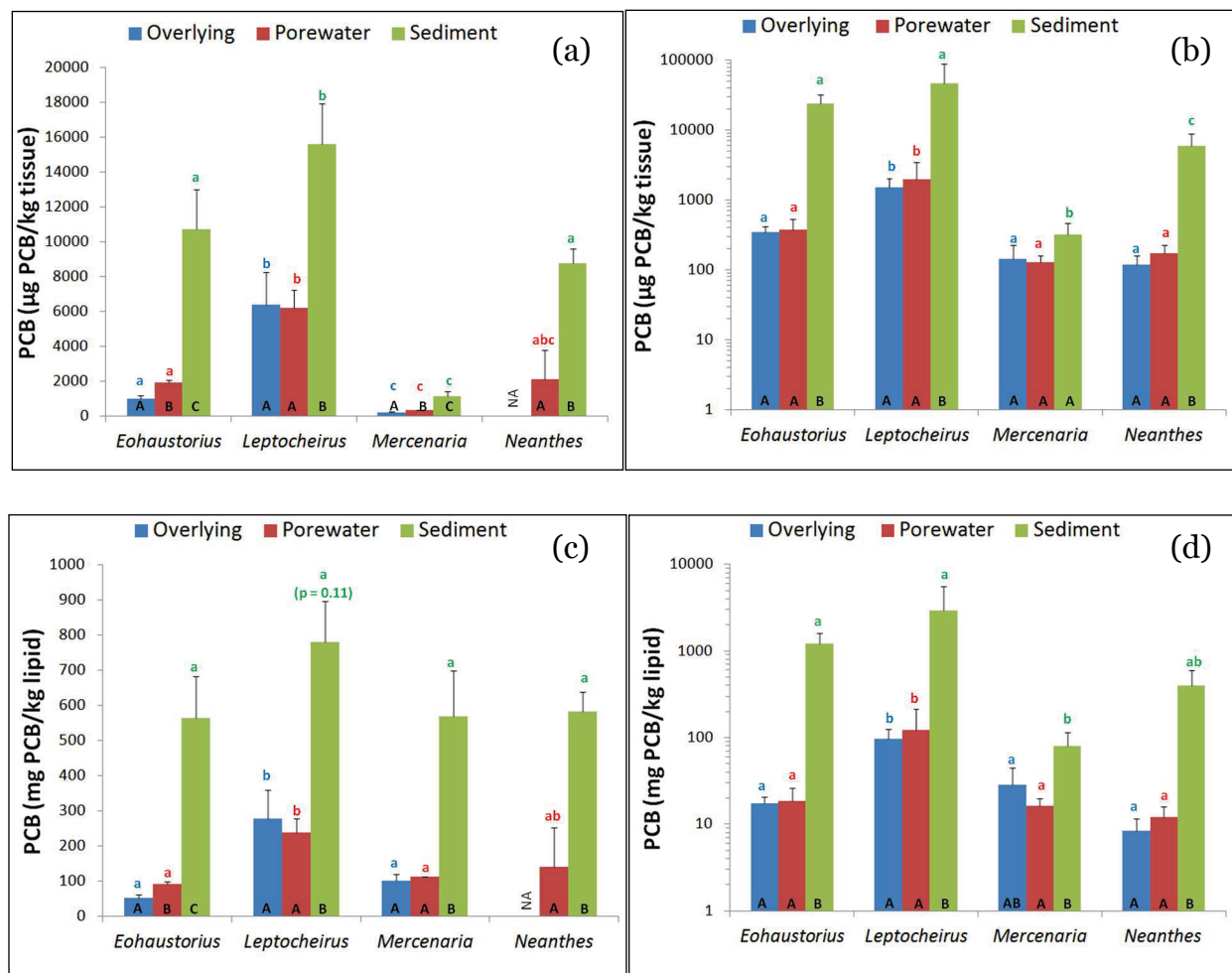
PEDs placed in the OW also confirmed the presence of dissolved PCB24/104 concentrations in both the water and within the three different PIC types for both sediment exposures (Figure 31c,d). In the NBH exposure, PCB24 concentrations were statistically similar within each type of PIC

(Figure 31c). Further, PCB24 concentrations were generally statistically similar across the different types of PICs. These data provide evidence that the four organisms received similar OW exposure conditions. PCB24/104 concentrations were significantly higher in the water above the OW-PICs (Figure 31c,d). This is likely due to placement of the PEDs 1 cm below the sand surface in the OW-PICs, resulting in lower direct exposure to the water. Results for PCB104 were similar to PCB24 in the NBH exposure (Figure 31d). Within the BNC exposure, analysis of PEDs also confirmed dissolved concentrations of PCB24/104 in both the OW and within the PICs (Figure S5). While trends discussed above for NBH (e.g., higher concentrations in water, OW-PICs and PW-PICs relative to WS-PICs and statistically similar PCB24/104 concentrations within each PIC type) generally held for BNC, larger data variability was apparent that precluded some comparisons. Generally, there was less difference in concentration between the OW-PICs (containing sand) and the WS-PICs, likely because the BNC consisted of a greater amount of coarser grained particles (Figure S5) that allowed more infiltration of PCB24/104 from the overlying water; this trend was most notable for PCB104 (Figure S5). These data in combination with total concentrations directly measured in the water (Table S5) confirm the successful dosing of PCB24/104 in the water and validity of comparison between species (species were generally exposed to similar conditions).

10.3.2 Bioaccumulation

Sufficient tissue was recovered for analytical determination of PCB residues in both sediment exposures with the exception of the *N. arenaceodentata* OW-PICs (NBH experiment). Generally, all four organisms in both sediment exposures accumulated significantly higher Σ PCB concentrations from the WS-PICs, followed by the PW-PICs and OW-PICs (Figure 32a, b). This is logical since the sediment PICs theoretically included three pathways (i.e., particle, PW, and OW), while PW-PICs theoretically included two pathways (i.e., PW and OW), and the OW-PICs included only one pathway (OW). However, the previously discussed PED-derived PW concentrations (Figure 31a, b) suggest the PW-PIC provided a similar exposure as the OW-PICs (i.e., OW only). Amphipods accumulated significantly higher Σ PCB than *N. arenaceodentata* while *M. mercenaria* accumulated significantly lower concentrations than other species. PCB24/104 concentrations were statistically higher in the PW and for tissue exposed within the OW-PICs and PW-PICs relative to the WS-PICs, likely due to higher porosity of the <60 μ m sand (used in both the OW-PICs and PW-PICs) and consequently greater OW infiltration.

Figure 32. Sum PCB congeners in organism tissue exposure in different pathway isolation chambers. Sum congeners in bulk tissue residues are presented for the (a) NBH and (b) BNC sediment exposures. In addition, lipid-normalized tissue residues are presented for (a) NBH and (b) BNC sediment exposures. Data for BNC sediment are presented on a log scale. Letter designations were previously described in Figure 31.



10.3.3 Bioaccumulation of sediment-associated congeners

PCB tissue residue data are presented first as bulk tissue to relate general differences in uptake between organisms. Then lipid-normalized tissue residues, BAFs and BSAFs are presented to discuss the role of organism specific attributes and sediment characteristics for determining bioaccumulation. Finally, differences in lipid-normalized residues between organisms for three PCB homolog groups are discussed. Two-way ANOVA (organism X PIC, Σ PCB) indicated *L. plumulosus* bioaccumulated the highest Σ PCB concentrations in bulk tissue from all PICs (both sediment exposures), followed by *E. estuarii*, *N. arenaceodentata* and *M. mercenaria* (Figure 32a, b). Since the focus of this section was bioaccumulation of congeners associated with the sediment, congeners delivered to the OW (PCB24/104) were excluded.

10.3.3.1 Whole sediment exposure

As expected, the whole sediment exposure (WS-PICs, both sediments) led to significantly higher bulk tissue concentrations in all four organisms (Figure 32) relative to the PW-PICs and OW-PICs. While statistically similar PED estimates of sediment PW concentrations indicated exposure conditions were successfully replicated in the WS-PICs within the four tanks (Figure 31a,b), significant differences in bulk tissue residues indicated organism-specific differences in PCB uptake in both the NBH (Figure 32a) and BNC sediments (Figure 32b) *L. plumulosus* > *E. estuarius* ≥ *N. arenaceodentata* > *M. mercenaria*. Other studies support that benthic deposit feeders accumulate more hydrocarbons than benthic filter feeders (Lake et al 1990, Kaag et al 1997, Hickey et al 1995, Burgess and McKinney 1999), as observed for *M. mercenaria* in this study. While overlying water is critical for filter feeding clams, it was previously noted that exposure to bedded sediment still contributes rather significantly to the tissue residues of filter feeding clams (Lohmann 2004). While others have reported that surface deposit feeders (e.g., *Macoma* spp. clams) bioaccumulate intermediate contaminant concentrations between bulk deposit feeders (e.g., polychaete worms) and filter feeders (Kaag et al 1997), which was not the case in this investigation as the surface deposit-feeding *L. plumulosus* accumulated the highest residues.

Interspecific differences in ΣPCB bioaccumulation could be at least partially accounted for by differences in lipid content (Figure 32c, d), with the exception of *M. mercenaria* (in the BNC exposure). Lipid normalization better standardized tissue residues in the NBH exposure, where lipid normalization resulted in statistically similar ΣPCB concentrations in *E. estuarius*, *N. arenaceodentata*, and *M. mercenaria*; only *L. plumulosus* lipid normalized residues remained significantly higher (Figure 32a), suggesting this amphipod experienced a unique exposure to the WS. Lipid normalization failed to standardize tissue residues between the two project sediments, suggesting sediment specific attributes were important (e.g., grain size, TOC, see discussion below). The clam bioaccumulated significantly lower lipid-normalized concentrations than the other organisms in the BNC WS-PICs. While the amphipods had much higher lipid normalized concentrations than *N. arenaceodentata* in the BNC sediment exposure, these differences were not statistically different (Figure 32b). Millward et al (2005) reported that *L. plumulosus* bioaccumulated 4.5 times more PCBs from WS than *N. arenaceodentata* on a lipid normalized basis. In the current investigation, *L. plumulosus* also accumulated more PCBs from WS,

though the difference between organisms was much less in NBH (1.3 times) and higher in BNC (7.4 times). This again reinforces the importance of the aforementioned sediment attributes other than bulk PCB concentration.

Statistical analysis of accumulation factors confirmed amphipods generally bioaccumulated greater concentrations of Σ PCBs into bulk tissue than *N. arenaceodentata* in both sediment exposures, while *M. mercenaria* consistently had the lowest BAFs (Figure 33a). Accumulation of Σ PCBs was significantly higher in amphipod tissue in the BNC sediment exposure relative to the NBH exposure. This likely was related to the higher TOC concentration of NBH reducing bioavailability. The higher Σ PCB concentrations in PW for the BNC relative to the NBH sediment (Figure 31a, b; green bars) supports this conclusion. Statistically similar BSAFs between organisms exposed in the WS-PICs for both sediments suggested much of the variability in bioaccumulation observed between species (Figure 32) could be accounted for by differences in tissue lipid content and sediment TOC (Figure 33b). The exception was for *M. mercenaria* exposed to the whole BNC sediment, where BSAFs were significantly lower than other organisms. This difference may relate to the larger grain size and lower concentrations of lower, log K_{ow} congeners in the BNC sediment PW. Sum PED-estimated PW concentrations were actually slightly higher in the WS-PICs for BNC sediment relative to the NBH sediment; lower uptake by the clam may be attributed to the shell reducing direct tissue contact with surrounding sediment and PW. The OW exposure pathway was also important to *M. mercenaria* exposed to the BNC sediment (see Section 13.3.4).

The relative importance of PCB homolog groups (i.e., degree of PCB congener chlorination and hydrophobicity) for determining bioaccumulation potential from sediment (WS-PICs) was also determined on a lipid-normalized basis. Tissue residues for all species were generally greater for the mono- to tri-chlorinated congeners in the NBH sediment (Figure 34), which contained relatively higher concentrations of these congeners (Table 20). However, tetra- to penta-chlorinated and the hexa to nona-chlorinated congeners in tissue were greater in the BNC sediment exposure, likely related to the much lower TOC of this sediment. Hexa to nona-chlorinated congeners, in particular, were much lower in organisms exposed to the NBH sediment despite similar concentrations in sediment (Table 20) suggesting low bioavailability (i.e., high TOC).

Figure 33. Summary of bioaccumulation factors for animals exposed to whole sediment. Panel (a) provides sediment BAFs and panel (b) provides BSAFs for each test organism exposed in the NBH and BNC whole sediment PICs. Panel (c) provides BSAFs for homolog groups. Letter designations were previously described in Figure 31.

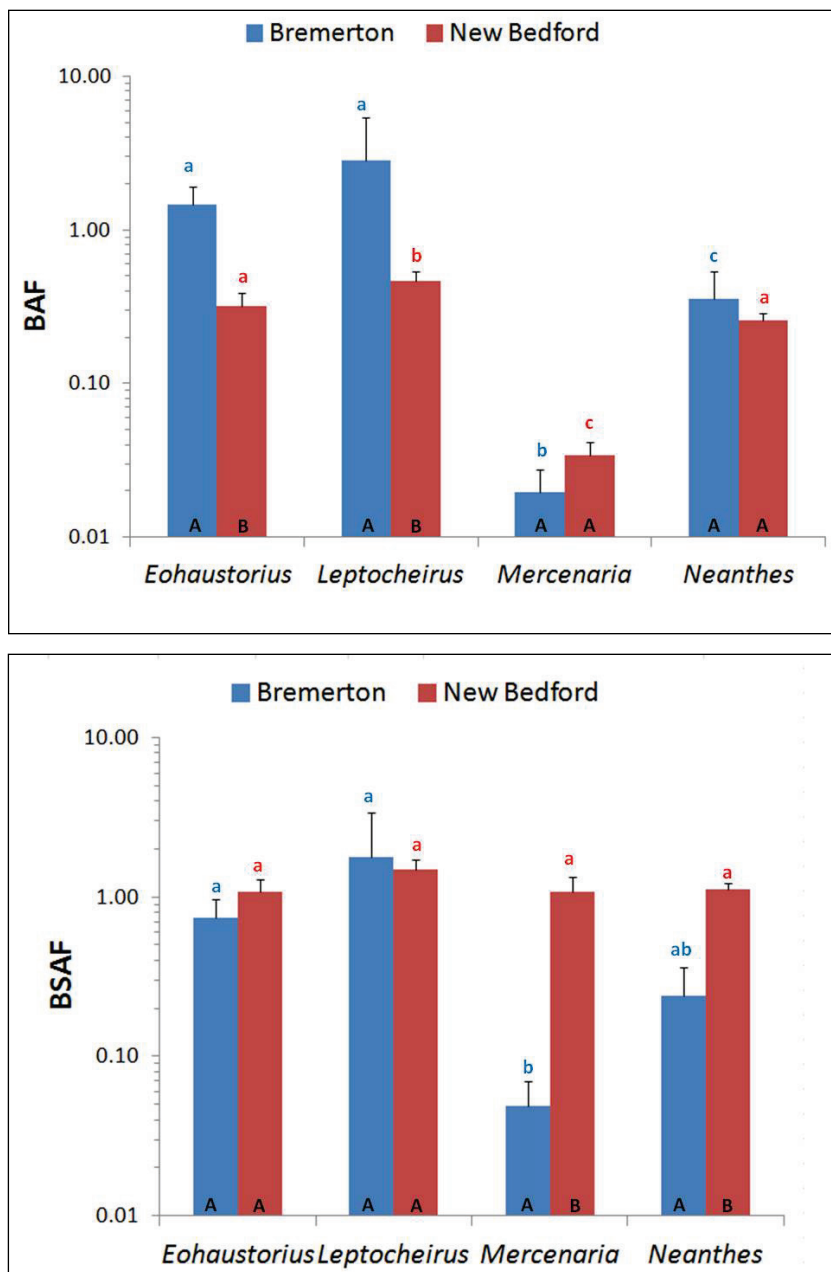
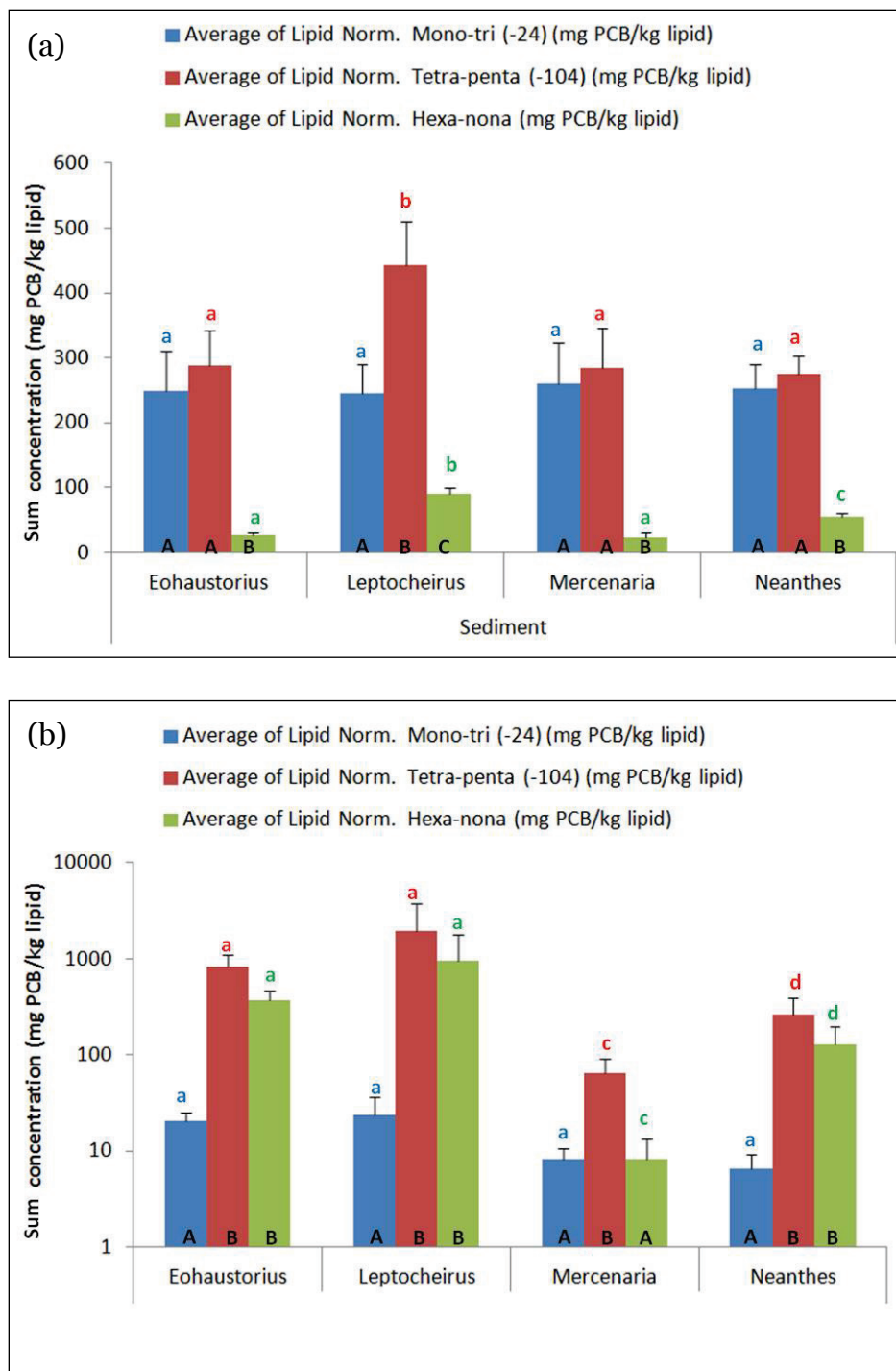


Figure 34. Lipid normalized tissue residues by homolog group for organisms exposed in the whole sediment pathway isolation chambers (PICs). Data area presented for (a) NBH and (b) BNC sediments. BSAFs for homolog groups are presented in the panel (c). Letter designations were previously described in Figure 31.



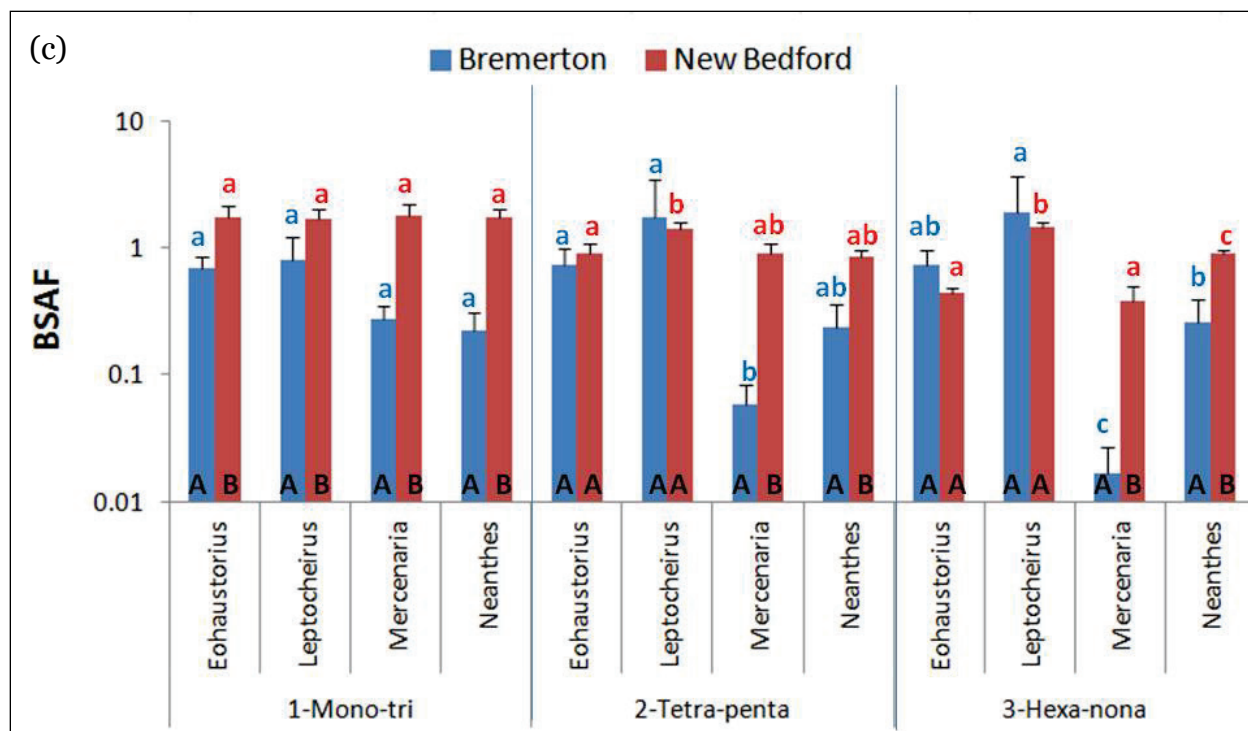


Table 19. Summary of the relative importance of different exposure pathways for the study organisms.

Organism	Importance of pathway for total bioaccumulation			
	Overlying	Whole sediment	Pore water	Sediment particles
<i>Eohaustorius</i>	Low	High	High	Low
<i>Leptocheirus</i>	Medium	High	High	High
<i>Mercenaria</i>	High	High	Medium	Medium*
<i>Neanthes</i>	Very low	High	High	NA

* only if particles are suspended in the water column

Supporting information in Appendix A: Supporting Data.

Table 20. Summary of sediment chemistry and characteristics.

Analysis	New Bedford	Bremerton
Sum PCBs (mg/kg)	33.7	16.6
Mono- to tri-chlorinated congeners (mg/kg)	9.3	0.3
Tetra- to penta-chlorinated congeners (mg/kg)	20.4	11.2
Hexa- to nona-chlorinated congeners (mg/kg)	4.0	5.0
Mono- to tri-chlorinated congeners (% of total)	28	2
Tetra- to penta-chlorinated congeners (% of total)	61	68
Hexa- to nona-chlorinated congeners (% of total)	12	30
Total organic carbon (%TOC)	6.4	1.0
Solids (%)	58.2	40.6
Clay (%)	7.0	11.3
Silt (%)	49.8	16.1
Sand (%)	42.2	69.5
<i>Fine sand (%)</i>	31.9	26.6
<i>Medium sand (%)</i>	8.3	27.2
<i>Coarse sand (%)</i>	2.0	15.7
Gravel (%)	1.0	3.1

Within both sediment exposures, all organisms bioaccumulated similar levels of mono- to tri-chlorinated congeners on a lipid-normalized basis (Figure 34). However, amphipods accumulated significantly higher lipid-normalized tissue residues of tetra- to penta-chlorinated and hexa to nona-chlorinated congeners than the clam and worm in both sediment exposures. In particular, *L. plumulosus* accumulated higher levels than *E. estuarius* in both sediments; this was statistically significant in the NBH exposure. These data support that amphipods, in particular *L. plumulosus*, were more exposed to the more hydrophobic (higher, low K_{ow}) congeners (less likely to partition to PW). Homolog specific BSAFs (Figure 34c) reduced differences between organisms exposed to the two different sediments, although the mono- to tri-chlorinated congener BSAFs were still significantly higher for all species in the NBH sediment. BSAFs for the higher log K_{ow} groups were significantly higher for the BNC sediment for clams and worms, but not amphipods (Figure 33c). No significant differences were observed for mono- to tri-chlorinated congeners in either sediment, suggesting less hydrophobic congeners bioaccumulated similarly across species. This provides evidence that PW concentrations are most important for determining bioaccumulation of this homolog group (see Section 13.3.3.2).

As previously discussed for lipid-normalized homolog tissue residues, BSAFs for the two higher log, K_{ow} groups were greater for amphipods (in particular *L. plumulosus*) relative to clams and worms. Statistically significant differences were found between some species for the tetra- to penta-chlorinated group while for the hexa- to nona-chlorinated group *L. plumulosus* BSAFs were consistently significantly greater than BSAFs for clams and worms.

These data suggest that all organisms are exposed similarly to less hydrophobic congeners (likely through the PW); however, *L. plumulosus* had higher exposure in the whole sediments than the other animals (albeit the other amphipod, *E. estuarius*, was similar, but trended lower). The authors speculated that the surface deposit feeding *L. plumulosus* directly consumed surface particles containing more hydrophobic PCBs less likely to partition to the PW. The clam had significantly lower lipid normalized residues and BSAFs for the more hydrophobic congeners than all other test species, indicating lower exposure through direct contact with sediment particles or through ingestion. This is logical as the shell protects the clam, and the clam suspension feeds from the OW (as long as it does not ingest high loads of resuspended sediment particles, which were not likely in the experiments). Overall, lipid and TOC appeared to normalize differences in bioaccumulation of lower, log K_{ow} homologs, while significant differences between species were apparent for higher, log K_{ow} groups.

10.3.3.2 Pore water exposure

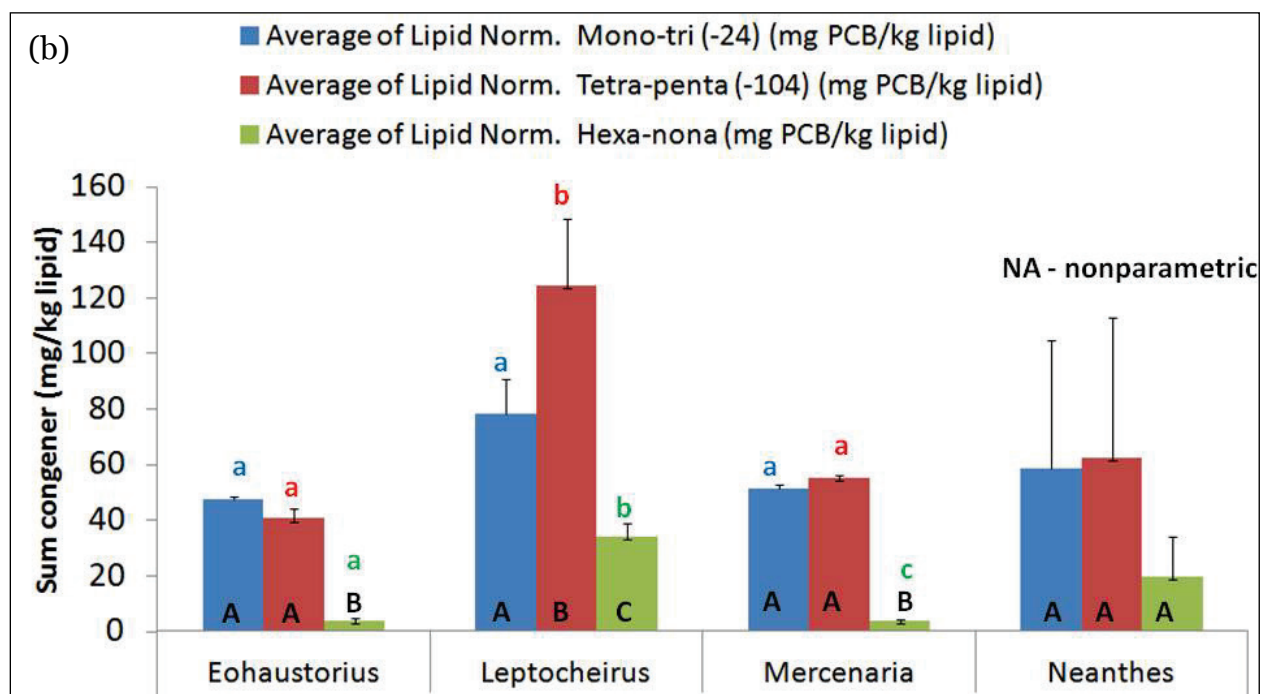
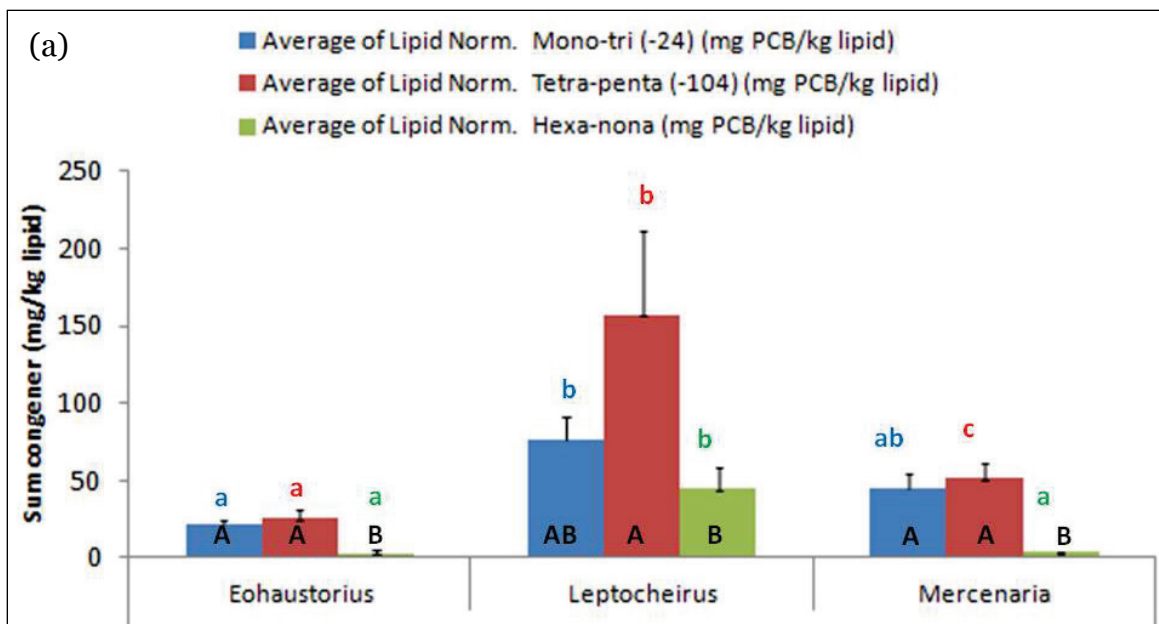
Here, we compare tissue residues in the PW-PICs to the WS-PICs to determine if sediment PW concentrations were successfully created in the PW-PICs. Next, we compare tissue residues in the PW-PICs to the OW-PICs to determine if the membrane created a unique PW exposure. Based on the exposure data (PED-estimated PW concentrations; Figure 31), the PW-PICs did not reproduce the PW concentrations of the WS-PICs; the PW-PIC concentrations were significantly lower. Further, the PW-PICs did not contain significantly higher PW concentration PCBs than the OW-PICs. However, statistically significantly higher bulk and lipid-normalized Σ PCB tissue residues for *E. estuarius* were found in the PW-PICs relative to the OW-PICs in the NBH exposure (Figure 32a,c), which suggests that PW-PICs at least partially accomplished the goal of exposing animals to a unique PW exposure. Bulk *M. mercenaria* tissue residues were also significantly elevated in the PW-PICs; however, this trend did not hold after lipid normalization for either sediment exposure. No significant

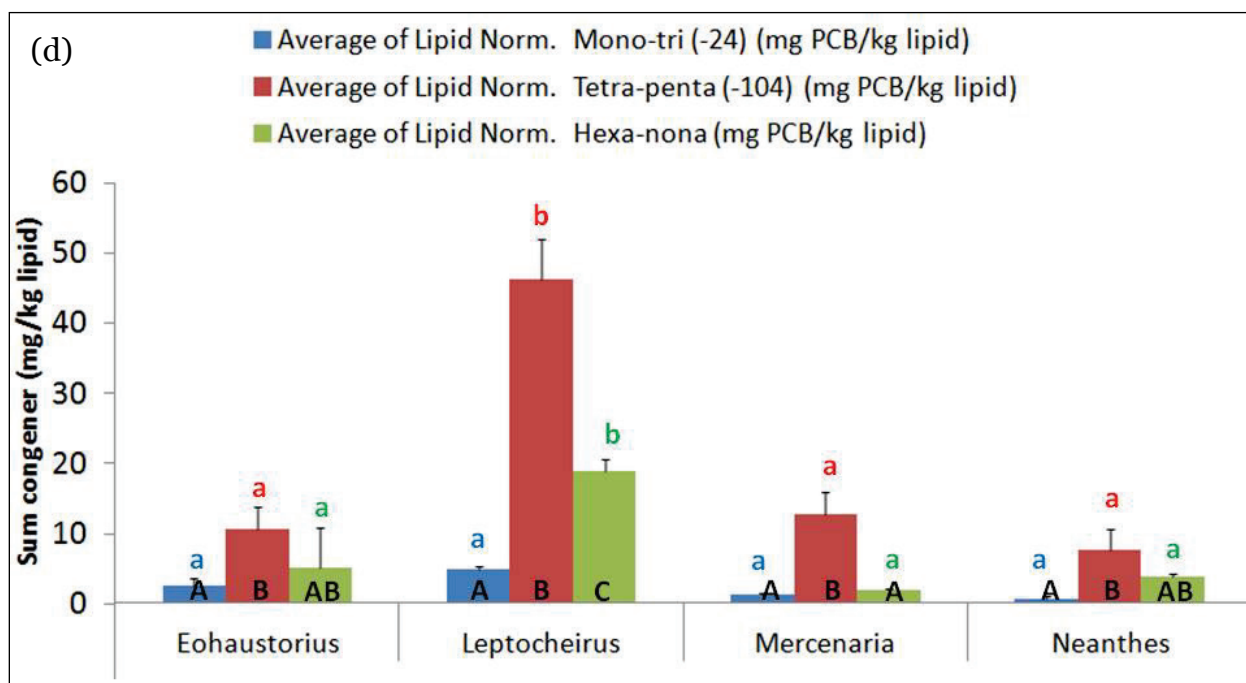
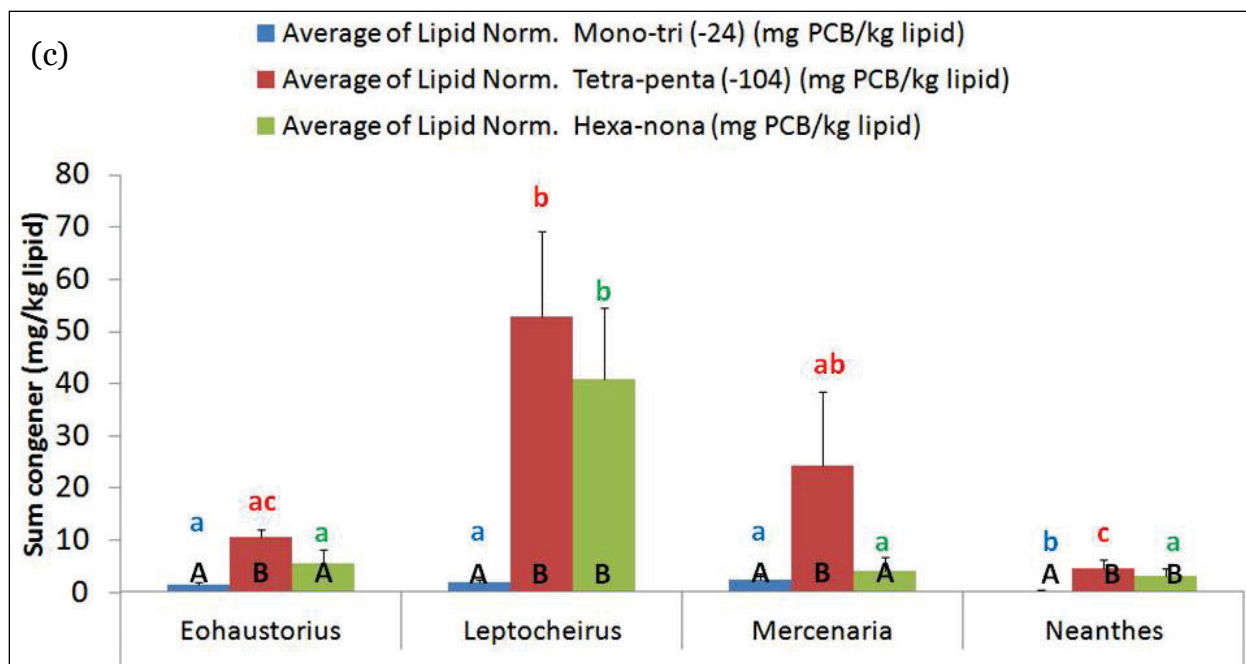
differences were found between PW-PICs and OW-PICs for *L. plumulosus* or *N. arenaceodentata*, nor were significant differences found for any test organism in the BNC exposure (Figure 32b, d). Comparison of homolog groups in the lipid normalized tissue residues of the four organisms exposed in the PW-PICs and OW-PICs (Figure 35) suggests similar bioaccumulation patterns for *L. plumulosus*, *M. mercenaria*, and *N. arenaceodentata* were acquired between these two PIC types. However, *E. estuarius* again bioaccumulated significantly higher lipid-normalized residues of both mono- to tri- and tetra- to penta-chlorinated congeners in the NBH exposure in the PW-PICs relative to the OW-PICs, while hexa- to nona-chlorinated (higher log K_{ow}) congeners were not different. While PED-estimates of PW concentrations indicate no differences between these PICs, elevated *E. estuarius* tissue residue suggest a unique exposure occurred in the PW-PICs.

These experimental data provide somewhat conflicting results between the PED-estimated PW concentrations and tissue data set; overall, there was not strong evidence that the PW-PICs consistently created a unique PW-only exposure throughout the entire area of the PIC after comparison with residues in organisms exposed within the OW-PICs. While passive movement of PCBs through the membrane was clearly shown in a smaller version of the PIC (Coleman et al 2014), this result was likely not replicated in this study due to the need for larger PICs to support animal health (high mortality was observed in smaller PIC chambers; SERDP ER-1750, unpublished data).

Thus, to make conclusions regarding the relative importance of the PW pathway for the study organisms, researchers must follow a multiple line of evidence approach. This included comparison of different sediment homolog groups in the different PICs and comparing PW-BCF values. As previously discussed in Section 13.3.3.1, all four test organisms bioaccumulated similar tissue residues of the two lower log K_{ow} homolog groups (mono- to tri- and tetra- to penta-chlorinated congeners) that were expected to more readily partition to the PW (Figure 34), while *L. plumulosus* bioaccumulated significantly greater tissue residues of the higher low K_{ow} homolog group (hexa- to nona-chlorinated congeners). This result may suggest that the four study organisms are exposed to sediment PW similarly, while *L. plumulosus* has a unique exposure to higher log K_{ow} congeners (e.g., through a route of exposure other than PW, such as direct particle exposure / consumption). However, the surface

Figure 35. Lipid normalized tissue residues by homolog group for organisms exposed in the overlying water and pore water pathway isolation chambers (PICs). Data for the NBH experiment are presented for the (a) overlying water PICs and (b) pore water PICs. Data for the BNC experiment are presented for the (c) overlying water PICs and (d) pore water PICs. Letter designations were previously described in Figure 31.





deposit-feeder *L. plumulosus* also had significantly higher levels of the two higher low K_{ow} homolog groups than the other test organisms in both the PW-PICs and OW-PICs where sediment particles were absent (Figure 35). This suggests that *L. plumulosus* is either a more efficient bioaccumulator of higher low K_{ow} PCBs, or this surface deposit-feeding amphipod was more exposed to surface deposits on the sand surface where the deeper-burrowing sediment feeding species (*E. estuarius*, *N. arenaceodentata*)

were less exposed. On the other hand, the clam was shielded by its shell or simply did not feed from the surficial substrate.

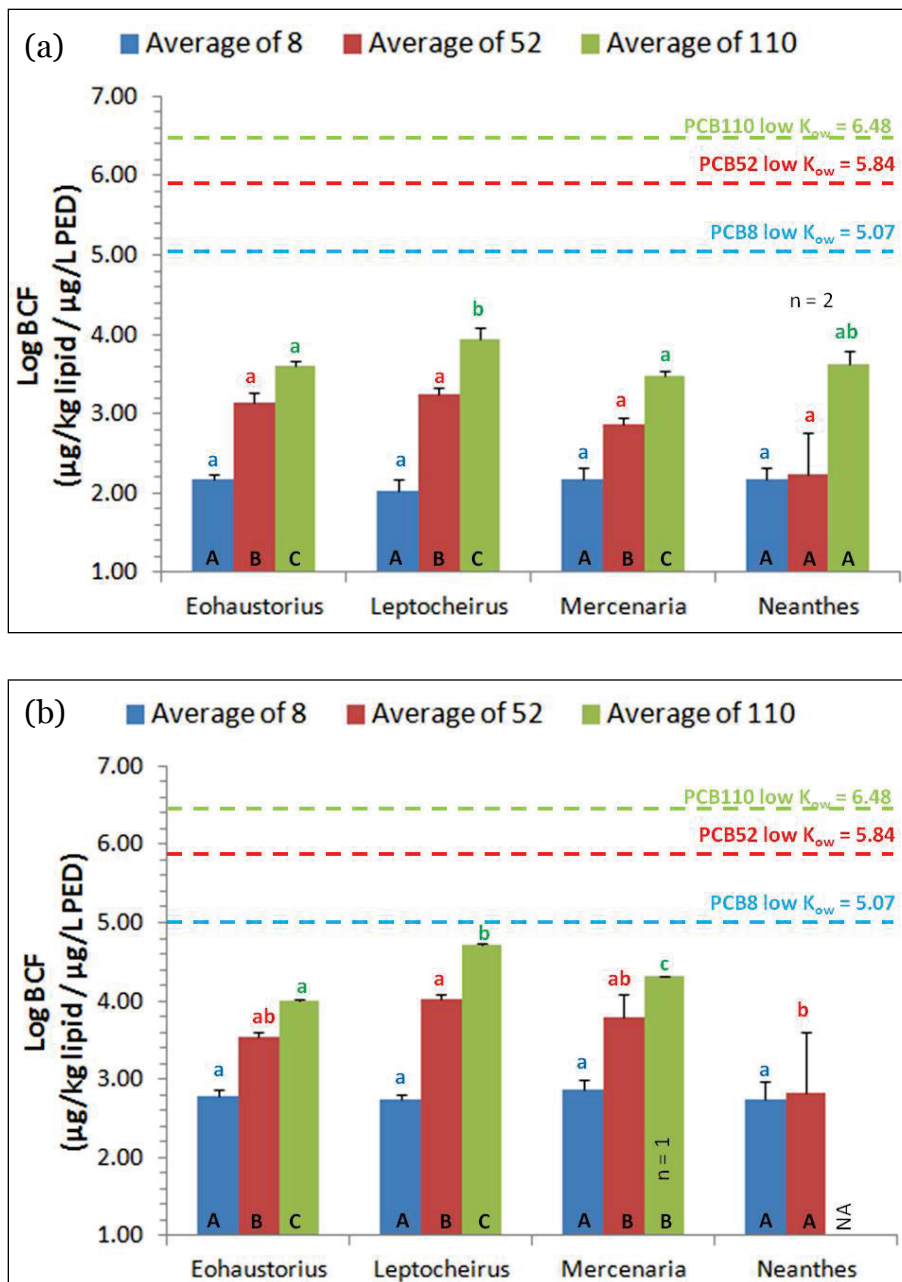
To analyze this finding further, lipid-normalized PW and standardized BCFs were generated for the four organisms exposed in all three PIC types by individually dividing the tissue residues of select congeners by PED-estimated PW concentrations for that congener. Compared with a range of low to medium log K_{ow} congeners (PCB8, 52, 110), higher log K_{ow} congeners in the PW bioaccumulated at higher concentrations, as expected (Figure 36). It was apparent that organisms did not bioaccumulate the full amount of PCBs predicted based on log K_{ow} values, regardless of species or PIC type. BCFs were consistently higher in the PW-PICs relative to the OW-PICs. Generally, all four organisms bioaccumulated the two lower log K_{ow} congeners with similar efficiency (statistically similar BCFs). However, *L. plumulosus* again bioaccumulated the higher log K_{ow} homolog group more efficiently (significantly higher BCFs). This result suggests that *L. plumulosus* more efficiently bioaccumulates the higher log K_{ow} congeners directly from the PW. This does not preclude the importance of consumption of surface particles or deposits, as the PED based PW estimates were from a single location within the PICs (1 cm below the surface) and cannot account for differences in test species position or feeding strategy.

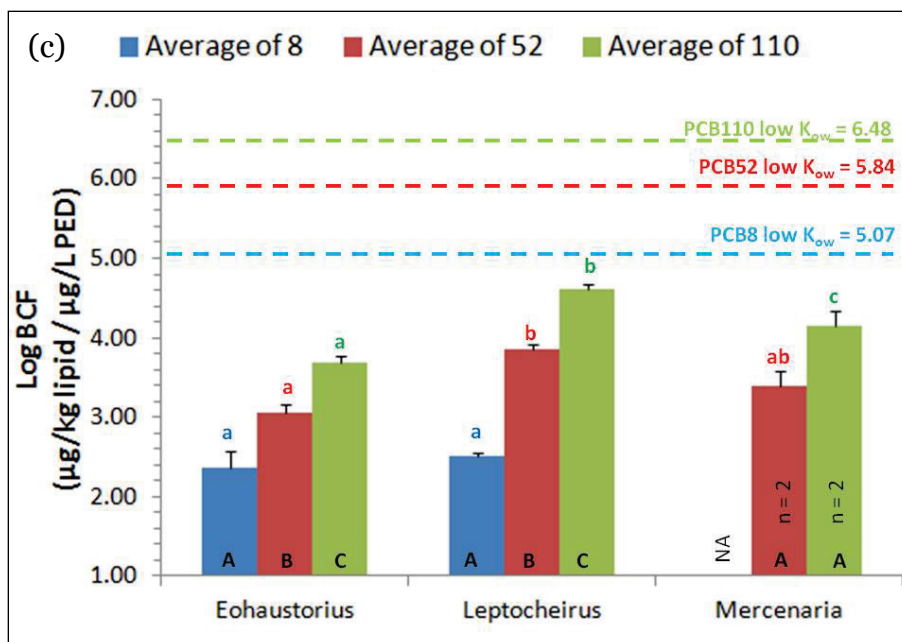
As discussed in the above analysis of the WS-PIC tissue data, comparison to PED-estimated PCB PW concentrations and similar lower, log K_{ow} congeners across the different test species suggests the importance of PW exposure. Significantly greater, high log K_{ow} congeners in *L. plumulosus* relative to other amphipods suggests exposure to surficial particle deposits (or the associated surficial PW) is likely important for determining this organism's tissue residues.

10.3.4 Bioaccumulation of overlying water (OW) congeners

Conclusions regarding the relative importance of the OW exposure pathway to the different test organisms were made by comparing: (1) Σ PCB tissue residues between the OW-PICs and the WS-PICs, (2) tissue residues of the water column delivered PCB24/104 concentrations between the OW-PICs and WS-PICs and (3) the percentage that sum PCB24 and 104 (delivered to the overlying water) made up of Σ PCB tissue residues in WS-PICs. Since all three types of PICs included open mesh tops to allow exposure to PCB24/104 in the OW (Figure 1b, Figure S2, SI), differences in congeners

Figure 36. Bioconcentration factors (BCFs) for study organisms standardized by lipid content and polyethylene devices (PEDs) predicted pore water concentration for select congeners. Data are presented for organisms exposed to the NBH sediment in the (a) whole sediment PICs, (b) pore water PICs, and (c) overlying water PICs. Data were not available for the *Neanthes* overlying water PICs. PCB8 was below detection in the *Mercenaria* overlying water PICs. Letter designations were previously described in Figure 31.





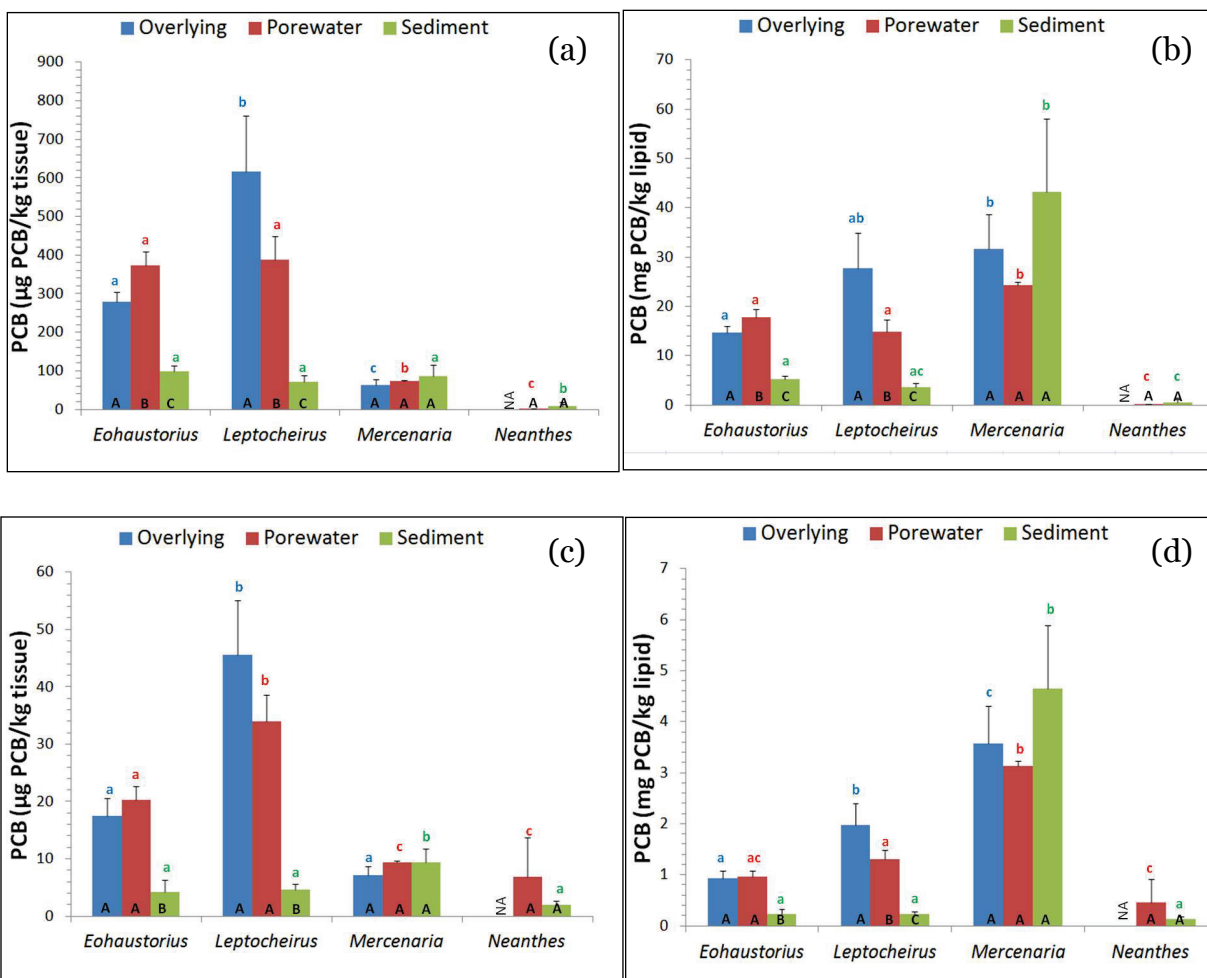
between the OW-PICs and WS-PICs could be attributed to substrate type and organism burrowing depth. Analysis of PCB24/104 directly measured in the OW (Table S5, measured in PEDs placed in the OW and PEDs placed within the PICs (Figure 31) provided evidence that the different organisms received similar exposure conditions. Since congeners other than 24/104 were detected in both tissue (Figure 32) and PEDs (Figure 31a) exposed in the OW-PICs (which only contained clean sand surrounded by all glass sides; thus no direct exposure to sediment), it was apparent that partitioning of some sediment-borne congeners occurred (Figure S3, SI). This occurred more prominently in the NBH experiment, which contained high concentrations of lower log K_{ow} congeners (Figure S3).

10.3.4.1 New Bedford experiment

In the NBH experiment, concentrations of both PCB24/104 were measured in bulk tissues (Figure 36a, c); the same general trend between test species and PICs was observed for both congeners. However, tissue residue of PCB24 were generally 8.9 to 15.9-fold higher than PCB104 in organisms exposed in the OW-PICs. This is logical provided the higher, stable concentrations of PCB24 in the OW (Table S5). While the same concentrations of PCB congeners 24 and 104 were delivered to the overlying water above all three types of PICs, different trends were observed depending on test species and PIC type. Pooling tissue residue data for all test organisms exposed to NBH, two-way ANOVA (organism x PICs) indicated that both PCB24 and 104 were statistically highest in the

OW-PICs, followed by the PW-PICs and the WS-PICs (Figure 37a, b). This is logical as the OW (containing PCB24/104) should better infiltrate the <60 µm sand in the PW-PICs and OW-PICs compared to the finer sediment in the WS-PICs. Thus, animals burrowed into the sediment in the whole sediment PICs were likely less connected to OW exposure.

Figure 37. Overlying water congeners (PCB24/104) in organisms exposed to New Bedford Harbor Sediment. Data are presented as (a) bulk PCB24 in tissue, (b) PCB24 on a lipid-normalized basis, (c) bulk PCB104 in tissue, (d) PCB104 on a lipid-normalized basis. Letter designations were previously described in Figure 31.



For both amphipod species, significantly elevated tissue concentrations of PCB24/104 were observed when exposed in the OW-PICs and PW-PICs relative to the WS-PICs. Within the PW-PICs and OW-PICs, significantly higher PCB24/104 concentrations were observed for *L. plumulosus* relative to *E. estuarius* in the OW-PICs, when expressed as bulk residues (Figure 37a,c) or lipid normalized residues (Figure 37b, d). Functional ecology supports this finding, as *L. plumulosus* tends to move to the surface to deposit feed (ASTM 2010), while *E. estuarius* generally remains

burrowed. These trends are especially true in sand. *L. plumulosus*, which is not well adapted to sand, remained on the surface, while *E. estuarius*, which prefers sandy sediments, remained burrowed. Thus, *L. plumulosus* did not burrow as deeply as *E. estuarius* in sand (or as deeply as it would have in a finer grained sediment), which increased direct exposure to the OW.

For the bulk deposit-feeding worm *N. arenaceodentata*, higher PCB24/104 concentrations were also observed when exposed within the PW-PICs (low tissue recovery precluded comparison to the OW-PIC) compared to very low PCB24/104 concentrations when exposed in the WS-PICs. This finding suggests that while exposure in sand substrate increased exposure to the OW, OW exposure is of relatively lower importance for the worm. Clearly significantly lower concentrations of PCB24/104 was accumulated in worm tissue residues on both a bulk (Figure 37a, c) and lipid-normalized basis (Figure 37b, d) relative to the other species. Further, when exposed in the fine-grained NBH sediment PICs, very low levels of PCB24/104 were measured in *N. arenaceodentata*, further supporting this claim.

For the clam *M. mercenaria*, however, statistically similar tissue residues of PCB24/104 were observed when exposed in all three PIC types (Figure 37a, c). This suggests equal importance of the OW exposure pathway for the suspension-feeding clam, regardless of substrate type. The clam burrows relatively shallowly into substrate to maintain a connection between the OW and its siphon. PCB24/104 tissue residues in the WS-PICs further support the relatively greater importance of OW exposure to *M. mercenaria*. While *M. mercenaria* typically accumulated statistically, significantly lower Σ PCB concentrations from sediment exposure relative to the other test species (Figure 32), the clam accumulated significantly more PCB104 from OW in the WS-PICs than the other test species (Figure 37c). While it appears that amphipods bioaccumulated more PCB24/104 from the OW based on bulk tissue analysis (Figure 37a, c), *M. mercenaria* actually bioaccumulated significantly more on a lipid-normalized basis than *E. estuarius* and *N. arenaceodentata* and effectively the same levels as *L. plumulosus* (Figure 37b,d). While *L. plumulosus* bioaccumulated similar levels of lipid-normalized PCB24/104 as the clam, this amphipod generally bioaccumulated much more PCB in general, such that the OW was still of relatively lower importance for determining total bioaccumulation compared to the clam. The importance of OW exposures for this clam is further supported in the literature (Bergen et al 1993; Kaag et al 1997).

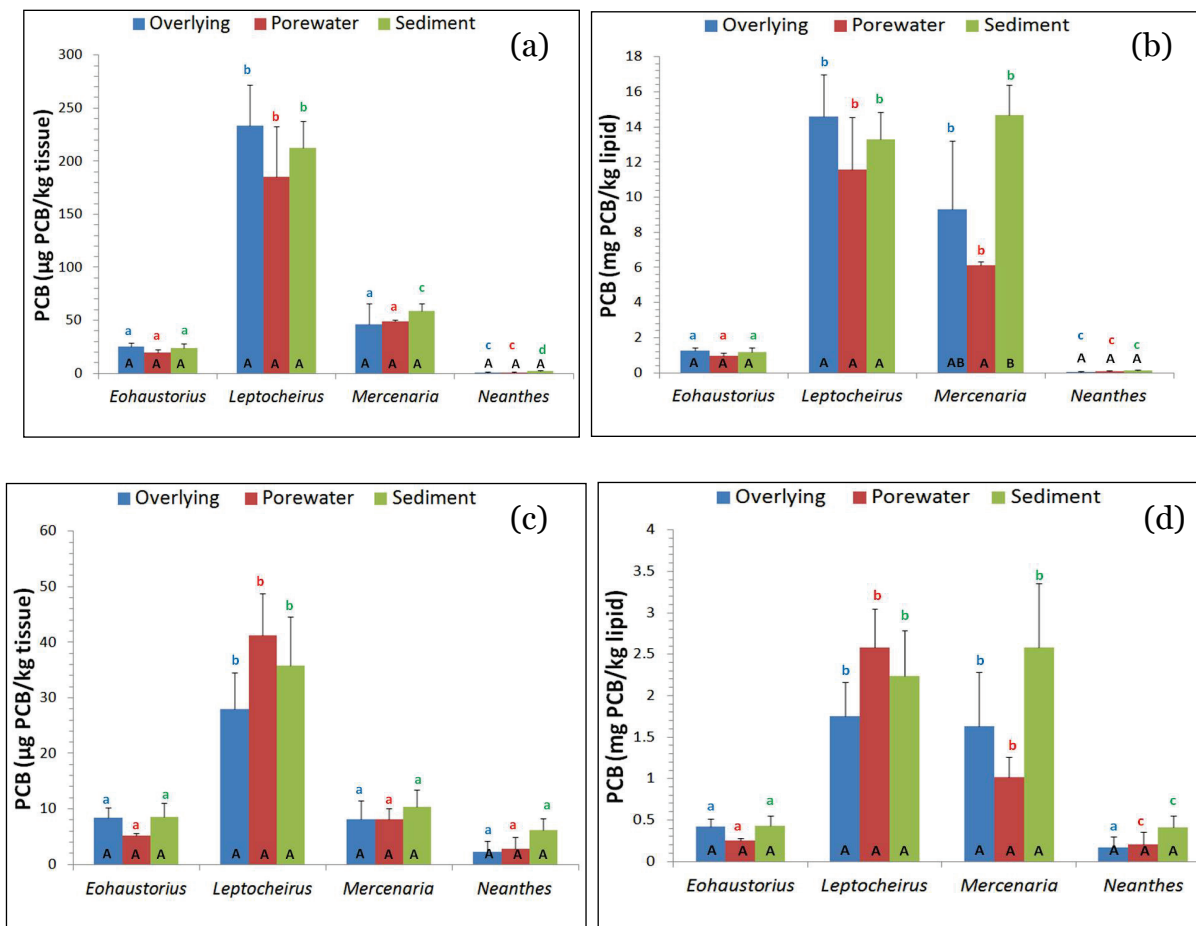
10.3.4.2 Bremerton experiment

Tissue concentrations of PCB24/104 delivered to the OW were lower in the BNC sediment exposure (Figure 38) relative to the NBH exposure (Figure 37). This result may relate to multiple factors including (1) more variable concentrations in the OW (Table S5)), (2) the use of smaller mesh-size PIC lids (0.5 vs. 1.0 mm) to reduce potential for *L. plumulosus* escapes, and (3) addition of airlines directly above all PICs to reduce sediment anoxia. One or a combination of these factors may explain the lower PCB24/104 tissue residues in the BNC experiment. However, PCB24/104 tissue residues in the BNC experiment were still high enough to confirm the trends observed in the NBH experiment. Bioaccumulation of PCB24/104 was more similar across PIC types for all organisms (bulk and lipid-normalized residues) relative to the NBH experiment results. This may relate to the much higher sand and gravel content of the BNC sediment (Table 20), which also contained gravel and shell hash. This coarser grained BNC sediment likely allowed penetration of greater concentrations of PCB24/104 from the overlying water into the substrate relative to the finer grained NBH sediment.

The BNC experiment provided data to support conclusions drawn from the NBH exposure on the relative importance of OW exposure to *M. mercenaria* and *N. arenaceodentata*. The suspension-feeding clam, again, showed no differences in accumulation of PCB24/104 among PICs types, suggesting it is consistently exposed to the water column in all conditions (Figure 38a, c). Lipid-normalized tissue residues, again, showed the high importance of OW exposure for the clam relative to the other organisms (Figure 38b, d). The worm *N. arenaceodentata*, again, accumulated relatively low residues of PCB24/104, further supporting relatively low importance of that pathway for determining total bioaccumulation potential. There is support in the literature that sediment exposure is more important for bulk deposit-feeding polychaete worms such as *N. arenaceodentata* than OW (Fowler et al 1978).

Thus, the BNC experiment generally confirms trends in overlying water exposure between species. However, differences in 24/104 accumulation between the OW-PICs and WS-PICs were less pronounced for the amphipods, suggesting amphipods did not remain burrowed as deeply in the coarser BNC sediment relative to the finer NBH sediment.

Figure 38. Overlying water congeners (PCB24/104) in organisms exposed to the Bremerton Navy Complex sediment. Data are presented as (a) bulk PCB24 in tissue, (b) PCB24 on a lipid normalized basis, (c) bulk PCB104 in tissue, (d) PCB104 on a lipid-normalized basis. Letter designations were previously described in Figure 31.

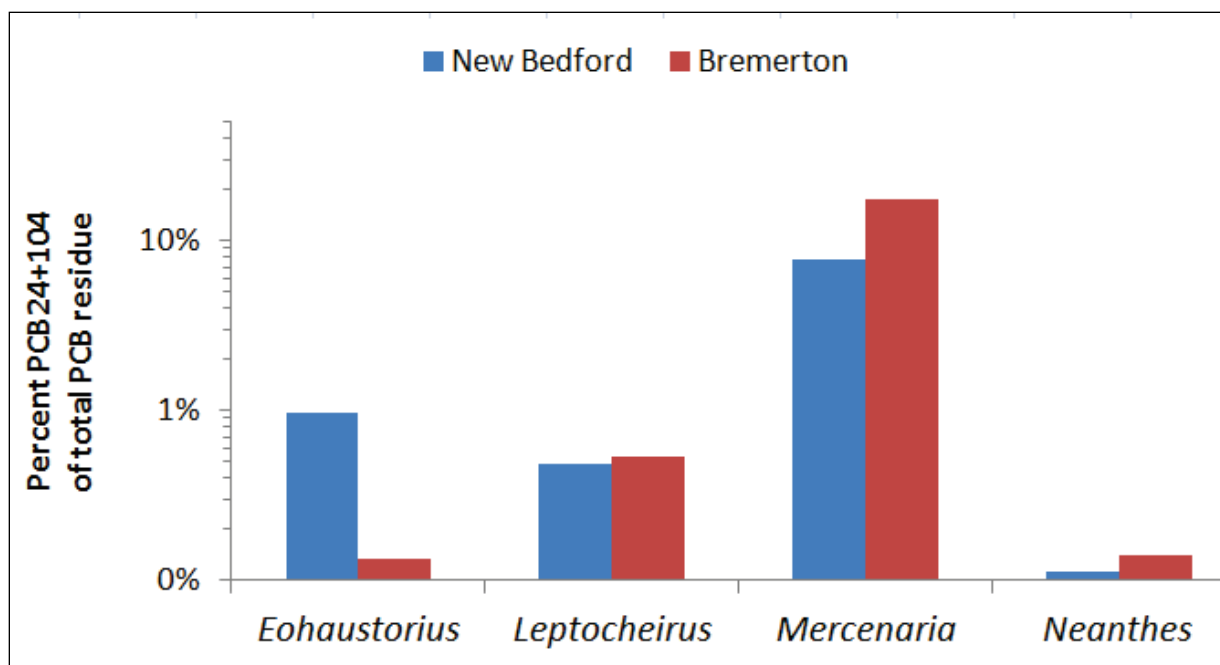


10.3.4.3 Overlying pathway conclusions

To determine the relative importance of the OW pathway for the different organisms in environmentally relevant conditions (i.e., WS), the percentage that the OW-dosed congeners (sum PCB24 and 104) made up of the Σ PCB tissue residues in the WS- PICs was determined for both the NBH and BNC experiments (Figure 39). These data do not quantify the overall importance of OW exposure to each organism since other sediment-sourced congeners likely partitioned to the water, and thus were available for uptake, as demonstrated by congeners other than 24/104 being detected in the PEDs placed in the PICs (Figure 31) and tissues exposed in the OW PICs (Figure 35, Figure 36). However, comparison of the relative percentage that sum PCB24/104 made up of total congener bioaccumulation from the sediments provides an expedient comparison between organisms. Results in Figure 39 clearly indicate OW exposure is most important for determining total

bioaccumulation potential of the suspension-feeding *M. mercenaria*. Overlying water exposure was least important to the deeper burrowing, bulk deposit-feeding *N. arenaceodentata* (Figure 39). A general summary of the importance of the different exposure pathways to each test organisms is provided in Table 19.

Figure 39. Importance of overlying water exposure to the test organisms living in whole sediment. Data are expressed as the percentage that the overlying water congeners (sum PCB24 + PCB104) make up of total congener bioaccumulation for organisms exposed in the whole sediment PICs. Caveats: (1) numbers are not representative of the total importance of overlying water exposure, since other congeners may have been in the water, and (2) numbers cannot be used to estimate the actual importance of overlying water exposure since the spiked levels of PCB24/104 were fairly low and may not be applicable to site-specific conditions.



10.3.5 Conclusion

The results show that the highest tissue residues were obtained from exposure in the WS-PICs, followed by the PW-PICs and OW-PICs. The amphipod *L. plumulosus* was the most efficient bioaccumulator of PCBs (most notably high, low K_{ow} congeners); this fact is partially accounted for by its relatively higher lipid content. In addition, the coarser grained BNC sediment appeared to induce a divergence in inter-specific burrowing behaviors (*L. plumulosus* stayed near top, *E. estuarius* and *N. arenaceodentata* burrowed (but not as deeply), *M. mercenaria* was not impacted by sediment type), leading to larger exposure and bioaccumulation differences than lipid and organic carbon normalization can explain. Similar BSAF values suggest differences between amphipods were mainly

related to TOC and lipid content, while *M. mercenaria* bioaccumulated significantly less PCBs (especially high low K_{ow} congeners; Figure 34) than would be expected based on organism lipid content.

The following conclusions are offered based on the analysis of exposure and bioaccumulation data for four functionally and phylogenetically distinct animals:

1. Whole sediment exposure clearly resulted in greatest bioaccumulation for all four species, as it included all pathways. However, deeper burrowing species (e.g., *N. arenaceodentata* and *E. estuarius*) are less exposed to the overlying water in a fine-grained, whole sediment than they would be in a coarse-grained sediment.
2. While the uptake of PCBs into bulk tissue varied greatly between organisms, lipid normalization accounted for much of that variability, with the exception of *L. plumulosus*, which bioaccumulated more PCBs than the other organisms. In addition, sediment type was a significant factor which can be partially addressed by normalizing to TOC using BSAFs (i.e., account for TOC). However, when substrate type modifies animal behavior (e.g., less borrowing of *L. plumulosus* in sand), there is a shift in the relative importance of pathways (e.g., OW more important for animals with a behavioral constraint that prevents full burrowing).
3. Pore water exposure was fairly similar between organisms after lipid normalization. The soft bodied, infaunal organisms (i.e., *N. arenaceodentata*, *E. estuarius*, *L. plumulosus*) bioaccumulated similar lipid-normalized concentrations of lower log K_{ow} homolog groups, while *M. mercenaria* generally accumulated lower concentrations than the other organisms related to protection from its shell and its connection with the overlying water.
4. The amphipod *L. plumulosus* bioaccumulated significantly higher concentrations of high log K_{ow} homolog groups than the other organisms (lipid-normalized), suggesting relatively greater exposure through direct sediment particle uptake / ingestion or simply more efficient uptake. While higher low K_{ow} congeners are more lipophilic, they are less likely to partition to the PW.
5. The OW pathway was by far the most important to the clam *M. mercenaria*. Not only does the clam have a shell that protects it from PW or direct sediment particle exposure, but also the clam accumulated the highest OW concentrations in all substrate types relative to different organisms (lipid normalized). While OW exposure had some importance

to the amphipod *L. plumulosus*, which comes to the substrate surface often, PW exposure and direct sediment particle exposure were by far more important factors for determining overall *L. plumulosus* tissue residues. The OW had lower importance for *E. estuarius* and was virtually irrelevant for the worm *N. arenaceodentata*.

6. PED estimations of PW concentrations were a vast improvement over bulk sediment concentration for predicting bioavailability; however, they cannot account for divergent animal behavior between species and substrate type. The PEDs were not able to predict that *L. plumulosus* would bioaccumulate significantly greater concentrations of high log K_{ow} congeners relative to the other organisms. In addition, PED estimates of PW concentrations are likely to overpredict bioaccumulation potential for the clam *M. mercenaria*. PEDs and other PW passive sampling devices are clearly most predictive of bioaccumulation potential for organisms for which PW is the predominate exposure pathway.

11 Task 2B: Model Development using RECOVERY

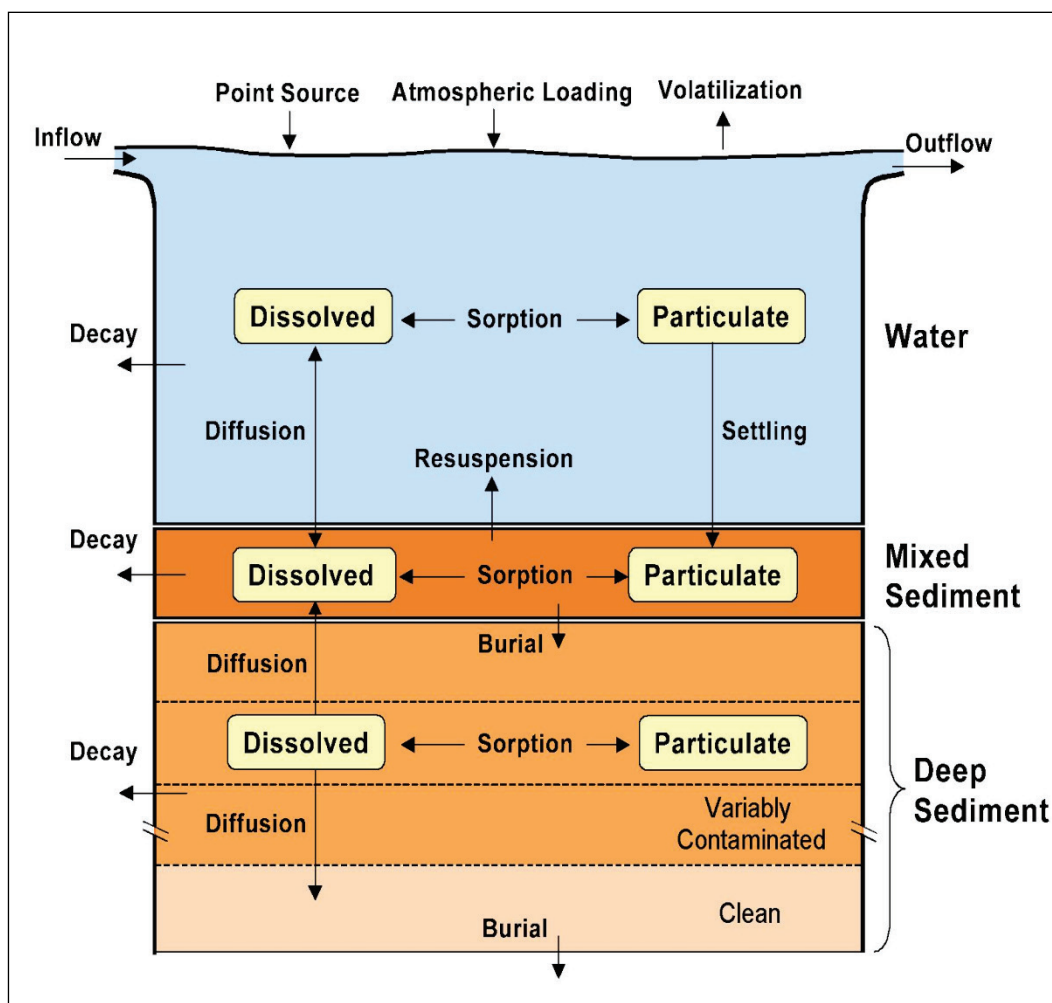
11.1 Introduction

The authors hypothesized that the functional attributes of benthic organisms will explain a substantial portion of observed variation in contaminant exposure and bioaccumulation among species. The objectives of the experimentation and modeling to follow were to investigate the relative importance of whole sediment, pore water, and overlying water bioaccumulation exposure pathways of PCBs to four phylogenetically and functionally distinct benthic macroinvertebrates by compartmentalizing their exposure using specially designed bioboxes, hereafter referred to as PICs.

The data collected during Tasks 1c (Section 12) and 2a (Section 13) were used as inputs to develop algorithms to describe exposure to benthic organisms having different functional attributes. These algorithms will be used to enhance the capability and predictive reliability of RECOVERY, an existing modeling framework for assessing contaminant processes in sediment systems.

The model is an extension of frameworks developed previously (Ruiz and Gerald 2001, Boyer et al. 1994, Chapra 1982, 1986, Chapra and Reckhow 1983). The system is idealized as a well-mixed surface water layer underlain by a vertically stratified sediment column (Figure 40). The sediment is well mixed horizontally, but segmented vertically into a well-mixed surface layer and a deep sediment. The latter, in turn, is segmented into layers of user-defined thickness, properties, and contaminant concentration, which are underlain by an uncontaminated region. The discretized sediment layer configuration is useful for capping scenarios and sites where contamination occurred over a long period of time; thus, contamination appears layered. The specification of a mixed surface layer is included because an unconsolidated layer is often observed at the surface of sediments due to a number of processes, including bioturbation and mechanical mixing. The contaminant is assumed to follow linear, reversible, equilibrium sorption, and first-order decay kinetics. Pathways incorporated in the RECOVERY model, in addition to sorption and decay, are volatilization, burial, resuspension, settling, and pore water diffusion.

Figure 40. Schematic of the sediment-water system as modeled in RECOVERY.



The partitioning coefficient for organic contaminants is computed by using the Karickhoff et al. method (1979). RECOVERY allows for different f_{oc} values for the water column, mixed layer, and the deep sediments. Analogous to other physico-chemical characteristics of the sediments, the f_{oc} can vary with depth (layers) in the deep sediments.

The model predicts the movement (i.e., flux) between specified sediment layers and the overlying water column. Likewise, has been used extensively to assess natural recovery processes and capping designs at contaminated sediment sites. Widdowson incorporated a reaction package into RECOVERY to address sequential electron acceptor reactions and PCB degradation (Widdowson 2002, Mobile 2008). The capability of simulating multiple contaminants was extended in the release of RECOVERY 4.2 (Ruiz et al 2007).

11.2 Materials and methods

Two general approaches could be taken to incorporate organism functional attributes into or coupled with RECOVERY: (1) exposure modeling using traditional applications of the EqP model and bioaccumulation processes (Morrison et al., 1996) with the incorporation of passive sampling data to account for uncertainties in EqP plus organism functional attributes, (2) a modified EqP model that takes into account multiple organic carbon phases (e.g., Accardi-Dey and Gschwend 2002, 2003), and bioaccumulation modeling following the form of Sun et al. (2009), with the incorporation of passive sampling measurements and functional attributes of different benthic species. These mechanistic approaches to describing exposure offer considerable value in terms of process-level insight and reduced uncertainty over simpler approaches (e.g., empirical derivation and use of BSAFs). Incorporating organism functional attributes and the interconnected contaminant exposure compartments will allow us to investigate the rate of exposure to each compartment and the ability of the organisms to integrate exposure across the compartments.

11.2.1 First approach

The first modeling approach would estimate the C_D of chemical in sediment pore water based on the C_P and f_{oc} in the sediment (Di Toro et al. 1991):

$$C_D = \frac{C_P}{K_{oc}f_{oc}} \quad (1)$$

Bioaccumulation would follow a form similar to:

$$\frac{dC_b}{dt} = U_w(t) + U_{food}(t) - R(t) - D_m(t) - D_d(t) \quad (2)$$

where C_b is the concentration of chemical in the benthos, U_w and U_{food} are the chemical intake from water and food respectively. R , D_m , and D_d are the primary routes of elimination to water (respiration, metabolism, and defecation, respectively) and passive sampling to refine the uncertainties in both EqP and bioaccumulation estimates:

$$C_D = \frac{C_{PS}}{K_{PS}} \quad (3)$$

where, C_{PS} is the passive sampler concentration and K_{PS} is the passive sampler partition coefficient.

In this approach, the dissolved concentration will be estimated from the RECOVERY model; analogous to Equation 1. The system will be simulated with RECOVERY to estimate dissolved and total concentration of the PCBs and/or congeners over time in the different PICs (reactors/boxes). The time series of total and dissolved concentration in the overlying water and the sediment will be used to estimate bioaccumulation using a modified Equation 2;

$$\frac{dC_b}{dt} = U_o(t) - R_o(t) \quad (4)$$

where, U_o and R_o are the overall chemical intake and elimination rates for the benthos.

11.2.2 Second approach

The second approach incorporates consideration for how both the black carbon formulation and treatment with AC in the experimental sediments impacts results. One can incorporate the black carbon model into Equation 1 resulting in:

$$C_D = \frac{C_P}{f_{OC}K_{OC} + f_{BC}K_{BC}C_D^n} \quad (5)$$

This model has also been successful at predicting bioavailable concentrations; however, as noted previously, considerable uncertainty still exists around the measurement of f_{BC} and values for K_{BC} and n ; bioaccumulation would be represented as:

$$\frac{d}{dt}C_b(t) = k_{abs}^i C_D(t) + k_{inj}^i \varepsilon \omega C_P - k_{dep} C_b(t) \quad (6)$$

where K_{abs} , K_{inj} , and K_{dep} are exchange rate (gill or tissue), ingestion rate, and depuration rate, respectively, for compartments $i=1-3$ (overlying water, sediment pore water, and sediment particulate matter), ε is the uptake efficiency, and ω is the sediment ingestion rate. Modifications to this approach would be made to include inputs resulting from passive sampling and the explicit incorporation of organism functional attributes.

Another alternative modeling approach to incorporate black carbon nonlinear sorption is using large f_{oc} s to simulate the less reversible partition coefficient associated with AC (black carbon) in RECOVERY. The approach will be evaluated against data generated in Task 2a (Section 13) using dissolved contaminant concentrations generated through the use of passive samplers, direct measurements of exposure media in PICs A-C, and measures of contaminant concentration in tissues. The influence of functional attributes, represented by different tissue concentrations produced within different PICs (A, B, and C), were incorporated into equations describing bioaccumulation and predictions were compared to the data for PIC D. The best modeling approach was adopted for further refinement, and the resulting algorithms was incorporated into the RECOVERY framework.

11.2.3 Exposure system

A recirculating exposure system was designed to contain experimental sediments, organisms (*Leptocheirus plumulosus*, *Eohaustorius estuarius*, *Mercenaria mercenaria*, *Neanthes arenaceodentata*), and PICs. Likewise, it was designed to passively dose unique PCB congeners into the overlying water (Figure 8, Figure 9, Figure 10). The PICs were constructed to modulate PCB exposure from the whole sediment:

1. overlying water only
2. pore water
3. whole sediment.

Two PCB congeners (24, 104) that were not detected in the sediment were dosed into the overlying water to quantify the extent to which the overlying water pathway contributed to overall contaminant exposure and tissue residues. These congeners are representative of relatively low to moderate log K_{ow} PCBs (log k_{ow} = 5.35 and 5.81, respectively).

11.3 Results and discussion

The first modeling task was to simulate the system to address equilibrium and to verify that the two congeners loaded into the exposure system could be simulated. The RECOVERY model was used to simulate the exposure system with a reactor detention time of 2.2 days, aquarium detention time of 2.4 days, and an overall detention time of 4.7 days.

Figure 41 shows the simulation of the exposure system using RECOVERY and a simple loading function. The simulation verifies that the exposure system can be loaded with congeners 24 and 104 over a short period, and the loading can be maintained for a long period. The exposure system was tested without a sediment bed in the aquariums. The system was further tested with Bremerton Harbor sediment and New Bedford sediment (previously described and characterized). Figure 42 and Figure 43 show the exposure system for the experiments: the New Bedford sediment and the Bremerton Harbor sediment both with the reactor loaded with congeners 24 and 104 in the water phase. The New Bedford Sediment (Figure 42) congener loadings were successful; however, the PCB 24 and 104 concentrations decreased over time, likely due to sorption into the sediment bed of the aquariums. In order to keep a long-term concentration similar to Figure 41, a higher loading of the permeable layer delivery system of the reactor tank would be needed, to account for the sorption losses. Loadings were successful since PCB congeners 24 and 104 concentrations were stable over the experimental period (28 days), the decrease over time was less than one order in magnitude, and losses were monitored and accounted for in the bed measurements. The Bremerton experiment exhibited results similar to the New Bedford experiment, including a decrease of the dissolved congeners 24 and 104 in reactor water and increased sorption in the sediment bed. Both experiments were loaded with congeners 24 and 104 and resulted in stable water phase concentration in the reactor and in the aquariums.

The second modeling task was to simulate the PCB dynamics in the exposure system. The RECOVERY model was used to simulate the exposure system (reactor and tanks). The reactor was simulated and verified with collected data in the prior task. The aquariums, as part of the exposure system, was simulated in this task.

Figure 44 shows the simulation of the exposure system with New Bedford sediment for total (sum of all congeners) PCBs using RECOVERY. The system was simulated with RECOVERY's K_{ow} database. The concentration in the water and the pore water (blue and pink lines respectively) show small concentrations of PCBs (sum of the congeners) in the dissolved phase in equilibrium with bulk NB sediment (33.7 mg/kg). Table 21 shows the data used in the RECOVERY simulations. To further refine the uncertainties in EqP , RECOVERY's PCB K_{ow} data was recalculated using PE data according to Equation 3. Using the estimated PCBs, PE, K_{ow} water,

Figure 41. Simulated PCB congeners 24 and 104 concentrations in reactor water.

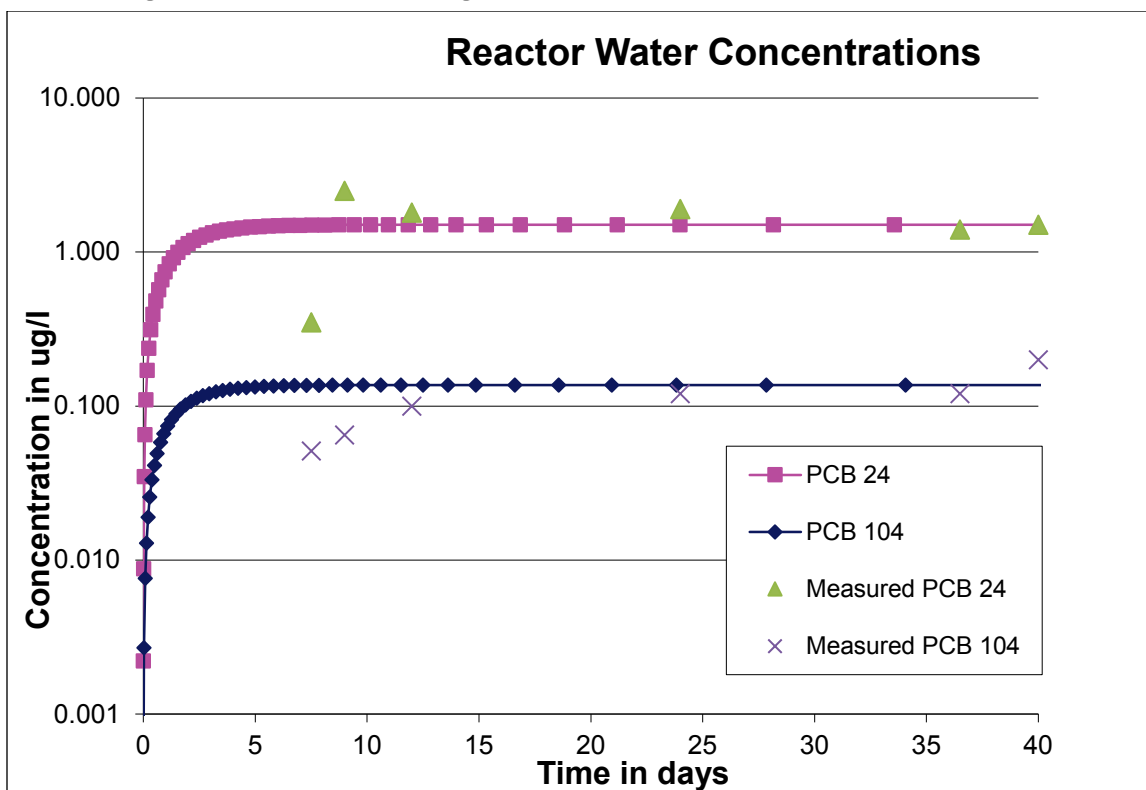


Figure 42. Simulated PCB Congeners 24 and 104 Concentrations in Reactor Water and New Bedford Sediment.

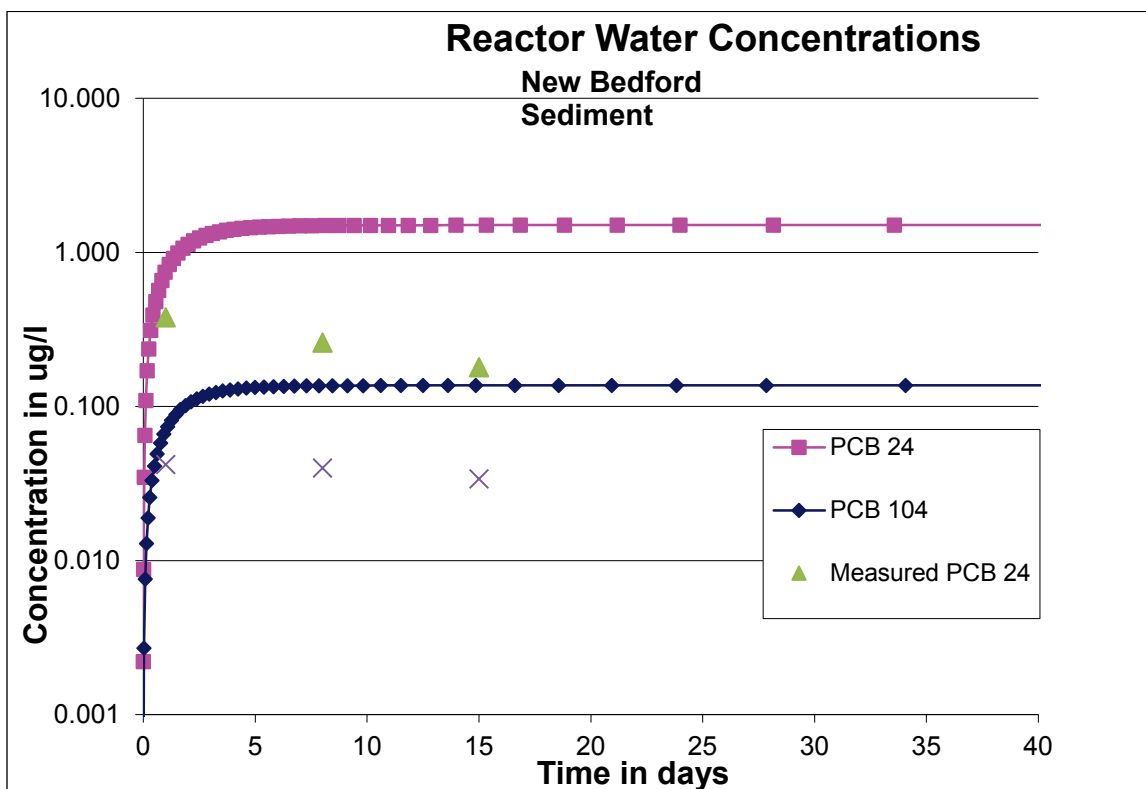


Figure 43. Simulated PCB Congeners 24 and 104 Concentrations in Reactor Water and Bremerton Sediment.

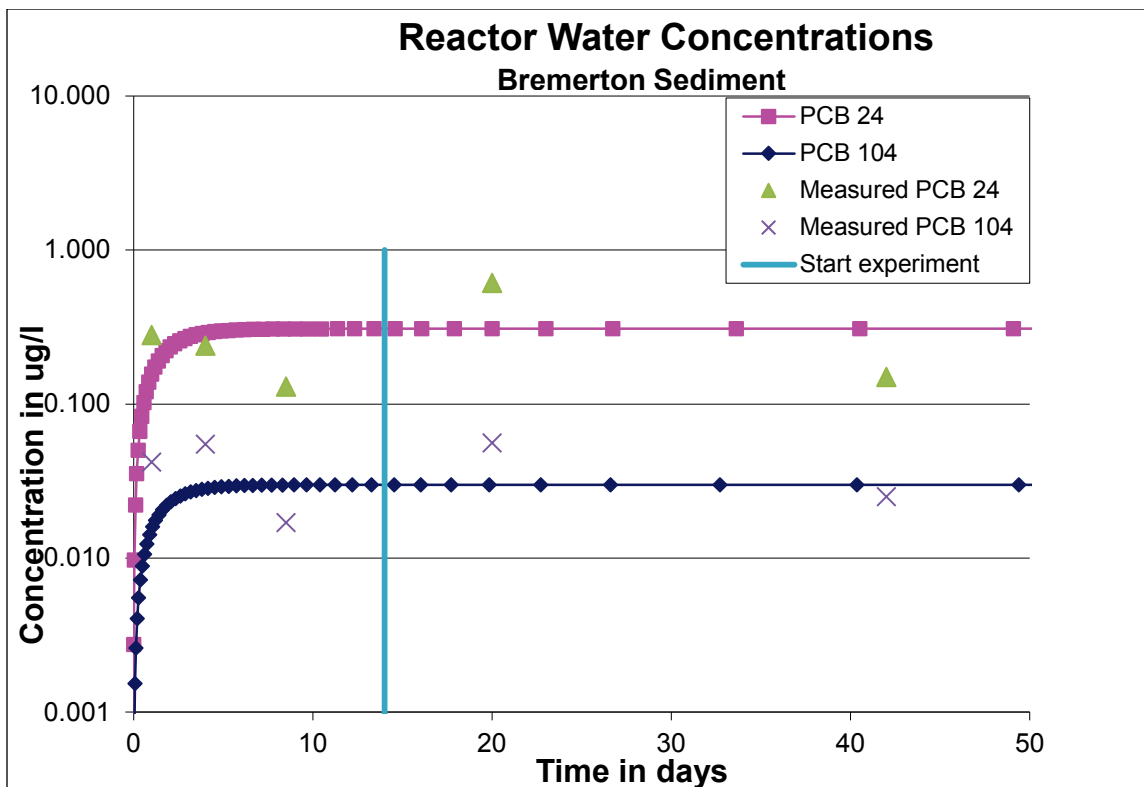
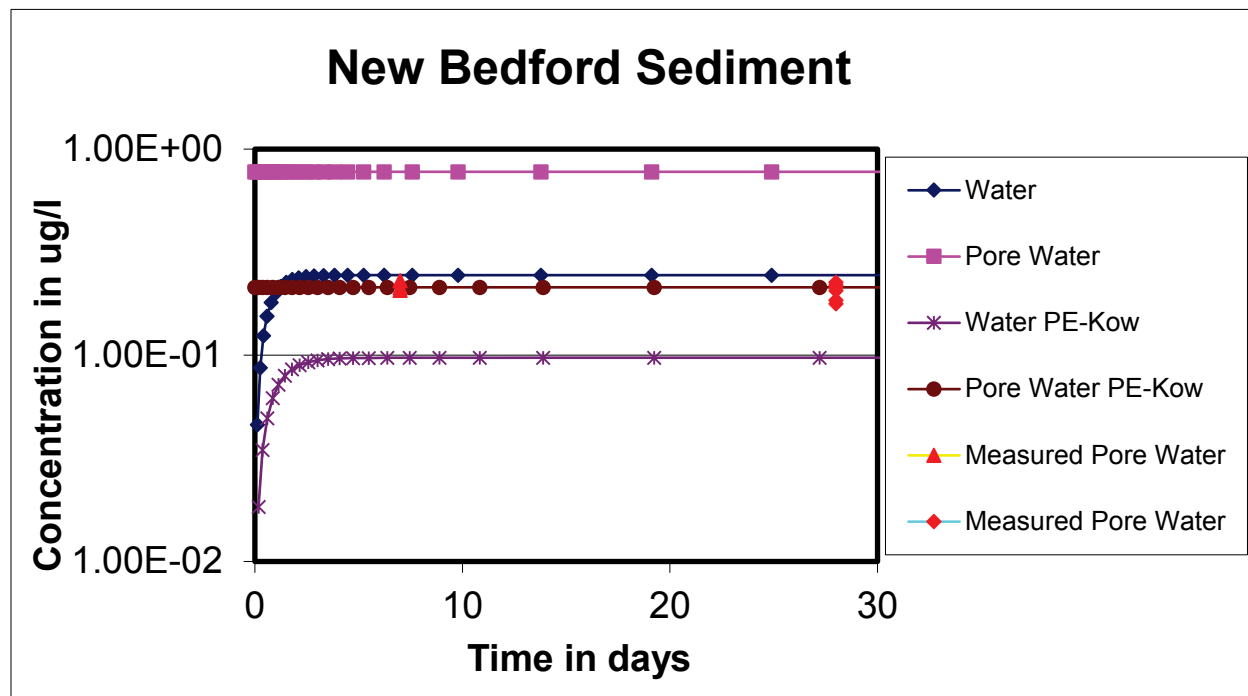


Figure 44. Simulated and Measured Total PCBs Concentrations in Exposure System with New Bedford Sediment.



and sediment pore water (lilac with stars and brown with circles lines respectively) show lower dissolved PCB concentrations and agrees with the collected PE data (measured data triangles and diamonds). After starting the experiment, the measured data was collected from outside the PIC as defined in section 11 at day 7 and day 28. Both the water and pore water concentrations look very stable, so even if the data collected were stable after ninety days (equilibrium period), the concentration in the water and the pore water would be the same concentration at 100 days and 200 days.

Table 21. Values used in the New Bedford Sediment Experiment.

Values Used in the New Bedford Sediment Experiment	
Parameter	Value
Mixed layer thickness (cm)	1
Initial contaminant concentration in mixed (mg/kg)	33.7
Porosity mixed sediment	0.8
Specific gravity of mixed sediment	2.7
F_{oc}	0.0640
Sediment thickness (m)	1
F_{oc}	0.0640
Porosity of sediment	0.6
Specific gravity of sediment	2.7
K_d for sediment	43436
Initial contaminant concentration in sediment (mg/kg)	33.7
Settling velocity (m/yr)	26
Burial velocity (m/yr)	0.0000001
Molecular diffusivity (cm^2/sec)	5×10^{-6}
Biodiffusion coefficient (cm^2/sec)	2×10^{-5}
Biodiffusion depth (cm)	0

The second part of simulating the exposure system was to simulate the PICs. The pore water PIC was simulated using sand layer over a New Bedford sediment layer. Pore water is able to diffuse across the layers. The sand layer has less than 1% organic carbon. The overlying water PIC was simulated with a sand layer isolated from the New Bedford sediment. PCBs can only be loaded to the overlying water PIC from the water column above the PIC. Figure 45 shows the one-year simulation of both PICs inside the aquarium for the different organisms. The simulation was run for one, two, and five years. If the authors ran the simulation for more than two years, both PICs would reach the same dissolved PCB concentration. It takes more than 100 days for the pore water in the sand of the pore water PIC (magenta line with stars) to be influenced by the pore water in the sediment; prior to that point, the surface layer of both PICs is loaded from the water column. The overlying PIC (green line with dashes) increased in concentration until it reached the level of the dissolved PCB in the water column. It takes at least two years for the PCB in the pore water in the overlying PIC to be equal to the pore water in the sediment. Both PICs will achieve the same concentration of PCB in the pore water since they have the same sand (with the same TOC). It is interesting to point out that after 100 days the pore water PIC was loaded predominately from the sediment; the diffusion path was longer, therefore the delay. The PIC was 4 cm wide, thus the dissolved PCBs from the sediment traveled at least 2 cm to reach the midpoint of the PIC, which was much closer from the water-sediment interface. The yellow line in Figure 45 shows the simulation using the theoretical PE K_{ow} . There were some minor modifications to the PE K_{ow} to be able to properly simulate the dynamics of the system (lines magenta and green).

Figure 46 is the same simulation, but the focus point is in the first two hundred days. It shows that the dissolved concentration in the sand PICs can be predicted. It also shows the state of equilibrium of the exposure system achieved during the experiment. The measured dissolved concentrations from the pore water PICs match the model simulation after several weeks (90 days); including the one month of the experiment. The overlying PIC and the pore water PIC show identical simulations for the first 70–90 days and remain very close throughout the experiment. The two PICs began to diverge significantly after 150 days. An increase in dissolved concentration of the pore water PIC during this time increased the water column concentration above the PIC (see water concentration line till with cross hatches), which eventually increased the water column concentration to levels close to those in Figure 44. The simulation for the sand PICs showed a greater level of variance (more dynamic) as compared to the whole sediment PIC and the sediment outside the PICs.

Figure 45. Simulated Total PCBs Concentrations in PICs Exposed to New Bedford Sediment.

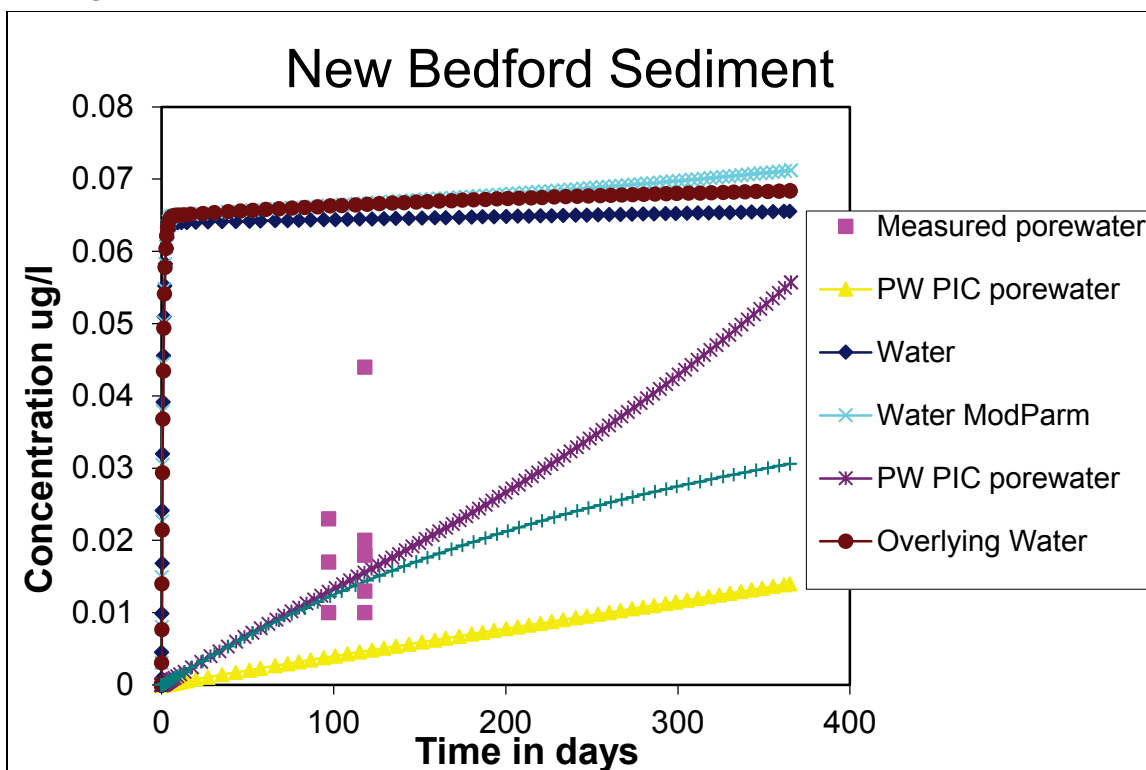


Figure 46. Simulated and Measured Total PCBs Concentration in PICs Exposed to New Bedford Sediment.

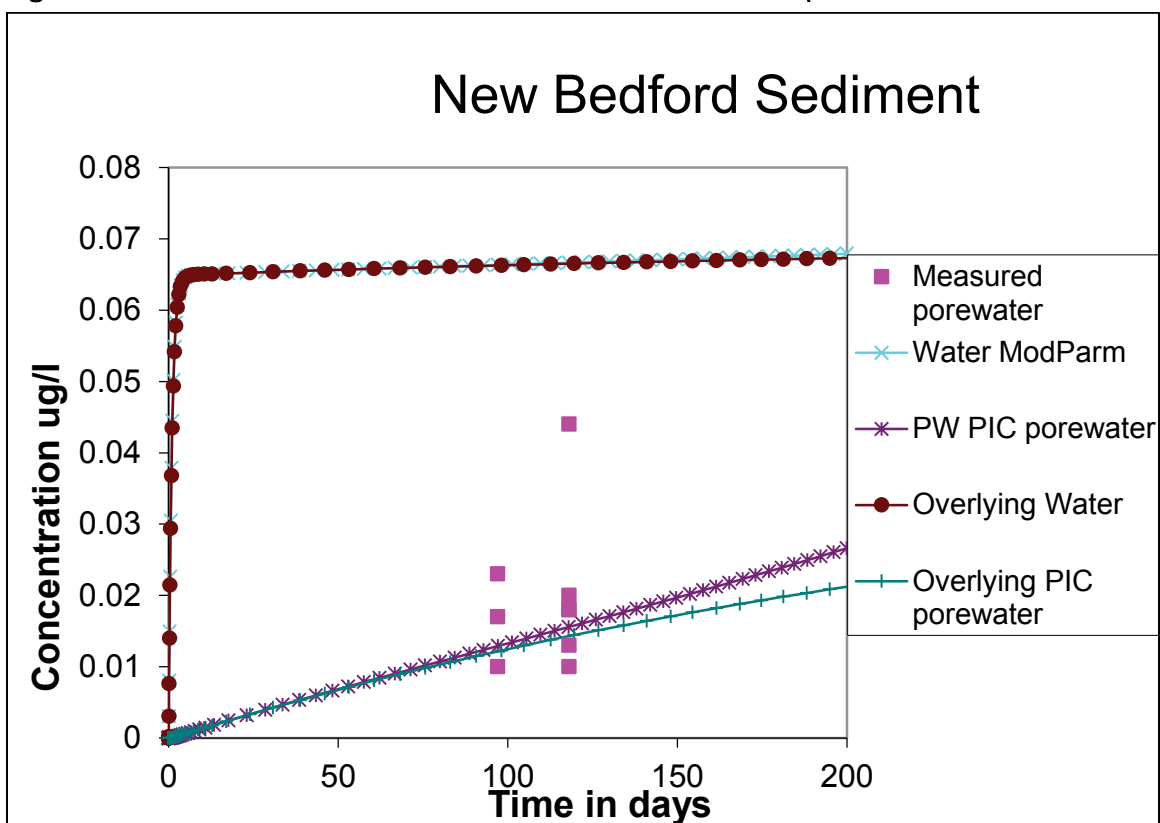
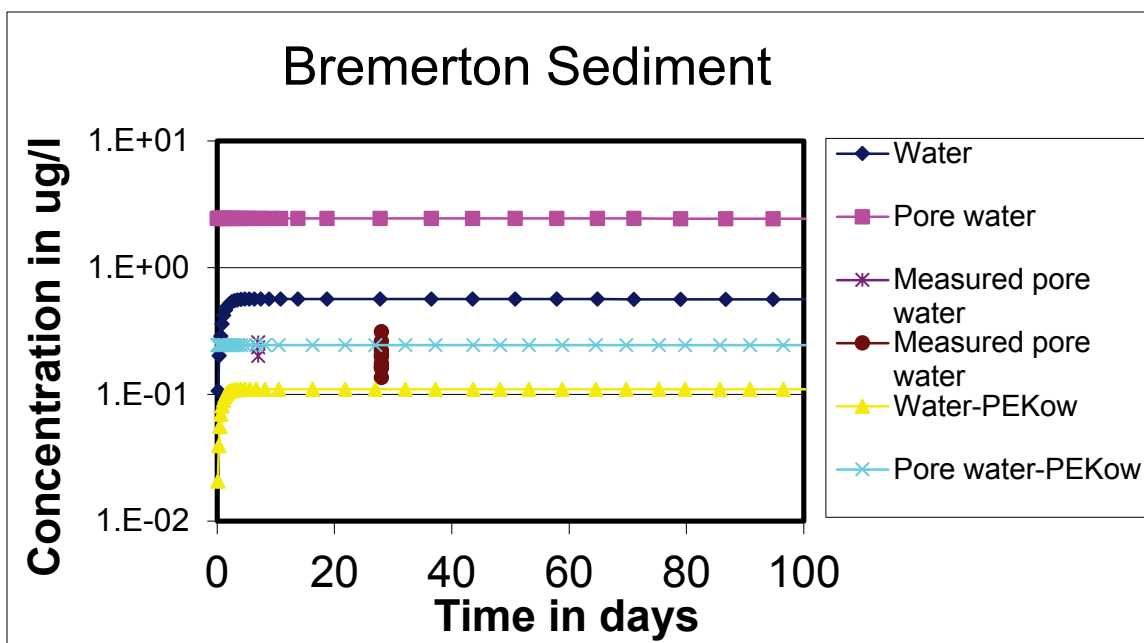


Figure 47 shows the simulation of the exposure system with Bremerton Harbor sediment for total (sum of all congeners) PCBs using RECOVERY. The system was simulated with RECOVERY's K_{ow} database. The concentration in the water and the pore water (blue and pink lines respectively) show the concentration of PCBs (sum of the congeners) in the dissolved phase in equilibrium with bulk BH sediment (16.6 mg/kg). Using the estimated PCBs, PE and K_{ow} from Equation 3, water and sediment pore water (yellow and cyan lines respectively) show the truly dissolved PCB concentrations measured by PEs. The measured data were collected from outside the PIC for the 7-day and 28-day experiments after 90 days of equilibration as defined in Section 13.

Figure 47. Simulated and Measured Total PCBs Concentrations in Exposure System with Bremerton Harbor sediment.



Simulation of the overlying PICs and pore water PICs for the Bremerton Harbor sediment follows the same procedures as the New Bedford sediment. Figure 48 shows the pore water PIC simulation inside the aquarium for the different organisms. The PCB concentrations at equilibrium is larger than the New Bedford sediment. Not only was the equilibrium concentration much higher, but the time to reach equilibrium (constant concentration) was longer for the Bremerton Harbor sediment compared to the New Bedford sediment (350 days versus 150 for NBH). The behavior captured with the PICs simulation should aid in the estimation of bioaccumulation and the effect of organic carbon in the sediment.

Figure 48. Simulated Total PCBs Concentrations in PICs Exposed to Bremerton Harbor Sediment.

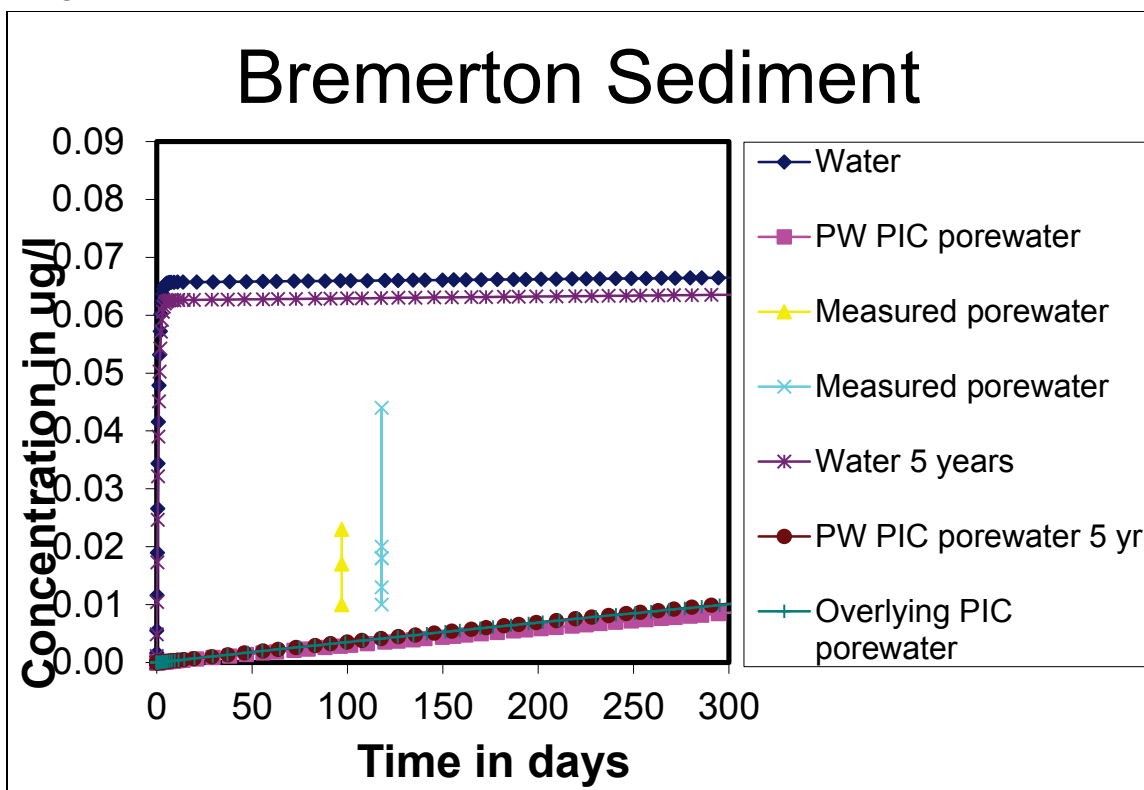
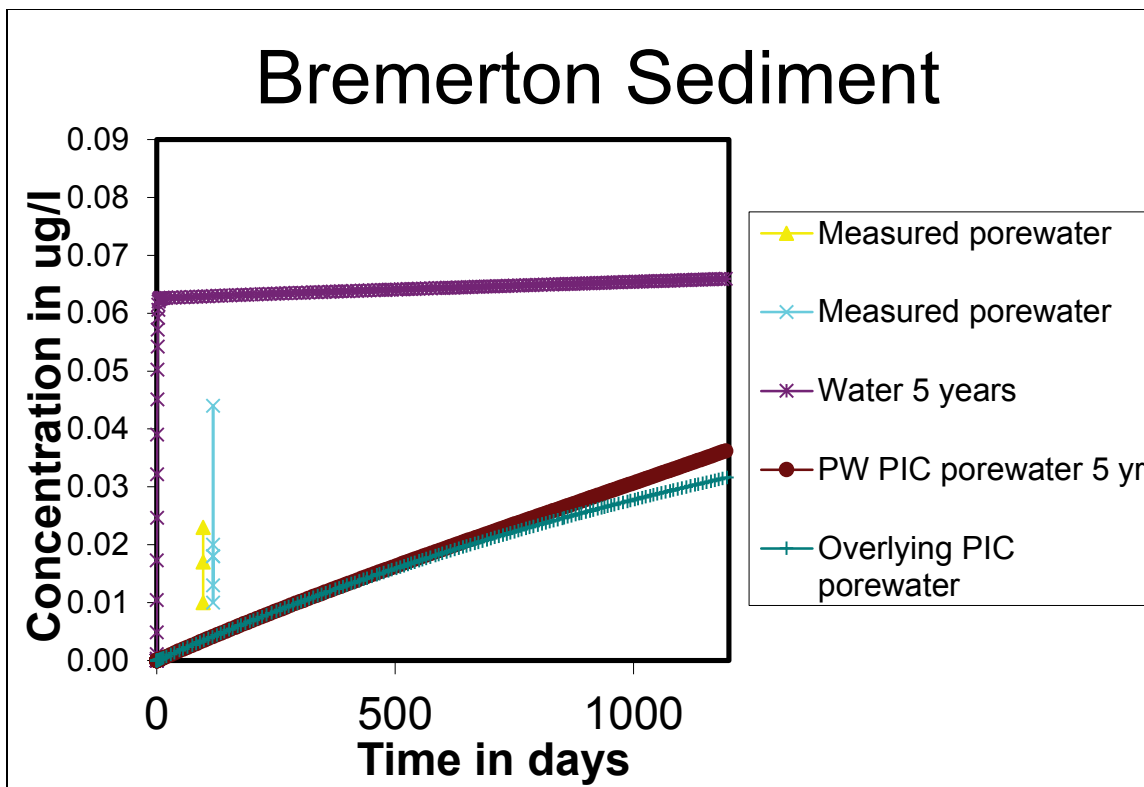


Figure 49 for the Bremerton sediment is analogous to Figure 46 for NBH. Similar to the New Bedford PICs, the flux is dominated by the water column followed by significant flux from the sediment bed after 500 days. The observation is similar to what was observed in the New Bedford PICs, although the time to reach equilibrium was longer. The authors wanted to make sure the dissolved concentration was similar to that in the sediment pore water; secondly, the authors wanted to ensure that the time that was allowed for equilibrium was adequate. The simulation shows that the pore water PIC was not fully loaded; it takes around 200 days to achieve equilibrium with the surrounding sediment. However, the concentration changes that take place over the period of the experiment are less than the variance of the analysis. Therefore, one can simulate the diffusion of the PCBs into the sand PICs and thus use the simulations in estimating both PCBs bioaccumulation and the functional attributes of the organisms.

Figure 49. Three-year simulation of Total PCBs Concentrations in PICs Exposed to Bremerton Harbor Sediment.



The third modeling task is to be able to simulate the PCB congeners, in particular 24 and 104, not only in the reactor and aquariums but also in the PICs. One needs to simulate the sorption and diffusion of the two congeners from the recirculated water into the sand PICs and the sediment PICs. In essence, the authors are estimating the losses pointed out in the first task and showed in Figure 42 and Figure 43. Figure 50 and Figure 51 show the PCB congener 24's simulation for four years and 200 days respectively. Figure 51 shows that the PICs were loaded with the external congener when the experiment was started. The simulation shows the loading and resulting water column concentration of PCB congener 24 if the reactor loading was maintained at a constant level. As discussed before, reactor loadings decreased by less than twenty percent throughout the experiment. The sand PICs exhibit the highest concentration because of the low TOC of the sand (f_{oc} less than one percent carbon). Both the PW PIC and the Overlying (OVL) PIC exhibit similar short term (less than one year) concentration and loading. Over time, since the f_{oc} below the sand layer is that of the sediment, the concentration of PCB congener 24 starts to deviate from that of the OVL PIC (see Figure 51, yellow line versus light blue). All the PICs pore water concentration will eventually reach that of the water column and reactor; in this case around five years (Figure 50).

Figure 50. Four-year simulation of PCB 24 Congener Concentration in PICs Exposed to New Bedford Sediment.

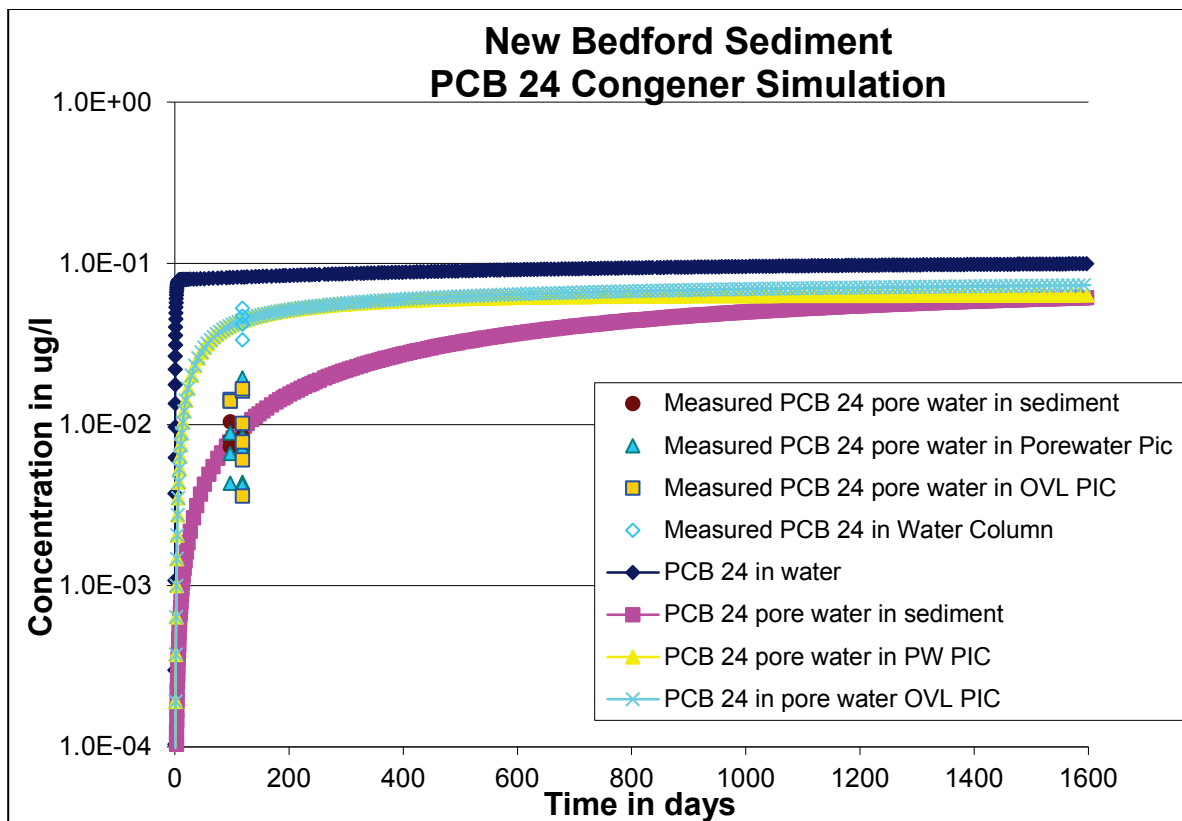


Figure 52 and Figure 53 show the PCB congener 104 simulation for four years and 200 days, respectively, for the New Bedford Sediment experiment. The simulations are similar to those for PCB congener 24. Congener 104 is less mobile than congener 24; it has a much higher K_{ow} , thus it has more affinity to organic carbon. The behavior is reflected in the lower loadings measured in the reactor and water column, and longer time to reach equilibrium versus congener 24. After four years, the concentration in the sediment pore water for congener 104 is still one order of magnitude less than the water column concentration, while that of congener 24 is less than five percent different. The RECOVERY model under-predicts the sediment pore water concentration and over-predicts the pore water in sand PICS for both PCB congener 24 and 104 as compared to the PE data. The difference could be the result of higher TOC in the sand PICS as compared to the measured bulk sand that was used in the experiment. Another difference could be cross contamination from the sediment PIC into the sand PICS in the setup or during the experiment.

Figure 51. Simulation of PCB 24 Congener Concentration in PICs Exposed to New Bedford Sediment.

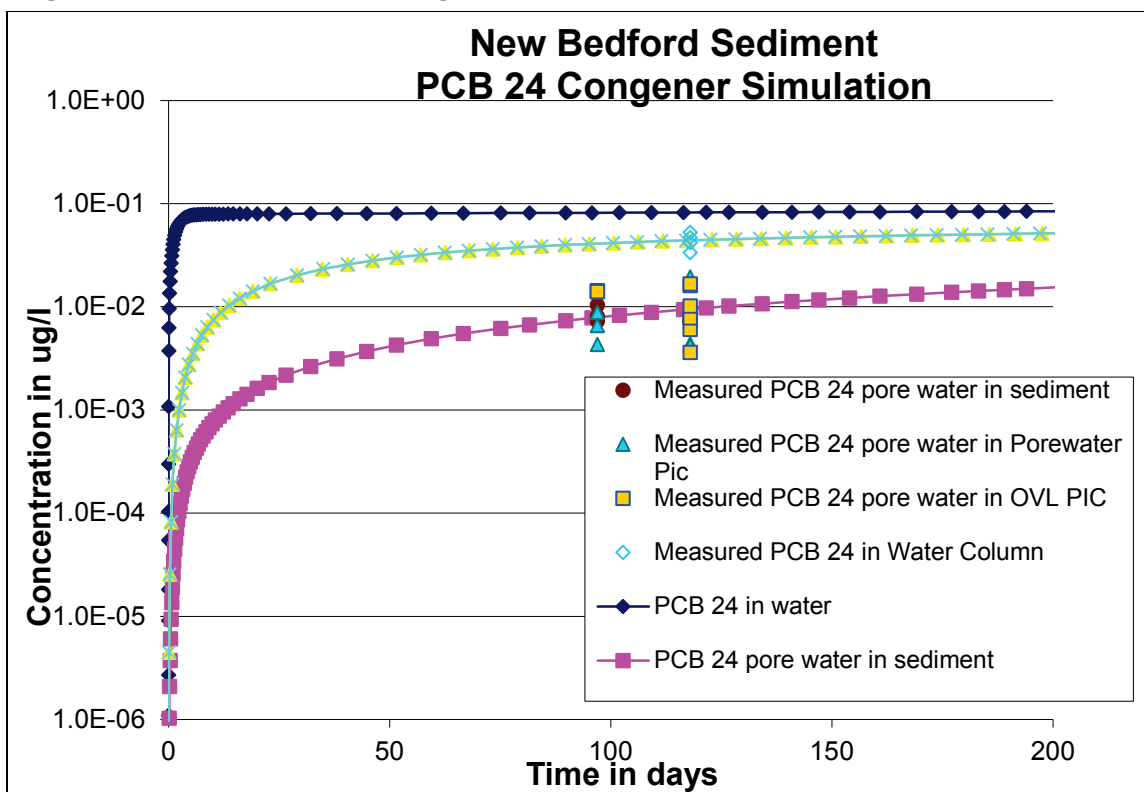


Figure 52. Four-year simulation of PCB 104 Congener Concentration in PICs Exposed to New Bedford Sediment.

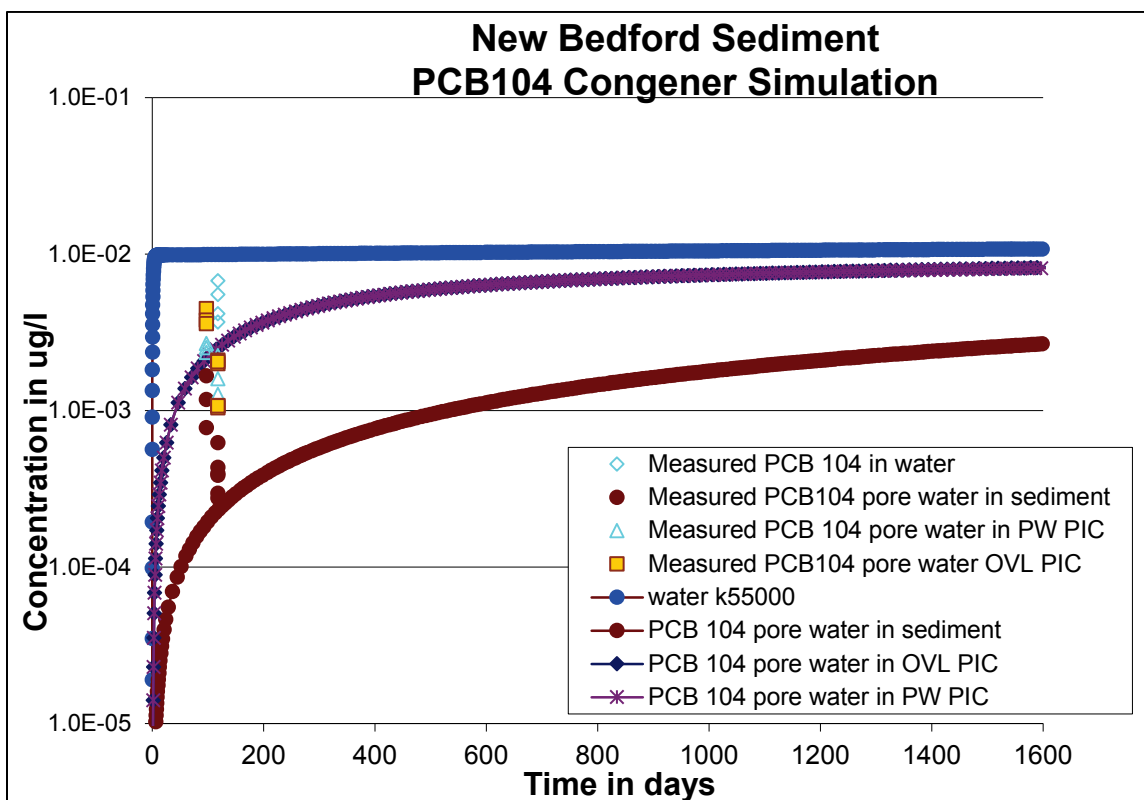


Figure 53. Simulation of PCB104 Congener Concentration in PICs Exposed to New Bedford Sediment.

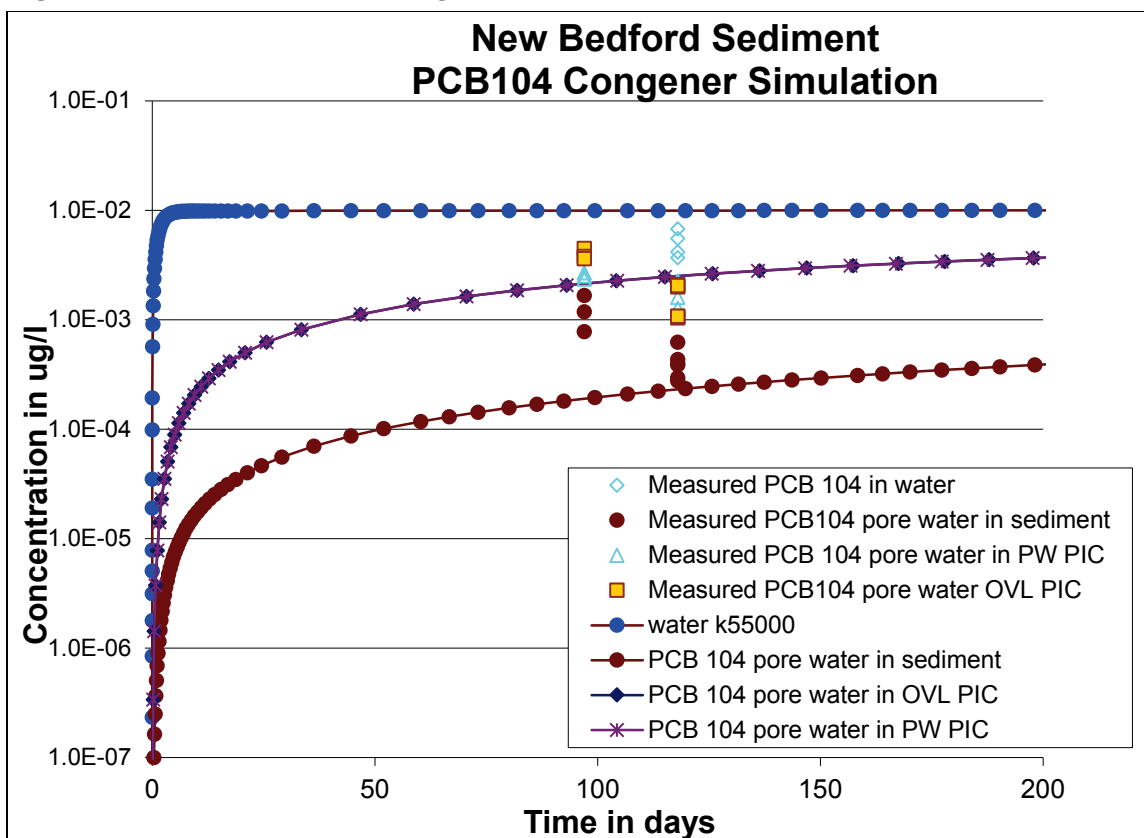


Figure 54 and Figure 55 show the simulation for PCB congener 24 loaded into the Bremerton Harbor sediment experiment. Similar to the New Bedford experiment, the RECOVERY model is able to simulate the system loading and the dynamics of the PICs. The RECOVERY simulation for PCB 24 congener in Bremerton sediment (pore water) is a closer match than the sand PICs (pore water), which are slightly under-predicted (Figure 55). The PE data are more spread out for the Bremerton experiment, especially that of the OVL PIC. The model under-predicts the sand PICs relative to the match of the New Bedford experiment. The PE data were not as complete; i.e., no PW PIC data and no water column data over the PICs were available. The simulation aids in the interpretation of the PIC behavior and shows that both the PW and the OVL PICs should have identical PCB 24 congener concentrations since both PICs are loaded from the water column and have identical geochemical properties (same sand, f_{oc} , grain size, porosity, and particle density).

Figure 54. Four-year simulation of PCB 24 Congener Concentration in PICs Exposed to Bremerton Harbor Sediment.

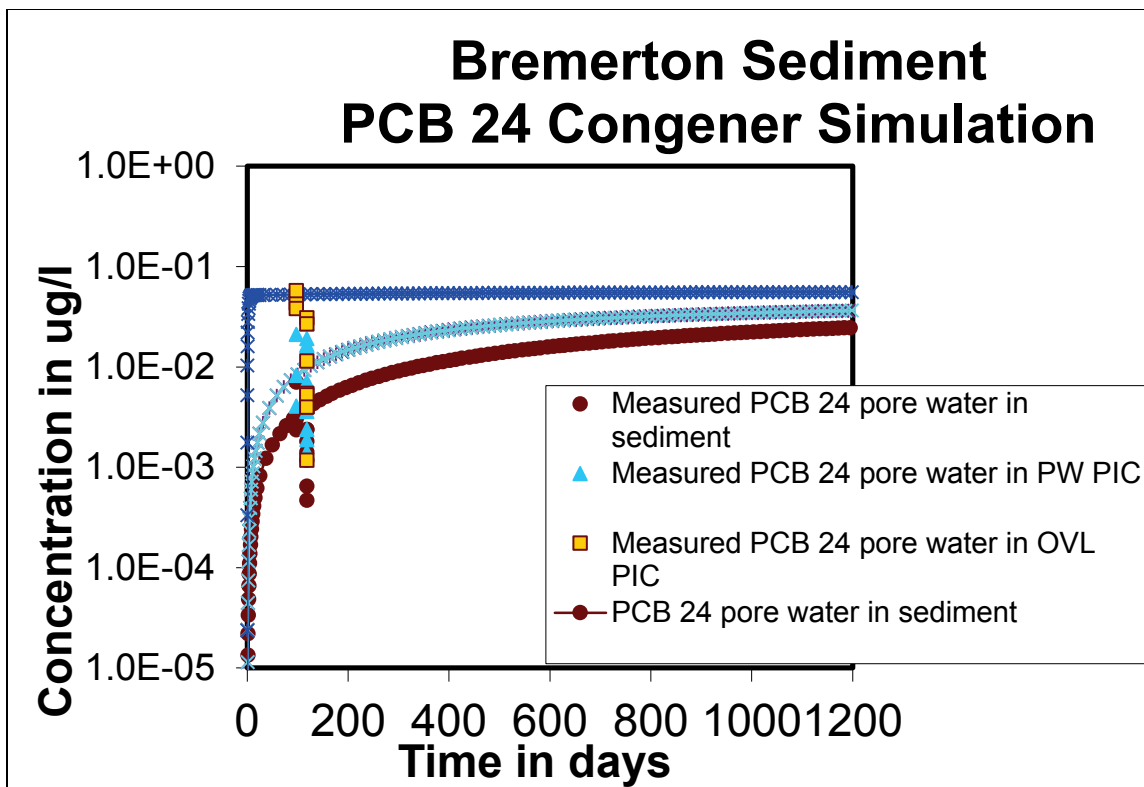


Figure 55. Simulation of PCB 24 Congener Concentration in PICs Exposed to Bremerton Harbor Sediment.

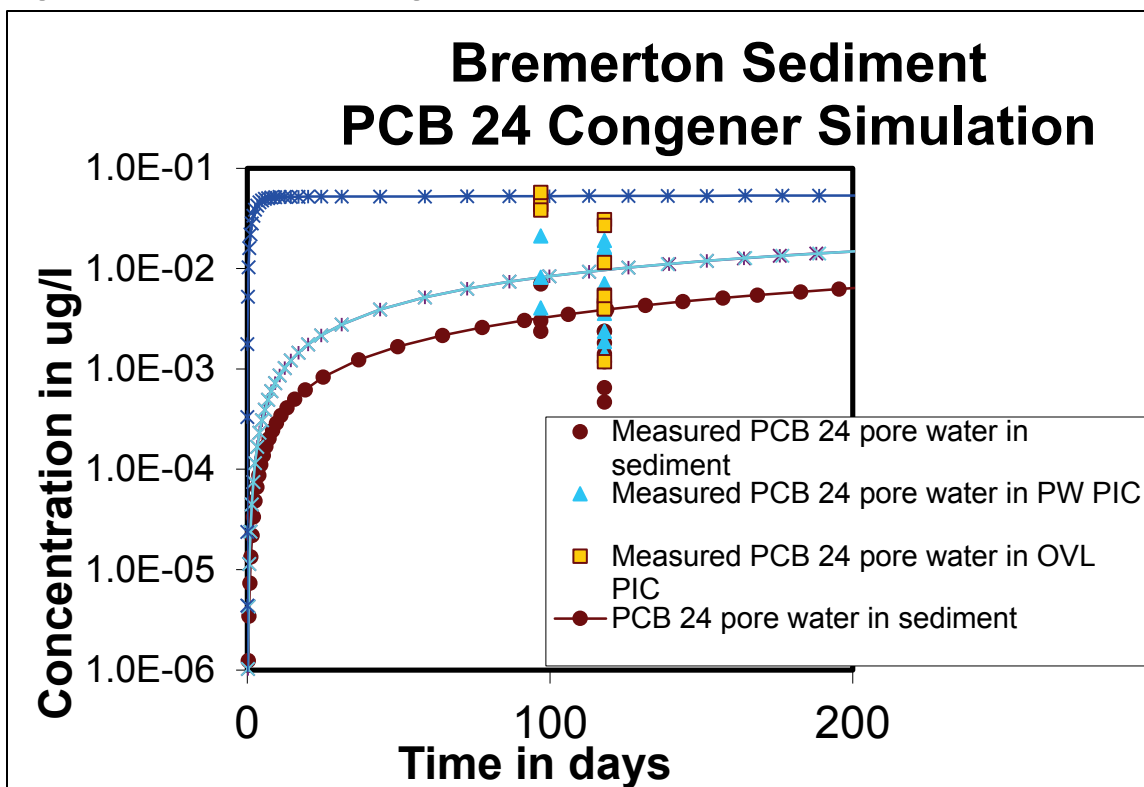


Figure 56 and Figure 57 show the simulation for PCB congener 104 loaded into the Bremerton Harbor sediment experiment. Similar to the New Bedford sediment results, the RECOVERY simulation under-predicts the concentration for PCB 104 congener in Bremerton sediment (pore water). In both cases, the extrapolation of the PE data does not closely match the expected concentration. The sand PICs (pore water) are also under-predicted (Figure 57), and the match is not as close as the New Bedford simulation. Again, it is important to point out that the authors are not fitting the data; instead, the authors simply use the K_d from the PE data to run the simulations for the truly dissolved concentration. The K_d s adjusted from the PE data are at least an order of magnitude greater than the literature K_{ow} s and K_{oc} s.

Figure 56. Four-year simulation of PCB 104 Congener Concentration in PICs Exposed to Bremerton Harbor Sediment.

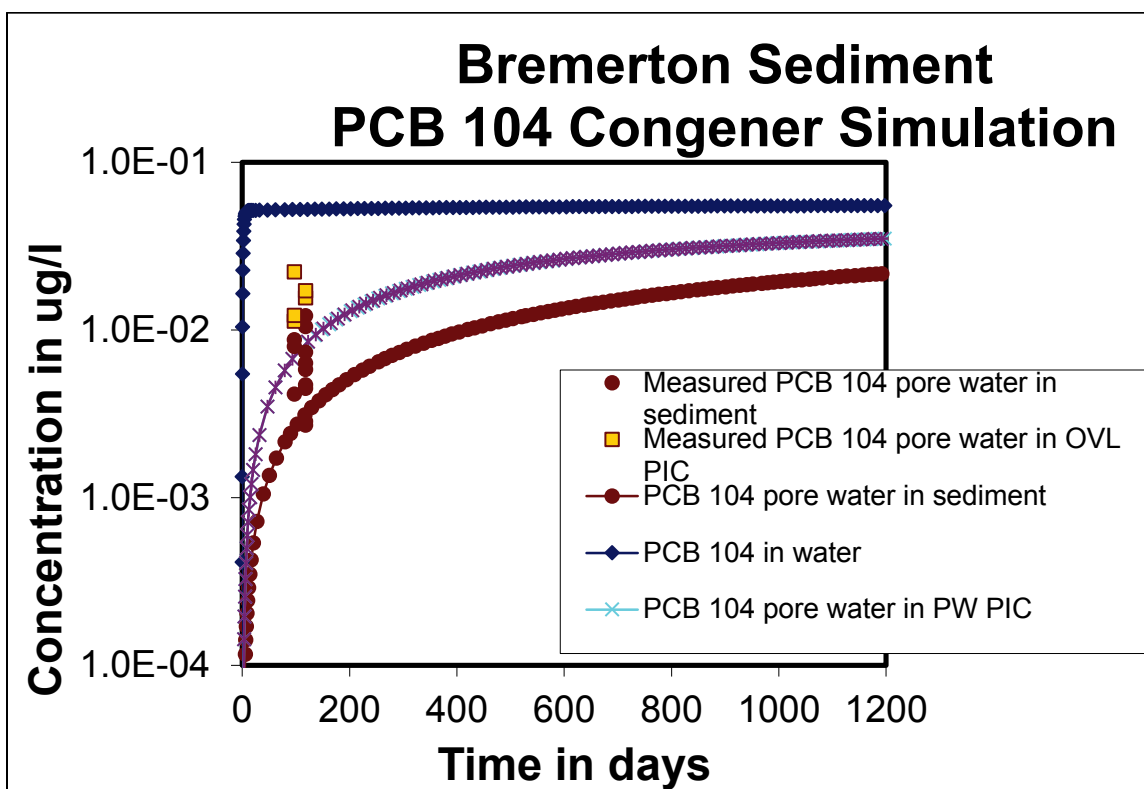
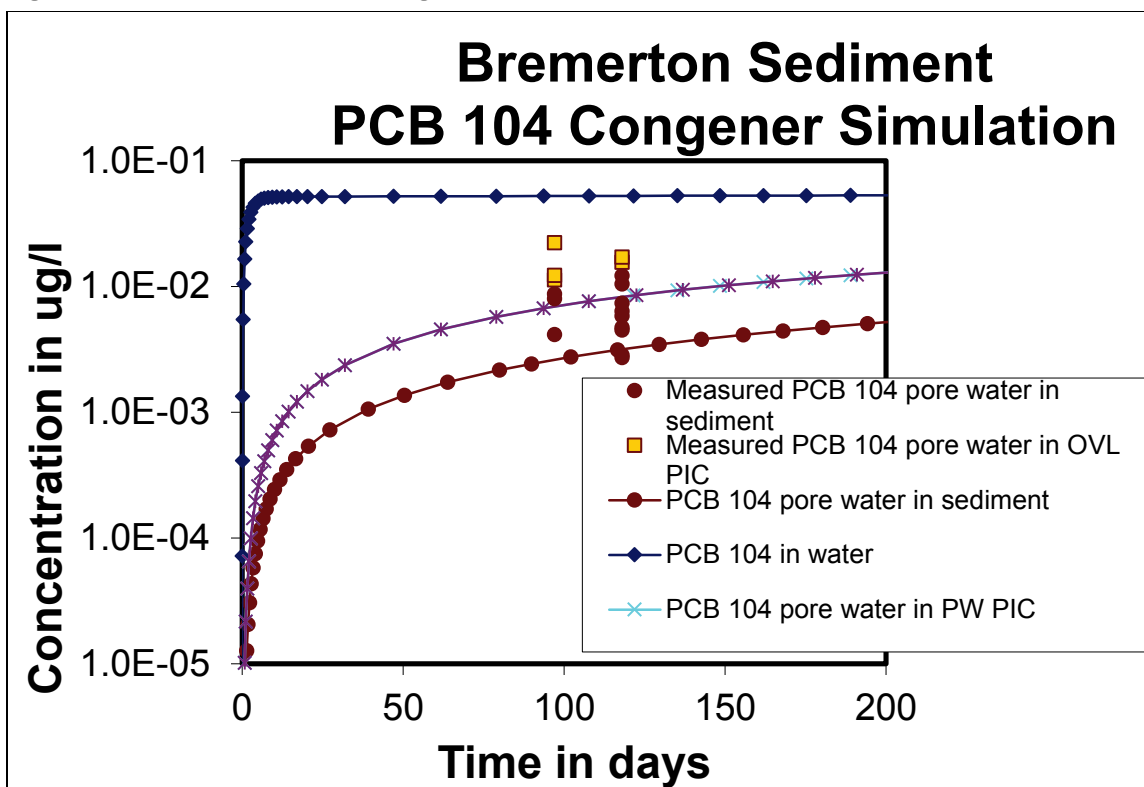


Figure 57. Simulation of PCB 104 Congener Concentration in PICs Exposed to Bremerton Harbor Sediment.



Overall, the RECOVERY model does a good job of predicting the trends, which allows researchers to infer difference in behavior due to sediment properties and chemical properties, factors that affect the functional behavior of organisms. It would be useful to collect PE data overtime (longer than 30 days) to see how the model is able to match the temporal PE data.

The last modeling task was to simulate the organism uptake, using the predicted PCB concentration of the different PICs, thus addressing the functional biology in bioavailability. Figure 58 and Figure 59 predict the tissue concentration of *Leptocheirus plumulosus* in the different PICs in New Bedford sediment. Equation 4 was solved using the coefficients estimated in sections 12.4.2 and 12.4.3 and the time variable concentration for all three PICs simulated by the RECOVERY model. Figure 58 shows the tissue concentration for the sum of the PCB congeners; the estimated average value for the *Leptocheirus plumulosus* in the sediment PIC was 15,990 ($\mu\text{g PCB/kg tissue}$), close to the value in Figure 32 of section 13.3.2. The estimated average PW PIC and the OVL PIC *Leptocheirus plumulosus* tissue concentration for the sum of all the PCB congeners was 584 and 700 ($\mu\text{g PCB/kg tissue}$) respectively.

Figure 58. Sum of PCBs Congeners *Leptocheirus plumulosus* Tissue Concentrations in PICs Exposed to New Bedford Sediment.

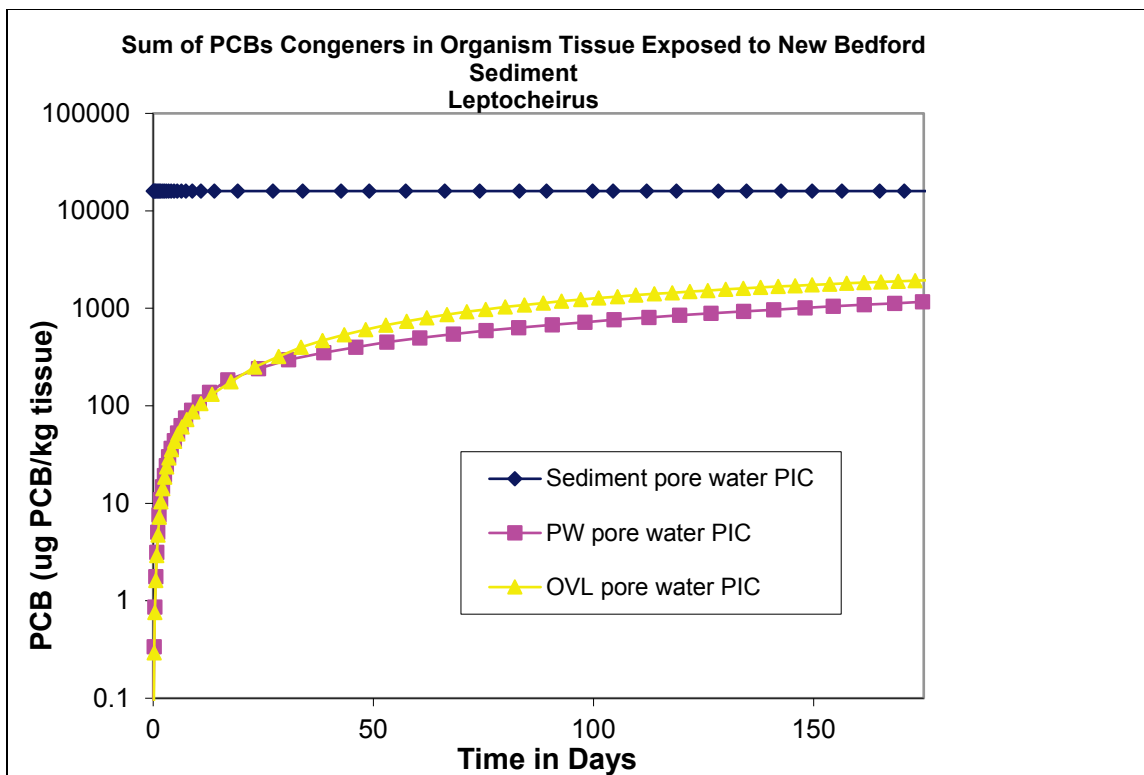


Figure 59. PCB 24 Congener *Leptocheirus plumulosus* Tissue Concentration in PICs Exposed to New Bedford Sediment.

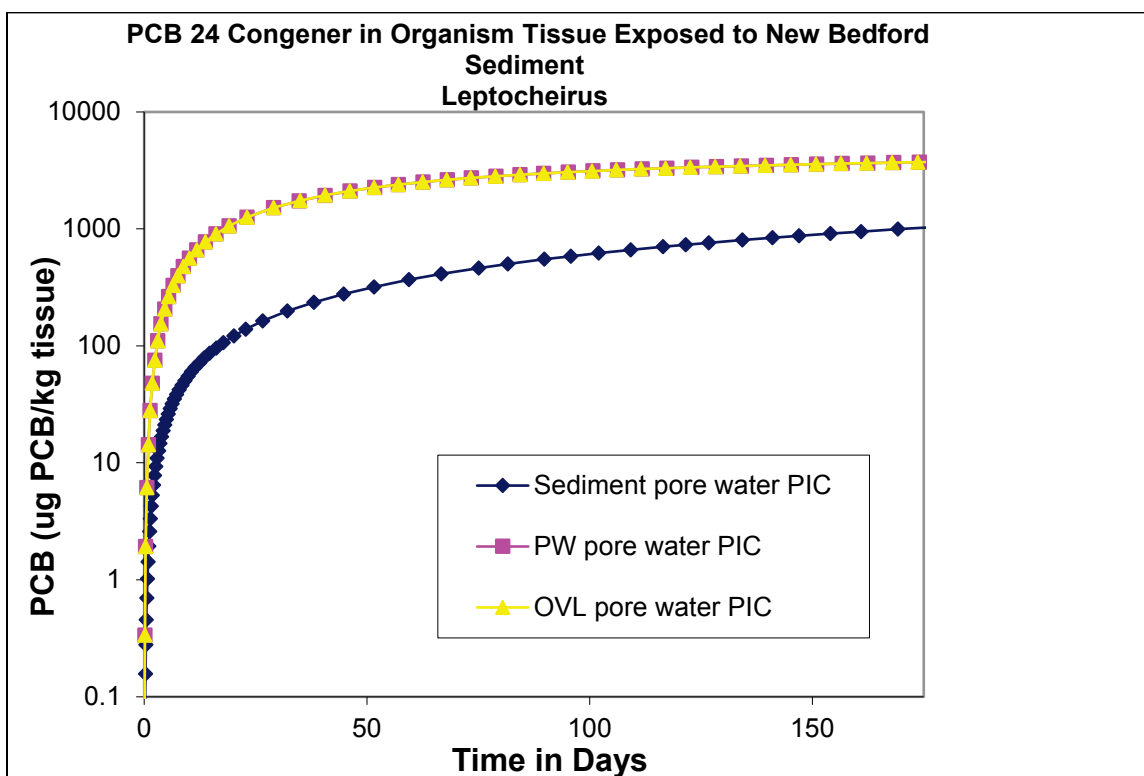


Figure 59 shows the time variable PCB 24 congener tissue concentration in *Leptocheirus plumulosus* exposed to the New Bedford sediment PICs. The values estimated for the PCB 24 congener were not as close (see Figure 37 in section 13.3.2) as those estimated for the total PCBs. One problem was that RECOVERY estimated the concentration in both sand PICs loaded with PCB 24 to be the same, which produced the same sand and f_{oc} results in equal concentration of PCB 24 congener. Therefore, those two PICs showed exact *Leptocheirus plumulosus* tissue concentration, which do not agree with Figure 37 in section 13.3.2. RECOVERY also predicted a much higher concentration in the sediment PIC resulting in very high PCB 24 congener tissue concentration as compared to Figure 37 in section 13.3.2.

11.4 Conclusion

As previously stated, RECOVERY does a good job at predicting the trends and difference in behavior due to sediment properties and chemical properties, except for the sand PICs loaded with PCB 24. In the OVL PIC, *Leptocheirus plumulosus* was able to uptake a higher concentration of PCB 24 than from the PW PIC; thus, something in the simulation is not fully capturing the loading from the water column into those two PICs. The simulation of the tissue update needs further refining to address the limitations of the predictions as shown in the two cases for *Leptocheirus plumulosus*.

12 TASK 3A: Experiments using management scenarios: impact of functional feeding group on efficacy

12.1 Introduction

The success of *in situ* remedies (e.g., capping or the use of amendments) will depend on the compatibility of those remedies with the biological attributes of the species to be protected. An understanding of how the exposure processes affected by remedies interact with the functional behavior of different benthic species is needed in order to properly design *in situ* remedies and to set realistic performance standards for such remedies.

In order to gain insight into the interaction of remedies with species functional attributes, the authors designed an experiment to evaluate changes in exposure (through the application of PEDs and measures of bioaccumulation) under two remedy conditions: (1) A thin layer cap of sand, and (2) a thin layer of granular activated carbon (GAC)-amended sediment. This experiment is an extension of the work described in Task 2a (Section 13).

12.2 Materials and methods

12.2.1 Test sediments and chemicals

Sediment was collected from BNC in Washington State (Pier 7; 47.558780 °N; 122.628896 °W). A different aliquot of BNC sediment was used from what was tested in Task 2a (Section 13). Therefore, new analysis for PCB congeners in this sediment was obtained. PCB congeners 24 (2,3,6-trichlorobiphenyl) and 104 (2,2',4,6,6'-pentachlorobiphenyl) were purchased from a commercial source (BZ#24, BZ#104 UltraScientific, N. Kingstown, RI, USA) for passive dosing into the overlying water. All analytical determinations were as described in Appendix A: Supporting Data (Table S1).

12.2.2 Benthic test organisms

The same four benthic macroinvertebrates were selected as used in Task 2a (Section 13) to represent a diversity of phyla (e.g., arthropods, annelids, and molluscs) and functional feeding strategies (e.g., surface deposit-feeders, infaunal deposit-feeders, suspension-feeders). These organisms were the surface deposit-feeding amphipod *Leptocheirus plumulosus*, the infaunal deposit-feeding amphipod *Eohaustorius estuarius*, the filter-feeding clam *Mercenaria mercenaria*, and the infaunal deposit-feeder polychaete *Neanthes areanaceodentata*. The rationale for selection and organism ecology was previously described in detail in Sections 8 and 13.

12.2.3 Organism chambers

The all-glass organism exposure chambers previously described in Section 13 for the overlying water exposure (see Figure 30 for illustration) were used in this experiment. To briefly review, 36 chambers were constructed of silanized glass plates that were sealed with marine grade caulk to have outer dimensions of 9 X 9 X 4 cm (see Section 13 for methodology). A stainless steel lid with 750 μ m mesh openings was caulked to the top of each chamber to prevent organisms from escaping, while allowing exchange with the surrounding overlying water. Glass tubes were inserted into lids to allow the addition of test organisms to the equilibrated exposure system as previously described (Section 15.2.3) and illustrated (Figure 62).

12.2.4 Exposure system

The same recirculating exposure system employed in Task 2a (see Sections 9 and Section 13 for detailed description) was used for this experiment. The system consisted of four silanized glass 5-gallon tanks, with each tank dedicated to exposure of one of the four organisms. Overlying seawater (25 ppt, Crystal Sea Marine Mix®, Enterprises International, Baltimore, MD, USA) was aerated and slowly recirculated at 3 ml/min through TFE tubing into each tank by piston pumps (Fluid Metering, Inc.) to maintain passively dosed concentrations in the overlying water. Water was recirculated to a divided 19.7 L ionized aluminum reactor box within which PCB 24 and 104 were passively dosed (see Section 13 for methods). These two congeners were not detected in the test sediment; thus, any detection of these congeners in tissue or PE samplers could be traced to a water column source. The exposure was maintained at 20 ± 1 °C using a recirculating

REMCOR heating/cooling unit (REMCOR Products Company, Glendale Heights, IL) with continuous florescent light.

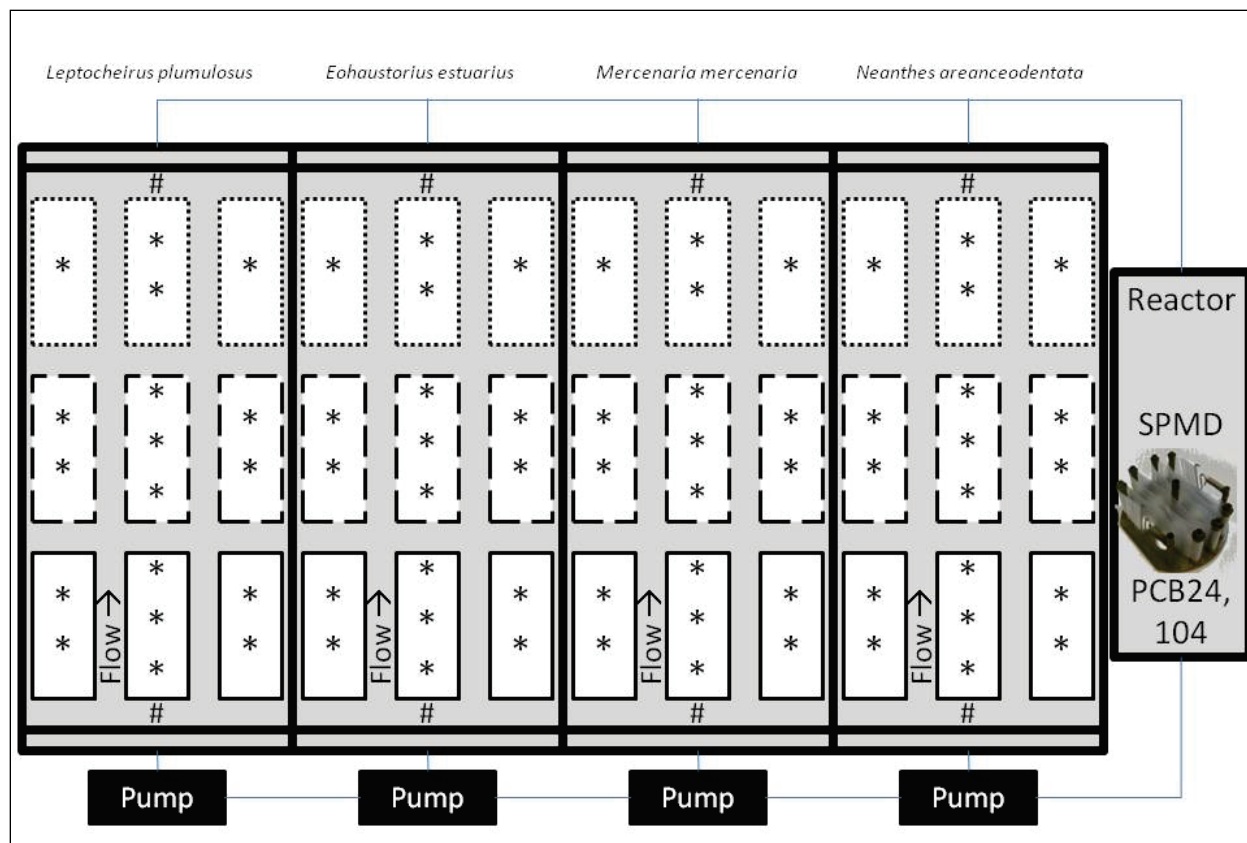
12.2.5 Sediment treatments

Three different sediment treatments (i.e., unamended sediment, sand cap, AC amendment) were employed to determine the efficacy of common remediation methods for contaminated sediments to reduce bioaccumulation of PCBs into organisms with different feeding strategies. Thirty-six chambers were placed into the exposure system, with 12 chambers dedicated to each of the three sediment treatments (4 organisms X 3 replicates per organism = 12 chambers for the treatment). The unamended sediment consisted of 427 g (or approximately 8.5 cm in the 9 cm high exposure chamber) of unmodified BNC sediment (wet weight) added to each of the 12 chambers to determine baseline bioaccumulation potential to compare to the amended sediment. To reduce cross contamination, the unamended sediment chambers were positioned so that they were downstream of the amended sediment treatments within each of the four, 5-gallon organism exposure tanks. The GAC amended BNC sediment was prepared by slowly adding 19.5 g GAC to 1500 g BNC (target concentrations: 2% GAC by dry mass giving at total TOC³ of 3%), while being mechanically stirred in a stainless steel container. Mechanical mixing continued for ten minutes and the mixture was added to the chambers shortly after mixing. To prepare the 12 GAC amended chambers, 327 g unamended BNC sediment was added (approximately 6.5 cm), followed by 101.3 g (approximately 2 cm) of the GAC amended BNC sediment layered evenly on top of the unamended sediment. The sand cap treatment was prepared by initially adding 327 g unamended BNC sediment (approximately 6.5 cm) to each of the 12 chambers, followed by adding an even layer (approximately 2 cm) of 123 g sand (< 60 µm in size). The 36 chambers containing the sediment treatments were then added to the exposure system, with each of the 4 tanks containing 9 chambers (3 sediment treatments X 3 replicates). A fine grained sand (< 60 µm) was added around the chambers within each of the four tanks to the height of the top of the chambers to simulate the experimental conditions used in Task 2a (Section 13). However, instead of using the experimental sediment as in Task 2a, sand with relatively low affinity for the PCB 24 and 104 dosed into the water column (see Section 13) was used in Task 3 to surround the exposure chambers. Overlying water (25 ppt, Crystal Sea Marine Mix®, Enterprises International, Baltimore,

³ Accounts for the 1.3% TOC of the BNC sediment.

MD, USA) was then slowly added over a 24-h period. Figure 60 provides an illustration of the layout of sediment treatments in the exposure system. The entire system was allowed seven days for equilibration of the GAC treatment with sediment pore water and the passively dosed PCB concentrations so that it could come to stability in the overlying water.

Figure 60. Diagram of exposure system: including position of sediment treatments, organisms, and polyethylene devices.



Large rectangles with thick lines represent the four glass tanks that housed PICs and organisms.

The nine smaller rectangles within each tank represent the PICs.

Solid-line rectangles: PICs with sand caps (12 total, 3 for each organism).

Dashed-line rectangles: PICs with GAC amended sediment (12 total, 3 for each organism).

Dotted-line rectangles: PICs with unamended sediment (12 total, 3 for each organism).

*PEDs in the substrate (positions indicated in panel b)

#PEDs in the overlying water

12.2.6 Bioaccumulation exposures

Following the seven-day equilibration period, each of the four test organisms were added to nine PICs (three unamended sediment, three GAC-amended sediment, and three sand capped sediment) held separately in the four glass tanks (Figure 60). Plastic transfer pipettes were used to add 35 *L. plumulosus*, 35 *E. estuarius*, 5 *M. mercenaria* or 5 *N.*

arenaceodentata to the equilibrated, in-place PICs using the previously described glass tubes. Exposure durations were 7 days for amphipods and 28 days for worms and clams, based on steady state estimates for these organisms in NBH sediment (Lotufo et al, in review). Since preliminary observations revealed that *M. mercenaria* ceased siphoning after 3 to 5 days when food was absent, approximately 6,000 cells/ml of Phytoplex (Kent Marine, Franklin, WI) was added to the test system to maintain filter-feeding, as previously described (Section 13.2.5). The exposures were conducted in basic accordance with ASTM (2010).

At the termination of each exposure, PICs were removed and sediment sieved (0.6 mm stainless steel mesh) to recover organisms. Amphipods and worms were purged for six hours in 1 L beakers containing clean seawater. Soft bristle paintbrushes were used to push remaining undigested sediment from worm guts, while clams were dissected to remove undigested material. All tissue was thoroughly rinsed with deionized water and frozen in 20 ml glass scintillation vials with TFE lid liners for analytical determination.

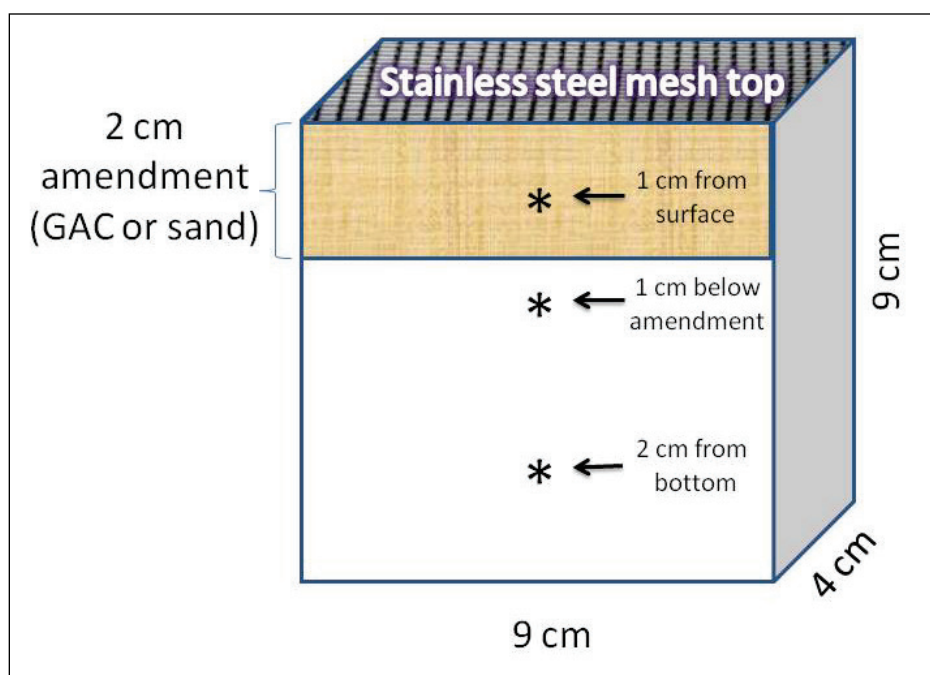
Due to low survival in the unamended sediment ($0 \pm 0\%$) and GAC-amended ($11 \pm 20\%$) treatments (survival was $95 \pm 4\%$ in the sand cap treatment suggesting organisms were healthy), the *E. estuarius* test was repeated for 4 days during the final portion of the 28 day exposure period used for *M. mercenaria* and *N. arenaceodentata*. Sediment treatments for the *E. estuarius* exposure repeat experiment were freshly prepared as previously described (Section 15.2.5). Survival in this four-day exposure was high for all treatments (81–95%). Adequate tissue mass was recovered for analytical chemistry.

12.2.7 Passive sampler exposures

PED samplers were constructed by cutting polyethylene sheets obtained from a commercial source (ACE Hardware Corp., Oak Brook, IL) into uniform size (0.5 by 2 cm). First, the PEDs were cleaned by soaking in dichloromethane (24 hours) and then in methanol (24 hours). The samplers were spiked with congeners 3, 14, 35, 69, and 88 (0.24 to 0.48 $\mu\text{g/L}$) in a 125 mL amber bottle for 30 days at the U.S. Environmental Protection Agency Office of Research and Development laboratory (Narragansett, RI), and then frozen until use. Two PEs were added to the overlying water of each of the four exposure tanks (eight total overlying water PEs). An additional PE was added to the reactor. PEDs were added 3 cm below the

substrate surface (1 cm below the GAC-amendment and sand cap) as the unamended BNC sediment was originally added to the chambers. In addition, PEs were added to each organism chamber 1 cm below the substrate surface. PEDs were added to the GAC and sand caps by inserting half of the amendment (by mass), adding the PE, and then inserting the other half of the amendment so that the PED was 1 cm below the surface. Unamended sediment PICs did not have the PED 3 cm below the surface. A “deep” PED (2 cm from bottom of chamber) was also added to the unamended BNC sediment to a single replicate of each of the sediment treatments (three deep PEDs per tank/organism). Figure 60 illustrates the position of the PEDs in the exposure system, while Figure 61 illustrates the position of the PEs within the chambers.

Figure 61. Diagram of polyethylene device (PED) position in the Pathway Isolation Chambers (PICs).



*represents PED position. All PICs contained a PED 1 cm from the substrate surface. All PICs with GAC and sand cap amendments contained a PED 3 cm below the surface, or 1 cm below the amendment (unamended sediment PICs did not have the 3 cm PED). The PED 2 cm from the bottom (or 7 cm from the substrate surface) was added to a single replicate with each animal treatment (see Figure 60).

The PEDs were sampled from the exposure system at the same time as organism recovery, rinsed thoroughly with deionized water, and then frozen in 20 ml glass scintillation vials with TFE lid liners for analytical determination. Data were expressed as ng PCB/ mg PED or ng/L. Due to

low PED recovery in the *L. plumulosus* and *E. estuarius* PICs, PEDs were pooled for one composite “amphipod” data set.

12.2.8 Analytical

Sediment, passive samplers, water, and tissue samples were analyzed at the ERDC Environmental Chemistry Branch (Vicksburg, MS) for PCBs congeners following USEPA 846 methodology (method 3665). Tissue samples were analyzed for organics by a micro-analytical technique, described in Jones et al (2006). Lipid analysis was conducted using a colorimetric method (Van Handel 1985). Lipid content for *N. areanaceodentata* from Lotufo et al (2000) was used because tissue recovery was insufficient to perform lipid analysis.

12.2.9 Data analysis

All statistical comparisons and determinations of data normality (Kolmogorov-Smirnov test) and homogeneity (Levene’s test) were performed using SigmaStat v3.5 software (SSPS, Chicago, IL, USA). One-way ANOVA was performed to determine statistically significant differences ($\alpha = 0.05$). If data failed normality or homogeneity tests, \log_{10} or square root transformations were performed. The Holm-Sidak method was employed as an all-pairwise multiple comparison procedure to determine statistical significance in bioaccumulation between different organisms and sediment treatments. Following transformation, normality could not be obtained in only one case (comparison of mono- to tri-chlorinated congeners for the unamended across test species). In this case, an ANOVA on ranks was used, applying Dunn’s method for multiple comparisons.

12.3 Results and discussion

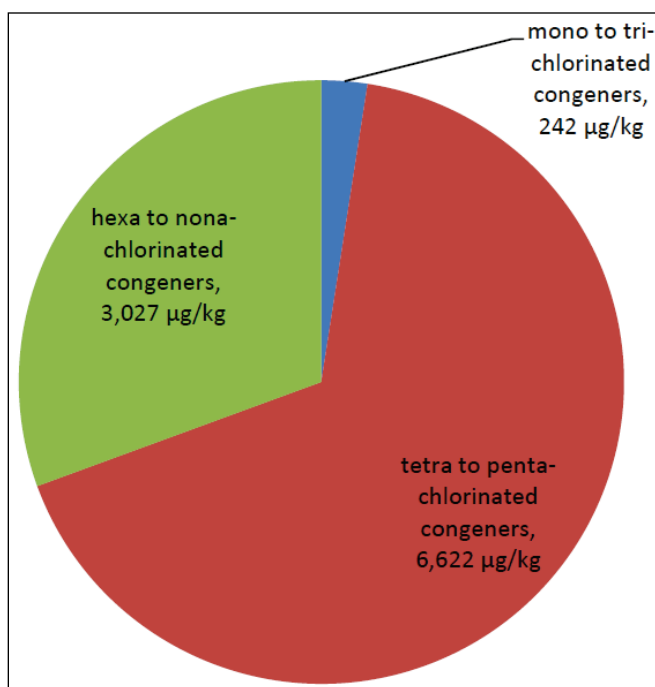
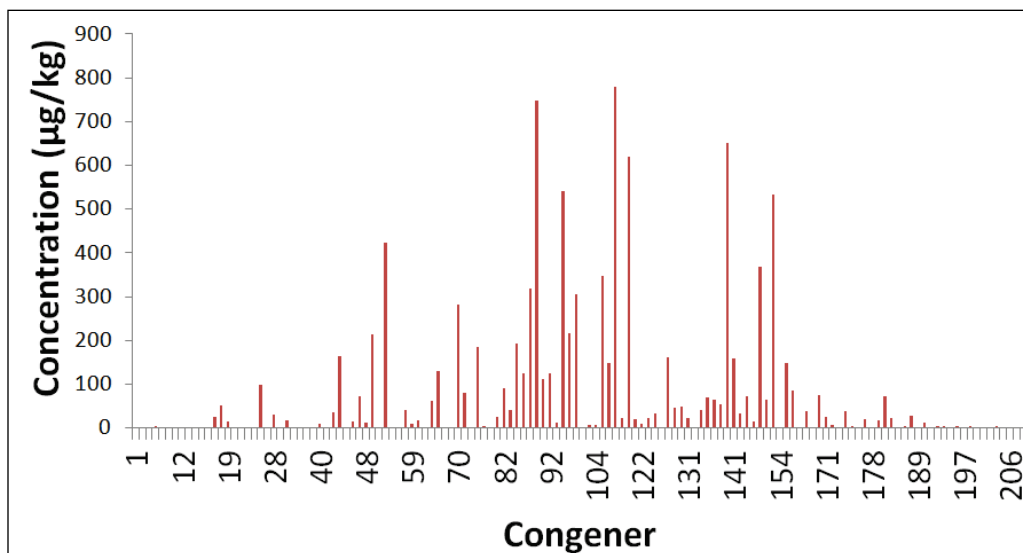
12.3.1 PCB congeners in sediment

Sum PCB congeners was 9,891 $\mu\text{g}/\text{kg}$ in the BNC sediment. The congener distribution and homolog groups are presented in Figure 63; much of the concentrations detected fell between congeners 50 through 150. TOC was 1.3%. The percentages of gravel, sand, silt, and clay were 0, 61, 28, and 10%, respectively.

Figure 62. Photographs of the exposure system. Panel (a) illustrates the position of organisms and sediment amendments in the exposure system. Panel (b) shows the entire exposure system including pumps and reactors. Panel (c) shows the addition of a PED before the final 1 cm sand was added. Panel (d) shows a sand cap on top of the sediment. Panel (e) shows a *Neanthes arenaceodentata* burrow. Panel (f) shows the different sediment treatments prior to the addition of sand around the chambers.



Figure 63. Distribution of PCB congeners in the Bremerton Naval Complex (BNC) sediment used in this exposure. Concentration of (a) all congeners and (b) homolog groups. Concentrations are provided as $\mu\text{g}/\text{kg}$.



12.3.2 Tissue recovery and residues

Organism recovery was relatively high with the exception of *N. arenaceodentata* (Table 23). Tissue masses were adequate for PCB analysis with one exception (*N. arenaceodentata* for the GAC amendment). Millward et al (2005) previously reported compromised *N. arenaceodentata* health (reported as low growth) in sediments amended

with GAC; lower individual *N. arenaceodentata* mass was also found in this investigation (Table 23). Survival of *L. plumulosus* was slightly lower in the sand cap (70%) relative to the sediment treatments ($\geq 81\%$), though recovered tissue mass was sufficient for chemical analysis. Previous work provides strong evidence of reduced *L. plumulosus* survival in sand (Emery et al 1997; Kennedy et al 2009) relative to finer grained sediment. Tissue mass recovered for *E. estuarii* and *M. mercenaria* was high in all treatments.

Table 22. Efficacy of different sediment treatments based on organism or functional feeding strategy.

Organism	2 cm GAC amendment		2 cm sand cap	
	Efficacy	Consideration	Efficacy	Consideration
<i>Leptocheirus</i>	None observed	Overlying water exposure, GAC did not significantly reduce pore water concentrations	Statistically significant reduction in bioaccumulation	Sand makes poor habitat
<i>Eohaustorius</i>	Statistically significant reduction	Mid-depth burrower, primarily sediment exposure, low overlying water, surficial sediment exposure	Statistically significant reduction in bioaccumulation	Can burrow past 2 cm
<i>Mercenaria</i>	None observed	Exposed mostly to overlying PCBs, significantly disturbs and mixes top 2–3 cm sediments	No reduction	Exposed to overlying PCBs, significantly disturbs and mixes top 2–3 cm sediments
<i>Neanthes</i>	None observed	Adverse health impacts; can burrow below the 2 cm amendment	Statistically significant reduction in bioaccumulation	Can burrow past 2 cm

Table 23. Summary of percent animals and tissue mass recovered.

Test organism	Treatment	Average Survival (%)	Average Total Recovered mass (mg)	Average Individual mass (mg)
<i>Leptocheirus plumulosus</i>	Unamended sediment	81 \pm 14	99.1 \pm 28.8	2.8 \pm 0.5
	GAC amendment	90 \pm 6	95.4 \pm 10.5	3.5 \pm 0.5
	Sand cap	70 \pm 9	68.5 \pm 22.2	3.0 \pm 0.1
<i>Eohaustorius estuarii</i>	Unamended sediment	83 \pm 8	122.8 \pm 14.8	4.9 \pm 0.5
	GAC amendment	95 \pm 6	153.7 \pm 15.1	4.7 \pm 0.2
	Sand cap	81 \pm 13	124.9 \pm 29.4	5.1 \pm 0.1

Test organism	Treatment	Average Survival (%)	Average Total Recovered mass (mg)	Average Individual mass (mg)
<i>Mercenaria mercenaria</i>	Unamended sediment	100 ± 0	345.4 ± 61.4	100.6 ± 6.1
	GAC amendment	100 ± 0	338.7 ± 57.2	115.1 ± 20.5
	Sand cap	100 ± 0	301.9 ± 18.2	112.9 ± 19.1
<i>Neanthes arenaceodentata</i>	Unamended sediment	53 ± 12	91.7 ± 19.5	45.9 ± 9.7
	GAC amendment	33 ± 42	62.8 ± 64.4	26.7 ± 13.3
	Sand cap	73 ± 12	85.3 ± 16.5	32.7 ± 6.9

12.3.3 Overlying water congeners concentrations and tissue residues

Both congeners 24 and 104 were detected in the overlying water throughout the exposure (Figure 64). PCB24 was measured at concentrations approximately 11-fold higher than PCB104 as was expected due to its lower log K_{ow} value (lower hydrophobicity). PCB104 concentrations were relatively stable throughout the exposure while PCB24 increased by approximately 1.8-fold by the 11th day of exposure, followed by a decline by day 21. These PCB24/104 water concentrations are comparable to those previously reported in Section 13.3.1.

Both PCB24 and 104 were detected in the tissues of all four test organisms, with significantly higher PCB24 concentrations in tissue, as expected based on the higher concentrations measured in the water (Figure 65a, b). Tissue concentrations of PCB24 and 104 mirrored one another when comparing organisms in the different sediment treatments, serving as good confirmation of the trends observed (Figure 65c, d). The amphipod *L. plumulosus* generally had the highest bulk tissue concentrations of PCB24/104, followed by *M. mercenaria*, *E. estuarius*, and *N. arenaceodentata*. Lipid normalization resulted in statistically similar PCB24 (Figure 65b) and 104 (Figure 64d) residues in *L. plumulosus* and *M. mercenaria*, suggesting similar relevance of water column exposure for these organisms. However, since *L. plumulosus* bioaccumulated significantly higher Σ PCB lipid-normalized residues relative to the clam (see Section 15.3.5), the importance of overlying water bioaccumulation relative to sediment associated bioaccumulation is relatively much lower for the amphipod. PCB24/104 concentrations for *E. estuarius* and *N. arenaceodentata* were significantly (and substantially) lower than *L. plumulosus* and *M. mercenaria*, indicating relatively low importance of water column exposure in all three sediment treatments. This finding further confirms conclusions in Section 13. The

GAC amendment did not appear to statistically impact the bioavailability of PCB24/104 from the overlying water for any of the test organisms relative to the unamended sediment (Figure 65). There was a non-significant trend of higher lipid normalized tissue residues of PCB24 (Figure 65b), but not PCB104 (Figure 65d), for *L. plumulosus*.

Figure 64. Concentrations of PCB 24 and 104 in the overlying water. Data are presented (a) as total measured water concentrations over the exposure duration and estimated dissolved concentrations from PEDs suspended in the water for (b) PCB 24 and (c) PCB104.

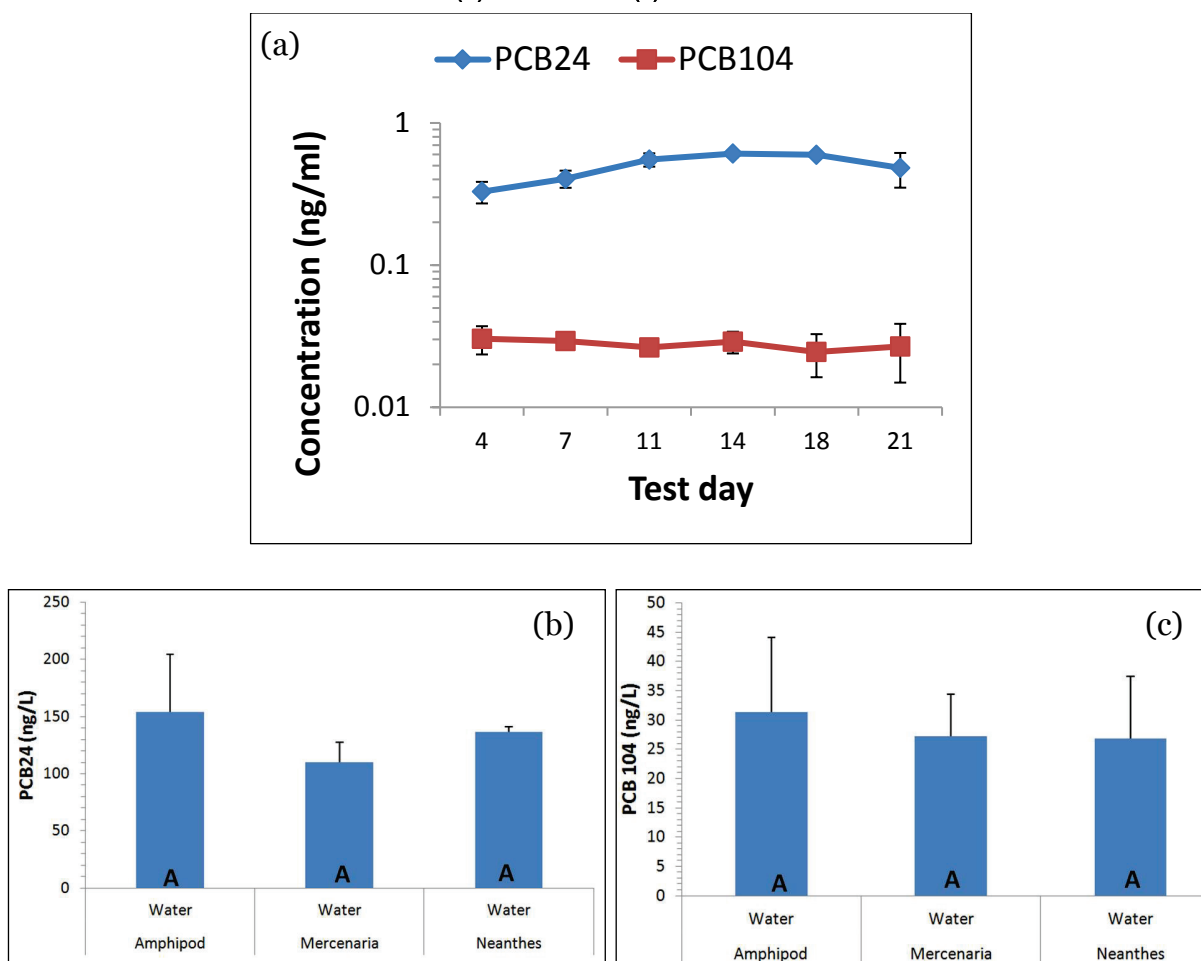
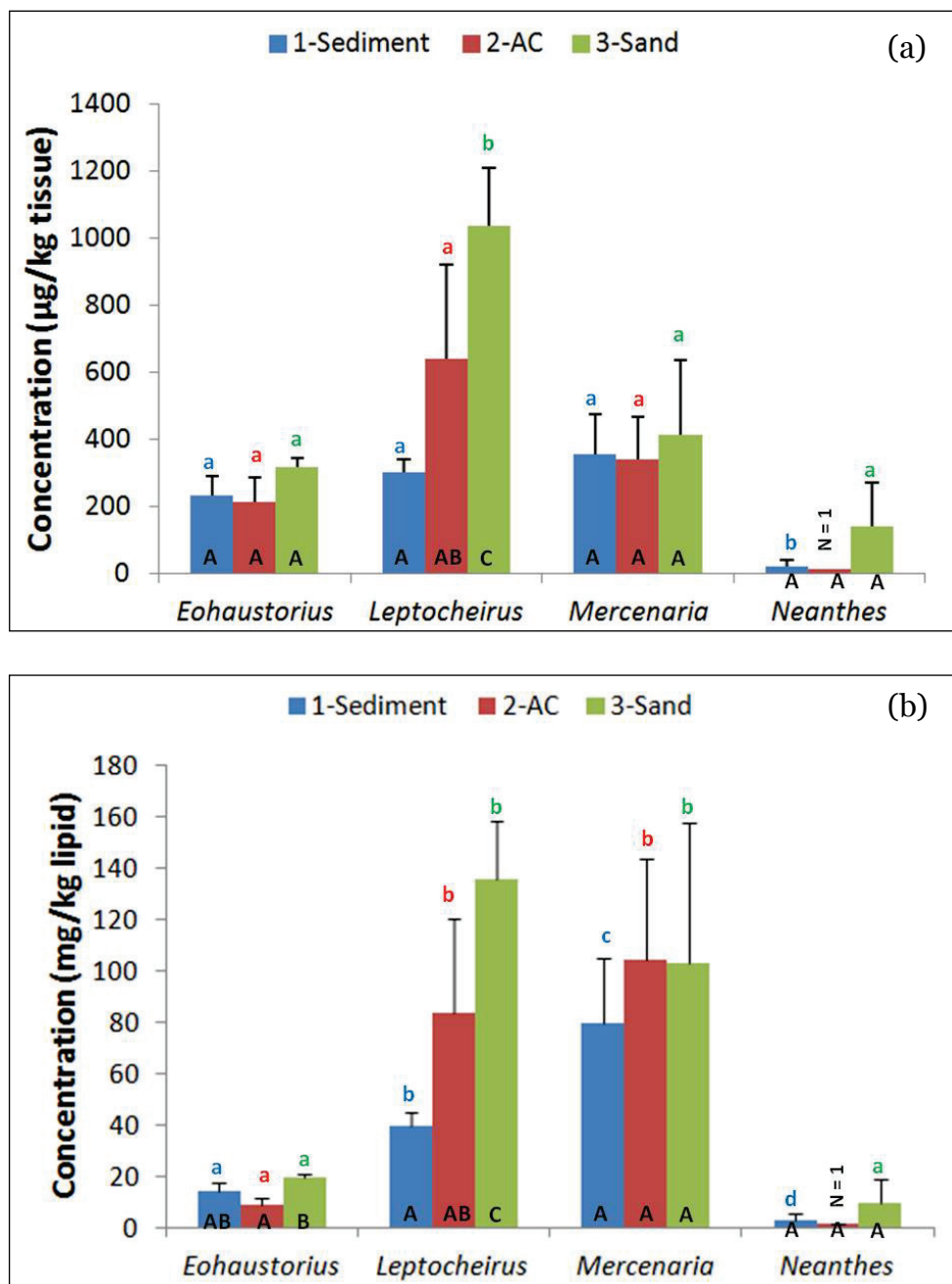
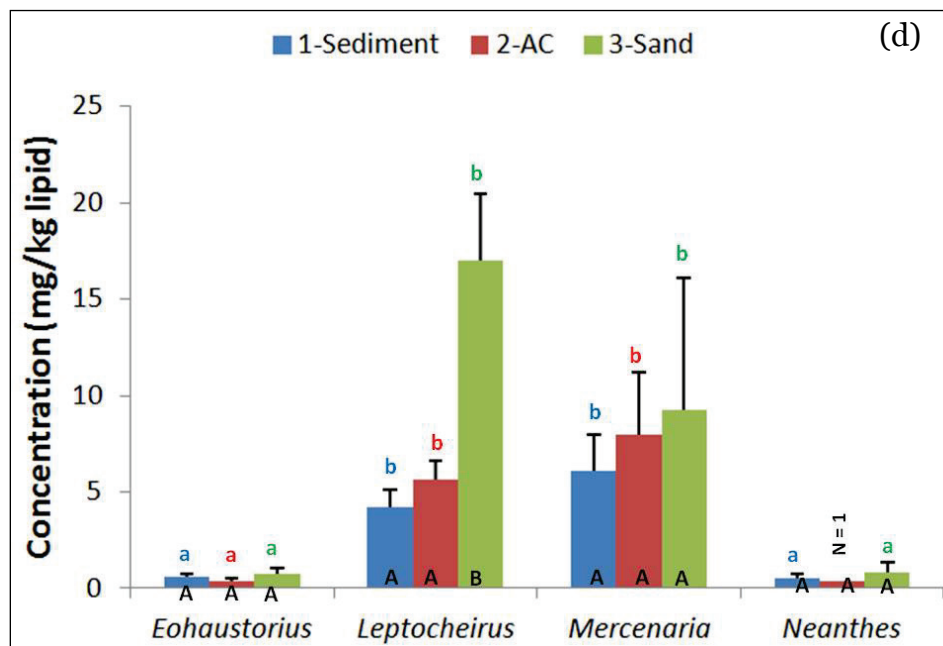
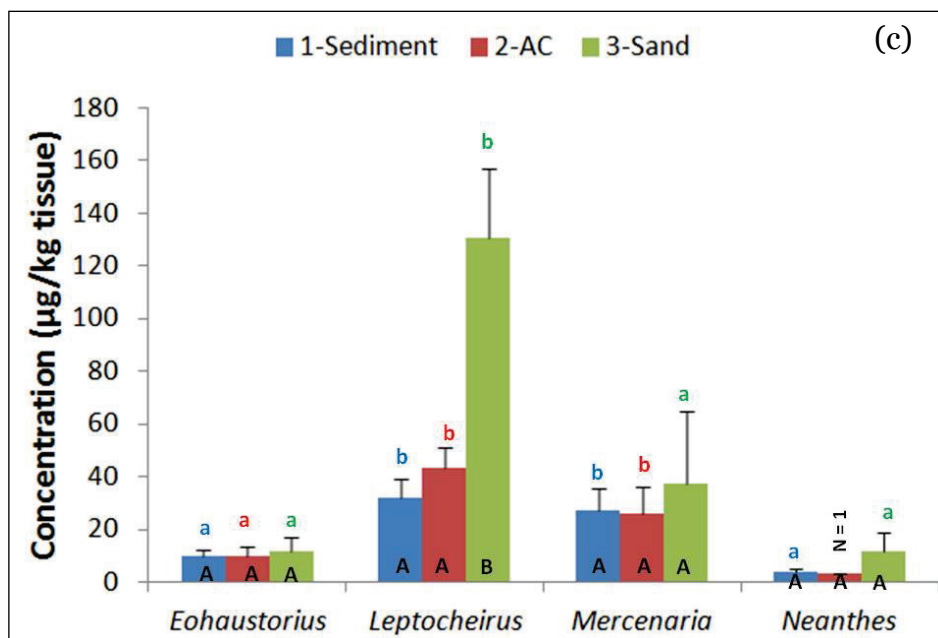


Figure 65. Concentrations of (a) PCB 24 and (b) PCB 104 in tissue. Concentrations of PCB24 are provided for (a) bulk tissue and (b) lipid-normalized tissue. Concentrations of PCB104 are provided for (c) bulk tissue and (d) lipid-normalized tissue. Black capital letters represent statistical comparisons within each organism. Lower case letters represent statistical comparisons within the same pathway (designated by color) across organisms. Data not sharing the same letter designation were statistically significant.





Concentrations of PCB24/104 were generally highest in amphipods exposed within the sand cap (Figure 65), which is consistent with greater infiltration of overlying water containing PCB24/104 into sand relative to the relatively finer grained BNC sediment. However, no differences in PCB24/104 tissue residues were observed for the clam or worm between sediment treatments. *M. mercenaria* was well connected with the water column regardless of substrate type, while *N. arenaceodentata* generally accumulated very low PCB24/104 residues, possibility due to deep

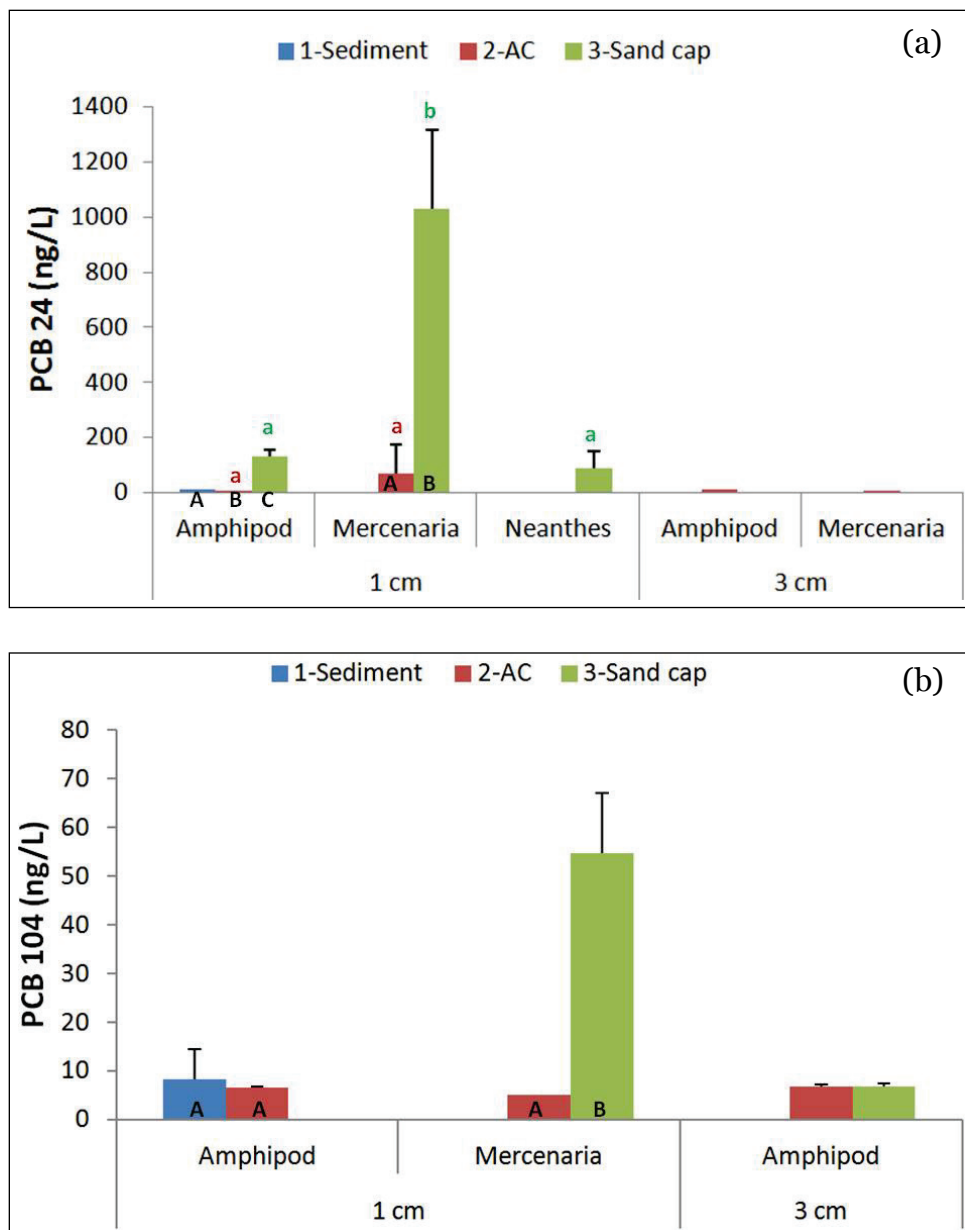
burrowing (as shown in Figure 62). The difference between PCB24/104 tissue residues between the whole sediment and sand cap was less pronounced than observed for the finer-grained NBH sediment (see Section 13.3.4); a trend that again can likely be explained by porosity and organisms with behavioral constraints that do not allow deep burrowing in sand (e.g., *L. plumulosus*). The increase in PCB24/104 concentration in the sand cap relative to the sediment treatment was greater for *L. plumulosus* than *E. estuarius* (Figure 65); this suggests *E. estuarius* remained burrowed deeper into the sand, or into the sediment below. Deeper burrowing by *E. estuarius* was expected because it prefers sandy sediments and can burrow efficiently in coarse-grained substrates (Section 8.2.2), while *L. plumulosus* prefers finer sediments (Section 8.2.2) and generally remains near the surface of sandy substrates. Use of overlying water PCB24/104 to confirm lower overlying water exposure of *E. estuarius* relative to *L. plumulosus* is strongly supported by similar data from Task 2a (Section 13).

Overall, overlying water bioaccumulation was highest for *L. plumulosus* and *M. mercenaria* but relatively low for *E. estuarius* and *N. arenaceodentata*. Due to the relatively lower Σ PCB tissue residues for the filter-feeding *M. mercenaria* compared to the other organisms (see Section 15.3.5), the overlying water pathway was most important to this clam. While the type of sediment treatment had some impact on exposure to and resulting bioaccumulation from the overlying water for the other three organisms, overlying water bioaccumulation in the clam was not impacted whether exposed in the sand cap, GAC amendment or unamended sediment.

12.3.4 Polyethylene device (PED) estimates of dissolved concentrations

Bulk PCB concentrations in PEDs were used to model estimates of dissolved PCBs in the water or sediment pore water (depending on where the PED were placed; see Figure 60). The resulting data were used to inform interpretation of the tissue residue data. The PED (Figure 66) data also confirmed similar concentrations of PCB24/104 in the water column in all four exposure tanks, suggesting organisms were exposed to basically the same conditions (Figure 64).

Figure 66. PED estimates of (a) PCB 24 and (b) PCB 104 in the sediment pore water in the animal exposure chambers. Black capital letters represent statistical comparisons within each organism. Lower case letters represent statistical comparisons within the same pathway (designated by color) across organisms. Data not sharing the same letter designation were statistically significant.



12.3.4.1 GAC amended sediment

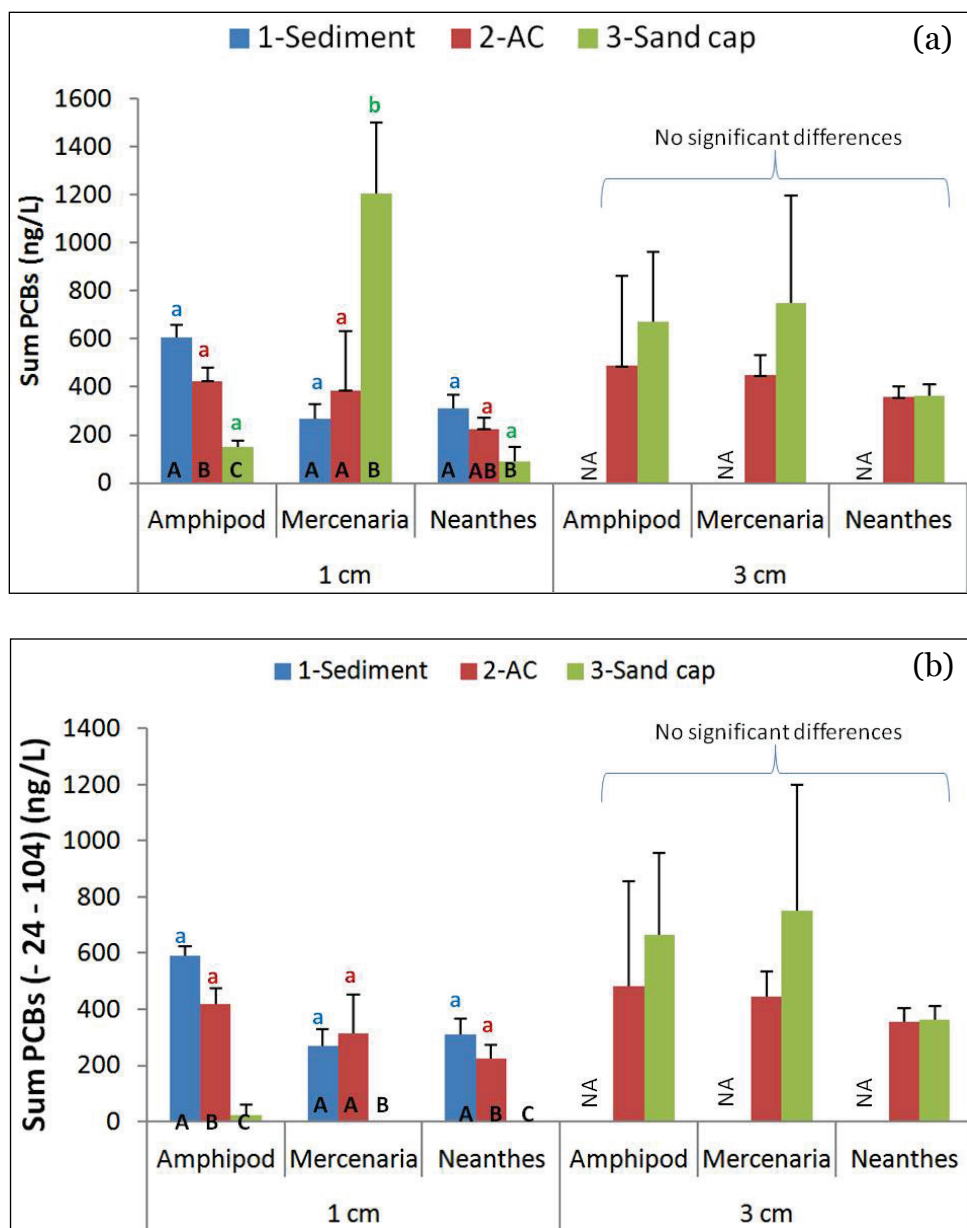
PED-derived Σ PCB concentrations sourced from the sediment (i.e., excluding PCB24/104) indicated that the AC amendment did slightly, but not statistically significantly, reduce pore water concentrations relative to the unamended sediment in the amphipod (30% reduction) and *N. arenaceodentata* (28% reduction) chambers (Figure 67). A greater

reduction was likely not achieved since the authors' methods attempted to simulate thin-layer deployments over realistic time periods (i.e., 30 minute mixing followed by seven-day *in situ* equilibration), rather than long term interactions that have been previously executed in laboratory investigations of the efficacy of GAC amendment (e.g., Millward et al 2005; Cho et al 2007). No reduction was observed in the *M. mercenaria* chambers. This is likely because the clams greatly disturbed the sediment when burrowing, resulting in greater mixing between the 2 cm AC amendment and the contaminated sediment below.

12.3.4.2 Sand cap

Generally the sand cap significantly reduced pore water concentrations of sediment associated PCBs (Figure 67). However, determinations of the efficacy of the sand cap depended on whether the sum of all PCBs was considered (Figure 67a) versus the sum of only the sediment-associated congeners (i.e., excluding PCB24/104; Figure 67b). That is, if all congeners were considered (including those in the water column), the pore water reduction by the sand cap was 75% and 71% in the amphipod and *N. arenaceodentata* exposure chambers, respectively. However, pore water concentrations were significantly and substantially higher in the *M. mercenaria* chambers within the sand cap relative to the unamended sediment; this again was likely due to the highly disruptive burrowing activity of the clam, allowing greater infiltration of PCB24 and 104 from the overlying water into the sand. However, when only the sediment associated congeners were considered (overlying water PCB24 and 104 excluded), the sand cap showed greater efficacy in reducing pore water concentrations (96, 98, and 100% reductions in the amphipod, *M. mercenaria*, and *N. arenaceodentata* chambers, respectively, relative to the unamended sediment). Thus, the data generated in this study suggest the sand cap method employed was the more effective remediation technique over the short term for reducing exposure to PCBs present in the contaminated sediment underneath the cap, with the caveat that exposure to PCBs in the overlying water may be higher.

Figure 67. PED estimates of dissolved concentrations in the animal exposure chambers at 1 cm and 3 cm below the surface. The PED placed at 1 cm was in the middle of the 2 cm AC or sand cap amendments. Data are presented for (a) sum of all PCBs and (b) sediment associated PCBs (i.e., sum PCBs minus concentrations of PCBs 24 and 104). Black capital letters represent statistical comparisons within each organism. Lower case letters represent statistical comparisons within the same pathway (designated by color) across organisms. Data not sharing the same letter designation were statistically significant.



12.3.5 Bioaccumulation of sediment associated congeners in tissue

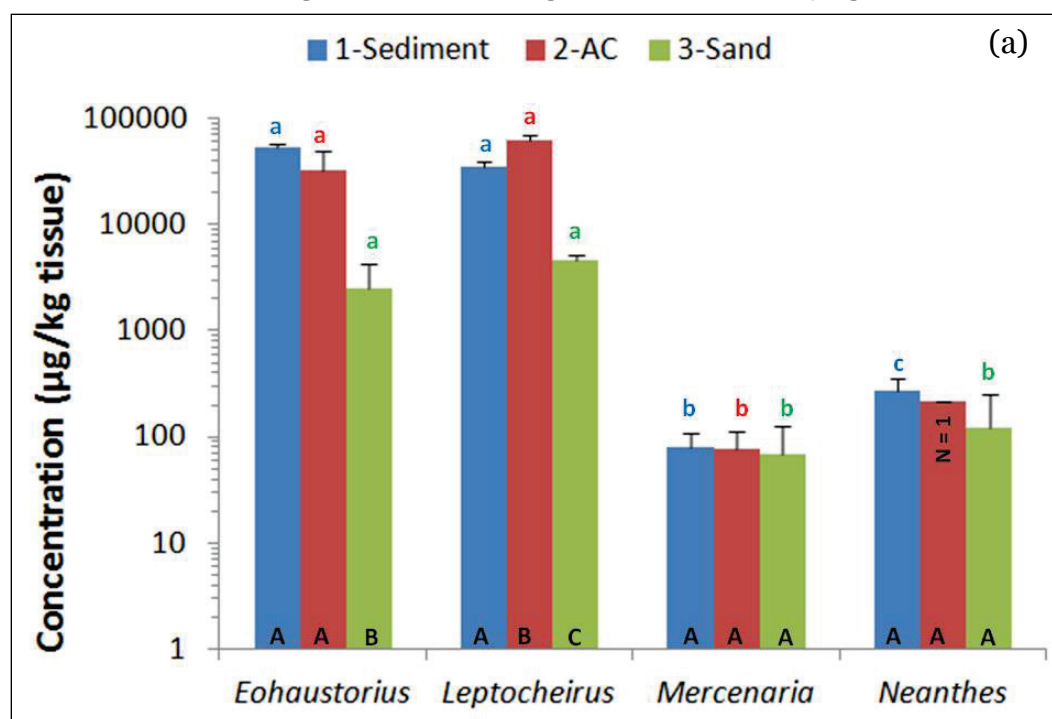
The following discussion and interpretation excluded PCB24 and 104 from the data analysis, since these congeners were delivered to the overlying water, and the focus on this section is bioaccumulation from sediment-

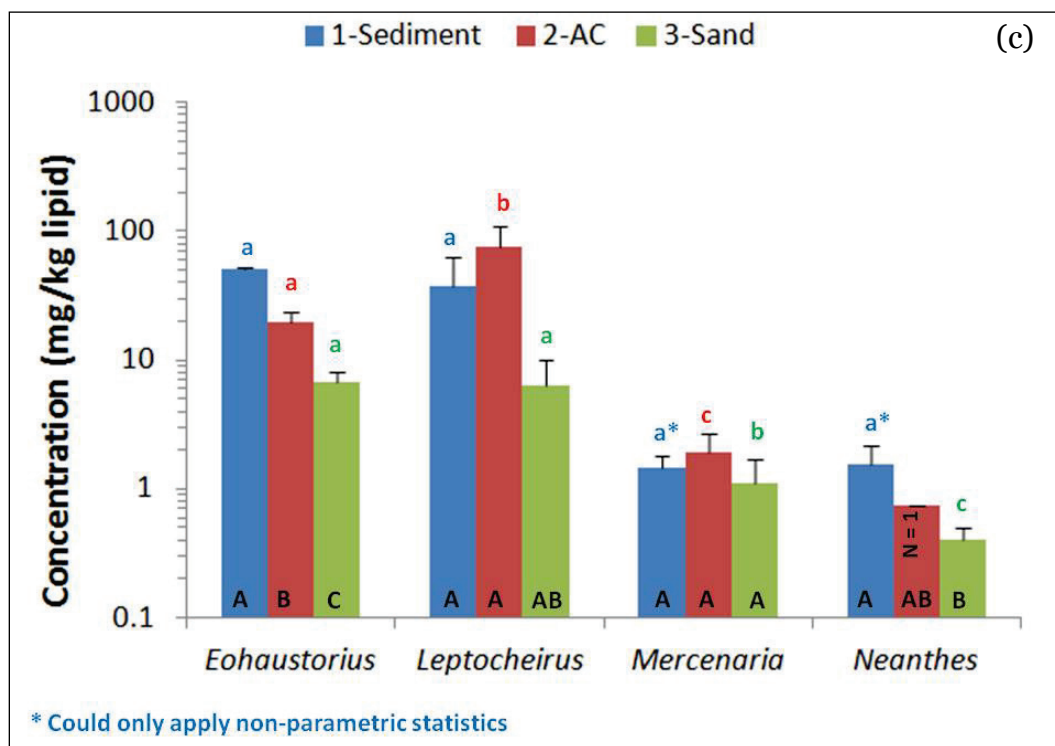
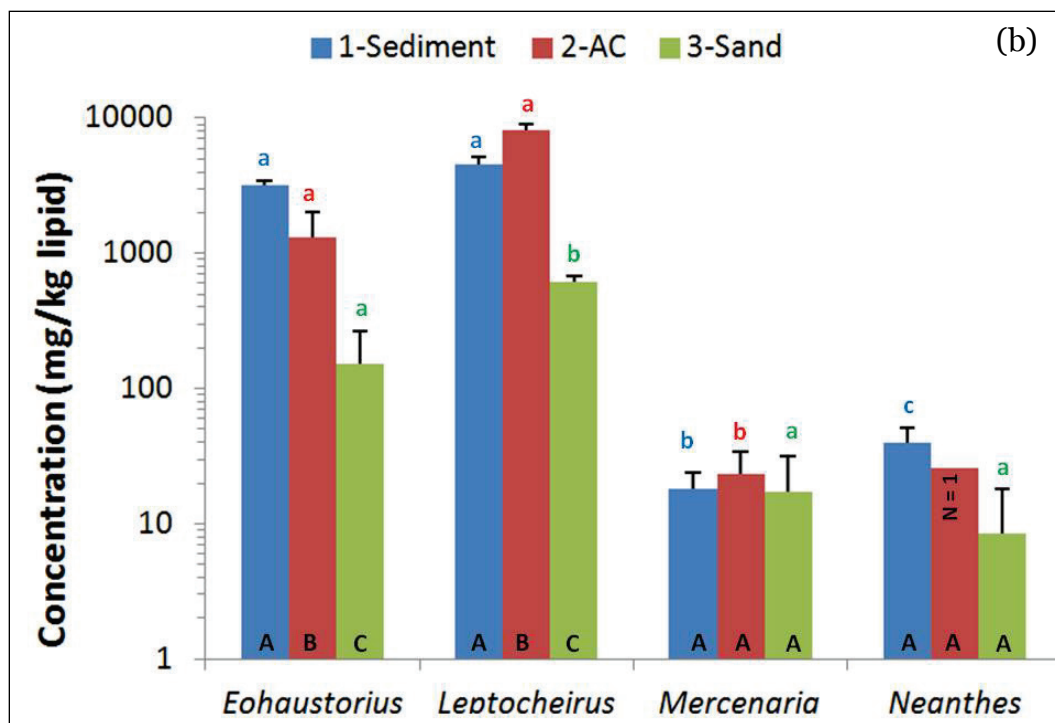
associated congeners. Thus, the Σ PCB and homolog group data are summarized such that the most likely source of bioaccumulation into the tissue was from sediment-associated congeners.

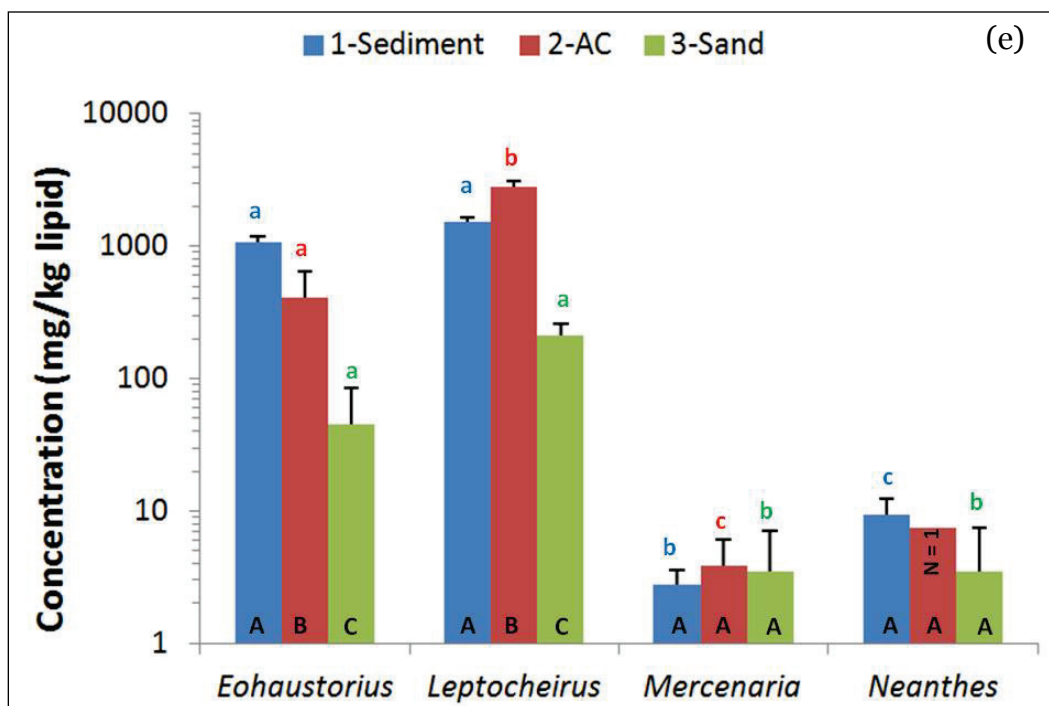
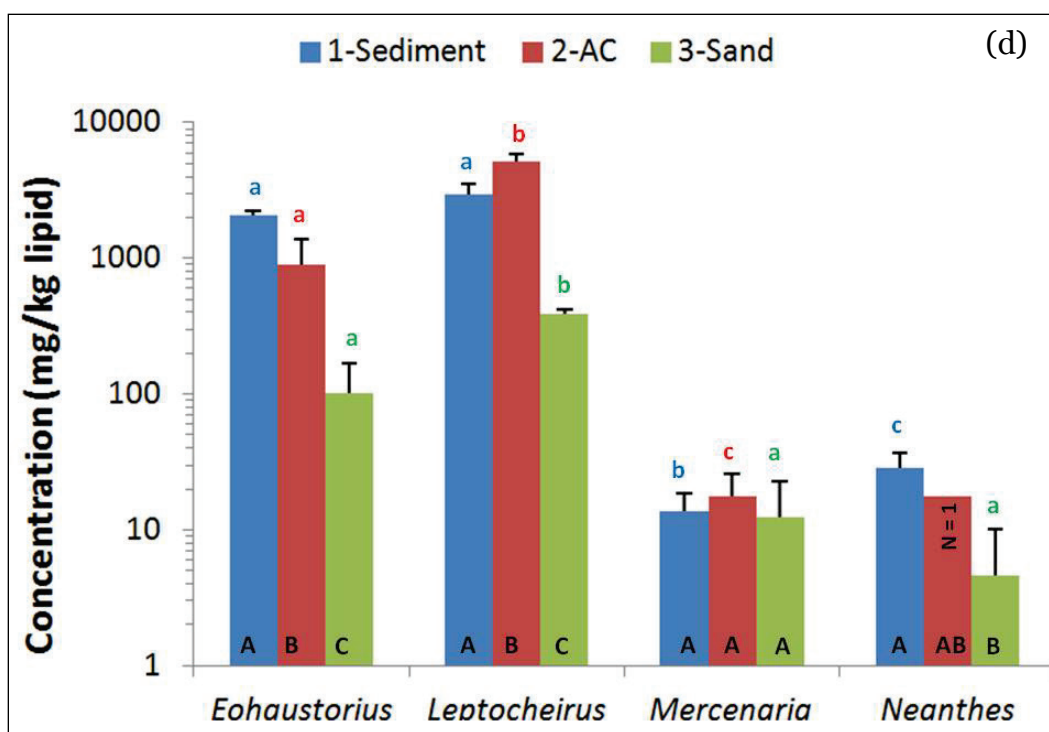
12.3.5.1 Comparison between PCB homolog groups

Trends in lipid-normalized tissue residues for the four organisms (Figure 68) were generally similar for all PCB homolog groups (sum of all congeners, mono/tri-, tetra/penta-, hexa/nona-chlorinated congeners). Residues of the different homolog groups were statistically similar between the two amphipod species in the unamended sediment treatment. However, *L. plumulosus* had significantly higher tissue residues of the two higher log K_{ow} homolog groups in the GAC-amended chambers relative to (1) *L. plumulosus* residues in the unamended sediment chambers and (2) *E. estuarius* residues in the GAC-amended sediment chambers (Figure 68). No statistically significant trends were observed between homolog groups for the other organisms.

Figure 68. Tissue residues for sum PCB congeners sourced from the sediment. Data are presented as (a) sum congeners in bulk tissue, (b) lipid-normalized sum congeners, (c) lipid-normalized mono- to tri-chlorinated congeners, (d) lipid-normalized tetra- to penta-chlorinated congeners, and (e) lipid-normalized hexa- to nona-chlorinated congeners. Black capital letters represent statistical comparisons within each organism. Lower case letters represent statistical comparisons within the same pathway (designated by color) across organisms. Data not sharing the same letter designation were statistically significant.







12.3.5.2 Comparisons between organisms

As previously discussed in Task 2A (Section 13), the amphipods accumulated significantly higher lipid-normalized PCB residues from all sediment treatments (Figure 68). Lipid-normalized tissue residues were

substantially and significantly lower for *N. arenaceodentata* and *M. mercenaria* in all three sediment treatments. The worm had slightly but significantly higher lipid-normalized residues of the higher low K_{ow} homolog groups relative to the clam (Figure 68), suggesting greater importance of direct sediment exposure for the worm. These findings between species support previous data generated in Task 2a (Section 13), where lipid normalization did not explain the differences in bioaccumulation for the coarser grained Bremerton sediment.

12.3.5.3 Comparisons between sediment treatments

12.3.5.3.1 Sand cap

The sand cap significantly reduced bioaccumulation of sediment sourced PCBs for both *E. estuarius* (95% reduction) and *L. plumulosus* (87% reduction), relative to baseline levels accumulated from the unamended sediment (Figure 68). A smaller reduction (78%) in Σ PCBs bioaccumulation was observed for *N. arenaceodentata* exposed in the sand cap. This reduction was not significant for Σ PCBs (Figure 68b) or the hexa- to nona-chlorinated homolog group (Figure 68e). However, the sand cap did significantly reduce residues of mono- to tri-chlorinated congeners by 74% (Figure 68c) and tetra- to penta-chlorinated congeners by 84% in *N. arenaceodentata* tissue (Figure 68d). These findings may suggest the sand cap reduced worm exposure to the pore water (where lower log K_{ow} congeners are expected) although the worm was still exposed to higher log K_{ow} congeners. The sand cap did not reduce bioaccumulation of Σ PCBs or any homolog group into *M. mercenaria*, which is more strongly influenced by exposure to overlying water. This was previously discussed in Task 2a (Section 13) as well as in this experiment (Section 15.3.3).

Differences greater than those observed for *N. arenaceodentata* bioaccumulation in unamended sediment compared to sand cap treatments were expected. Possible explanations for the lack of difference include: (1) the worms remained on the surface of the substrate in all treatments and were predominately exposed to overlying water or mobile PCBs from the sediment; or (2) the worms were able to burrow below the 2 cm sand cap and GAC amendments, and thus were exposed to the BNC sediment below. Bioaccumulation into *N. arenaceodentata* was similar between sediment treatments for the more mobile mono- to tri-chlorinated homolog groups and the less mobile, hexa- to nona-chlorinated homolog groups. The majority of the accumulation was from the tetra- to penta-chlorinated

homolog groups that should not have come through the sand cap, as PED data indicate sediment associated congeners were not in the sand cap pore water (Figure 67). This finding suggests that *N. arenaceodentata* was able to burrow through the 2 cm amendment, which is consistent with the fact that most of the PCBs in their tissue were sourced from the sediment, not the overlying water.

12.3.5.3.2 GAC amendment

Amendment of the top 2 cm sediment with GAC generally did not result in a significant reduction in bioaccumulation. However, a statistically significant, 39% reduction in lipid-normalized tissue residues of Σ PCBs and all three homolog groups was observed for the GAC amended sediment, relative to the unamended sediment, for the amphipod *E. estuarius* (Figure 68b,c,d,e). Significant reductions were not observed for the other three organisms. This is not surprising since only a 30% reduction in pore water concentrations derived from PED data was observed (Figure 67). Lack of efficacy for the GAC treatment is logical for *N. arenaceodentata*, which likely burrowed below the 2 cm amendment (Figure 62), and thus was exposed to the underlying, unamended sediment. The clam *M. mercenaria* was observed to bioturbate the top few centimeters and was considered to be more connected with overlying water exposure than with sediment exposure; therefore, GAC amendment of the surface sediment is inconsequential for the clam. Surprisingly, the two higher log K_{ow} homolog groups were significantly higher in *L. plumulosus* residues exposed in the GAC-amended chambers relative to *L. plumulosus* residues in the unamended sediment chambers (Figure 68d, e). There was no significant difference for the lower log K_{ow} homolog groups (Figure 68c). This result suggests that the more hydrophobic congeners were significantly more available to *L. plumulosus* in the GAC chambers. While this result was unexpected, it may relate to exposure to and/or consumption of particles. In addition, the intention of this GAC-amendment was to simulate an in situ deployment (e.g., Cho et al 2009). Previous laboratory studies have involved more robust interaction methods (e.g., continuous roller mills for 30+ days) between GAC and contaminated sediment (Millward et al 2007, Cho et al 2007, Cho et al 2009) that are undoubtedly more robust for reducing pore water concentrations. The 30% reduction in pore water concentrations (Figure 67) may have been insufficient to effectively result in the reduction in bioaccumulation of sediment associated PCBs for all organisms.

12.3.6 Conclusion

The following conclusions can be made from this investigation and are summarized in Table 22:

1. Overlying water exposure is most important for *M. mercenaria* and *L. plumulosus*.
 - a. The relative importance of overlying water exposure for determining total tissue residues is much higher for *M. mercenaria*. However, sediment or sediment pore water exposure dominates total *L. plumulosus* residues.
 - b. Overlying water exposure was generally of lower importance for *E. estuarius* and *N. arenaceodentata*.
 - c. GAC amendment did not reduce bioaccumulation of water column PCBs.
 - d. The sand cap increased exposure and bioaccumulation of water column PCBs to the amphipods. However, the sand cap did not change bioaccumulation into the clam.
2. The GAC-amendment resulting in a 30% reduction in pore water concentrations showed efficacy to reduce body residues only for *E. estuarius*.
 - a. The worm has the ability to burrow beneath the 2 cm amendment, leading to direct exposure to the unamended sediment.
 - b. The clam is more connected to the water column.
 - c. Organism exposure to (or consumption of) particles may have reduced efficacy.
 - d. A higher GAC concentration or longer mixing/equilibration is likely needed for *in situ* deployments. Further, 2 cm is likely an inadequate amendment depth to reduce PCB bioavailability to deeper burrowing organisms.
3. Sediment-associated bioaccumulation is significantly reduced by the sand cap.
 - a. The largest reduction in bioaccumulation was observed for the amphipods.
 - b. Significant reduction in bioaccumulation for the worm was only observed for the higher log K_{ow} congeners. The worm likely has the ability to burrow beneath the 2 cm cap and was exposed to sediment pore water and particles.

- c. No significant reduction in bioaccumulation was observed for the filter-feeding clam.
- d. Sand caps may increase exposure to water column contaminants to organisms.

13 Sediment particle and solute mixing

13.1 Objective

It is well established that benthic organisms through their life activities affect geochemical and physical properties of the sediment, including sediment permeability, distribution of organic matter, microbial activity, as well as contaminants partitioning and their bioavailability (Krantzberg, 1985, Maire et al, 2008). The objective of this work is to provide more insight into processes governing bioaccumulation of contaminants by characterizing how test organisms interact with sediment and water, and how sediment-related contaminants affect this interaction. Information obtained from this work can then be incorporated into a model of functional benthic exposure processes. The objective was addressed by quantifying and comparing particle and solute mixing parameters of deposit-feeding *Leptocheirus plumulosus* and filter-feeding *Mercenaria mercenaria* in clean and contaminated sediments. Additionally, a generic 3-D transport reaction model for solute transport by larger, burrow constructing animals was developed.

13.2 Background

Benthic organisms shape their environment by moving particles, feeding selectively on particles, altering sediment porosity, pumping water, altering redox conditions, secreting mucus and metabolites, and building structures and lining them with semi-permeable materials (e.g. McCall and Tevesz, 1982). For hydrophobic, organic compounds, bioturbation will affect such important processes as burial / resuspension, desorption, and microbial degradation (Qin et al, 2010) as well as distribution of organic matter, which is the major agent reducing concentration of dissolved (most bioavailable) PCBs in the interstitial water (DiToro et al, 1991). The partitioning behavior of different organic chemicals between sediments, organic matter, and water leads to unpredictable exposures for different combinations of chemicals and organisms. Different functional attributes of different benthic organisms may explain these differences in exposure, uptake, and bioaccumulation.

13.3 Materials and methods

13.3.1 Materials

Seawater used for maintaining organism cultures and during the experiments was prepared by dissolving Crystal Sea Marinemix manufactured by Marine Enterprises International Inc. Salinity of 20 parts per thousand (ppt) was used for *Leptocheirus plumulosus*, while for *Mercenaria mercenaria* 28 ppt seawater was used. The water was continuously oxygenated by bubbling with air.

Sediment particle radiotracer was made by adding 70 μCi of carrier-free ^{137}Cs to a distilled water suspension of sieved ($<40\text{ }\mu\text{m}$) illite-rich sediment ($\sim 10\text{ g}$) derived from the Chagrin Shale member of the Ohio Shale near Cleveland, OH. Labeled illite was isolated by decanting and then resuspending in 250 mL of 1 M non-radioactive CsCl to remove easily exchangeable radioactive cesium ions. Salinity was then adjusted to 20 ppt. After a few months, ^{137}Cs is incorporated into illite mineral lattices where it is effectively immobilized (Robins et al, 1979).

A 100 μCi ^{22}Na standard was purchased from Perkin Elmer Inc. in a carrier-free solution of NaCl. A stock solution containing 2 $\mu\text{Ci/mL}$ was prepared by diluting the standard in 50 mL of 20 ppt seawater. A working ^{22}Na solution with an activity of 0.02 $\mu\text{Ci/mL}$ was prepared by 100 times dilution of the stock solution and was used as a solute tracer.

13.3.2 Organisms

L. plumulosus was obtained from the ERDC in Vicksburg, MS. The organisms were kept in 1 L glass beakers containing about 2 – 3 cm of uncontaminated Sequim Bay sediment and 15 cm of 20 ppt seawater. As recommended by the *L. plumulosus* toxicity test manual of the U.S. EPA (U.S. EPA, 2001), three times a week about 60% of the overlying water from the cultures was decanted and replaced with clean seawater, followed by feeding the cultures with finely ground TetraMin® tropical flakes, about 1 mg per animal. For temperature control, the culture beakers were kept in larger aquaria filled with water and maintained at $20 \pm 2\text{ }^{\circ}\text{C}$. Vigorous aeration of the overlying water was provided by placing air stones in each beaker.

Bay Shellfish Company, located in Terra Ceia, collected *M. mercenaria* in lower Tampa Bay, FL for experiments conducted for this study. Juveniles of about 20 mm in length were used in this work. The cultures were kept in 1-gallon buckets filled with about 3 cm of native sediment (sand) from the collection site and overlying 28 ppt seawater maintained at 24 ± 2 °C. Three times a week about 60% of the water was removed and replaced with clean seawater, and the animals were fed with DT's Live Marine Phytoplankton.

13.3.3 Sediments

Contaminated sediment treatment for both *L. plumulosus* and *M. mercenaria* was conducted in NBH sediment. Control sediment for *L. plumulosus* was Sequim Bay sediment, whereas for *M. mercenaria* three clean sediments were used, Eel Pond mud, sandy mud from Florida, and lower Tampa Bay sand. All sediments were refrigerated and sieved through 1 mm sized mesh prior to use.

13.3.4 Experimental setup

Experimental microcosms were made of acrylic and had dimensions 5 x 1 x 25 cm for *L. plumulosus*, and 4.7 x 2.6 x 25 (W x D x H) cm for *M. mercenaria*. Cells were filled with 8 cm of sediment, which was more than twice the maximum observed burrowing depth for the organisms used. After adding the sediment, cells were filled with seawater and stored in a refrigerator for a minimum of two weeks to allow the sediment to compact. In the particle tracing experiments, the overlying water was changed a day prior to the start of the experiment to ensure proper salinity and to dilute any potential sediment borne contaminants and bacterial metabolites. Aeration of the cells started 24 hours before the experiment. The ^{137}Cs tracer was then gently injected as a water suspension into the overlying water and allowed to settle for about an hour to form a sub-millimeter layer on the sediment-water interface. In the solute tracer experiments, the overlying water was siphoned at the start of the experiment and replaced with ^{22}Na -spiked water using a peristaltic pump. One clam per cell was used in all *M. mercenaria* experiments (population density of about 800 indiv/m²), whereas in *L. plumulosus* 5, 10, or 20 organisms per cell (corresponding to population densities of 8, 16, and 32 thousand organisms per m²) were used.

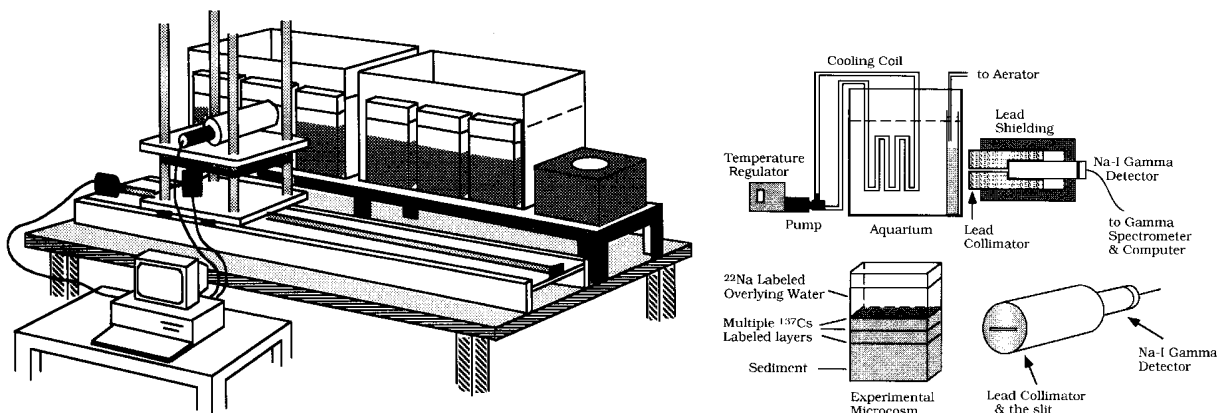
In both the particle (^{137}Cs) and solute (^{22}Na), transport experiments oxygenation was provided through silicone tubing placed in each cell, and the suitable temperature for the microcosms was provided by placing them in a temperature controlled water bath. In ^{137}Cs experiment, 60% of overlying water was replaced with clean seawater three times a week, followed by feeding. In the solute tracer experiment, 25% of the water was removed daily and replaced with fresh ^{22}Na -spiked seawater. This water change routine created a constant radionuclide concentration in water column throughout the experiment duration. The animals were fed following water change on day two of the experiment duration, which was consistent with the three times per week pattern of feeding in ^{137}Cs experiment. Because solute transport experiments were terminated after four days, feeding at day four was not necessary.

Vertical profiles of the ^{137}Cs and ^{22}Na activity were obtained by using a gamma scanner system (Wang and Matisoff, 1997). The system includes NaI gamma detector well shielded from any incident radiation, except that passing through 0.4 x 5 cm collimated slit. The detector, coupled with a multi-channel analyzer, is attached to a precise X-Y positioning system (accuracy 0.01 mm) and controlled by a computer (Figure 69). Vertical profiles of tracer activity were obtained at depth intervals of 2 mm (all *L. plumulosus* experiments and *M. mercenaria* particle mixing) or 4 mm (*M. mercenaria* solute mixing). Because the width of the detector slit covered the entire width of the experimental microcosms, measured gamma activity at each depth was the horizontal average over the full width of the cell. Time series of the activity profiles were obtained by repetitive scanning of the microcosms throughout the experiment duration. The experimental durations for each organism and type of sediment are presented in Table 24.

Table 24. Experimental duration

Sediment	Tracer	organism	
		<i>L. plumulosus</i>	<i>M. mercenaria</i>
Clean	^{22}Na	4	4
	^{137}Cs	14	39
Contaminated	^{22}Na	4	4
	^{137}Cs	7	21

Figure 69. Sketch of the experimental gamma scan system. The top illustration shows the general layout of the equipment. The system consists of three aquaria, which house the experimental microcosms (top illustration), a collimator/detector (bottom illustration), and a gamma spectrometer/counting system (middle figure).



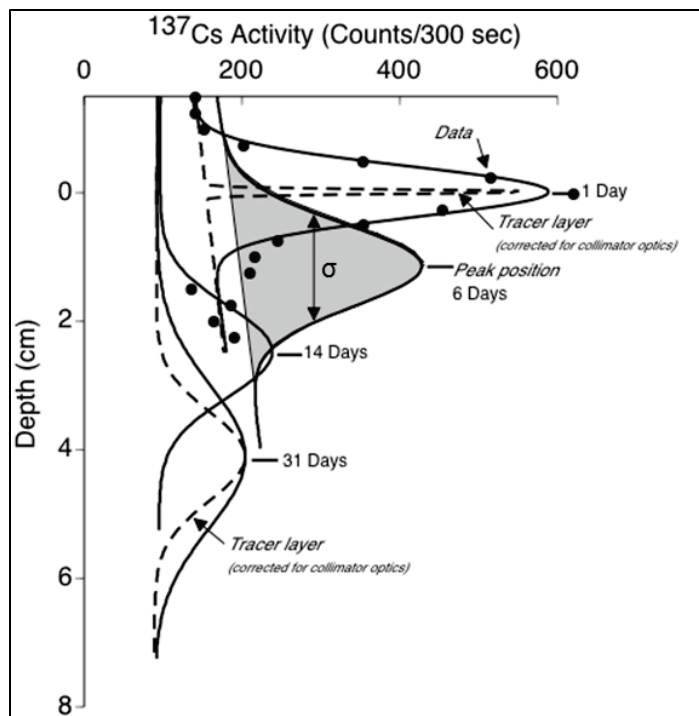
13.3.5 Mixing parameters

Detected activity of a ^{137}Cs tracer layer placed as a thin horizontal layer of radiolabeled particles can be well described by a Gaussian (McCall et al, 1995). In order to quantify spreading and movement of the tracer, a Gaussian was fitted to the gamma scan data for each microcosm. Two parameters of the fitted curve were then extracted: peak position, being the depth of the peak maximum, and peak spread (σ), being the measure of peak's width at half of its height. Analysis of the change of peak position and peak broadening in time series enables determination of burial rate and particle biodiffusion coefficient, respectively (Figure 70). More precisely, the value of burial rate (burial velocity, W_b) is obtained from the slope of the line fitted to data representing position of the peak (cm below sediment-water interface, positive down) vs. time. The second particle mixing parameter, the biodiffusion coefficient, D_b , is a measure of the random redistribution of particles by biota, which were mathematically analogous to molecular diffusion (Wheatcroft et al, 1990). The biodiffusion coefficient is quantified by measuring the change in broadening of the Gaussians fitted to the peak's activity profiles with time according to the equation (McCall et al, 1995):

$$\sigma^2 = D_b 2t$$

where σ is the peak's width at half its height (cm), t is time (yr). It can be seen then that slope of the line plotting σ^2 versus $2t$ gives the value of biodiffusion coefficient. Obtained coefficients were corrected for non-biological particle mixing using D_b in a control cell without organisms.

Figure 70. A Gaussian is fit to each scan for each cell to obtain the peak position and the spread of the peak. These data are collected for each layer at each time and plotted as a function of time to obtain the burial rate (burial velocity) and the particle biodiffusion coefficient.



Diffusion of solute from the overlying water into the sediment in the presence of *L. plumulosus* was analyzed using an enhanced diffusion model. The model is described in more detail by Wang and Matisoff (1997). Briefly, the sediment is divided in two zones: an upper, bioturbated layer, which is assumed to be uniformly and thoroughly mixed by the biota and where solute transport is enhanced over molecular diffusion, and a lower layer that is unmixed and where solute transport is assumed to be exclusively due to molecular diffusion. Diffusion is modeled using following equation:

$$\frac{\partial C_i}{\partial t} = D \frac{\partial^2 C_i}{\partial x^2} - \lambda C_i$$

where C_i is the activity of the tracer (decays/s), t is time (s), x is depth from the sediment-water interface (cm, positive downward), and λ is the radioactive decay constant (s^{-1}). Since the experiments were conducted only for four days and the half-life of ^{22}Na is 2.6 years, the loss of tracer due to radioactive decay can be neglected.

Processing of the experimental data starts with obtaining the molecular diffusion coefficient below the mixing zone from the control cell, and then enhanced diffusion coefficient (D_e) can be modeled by fitting the diffusion equation to data for the bioturbated layer of sediment. *M. mercenaria* did not create a uniformly mixed top layer of sediment, as it is assumed by enhanced diffusion model; so, the solute transport was modeled by fitting one value of diffusion coefficient for the entire length of sediment column in each cell.

13.3.6 3-D burrow model of dissolved oxygen

A 3-D model of oxygen transport and reaction was developed for a generic burrow to gain insight about the solute concentrations around a burrow and the exposure of a burrow-dwelling organism to a reactive solute. The model accounts for the diffusive transport of oxygen from both the water column and from the inside of the burrow into the sediments where it is consumed by a first order respiration reaction (bacterial aerobic respiration). Water is pumped through the burrows at a constant velocity, and animal respiration consumes some of the oxygen. For steady state to be reached, a balance between the rate of oxygen flux into the sediment and the rate of aerobic respiration must be achieved. The model is used to calculate the steady state flux of oxygen into the sediment (the sediment oxygen demand (SOD)) as a function of burrow density.

Model construction requires knowledge of burrow dimensions, water flow velocity through the burrow, animal respiration rate, the diffusion coefficient for oxygen in water and in the sediment, the oxygen concentration in the water, and the aerobic respiration rate by the bacteria in the sediment. Burrow densities were determined by adjusting the volume of sediment surrounding a single burrow. The model includes three domains: water, burrows, and sediment. Within each domain all physical and chemical properties, such as porosity, dispersivity, diffusivity, initial oxygen concentrations, bulk density, oxygen respiration rate coefficients, and adsorption coefficients are constant. The model was solved using the time-dependent finite element code COMSOL Multiphysics and run to steady state. The finite elements ranged in size from 0.04 to 4 cm and the time step was 1000 sec. The model ran for 100000 sec to steady state. The flux of oxygen across the sediment-water interface at steady state was calculated as a function of the burrow density (the number of burrows/m²) and those data were determined both with and without the inclusion of animal-oxygen respiration.

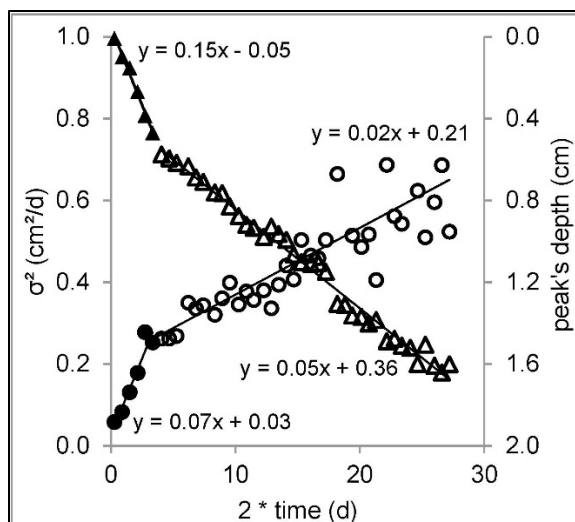
13.4 Results and discussion

13.4.1 *L. plumulosus*

13.4.1.1 Particle mixing by *L. plumulosus*

Particle mixing in the various treatments was not constant in time. Both burial and spreading of the peak layer occurred at a higher rate for the first few days of the experiments, and then decreased, in some cases reaching a steady state with no additional change. Particle mixing rates were extracted from the vertical activity profile by plotting the position of the peak maximum with time and the square of the peak width as a function of time. To visualize the bioturbation that was analyzed and quantified, the data from one treatment (16000 *L. plumulosus* / m² in Sequim sediment) are shown in Figure 71. Note that for the purpose of comparison between the two plots, peak position was plotted against $2 \cdot t$ (time), not t ; thus the apparent slope of the line, W_b , is two times smaller than in reality. In the first two days of this experiment, the tracer was buried at 0.30 cm/day or 110 cm/yr, (W_b initial; in Figure 70 visible as 0.15 cm/day, $R^2 = 0.99$), and the biodiffusion coefficient (D_b initial) had a value of 0.07 cm²/day or 26 cm²/yr ($R^2 = 0.92$). After day two, the rates of both processes decreased by about a factor of three; secondary W_b and D_b achieved values of 0.10 cm/day or 37 cm/yr (in Figure 70, 0.05 cm/day; $R^2 = 0.99$) and 0.02 cm²/day or 7.3 cm²/yr ($R^2 = 0.70$), respectively. Similar patterns of mixing were observed in all experimental treatments, so both initial and secondary rates are reported.

Figure 71. Obtaining burial rate and particle biodiffusion coefficient from the scanner data.



The biodiffusion coefficient is obtained from Equation (1) by plotting the square of the peak's spread, σ^2 vs. $2 \times \text{time}$ (circles). Burial velocity is determined by plotting the position of the peak's maximum vs. time (triangles; in Figure 71 peak's position was plotted against $2 \times \text{time}$, so obtained burial velocities have to be doubled). Closed symbols – initial rates; open symbols – secondary rates. Experiment with 16000 indiv/m² in Sequim sediment.

Burial velocities of the tracer peak are summarized in Figure 72 and Figure 73. Figure 72 shows the rate of burial of the tracer layer, which was positioned at the sediment-water interface at the beginning of the experiment ($t = 0$). While burrowing, *L. plumulosus* brings up unlabeled particles from depth into the water column; eventually the particles settle, causing burial of the surface tracer layer. Measured positions were corrected for compaction by subtracting peak burial rates in the control cell, so the reported values resulted exclusively from the sediment reworking activities of *L. plumulosus*. Much higher rates of burial were observed in clean (Sequim) sediment than in contaminated (New Bedford) sediment. No experiments were conducted with contaminated sediment for the lowest population density of 8000 indiv/m² because no measurable effect would have been detected. Even for the medium abundance in contaminated mud, burial velocities were 0 cm/yr. Only the highest population density of 32000 indiv/m² caused measurable burial of the peak, with initial burial of 28.7 ± 4.1 cm/yr (mean \pm 1 SD) and secondary burial of only 2.3 ± 1.7 cm/yr. Conversely, in clean sediment the tracer burial velocity was significant even in the lowest abundance treatment: 26.4 ± 1.8 cm/yr initially, and 9.1 ± 7.7 cm/yr afterwards (2.9 factor difference). In the two higher population density treatments, 16000 and 32000 indiv/m², the burial velocities were even higher with initial burial velocities of 65.6 ± 20.3 cm/yr and 67.8 ± 3.7 cm/yr, respectively, and secondary burial velocities of 22.9 ± 5.0 cm/yr and 18.7 ± 7.5 cm/yr, respectively. The resulting ratios between initial and secondary burial rates were 2.9 and 3.6, respectively. A trend of faster burial at higher population densities was observed (one-way ANOVA, $p = 0.066$), yet there was no statistically significant difference in the magnitude of burial velocities between the two higher abundances (paired t-test, $p = 0.905$) due to one of the medium density treatments scoring exceptionally high, and thus significantly increasing the replicate standard deviation. Given these uncertainties there was an approximately 3-fold difference (3.1 ± 0.3) between the initial and secondary rates of burial at each population density. Since this factor between the initial and

Figure 72. Tracer burial velocity (average from three replicates, one standard deviation error bar). Circles represent clean sediment treatment; triangles represent contaminated sediment treatment; closed symbols represent initial burial velocities; open symbols represent secondary burial velocities.

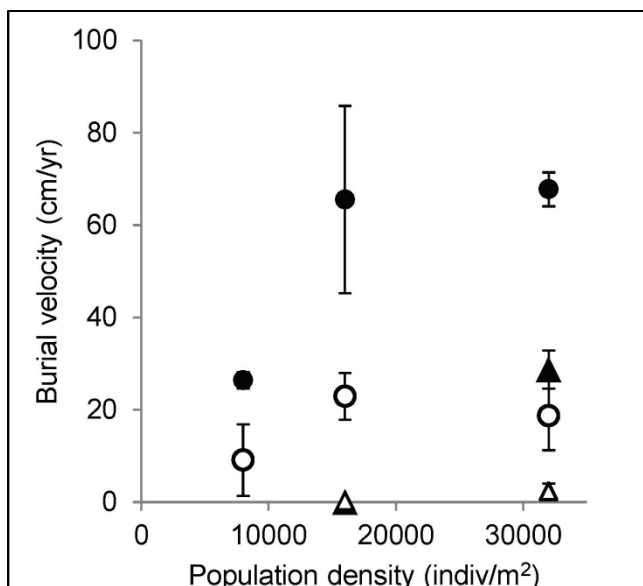
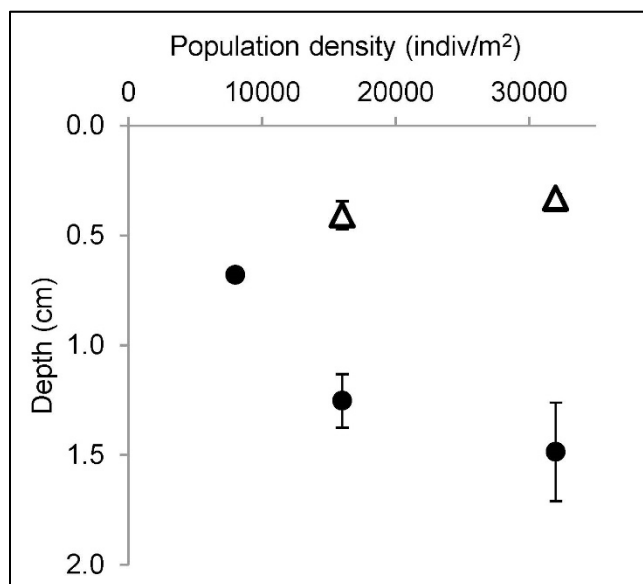


Figure 73. Depth of the tracer layer at the end of the experiment. (Average from three replicates, one standard deviation error bar). Circles represent clean sediment treatment; triangles represent contaminated sediment treatment.



secondary velocities is approximately constant data collected during the first few days of the experiment, it is sufficient to characterize the organism behavior. Contaminated sediment significantly affects (2.4-fold difference for 32000 indiv/m²) or practically ceases (16000 indiv/m²) burial of the surface layer, so this parameter is a sensitive indicator of behavioral effects of pollution on *L. plumulosus*.

The peak position at the end of the experiment is presented in Figure 73. This is a measure of the maximum depth of mixing by *L. plumulosus* because the tracer cannot be buried any deeper than the maximum depth of mixing. In clean sediment, the maximum depth of burial increased with population density and achieved values of 0.68 ± 0.03 cm, 1.24 ± 0.12 cm and 1.49 ± 0.23 cm for densities of 8000, 16000, and 32000 indiv/m², respectively, although two higher abundances were not statistically different (paired t-test, $p = 0.014$). Correlation of the maximum depth of burial with population density was expected; the more individuals, the more crowded it is, so the population will burrow deeper in the sediment to gain access for space and food. In contaminated sediment, the maximum depths of burial did not correlate with population density at 0.05-significance level (paired t-test, $p = 0.183$). The mean values of the maximum mixing depth in contaminated sediment were 0.41 ± 0.06 cm and 0.33 ± 0.02 cm for 16000 and 32000 indiv/m², respectively, which is 3.0 and 4.5 times less than the corresponding values in clean sediment. This is in agreement with visual observations that showed that even though the animals were alive throughout the experiment duration, their life activities were extremely reduced. Most individuals did not burrow deeper than 0.5 cm below the interface, they changed their location very rarely, caused very limited particle re-suspension, and consequently there was limited burial of the surficial sediment.

It should be noted that although the clean sediment treatment ran for 14 days and the contaminated treatment ran for 7 days, the authors' comparisons are still valid due to very slow burial observed after 2.5 half days (data not shown) in contaminated sediment. The secondary burial rates presented in Figure 71 for contaminated sediment yielded an average maximum burial velocity of 2.3 cm/yr leading to an additional 0.04 cm of burial if the experiments were continued for an additional 7 days. This is much less than the resolution of the authors' measurement (0.2 cm).

Particle biodiffusion enhancement factors were calculated from the ratio of the particle biodiffusion coefficient in the presence of benthos to the particle diffusion coefficient in the control cell to account for any non-biological particle mixing (Figure 74). The presence of *L. plumulosus* in the clean sediment enhanced initial particle diffusion by a factor of 13.8 ± 3.3 , 34.2 ± 12.0 , and 40.5 ± 10.5 for 8000, 16000, and 32000 indiv/m², respectively. While the biodiffusion coefficient seems to increase with population density, variability in the small number of trials was such that there is no compelling statistical difference between the treatments (ANOVA, $p = 0.066$). In contaminated sediment, the initial biodiffusion coefficient was significantly lower: 2.3 ± 0.7 and 4.3 ± 0.5 for 16000 and 32000 indiv/m², hence over 10 times slower than those obtained in clean sediment. Similar to burial velocities, particle biodiffusion was fastest at the beginning of the experiment, with secondary biodiffusion coefficients more than three times lower than the initial biodiffusion coefficients. Secondary biodiffusion enhancement factors for contaminated sediment were close to one, which means that biological mixing of tracer ceased. The values of particle biodiffusion coefficients obtained for microcosms with biota and corresponding control cells are presented in Table 25.

Figure 74. Particle biodiffusion enhancement factors. Circles represent clean sediment treatment; triangles represent contaminated sediment treatment; closed symbols represent initial coefficient; open symbols represent secondary coefficient. Error bars equal to one standard deviation within the triplicate.

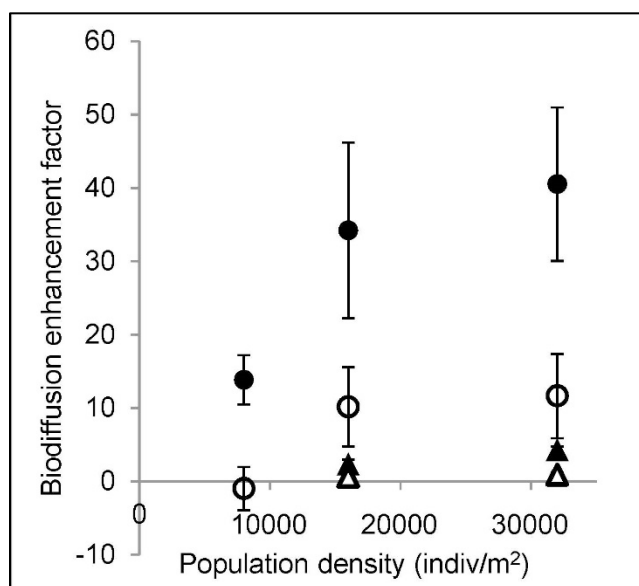


Table 25. Measured particle biodiffusion coefficients and average particle biodiffusion enhancement factors. Enhancement factors were calculated by dividing D_b initial (D_b ini) or D_b secondary (D_b sec) by corresponding diffusion coefficient in the control cell. Values of D_b enhancement factor lower than one marked with an asterisk result most likely from collapsing of abandoned burrows (secondary compaction faster than peak's spreading rate).

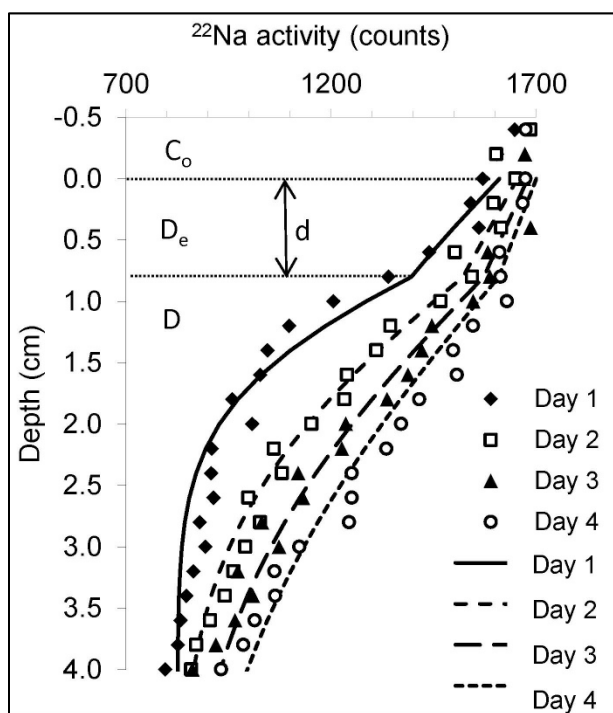
Sediment type and <i>L. plumulosus</i> population density	<i>D_b ini</i> (cm ² /yr)	<i>D_b sec</i> (cm ² /yr)	<i>D control</i> (cm ² /yr)	Average <i>D_b ini</i> enhancement factor	Average <i>D_b sec</i> enhancement factor
Sequim					
32000 indiv/m ²	27.0	10.0	0.5	40.5	11.6
	14.0	4.7	0.5		
	58.7	8.8	1.4		
16000 indiv/m ²	15.2	4.6	0.5	34.2	10.2
	25.8	8.8	0.5		
	31.7	5.9	1.4		
8000 indiv/m ²	9.5	-2.1	0.5	13.8	-1.0 *
	6.2	-0.9	0.5		
	15.4	4.3	1.4		
New Bedford					
32000 indiv/m ²	6.1	2.2	1.7	4.3	0.9 *
	7.5	1.5	1.7		
	8.0	0.8	1.7		
16000 indiv/m ²	3.6	1.7	1.7	2.3	0.6 *
	5.4	0.9	1.7		
	2.7	0.5	1.7		

13.4.1.2 Solute transport by *L. plumulosus*

Diffusion of solutes from the overlying water into the sediment occurs both with and without biota, but infaunal benthic organisms increase the diffusive flux by burrow construction and irrigation. The authors modeled this process using Equation 17-2 to obtain an estimate of the enhanced flux induced by *L. plumulosus*. The model fits the vertical ²²Na activity profile for an enhanced diffusion coefficient in the bioturbated zone when the activity of the tracer in the overlying water, thickness of the bioturbated zone, and molecular diffusion in undisturbed sediment below bioturbated zone are known (Figure 75). The activity of the ²²Na tracer in the overlying water (C_o) was obtained by averaging all measurements of the ²²Na activity above sediment-water interface (depth < 0). The molecular diffusion coefficient in the sediment, D , was obtained by least square fitting the diffusion equation to the tracer activity profile obtained from the control cell containing no organisms. The thickness of the

bioturbated zone (d) was assessed by visual examination of trends of activity change with depth. The enhanced solute diffusion coefficient, D_e , was then determined by minimizing the total sum of squares when fitting the diffusion equation to the data from the four days of scanning.

Figure 75. Vertical profiles of the ^{22}Na activity obtained over four days from one of the microcosms. Symbols represent measured data; lines represent modeled values; C_o represents overlying water activity of the tracer; D_e represents enhanced diffusion coefficient in the bioturbated zone; D represents molecular diffusion coefficient below the mixing zone; d represents mixed zone thickness.



The authors define a solute biodiffusion enhancement factor as the value of the enhanced diffusion coefficient in the presence of organisms divided by the value of the diffusion coefficient in the control cell. The results obtained in cells containing 16000 and 32000 *L. plumulosus* per m^2 are presented in Figure 76. In both clean and contaminated sediment, the presence of biota significantly increased the solute flux (1-sided t-test, $\mu = 1$ vs. > 1 , $p = 0.003$ for clean sediment and $p = 0.002$ for contaminated sediment). In clean sediment, the average enhancement factor was slightly higher: 2.81 ± 0.89 and 2.26 ± 0.44 for 16000 and 32000 indiv/ m^2 , respectively, while in contaminated sediment the solute diffusion was enhanced by a factor of 1.56 ± 0.26 and 1.72 ± 0.35 in the presence of

16000 and 32000 indiv/m², respectively. Due to the variation within replicates, the differences between solute diffusion enhancement factor in clean and contaminated sediments were statistically insignificant (paired t-test, $p > 0.10$). The authors attribute the relatively little effect that sediment pollution had on solute transport by *L. plumulosus* to the fact that the organism does not actively irrigate its burrows once they are constructed. Rather, it was the presence of the burrow itself that caused increased solute diffusion by providing extra surface area for solute exchange, and not the direct irrigation of burrows by the organisms. Values of solute diffusion coefficients in the presence of biota and in corresponding control cells are presented in Table 26.

Figure 76. Mean solute biodiffusion enhancement factors with one standard deviation error bars. Circles represent clean sediment treatment; triangles represent contaminated sediment treatment.

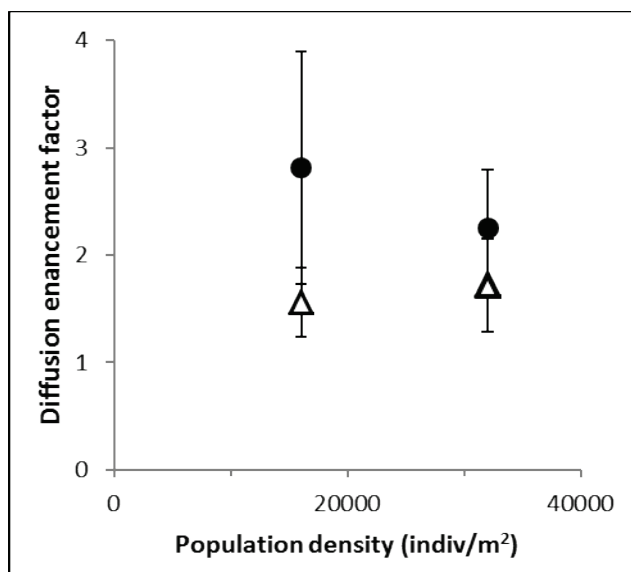


Table 26. Solute diffusion coefficients for bioturbated cells and corresponding control cells.

Sediment type and <i>L. plumulosus</i> population density	D_b (cm ² /d)	$D_{control}$ (cm ² /d)	Diffusion enhancement factor	Average
Sequim				
32000 indiv/m ²	1.99	1.09	1.83	2.26
	2.26	1.09	2.08	
	1.64	0.57	2.87	
16000 indiv/m ²	4.22	1.09	3.87	2.81
	3.12	1.09	2.87	
	0.98	0.57	1.70	

Sediment type and <i>L. plumulosus</i> population density	D_b (cm ² /d)	$D_{control}$ (cm ² /d)	Diffusion enhancement factor	Average
New Bedford				
32000 indiv/m ²	1.73	1.24	1.40	1.72
	2.73	1.24	2.21	
	1.11	0.72	1.54	
16000 indiv/m ²	1.48	1.20	1.20	1.56
	2.19	1.78	1.78	
	1.24	1.72	1.72	

13.4.1.3 *L. plumulosus* particle and solute mixing summary

Contamination of the sediment has a significant effect on particle mixing and solute transport by *L. plumulosus*. The velocity of surficial sediment burial at high amphipod population density decreased from the average of 68 cm/yr in clean sediment to 29 cm/yr in contaminated sediment, with burial in contaminated sediment practically ceased at lower animal abundance. In addition, maximum mixing depth was significantly altered in the presence of contamination, achieving mean depth of 1.5 cm in clean sediment, and only 0.4 cm in contaminated sediment. Finally, the average ratio of biologically induced particle mixing to the non-biological solids movement (particle biodiffusion enhancement factor) decreased from about 34 and 41 cm²/yr for medium and high amphipod population densities, respectively, to 2 and 4 cm²/yr for corresponding animal abundances in contaminated sediment. Polluted sediment caused over two times slower burial velocity, three times lower mixing depth (reduction in bioturbated zone thickness), and 10 times slower particle biodiffusion when compared to clean sediment. Thus, particle biodiffusion, measured as surficial peak broadening, is the most sensitive of the three measured particle-mixing parameters. Additionally to decreased rates of mixing and presence of thinner bioturbated zone in the contaminated sediment, reworking activities of *L. plumulosus* practically ceased about 2.5 days after the initiation of the experiment (secondary burial velocities close to 0 cm/yr and particle biodiffusion enhancement factors close to 1). In clean sediment the biological sediment reworking was still observed even after 14 days (for higher population densities).

The results show that sediment-reworking activities are strongly affected by sediment contamination, with particle biodiffusion, measured as surficial peak broadening, being most sensitive out of the three analyzed

particle-mixing coefficients. The presence of *L. plumulosus* significantly increased solute flux compared to control cells; however, the difference between clean and contaminated sediment treatments were statistically negligible due to the data scatter.

13.4.2 *M. mercenaria*

13.4.2.1 Particle mixing by *M. mercenaria*

Burial velocity of the surficial labeled layer of sediment and particle biodiffusion rates are obtained in the same manner as for *L. plumulosus*. Slope of the line on tracer peak depth vs. time quantifies burial velocity and slope of the line on the square of peak's spread (σ) vs. $2 \times \text{time}$ constitutes particle biodiffusion coefficient. For more details, refer to section 15.4.1.1. Both mixing parameters display faster rates for the first 10 days of the experiment than afterward. Although it is unclear why the observed pattern holds for control cells as well, by comparing all treatment samples to the control, the authors are able to extract changes resulting from biological activity only. The exception is one cell in which an intense and rapid episode of mixing took place between the measurement on day 28 and day 32 (Figure 77). After two weeks of no significant changes in peak's position and peak's spread (σ), sudden increase in both the parameters was observed. Peak's depth increased from 0.3 to 0.6 cm, and peak's spread from 0.35 to 0.82 cm². Since such episode was recorded in only 1 out of 6 bioturbated cells, the three exceptional data points were not included in the analysis of the overall trends. More replicates and longer term experiments would be useful to establish frequency of such an event and its significance for sediment geochemistry changes, including contaminants partitioning and bioavailability.

Data from peak position with fitted trend lines used for burial velocity and particle biodiffusion coefficient calculations are presented in Figure 78 and Figure 79. As mentioned before, different trends were observed for the first 10 days than afterwards, so data from each cell was divided into two parts: initial (up to day 10) and secondary (days 10 +). Black circles and black bold lines indicate results for the control cell (no organism), and the colored data are for the microcosms with *M. mercenaria*.

Figure 77. Peak's position and peak's spread change in time. After very little change from day 10 to day 28, a sudden increase in both measurements was observed.

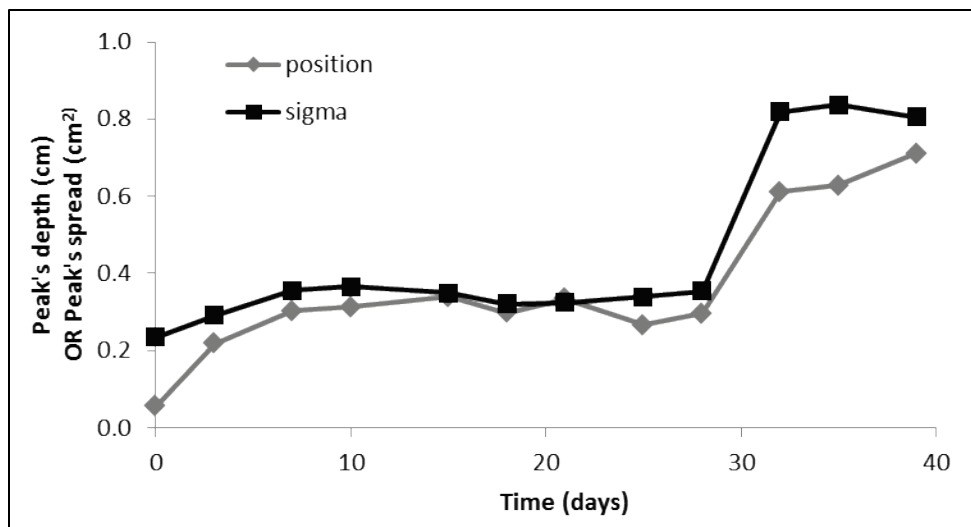


Figure 78. Change of peak position with time for clean (left hand side panel) and contaminated (right hand side panel) sediments. Black data indicates control cell for each treatment (no organisms); colored data refers to microcosms with *M. mercenaria*.

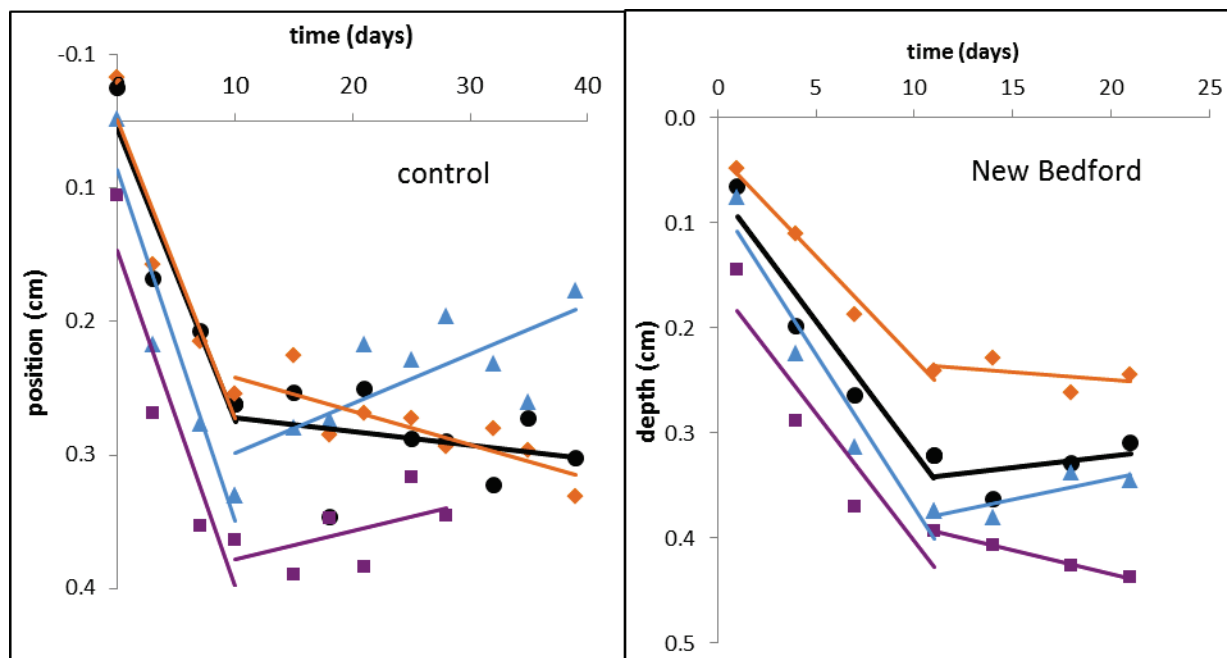
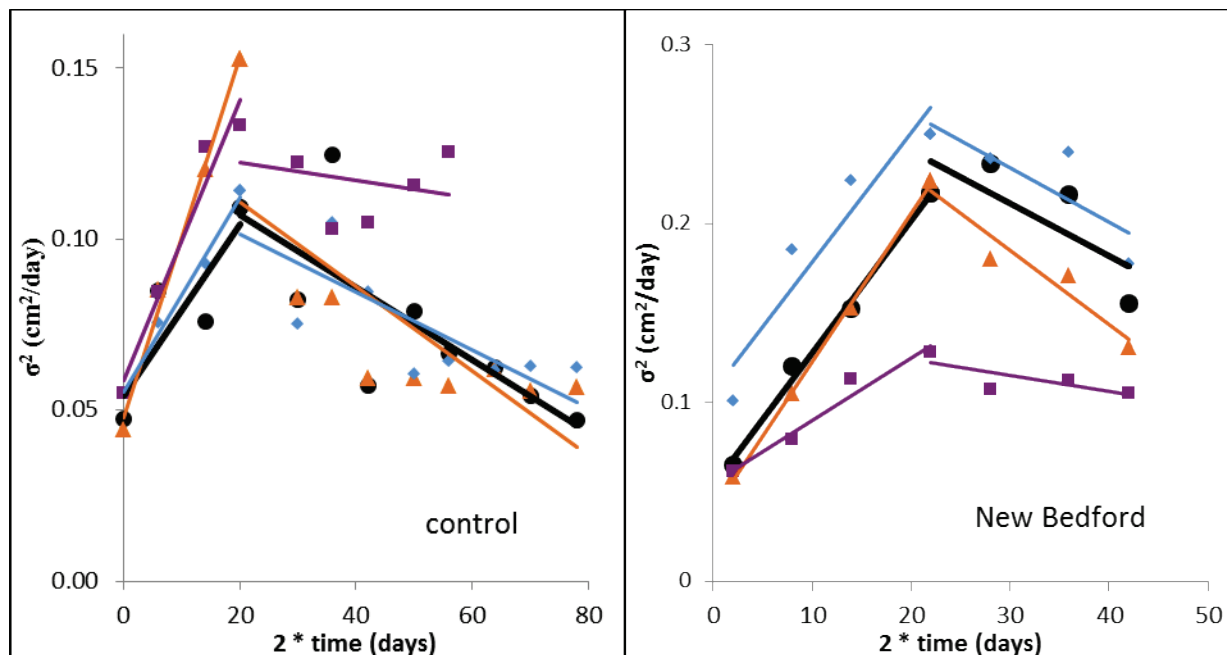


Figure 79. Squared peak's spread (σ^2) vs. $2 \times$ time plots used for particle bioturbation coefficient determination. Left hand side panel refers to uncontaminated sediment, and right hand side panel shows data for contaminated sediment. Black represents data for control cells (no organisms), and colored represents data cells with *M. mercenaria*.

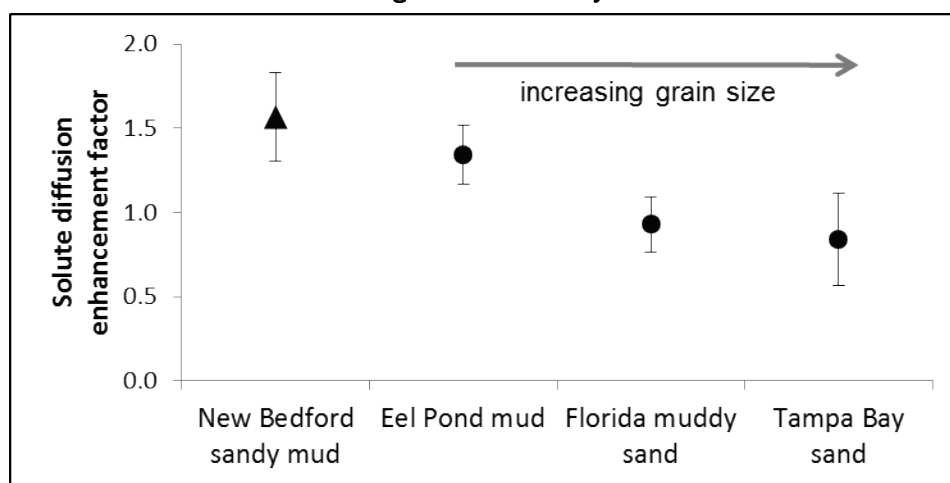


The left hand side panel in Figure 78 shows the results of peak burial for uncontaminated sediment, and the right hand side panel refers to contaminated sediment (New Bedford). Analysis conducted on the slopes of the lines with ANOVA General Linear Model showed that for both sediments, initial slopes of peak position vs. depth data in cells with clams are statistically equal to the corresponding control cells ($P = 0.645$ and $P = 0.941$ for clean and contaminated sediments, respectively). Secondary slopes are also indistinguishable from the control cells at 0.05 significance level, except one cell in clean sediment treatment (blue triangles, left panel, $P = 0.015$). That means that neither for clean nor contaminated sediment, measurable effect of *M. mercenaria* activity on peak burial was observed. That is also true for peak spread (σ) shown in Figure 79. ANOVA General Linear Model indicates that both initial and secondary slopes for the lines fitted to data from bioturbated cells are not significantly different from the corresponding control cells (0.05 significance level), with the exception of the initial slope of the dataset presented in purple squares for New Bedford sediment treatment. However, this slope is lower, and not higher than the control further supporting the conclusion of no effect of *M. mercenaria* on diffusive spreading of the surficial sediment layer.

13.4.2.2 Solute transport by *M. mercenaria*

Solute exchange results for *M. mercenaria* are presented in Figure 80 as diffusion enhancement factors, defined as the ratio of biodiffusion coefficient in the presence of benthos to the diffusion in control cell. The highest solute increased was observed in New Bedford contaminated mud (factor of 1.57 ± 0.27) and Eel Pond mud (1.35 ± 0.18), however the difference between the two is not statistically significant (paired T-test, $P = 0.187$). Diffusion enhancement factors in both Florida muddy sand and Tampa Bay sand had values of 0.93 ± 0.17 and 0.84 ± 0.28 , respectively, and were both statistically insignificant ($P > 0.05$). Results for the two finest sediments (New Bedford and Eel Pond) indicate that there is no measurable effect of contamination on solute exchange. Comparison of solute biodiffusion for the three uncontaminated sediments with different grain sizes shows no effect in the bivalve's native sands from Florida, while showing significant solute transport enhancement in fine-grained Eel Pond mud. This is somewhat contrary to what could be expected, as the sand-burrowing organisms such as *M. mercenaria* placed in a sediment of preference should maintain maximum activity. The results may indicate that the organism becomes more active in the lack of appropriate support of the foot during movement in fine-grained sediments.

Figure 80. Solute diffusion enhancement factors for *M. mercenaria*. The triangle shows data for treatments in contaminated sediment (New Bedford), circles denote treatments in uncontaminated sediment with varying grain size, increasing from left to right as indicated by the arrow.



13.4.2.3 *M. mercenaria* particle and solute mixing summary

Particle mixing experiments revealed that for the tested population density of about 800 *M. mercenaria* juveniles (20 mm in length) per m² no

measurable particle redistribution was observed. The exception was one cell where a rapid episode of mixing resulted in dramatic peak broadening and burial occurred after 28 days of the experiment. That proves necessity of using much larger number of clams and longer experimental duration to properly describe long-term population level effects of mixing and bioaccumulation. Solute transport measurements showed that *M. mercenaria* significantly affects diffusion in fine-grained sediments (mud and muddy sand, factor of 1.35 and 1.57, respectively), but there is no effect of its presence for sandy sediments, which could indicate that the organism moves more when no proper support for the foot is provided. No significant difference was observed between clean and contaminated sediment treatments.

13.4.3 3-D burrow model of solute flux

A color contour plot of a 2-D cross section through the center of the burrow of the steady state model result is shown in Figure 81. The blue represents material with a high oxygen concentration (164 μM), and the dark red represents material with a low (0 μM) concentration. In this simulation, the overlying water is fixed at its half saturation value, so it is uniformly blue, whereas some oxygen has diffused into the sediment and the rainbow of colors from blue to red represents the diffusion boundary. The depth of oxygen penetration into the sediment by diffusion is about 1 cm. Note that oxygen not only diffuses from the water column into the sediment, but that it also diffuses from the burrow into the sediment. Thus, the presence of irrigated burrows would be expected to increase the sediment-oxygen demand, which is what is observed in Figure 82. As water is transported through the burrows, it diffuses into the sediment and, in the bottom of the burrow, where the organism consumes it. This can be seen in Figure 81 where the oxygen concentrations form a halo around the burrow and decrease along the length of the bottom section of the burrow where animal respiration occurs. The outflow water from the burrow has a lower oxygen concentration (~6% O_2 saturation) than the inflow water (50% O_2 saturation). The plume of low oxygen water that emerges from the burrow is not apparent in the overlying water because the model assumes a well-stirred overlying water of fixed concentration. To account for the effect of animal respiration and to gain insight to the magnitude of the enhanced demand caused by diffusion, the animal respiration was subtracted from the total oxygen demand. This 'corrected' oxygen flux is also shown in Figure 83. Although animal respiration represents only a small fraction of the total sediment-oxygen demand at

low densities, it accounts for up to 1/3 of the SOD at the highest densities considered here. The results in Figure 82 show that the sediment-oxygen demand increases by about a factor of 10 from $\sim 1 \times 10^{-12}$ mol/cm²/s in the absence of burrows to $\sim 1 \times 10^{-11}$ mol/cm²/s at densities of about 500 indiv/m². The increase in SOD is significant, even at small organism densities. At the highest densities considered only about 10% of the increase in SOD can be related to an increase in available surface area through which oxygen diffuses. In this model, it is not possible to calculate the sediment-oxygen demand at burrow densities greater than about 650/m² without intersecting or overlapping adjacent burrows so the calculations did not consider higher densities.

Figure 81. A color contour plot of a 2-D cross section through the center of the burrow of the steady state model. The blue represents material with a high oxygen concentration (164 μ M), and the dark red represents material with a low (0 μ M) concentration. The colors represent the diffusion of oxygen across the sediment-water interface and across the burrow wall and its consumption in the anaerobic sediment.

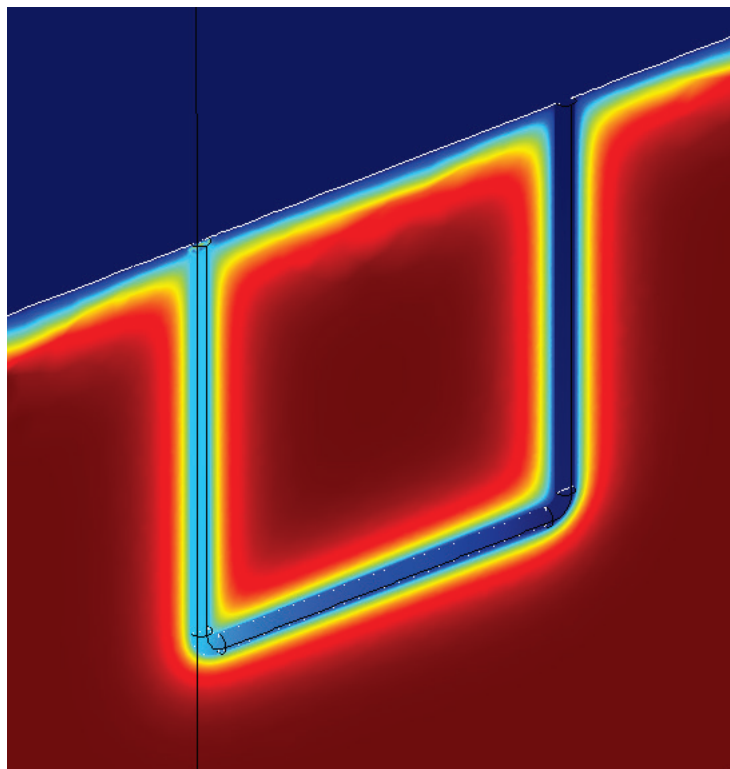


Figure 82. Increase in solute flux (oxygen) as a function of burrow density. The model results are shown both with and without animal respiration and indicate that the flux increases by about a factor of 8 as the burrow density increases from 0 to 600 indiv/m².

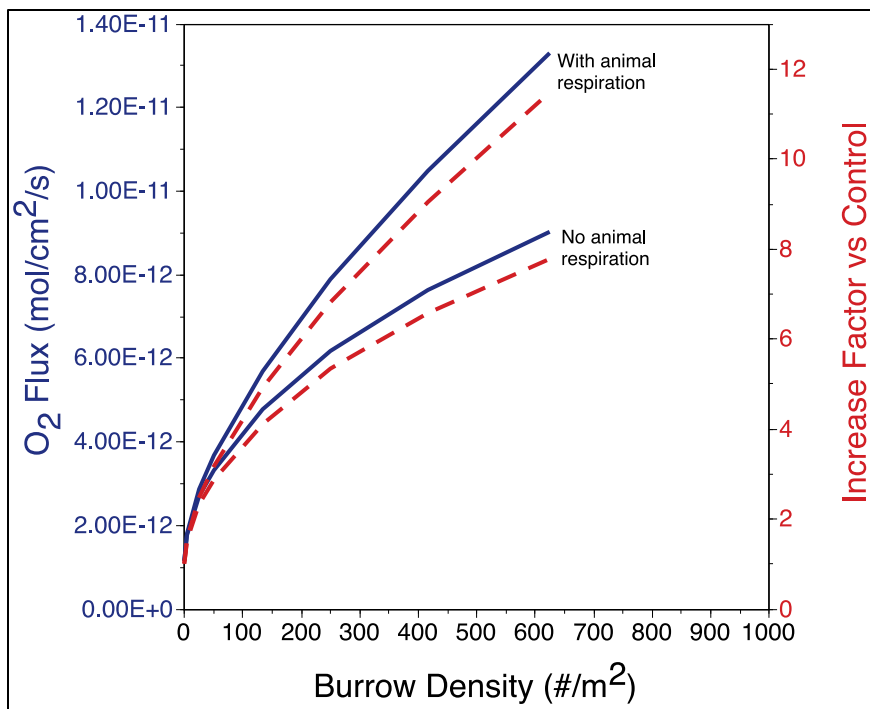
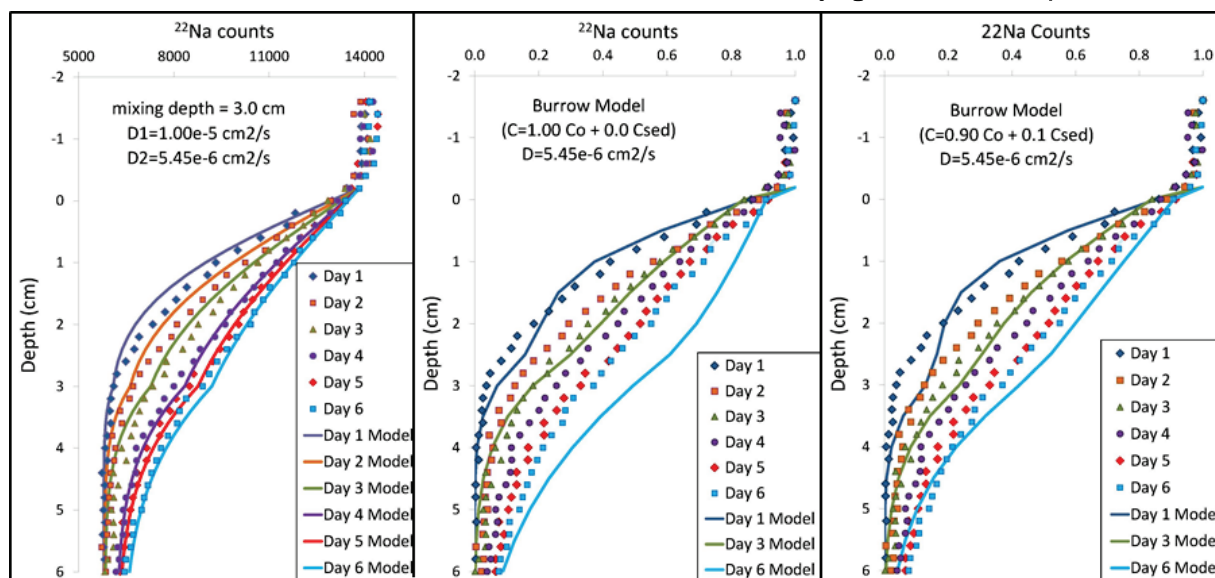


Figure 83. Comparisons of models of solute transport by *Y. limatula*. The left figure illustrates the best fit results for a 2-layer enhanced diffusion model, the same model as presented above for the *L. plumulosus* experiment. The center figure is the best fit results for a 3-D model where the *Yoldia* burrow is characterized by a cylindrical hole consisting of pure overlying water. The figure on the right is also a 3-D model of a *Y. limatula* burrow, but it is filled with water that consists of 90% overlying water and 10% pore water.



The significance of these model simulations is not in the calculation of a specific value of the sediment-oxygen demand, nor is it in the calculation of an exact distribution of oxygen around a single burrow. Rather it is the finding that it takes only a few bioirrigating animals to significantly increase the sediment-oxygen demand. In essence, the presence of an irrigated burrow significantly increases aerobic respiration at the burrow wall and the flow of water through the burrow maintains a high oxygen gradient resulting in an enhanced diffusive flux across the burrow walls. Higher burrow densities do not result in significantly higher oxygen fluxes because the diffusion halos will overlap.

While this model cannot be applied to a single *Leptocheirus plumulosus* burrow, it has application to larger solitary bioirrigating infauna that might see use in other toxic sediment exposure experiments. In fact, it does predict solute transport by the larger (1–3 cm length) *Yoldia limatula* clams that were contemplated as a test organism in the original SERDP proposal (and whose supply of experimental organisms has been cut off due to a disease outbreak). An example of this is shown in Figure 83, where the 3-D burrow model indicates that to explain the concentrations of ^{22}Na , the burrow around the clam must consist of a mixture of pore water and overlying water.

14 Comparison of fluorescent and radioactive particle tracers

14.1 Objective

^{137}Cs was successfully used as a particle tracer to characterize mixing coefficients, such as the burial rate and the biodiffusion coefficient (e.g. Matisoff and Wang, 2000), however this method has several limitations, including expensive waste disposal. The objective of the work presented in this section was to assess usefulness of an alternative tracer - fluorescent particles (luminophores) for non-destructive time series measurements of mixing parameters. The methodology used for luminophores redistribution measurements was evaluated by comparing the results with those obtained with ^{137}Cs particle tracer.

14.2 Background

^{137}Cs labeled clay placed on sediment water interface or as a multiple subsurface layer was used to quantify particle redistribution due to biological activity (e.g. Matisoff and Wang, 2000). Emitted gamma radiation is measured for each depth interval creating depth vs. tracer activity profiles. The authors employed this method in the *L. plumulosus* and *M. mercenaria* mixing experiments described in Section 15. The details of the experimental setup and mixing parameters calculation are described in Sections 15.3.4 and 15.3.5. Although this method was successfully used (Robbins et al, 1979; McCall et al, 1995; Muslow, et al, 2002; Landrum et al 2002), it has some limitations. First, the measurements are taken through a collimated slit, which is 4 mm tall and horizontally averages the readout. Thus, no information about the lateral particle transport can be obtained, and the vertical resolution of the measurement is limited. Furthermore, the method uses radioactive material, which requires special laboratory procedures and certifications and is costly to dispose of after experiment termination. Additionally, the gamma emitting element is sorbed to clay mineral, meaning the tracer fits well with studies conducted in finely-grained sediments, but may not be appropriate for experiments conducted in substrates with large percentages of coarser particles (e.g. sand). Finally, each horizontal line of the scan takes about five minutes, causing time difference between the bottom and the top of the scan, which could

potentially be an issue for large scan depths and/or rapidly mixing organisms.

Fluorescent particles (luminophores) have been used quite frequently and offer an alternative for measuring particles redistribution. However, a majority of studies quantify particle redistribution destructively by slicing a core and then counting the particles in each depth interval (e.g. Mahaut and Graf, 1987; Gerino, 1990; Quintana et al, 2007). As a result of such handling, no real-time series measurements are possible, and the results are horizontally averaged for each depth interval. The sections of the core are dried, homogenized, and then a sample is taken to count fluorescent particles under UV microscope, meaning the processing is also quite time consuming.

At this juncture, the authors used luminophore methodology that allows obtaining non-destructive time series 2-dimensional high resolution measurements. The layer of the particles can be placed either on the sediment – water interface to measure the burial, or as a subsurface layer to track the upward movement of buried particles. Particle redistribution by benthic biota is recoded using a digital photo camera. Varieties of colors are available, which permits possible simultaneous measurement of both processes. The advantages of this method are that it is non-toxic, the measurements are very quick (on the order of seconds), it does not require expensive instrumentation, and it permits great two-dimensional resolution limited only by the image pixel size. Two-dimensional measurements of luminophores redistribution have been previously used (e.g. Solan et al, 2004; Maire et al, 2007); however, this is the first work comparing 2-D fluorescent measurements to those obtained from horizontally averaged radiotracer scanners.

14.3 Materials and methods

14.3.1 Materials

Seawater of salinity 28 ppt and ^{137}Cs tracer were the same as described in Section 15.3.1. Silt sized yellow luminophores were purchased from Environmental Tracing Systems Ltd, Helensburgh, Scotland. The luminophores have a density of 2.65 g/cm^3 and emit at a wavelength of about 525 upon excitation with UV light. Prior to use luminophores were suspended in water by mixing 3 g of the tracer with 6 g of water. The suspension was vigorously shaken before each use.

14.3.2 Organisms and sediment

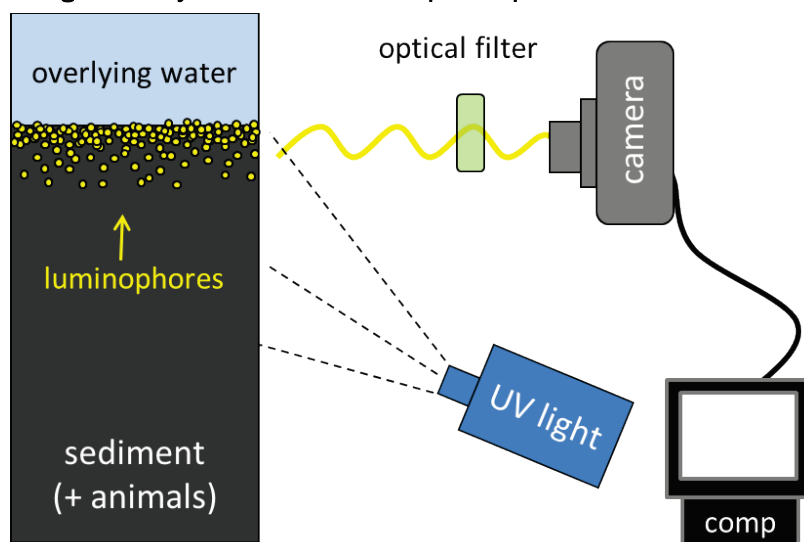
M. mercenaria juveniles (about 20 mm in length) and the sediment were collected by Bay Shellfish Co., Terra Ceia, FL. The specifics of animal care are described in Section 15.2.2. Sediment used for this study was a muddy sand collected in Florida.

14.3.3 Experimental setup

This experiment consisted of four Plexiglass cells sized 4.7 x 2.6 x 25 cm (W x D x H). The cells were filled with about 8 cm of sediment column and overlying 28 ppt sea water, and allowed to compact for two weeks in the fridge. A day prior to the start of this experiment, most of the water from each cell was siphoned and replaced with fresh sea water to ensure proper salinity, and the cells were placed in a water bath to provide adequate temperature for *M. mercenaria* (24 ± 2 °C). One cell was used as a control (no organisms). In the other three cells, two clams per cell were gently placed on top of the sediment and allowed to burrow. Organisms that failed to burrow were replaced. After all organisms burrowed, a 300 µL of luminophores suspension, 300 µL of ^{137}Cs -labeled clay, and again 300 µL of luminophores were added in 20 minute intervals between each layer to allow the particles to settle onto the sediment surface. The cells were kept in a water bath for temperature control. About 60% of water was siphoned out of each cell and replaced with clean seawater three times per week. In addition, the animals were fed with DT's Live Marine Phytoplankton.

Redistribution of ^{137}Cs tracer was measured about twice a week using the gamma scanner with precise X-Y positioning, as described in Section 15-3-4 and in Wang and Matisoff (1997). On the same days, the distribution of luminophores was recorded using the system schematically presented in Figure 84. A high-resolution Canon EOS 50D digital camera with a macro lens was positioned directly in front of the cell. The luminophores in the cell were excited using a UV light, and the emitted light was collected by the camera after passing through a 520 ± 10 nm optical filter (Intor, Inc., Socorro, NM) to eliminate all reflected light. The whole system was contained in a black box to minimize the amount of noise from external light sources. An ISO of 800 and a 30-second exposure time was sufficient to obtain good quality images. Both the front and back of each cell were photographed.

Figure 84. System used for luminophores position measurements.



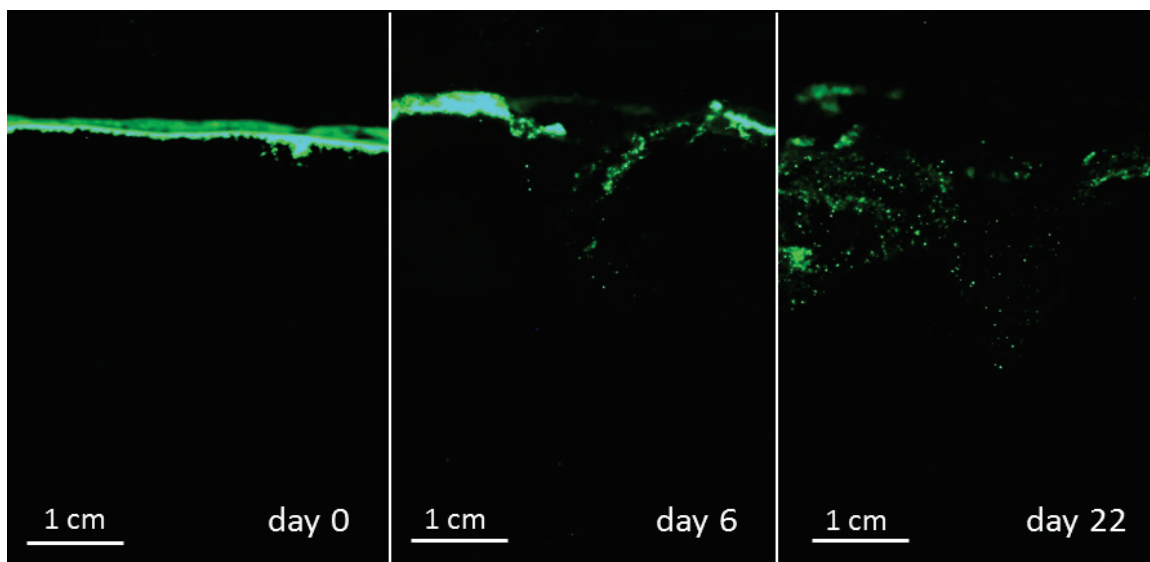
14.3.4 Data processing

The luminophore images were processed using Image J 1.43u, which were obtained at no cost from the National Institutes of Health website. After cropping the picture to the desired size, fluorescence intensity of each pixel was obtained by transforming the image into a text file, which can then be imported to Microsoft Excel for further processing. After establishing threshold light intensity for the background noise, the matrix of pixels was converted into a binary where the fluorescent particle is either present or absent. The information can then be used to construct high-resolution (0.1 mm) intensity vs. depth profiles, vertically averaged intensity data for horizontal transport models, or 2-D distribution maps. However, the purpose of this study was to compare the results using luminophores with those obtained using ^{137}Cs tracer. Since the height of the gamma detector collimated slit was 4 mm, the authors averaged the measurement for each 4 mm depth interval.

14.4 Results and Discussion

The example of time series measurement of luminophore redistribution by *M. mercenaria* is presented in Figure 85. On day zero of the experiment, luminophores were present as a thin layer on the sediment-water interface. On day six, the layer was destroyed in the middle section; however, it was still present on right and left ends of the cell. On day 22, no surficial luminophore layer was visible, and the particles appeared down to depth of about 2.5 cm.

Figure 85. Progression of fluorescent particles redistribution for one of the experimental cells. Undisturbed layer of luminophores (day 0), luminophore layer partly mixed (day 6), and surficial layer of luminophores completely redistributed (day 22).



Luminophores distribution was measured on both the front and back of the experimental cells because the mixing was not perfectly uniform across the cell. Cell #30 showed the largest contrast between the two sides; As a result, it was used to assess whether data from two sides of the cell could be a reasonable indicator of the mixing activity within the entire volume of the sediment. Figure 86 presents images taken on the front and back of cell 30 on day 19 of the experiment. The two images show a different extent of bioturbation, with little mixing visible on the front side, and significant particle redistribution down to about 3 cm on the reverse side. That emphasizes the need of measuring both sides of the cell, as well as using cells as narrow as possible. Processing of the data for each cell is illustrated in Figure 87. The plot on the left hand side shows the counts of fluorescent luminophores vs. depth for the front (30a) and the back (30b) of the cell. On the right hand side, the two profiles were averaged to get the overall fluorescence intensity profile for the analyzed microcosm and the ^{137}Cs data profile is presented for comparison.

Figure 86. Comparison of two sides of the same cell. Each division on the scale bar on the left hand side of the pictures is 1 cm. The dashed line indicates position of sediment-water interface at the beginning of the experiment.

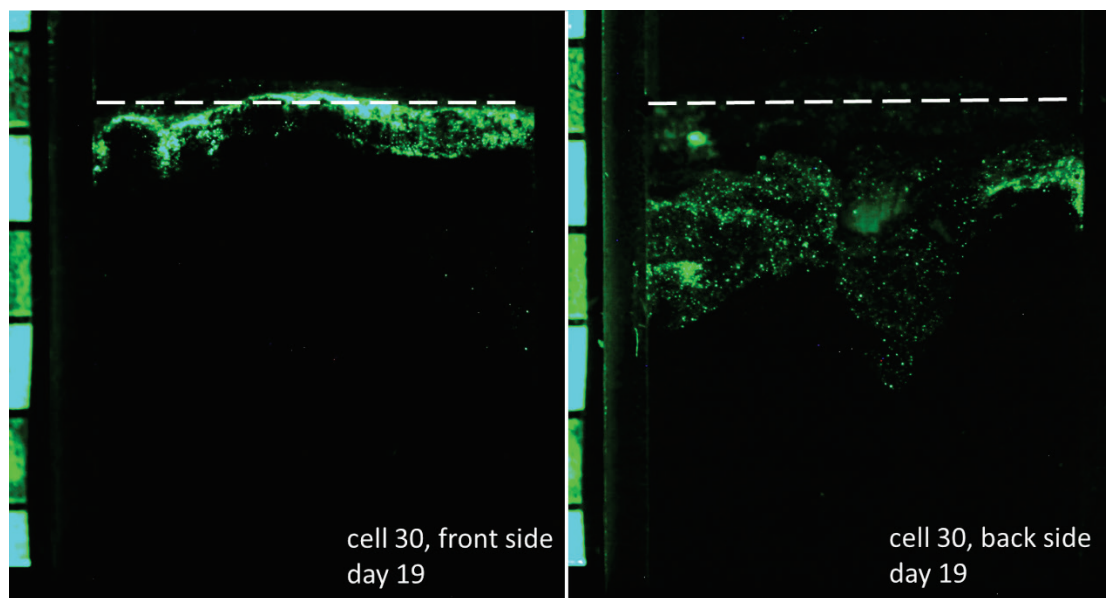
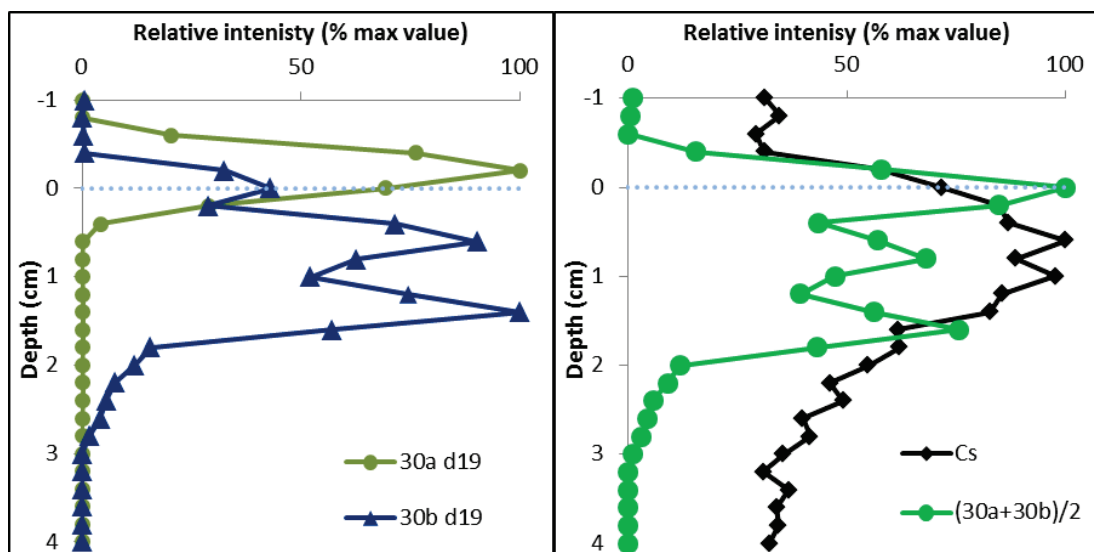


Figure 87. Fluorescent intensity profiles for the front (30a) and back (30b) of cell 30 (left panel). Averaged fluorescence intensity $(30a+30b)/2$ profile for cell 30 with corresponding ^{137}Cs data for the same cell.

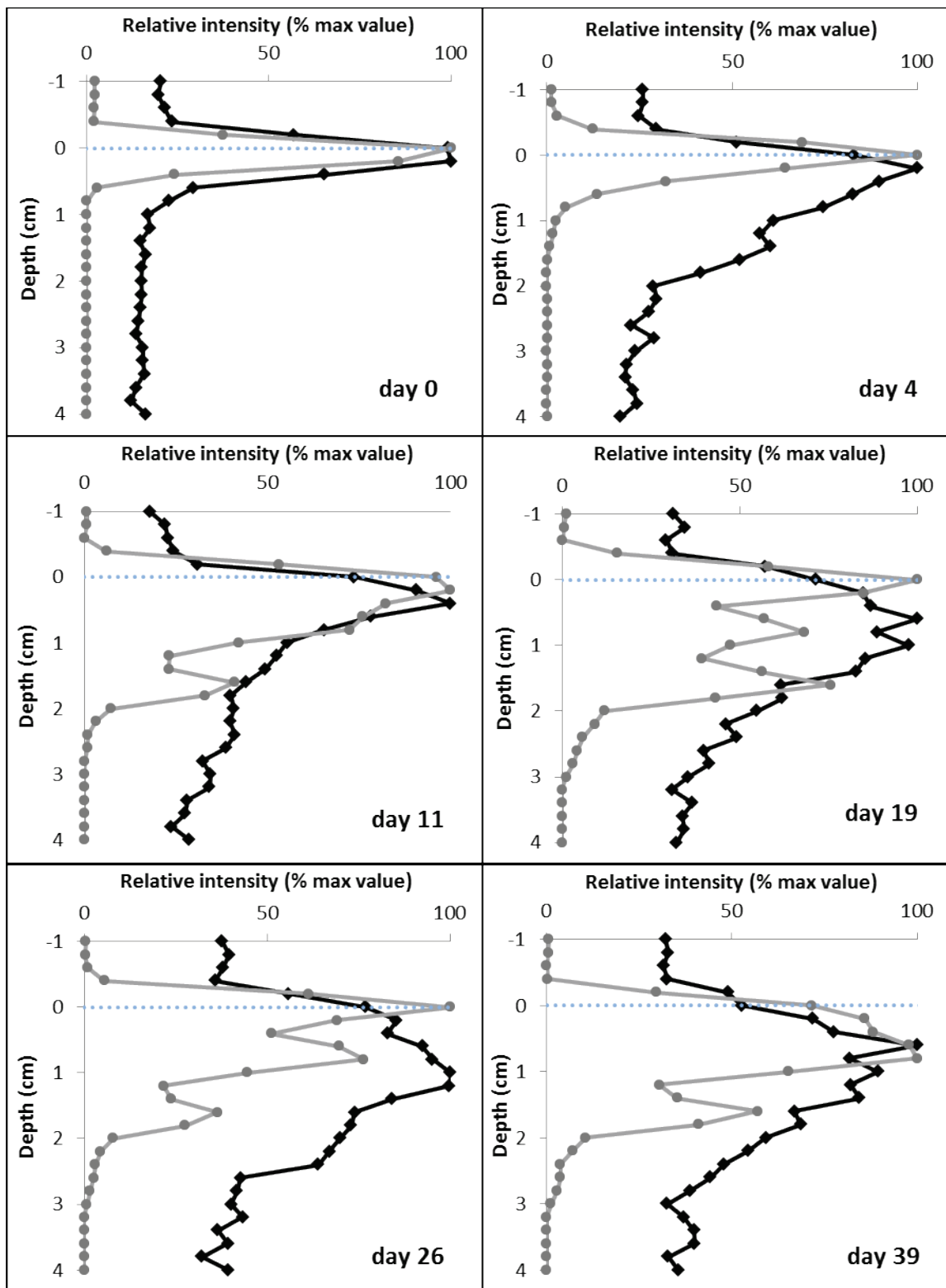


The comparisons of the profiles obtained using ^{137}Cs and luminophores over the course of the experiment (results averaged to 4 mm depth intervals) are presented in Figure 88 (both datasets were normalized to percent of maximum counts within a profile). On day zero, both tracers show a similar peak spread and peak position at a depth of 0 cm, consistent with the initial placement of the tracers on top of sediment-water interface. On day four,

both methods show a peak maximum near the initial sediment-water interface, however ^{137}Cs is observed down to about 2 cm, while luminophores are visible down to only about 1 cm. On days 11 through 39, both tracers show similar profiles, where ^{137}Cs is mixed deeper and sooner than the luminophores. The time difference between ^{137}Cs and luminophores reaching a particular depth could be the result of the radiotracer consisting of a slightly smaller grain size clay, while luminophores are silt. On the other hand, it is most likely because the gamma scanner measures tracer profiles through the entire slice of the sediment, while luminophore profiles are an outcome of averaging information from the front and the back walls of the cell only. Thus, if the mixing takes place in the middle of the cell, it will not be visible for the fluorescence measurements until the mixed volume of sediment reaches the cell walls.

Overall, the authors observed good agreement of the two datasets. Luminophores offered much better resolution than the ^{137}Cs tracer (limited by image pixel size, in this case 0.1 mm), much less background noise, and could be used to model lateral transport of particles or to better understand small-scale mixing behavior of organisms. For example, the authors observed the formation of a second radiotracer peak in some cells. Analysis of the fluorescence data showed that the tracer was non-uniformly mixed throughout the cell. For example, on the front side of the cell, the peak was still near the sediment-water interface and relatively intact, while on the back of the cell, the peak was significantly broadened and buried. Since fluorescence data collection takes less than a minute, this method was also more suitable for rapidly mixing species when the time difference between the top and the bottom of a radiotracer scan is no longer negligible. However, because the luminophore method only captured particle transport against the walls of the experimental cell, it was important to use narrow microcosms.

Figure 88. Comparison of ^{137}Cs (black line) and luminophore (grey line) profiles. The blue dotted line indicates the position of sediment-water interface.



15 Conclusions and implications for future research/implementation

The experimental results provided in this final report demonstrate that the functional attributes of species can affect the nature of their exposure to environmental contaminants associated with sediment. These findings have implications for future research and the conduct of risk assessment and management activities at contaminated sites.

Different species can exhibit substantially different bioaccumulation kinetics when exposed to PCB contaminated sediments. These results are consistent with previous findings, which show that biological attributes (e.g., organism size, lipid content, physiology) will affect the uptake and fate of contaminants within organism tissues. The observation of substantially different BSAFs among species exposed to the same sediment, and substantially different BSAFs for the same species exposed to two different sediments, raises numerous questions regarding the use of experimentally derived BSAFs in risk assessments. It is common practice for exposure modeling at contaminated sites to be based on relatively small amounts of bioaccumulation data that are derived from a limited number of species. The variation in bioaccumulation observed in the present study represents a significant source of uncertainty in the results of risk assessments based on benthic bioaccumulation data from a limited number of species and spatially distributed samples.

The experimental results of this study also illustrate that benthic species, as a result of variation in their functional attributes, will vary in their susceptibility to different exposure pathways, e.g., exposure to overlying water or bedded sediments. One of the obvious implications of these findings relates to how monitoring is conducted at field sites following the implementation of an *in situ* remedy. For example, in the case of a thin-layer capping remedy, functional groups that are strongly influenced by overlying water exposures would be more susceptible to ongoing sources of contamination than would functional groups that are primarily exposed through contact with bedded sediments. An understanding of the susceptibility of a particular functional group to exposures originating from overlying water, in contrast to sediments below the cap or sediment layer amended with activated carbon, could affect conclusions about the

performance of remedy and the need for additional engineering intervention.

The experimental evaluation of applying very thin (2 cm) layers of clean sand or activated carbon amended sediment provided insights regarding the efficacy limits of *in situ* approaches. A 2-cm layer of sand did result in substantial reductions in exposures to bedded sediments; by contrast, a 2-cm layer of activated carbon produced a limited effect. While it is possible that allowing for a longer contact period between the activated carbon and the contaminated sediment before exposing organisms might have produced a more substantial reduction in exposure, it is nevertheless true that the application of the 2-cm sand cap produced an immediate, positive effect. These results highlight the need for investigations of the temporal aspect of *in situ* remediation, especially in cases where minimal levels of intervention (thin-layer applications) are employed.

In addition to the above conclusions, the experimental results also demonstrate the value and limitations associated with passive sampling methods, in this case, through the use of PED. While passive sampling provides the means for obtaining important insight regarding bioavailability and the significance of different exposure pathways (e.g., overlying water vs. bedded sediment), the experimental results indicate that passive sampling may not be an entirely sufficient tool for characterizing the functional differences among different groups of benthic invertebrates. It is unrealistic to expect passive sampling to be a “silver bullet” approach for characterizing exposure for organisms exposed to contaminated sediments. While passive sampling, through PED or other approaches, provides important information that cannot be obtained from bulk chemistry data alone, such techniques should be used as a part of a multiple lines-of-evidence approach for characterizing the complexity of exposures to contaminated sediment.

References

- Accardi-Dey, A., and P. M. Gschwend. 2002. Assessing the combined roles of natural organic matter and black carbon as sorbents in sediments. *Environ Sci Technol* 36(1):21–29.
- Accardi-Dey, A., and P. M. Gschwend. 2003. Reinterpreting literature sorption data considering both absorption into organic carbon and adsorption onto black carbon. *Environ. Sci. Technol.* 37(1): 99–106.
- Adams, W. J. 1987. Bioavailability of neutral lipophilic organic chemicals contained in sediments: a review. In. *Fate and Effects of Sediment-bound Chemicals in Aquatic Systems*, ed. K. L. Dickson, A. W. Maki, and W. A. Brungs, 219–244. Elmsford, New York: Pergamon Press.
- Adams, R. G., R. Lohmann, L. A. Fernandez, J. K. MacFarlane, and P. M. Gschwend. 2007. Polyethylene devices: Passive samplers for measuring dissolved hydrophobic organic compounds in aquatic environments. *Environ Sci Technol* 41(4): 1317–1323.
- Allan, I. J., K. Booij, A. Paschke, B. Vrana, G. A. Mills, and R. Greenwood. 2009. Field performance of seven passive sampling devices for monitoring of hydrophobic substances. *Environ Sci Technol* 43(14): 5383–5390.
- Allan, I. J., A. Ruus, M. T. Schaanning, K. J. Macrae, and K. Naes. 2012. Measuring nonpolar organic contaminant partitioning in three Norwegian sediments using polyethylene passive samplers. *Science of the Total Environment* 423: 125–131.
- Alvarez, D. A. 2010. Guidelines for the use of the semi-permeable membrane device (SPMD) and the polar organic chemical integrative sampler (POCIS) in environmental monitoring studies. *U.S. Geological Survey, Techniques and Methods* 1–D4: 28.
- American Society of Testing Materials (ASTM). 2008. Standard test method for measuring the toxicity of sediment-associated contaminants with estuarine and marine Invertebrates. E1367-03. West Conshohocken, PA: ASTM International.
- American Society of Testing Materials (ASTM). 2010. Standard guide for determination of the bioaccumulation of sediment-associated contaminants by benthic invertebrates. Designation E 1688-10. West Conshohocken, PA: ASTM International.
- Backhus, D.A., and P.M. Gschwend. 1990. Fluorescent polycyclic aromatic hydrocarbons as probes for studying the impact of colloids on pollutant transport in groundwater. *Environ. Sci. Technol.* 24(8): 1214–1223.
- Bao, L. J., S. Xu, Y. Liang, and E. Y. Zeng. 2012. Development of a low-density polyethylene-containing passive sampler for measuring dissolved hydrophobic organic compounds in open waters. *Environ Toxicol Chem* 31(5): 1012–1018.

- Bao, L. J., and E. Y. Zeng. 2011. Passive sampling techniques for sensing freely dissolved hydrophobic organic chemicals in sediment porewater. *Trends in Analytical Chemistry* 30(9):1422–1428.
- Beckingham, B., and U. Ghosh. 2010. Comparison of field and laboratory exposures of *Lumbriculus variegatus* to polychlorinated biphenyl-impacted river sediments. *Environ.Toxicol.Chem.* 29(12):2851–2858.
- Bergen, B. J., W. G. Nelson, and R. J. Pruell. 1993. Bioaccumulation of PCB congeners by blue mussels (*Mytilus edulis*) deployed in New Bedford Harbor, Massachusetts. *Environ Toxicol Chem* 12(9): 1671–1681.
- Boehm, P. D., and J. G. Quinn. 1976. The effect of dissolved organic matter in sea water on the uptake of mixed individual hydrocarbons and Number 2 fuel oil by a marine filter-feeding bivalve (*Mercenaria mercenaria*). *Estuarine and Coastal Marine Science* 4(1): 93–105.
- Boese, B. L., H. Lee, D. T. Specht, R. C. Randall, and M. H. Winsor. 1990. Comparison of aqueous and solid-phase uptake for hexachloro-benzene in the tellinid clam *Macoma nasuta* (Conrad): a mass balance approach. *Environ Toxicol Chem* 9(2): 221–231.
- Boese, B. L., H. Lee, and S. Echols. 1997. Evaluation of a first-order model for the prediction of the bioaccumulation of PCBs and DDT from sediment into the marine deposit-feeding clam *Macoma nasuta*. *Environ Toxicol Chem* 16(7): 1545–1553.
- Booij, K., H. E. Hofmans, C. V. Fischer, and E. M. Weerlee. 2003. Temperature-dependant uptake rates of nonpolar organic compounds by semipermeable membrane devices and low-density polyethylene membranes. *Environ. Sci. Technol.* 37(2): 361–366.
- Boudreau, B. P. 1986. Mathematics of tracer mixing in sediments. II. Nonlocal mixing and biological conveyor belt phenomena. *Am. J. Sci.* 286: 199–238.
- Boyer, J. M., S. C. Chapra, C. E. Ruiz, and M.S. Dortch. 1994. *RECOVERY, a mathematical model to predict the temporal response of surface water to contaminated sediments*. TR W-94-4. Vicksburg, MS: U.S. Army Engineer Waterways Experiment Station.
- Bricelj, V. M. 1993. Aspects of the biology of the northern quahog *Mercenaria mercenaria*, with emphasis on growth and survival during early life history. In *Proceedings, of the 2nd Rhode Island shellfish industry Conference*, 4 August 1992, Narraganset, RI, ed. M. A. Rice and D. Grossman-Garber, 29–61. Rhode Island Sea Grant, Narraganset
- Bridges, T. S., J. D. Farrar, E. V. Gamble, and T. M. Dillon. 1996. Intraspecific density effects in *Nereis (Neanthes) arenaceodentata* Moore (Polychaeta: Nereidae). *Journal of Experimental Marine Biology and Ecology* 195(2):221–235.
- Buckman, A. H., C. S. Wong, E. A. Chow, S. B. Brown, K. R. Solomon, and A. T. Fisk. 2006. Biotransformation of polychlorinated biphenyls (PCBs) and bioformation of hydroxylated PCBs in fish. *Aquat Toxicol* 78(2): 176–185.

- Burgess, R. M., and R. A. McKinney. 1999. Environmental pollution: Importance of interstitial, overlying water and whole sediment exposures to bioaccumulation by marine bivalves. *Environ. Poll* 104(3): 373–382
- Carter, C. W., and P. M. Suffet. 1982. Binding of DDT to dissolved humic materials. *Environ. Sci. Technol.* 16(11): 735–740.
- Chapra, S. C. 1982. Long-term models of interaction between solids and contaminants in lakes. Ph.D. diss., University of Michigan, Ann Arbor, MI.
- Chapra, S. C. 1986. Toxic substance modeling. Intensive course notes: Mathematical modeling of lake and reservoir water quality. Duke University School of Forestry and Environmental Studies, Durham, NC.
- Chapra, S. C., and K. H. Reckhow. 1983. Engineering approaches for lake management, Vol. 2: Mechanistic modeling. Woburn, MA: Butterworth Publishers.
- Charrasse, B., C. Tixier, P. Hennebert, and P. Doumenq. 2014. Polyethylene passive samplers to determine sediment-pore water distribution coefficients of persistent organic pollutants in five heavily contaminated dredged sediments. *Science of the Total Environment* 472: 1172–1178.
- Cho, Y. M., D. W. Smithenry, U. Ghosh, A. J. Kennedy, R. N. Millward, T. S. Bridges, and R. G. Luthy. 2007. Field methods for amending marine sediment with activated carbon and assessing treatment effectiveness. *Mar Environ Res* 64(5):541–555.
- Cho, Y. M., U. Ghosh, A. J. Kennedy, E. Grossman, G. Ray, J. E. Tomaszewski, D. W. Smithenry, T. S. Bridges, and R. G. Luthy. 2009. Field application of activated carbon amendment for In-Situ stabilization of polychlorinated biphenyls in marine sediment. *Environmental Sci Technol* 43(10):3815–3823.
- Coleman, J. G., G. R. Lotufo, A. J. Kennedy, A. R. Poda, T. S. Rushing, C. E. Ruiz, and T. S. Bridges. 2014. Testing of various membranes to design a novel sediment porewater isolation chamber for infaunal invertebrate exposure to PCBs. In Submission, *Chemosphere*.
- Conder, J. M., T. W. La Point, G. R. Lotufo, and J. A. Steevens. 2003. Nondestructive, minimal-disturbance, direct-burial solid-phase microextraction fiber technique for measuring TNT in sediment. *Environ Sci Technol* 37(8): 1625–1632.
- Cornelissen, G., Ö. Gustafsson, T. D. Bucheli, M. T. O. Jonker, A. A. Koelmans, and P. C. M. Van Noort. 2005. Extensive sorption of organic compounds to black carbon, coal, and kerogen in sediments and soils: Mechanisms and consequences for distribution, bioaccumulation, and biodegradation. *Environ Sci Technol* 39(18):6881–6895.
- Cornelissen, G., A. Pettersen, D. Broman, P. Mayer, and G. Breedveld. 2008. Field testing of equilibrium passive samplers to determine freely dissolved native polycyclic aromatic hydrocarbon concentrations. *Environ. Toxicol. Chem.* 27(3): 499–508
- DeWitt, T. H., R. J. Ozretich, R. C. Swartz, J. O. Lamberson, D. W. Schults, G. R. Ditsworth, J. K. P. Jones, L. Hoselton, and L. M. Smith. 1992. The influence of organic matter quality on the toxicity and partitioning of sediment-associated fluoranthene. *Environ Toxicol Chem* 11(2):197–208.

- Ding, Y. P., P. F. Landrum, J. You, and M. J. Lydy. 2013. Assessing bioavailability and toxicity of permethrin and DDT in sediment using matrix solid phase microextraction. *Ecotoxicology* 22(1):109–117.
- DiToro, D. M., C. S. Zarba, D. J. Hansen, W. J. Berry, R. C. Swartz, C. E. Cowan, S. P. Pavlou, H. E. Allen, N. A. Thomas, and P. R. Paquin. 1991. Technical basis for establishing sediment quality criteria for nonionic organic chemicals using equilibrium partitioning. *Environ Toxicol Chem* 10(12):1541–1586.
- Driscoll, S. K., L. C. Schaffner, and R. M. Dickhut. 1998. Toxicokinetics of fluoranthene to the amphipod, *Leptocheirus plumulosus*, in water-only and sediment exposures. *Mar Environ Res* 45(3): 269–284.
- Emery, V. L., D. W. Moore, B. R. Gray, B. M. Duke, A. B. Gibson, R. B. Wright, and J. D. Farrar. 1997. Development of a chronic sublethal sediment bioassay using the estuarine amphipod *Leptocheirus plumulosus* (Shoemaker). *Environ Toxicol Chem* 16(9):1912–1920.
- Escher, B. I., and R. P. Schwarzenbach. 1996. Partitioning of substituted phenols in liposome-water, biomembrane-water, and octanol-water systems. *Environ. Sci. Technol.*, 30(1): 260–270.
- Fernandez, L. A., C. F. Harvey, and P. Gschwend. 2009. Using performance reference compounds in polyethylene passive samplers to deduce sediment porewater concentrations for numerous target chemicals. *Environ Sci Technol* 43(23): 8888–8894.
- Fernandez, L. A., J. K. MacFarlane, A. P. Tcaciuc, and P. M. Gschwend. 2009. Measurement of freely dissolved PAH concentrations in sediment beds using passive sampling with low-density polyethylene strips. *Environ Sci Technol.* 43(5): 1430–1436.
- Fernandez, L. A., W. J. Lao, K. A. Maruya, C. White, and R. M. Burgess. 2012. Passive sampling to measure baseline dissolved persistent organic pollutant concentrations in the water column of the Palos Verdes shelf superfund site. *Environ Sci Technol.* 46(21): 11937–11947.
- Fowler, S. W., G. C. Polikarpov, D. L. Elder, P. Parsi, and J. P. Villeneuve. 1978. Polychlorinated biphenyls: Accumulation from contaminated sediments and water by the polychaete *Nereis diversicolor*. *Mar Biol* 48(4):303–309.
- François, F., J. C. Poggiale, J. P. Durbec, and G. Stora. 1997. A new approach for the modeling of sediment reworking induced by a macrobenthic community. *Acta Biotheoretica* 45(3): 295–319.
- Fredette, T. J., and G. T. French. 2004. Understanding the physical and environmental consequences of dredged material disposal: history in New England and current perspectives. *Marine Pollution Bulletin* 49 (1-2):93–102
- Friedman, C. L., R. M. Burgess, M. M. Perron, M. G. Cantwell, K. T. Ho, and R. Lohmann. 2009. Comparing polychaete and polyethylene uptake to assess sediment resuspension effects on PCB bioavailability. *Environ Sci Technol* 43(8): 2865–2870.

- Gaston, G. R., C. F. Rakocinski, S. S. Brown, and C. M. Cleveland. 1998. Trophic function in estuaries: response of macrobenthos to natural and contaminant gradients. *Marine and Freshwater Research* 49(8), 833 – 846.
- Gerino, M. 1990. The effects of bioturbation on particle redistribution in Mediterranean coastal sediment. Preliminary results. *Hydrobiologia* 207(1): 251–258.
- Gerino, M., R. C. Aller, C. Lee, J. K. Cochran, J. Y. Aller, M. A. Green, and D. Hirschberg. 1998. Comparison of different tracers and methods used to quantify bioturbation during spring bloom: 234-thorium, luminophores and chlorophyll α . *Estuarine, Coastal and Shelf Science* 46(4): 531–547.
- Germano, J. D., D. C. Rhoads, and J. D. Lunz. 1994. An integrated, tiered approach to monitoring and management of dredged material sites in the New England region. DAMOS Contribution No. 87, Report No. SAIC-90/7575&234. Waltham, MA: U.S. Army Corps of Engineers.
- Goerke, H., and K. Weber. 2001. Species-specific elimination of polychlorinated biphenyls in estuarine animals and its impact on residue patterns. *Mar Environ Res* 51(2): 131–149.
- Gschwend, P. M., J. K. MacFarlane, D. D. Reible, X. Lu, S. B. Hawthorne, D. V. Nakles, and T. Thompson. 2011. Comparison of polymeric samplers for accurately assessing PCBs in porewaters. *Environ Toxicol Chem* 30(6): 1288–1296.
- Hale, S. E., J. E. Tomaszewski, R. G. Luthy, and D. Werner. 2009. Sorption of dichlorodiphenyltrichloroethane (DDT) and its metabolites by activated carbon in clean water and sediment slurries. *Water Res.* 43(17): 4336–4346.
- Harkey, G. A., P. F. Landrum, and S. J. Klaine. 1994. Comparison of whole-sediment, elutriate and pore-water exposures for use in assessing sediment-associated organic contaminants in bioassays. *Environ Toxicol Chem* 13(8): 1315–1329.
- Hawker, D. W., and D. W. Connell. 1988. Octanol-water partition coefficients of polychlorinated biphenyl congeners. *Environ. Sci. Technol.* 22(4): 382–387.
- Hawthorne, S. B., C. B. Grabanski, D. J. Miller, and J. P. Kreitinger. 2005. Solid-phase microextraction measurement of parent and alkyl polycyclic aromatic hydrocarbons in milliliter sediment porewater samples and determination of K_{DOC} values. *Environ Sci Technol.* 39(8):2795–2803.
- Hawthorne, S. B., C. B. Grabanski, and D. J. Miller. 2007. Measured partitioning coefficients for parent and alkyl polycyclic aromatic hydrocarbons in 114 historically contaminated sediments: part 2. Testing the K_{oc}K_{bc} two carbon-type model. *Environ Toxicol Chem.* 26(12): 2505–2516.
- Hickey, C. W., D. S. Roper, P. T. Holland, and T. M. Trower. 1995. Accumulation of organic contaminants in two sediment-dwelling shellfish with contrasting feeding modes: deposit- (*Macomona liliana*) and filter-feeding (*Austrovenus stutchburyi*). *Archives of Environmental Contamination and Toxicology* 29(2): 221–231.

- Hilal, S. H., S. W. Karickhoff, and L. A. Carreira. 2003. Verification and validation of the SPARC Model. EPA/600/R-03/033. Athens, GA: U.S. Environmental Protection Agency, Ecosystems Research Division.
- Hoke, R. A., G. T. Ankley, A. M. Cotter, T. Goldenstein, P. A. Kosian, G. L. Phipps, and F. M. VanderMeiden. 1994. Evaluation of equilibrium partitioning theory for predicting acute toxicity of field-collected sediments contaminated with DDT, DDE and DDD to the amphipod *Hyalella azteca*. *Environ Toxicol Chem.* 13(1):157–166.
- Inouye, L. S., and G. R. Lotufo. 2006. Comparison of macro-gravimetric and micro-colorimetric lipid determination methods. *Talanta* 70(3):584–587.
- Jones, R. P., R. N. Millward, R. A. Karn, and A. H. Harrison. 2006. Microscale Analytical Methods for the Quantitative Detection of PCBs and PAHs in Small Tissue Masses. *Chemosphere* 62(11): 1795–1805.
- Kaag, N. H., E. M. Foekema, M. C. T. Scholte, and N. M. van Straalen. 1997. Comparison of contaminant accumulation in three species of marine invertebrates with different feeding habits. *Environ. Toxicol. Chem.* 16(5): 837–842.
- Karickhoff, S. W., D. S. Brown, and T. A. Scott. 1979. Sorption of hydrophobic pollutants on natural sediments. *Water Research* 13(3): 241–248.
- Kennedy, A. J., J. A. Steevens, G. R. Lotufo, J. D. Farrar, M. R. Reiss, R. K. Kropp, J. Doi, and T. S. Bridges. 2009. A comparison of acute and chronic toxicity methods for marine sediments. *Mar Environ Res* 68:118–127.
- Kennedy, A. J., G. R. Lotufo, J. Steevens, and T. S. Bridges. 2010. *Determining steady-state tissue residues for invertebrates in contaminated sediment*. ERDC/EL TR-10-2. Vicksburg, MS: U.S. Army Engineer Research and Development Center, Dredging Operations and Environmental Research Program.
- Krantzberg, G. 1985. The influence of bioturbation on physical, chemical, and biological parameters in aquatic environments: a review. *Environmental Pollution (Series A)* 39(2): 99–122.
- Kravitz, M. J., J. O. Lamberson, S. P. Ferraro, R. C. Swartz, B. L. Boeses, and D. T. Specht. 1999. Avoidance response of the estuarine amphipod *Eohaustorius estuarius* to polycyclic aromatic hydrocarbons-contaminated, field collected sediments. *Environ Toxicol Chem* 18(6):1232–1235.
- Kreitinger, J. P., E. F. Neuhauser, F. G. Doherty, and S. B. Hawthorne. 2007. Greatly reduced bioavailability and toxicity of polycyclic aromatic hydrocarbons to *Hyalella azteca* in sediments from manufactured-gas plant sites. *Environ Toxicol and Chem*, 26 (6): 1146–1157.
- Kukkonen, J., and P. F. Landrum. 1994. Toxicokinetics and toxicity of sediment-associated pyrene to *Lumbriculus variegatus* (Oligochaeta). *Environ Toxicol Chem* 13(9): 1457–1468.
- Kukkonen, J. V. K., and P. F. Landrum. 1998. Effect of particle-xenobiotic contact time on bioavailability of sediment-associated benzo(a)pyrene to benthic amphipod, *Diporeia* spp. *Aquat Toxicol* 42(3):229–242.

- Lake, J. L., N. I. Rubinstein, H. Lee, C. A. Lake, J. Heltshe, and S. Pavignano. 1990. Equilibrium partitioning and bioaccumulation of sediment-associated contaminants by infaunal organisms. *Environ Toxicol Chem* 9(8):1095–1106.
- Landrum, P. F. 1989. Bioavailability and toxicokinetics of polycyclic aromatic hydrocarbons sorbed to sediments for the amphipod *Pontoporeia hoyi*. *Environ Sci and Technol* 23(5): 588–595
- Landrum, P. F., H. Lee, and M. J. Lydy. 1992. Toxicokinetics in aquatic systems: Model comparisons and use in hazard assessment. *Environ Toxicol Chem* 11(12): 1709–1725.
- Landrum, P. F., E. A. Tigue, S. K. Driscoll, D. C. Gossiaux, P. L. Van Hoof, M. L. Gedeon, and M. Adler. 2001. Bioaccumulation of PCB congeners by *Diporeia* spp.: Kinetics and factors affecting bioavailability. *J Great Lakes Res* 27(2): 117–133.
- Landrum, P. F., M. L. Gedeon, G. A. Burton, M. S. Greenberg, and C. D. Rowland. 2002. Biological responses of *Lumbriculus variegatus* exposed to fluoranthene-spiked sediment. *Archives of Environmental Contamination and Toxicology* 42(3): 292–302.
- Lee Li, H., B. L. Boese, R. C. Randall, and J. Pelletier. 1990. A method for determining gut uptake efficiencies of hydrophobic pollutants in a deposit-feeding clam. *Environ Toxicol Chem* 9(2): 215–219.
- Leppanen, M. T., and J. V. K. Kukkonen. 1998. Relative importance of ingested sediment and porewater as bioaccumulation routes for pyrene to oligochaete (*Lumbriculus variegatus*). *Environ Sci and Technol*. 32(10): 1503–1508.
- Lohmann, R., R. M. Burgess, M. G. Cantwell, S. A. Ryba, J. K. MacFarlane, and P. M. Gschwend. 2004. Dependency of polychlorinated biphenyl and polycyclic aromatic hydrocarbon bioaccumulation in *Mya arenaria* on both water column and sediment bed chemical activities. *Environ Toxicol Chem* 23(11):2551–2562.
- Lohmann, R., and D. Muir. 2010. Global Aquatic Passive Sampling (AQUA-GAPS): Using Passive Samplers to Monitor POPs in the Waters of the World. *Environ Sci Technol* 44(3): 860–864.
- Lohmann, R., K. Booij, F. Smedes, and B. Vrana. 2012. Use of passive sampling devices for monitoring and compliance checking of POP concentrations in water. *Environmental Science and Pollution Research* 19(6): 1885–1895.
- Lohmann, R., J. K. MacFarlane, and P. M. Gschwend. 2005. Importance of black carbon to sorption of native PAHs, PCBs, and PCDDs in Boston and New York, Harbor sediments. *Environ Sci Technol* 39(1):141–148.
- Lohrer, A. M., L. D. Chiaroni, J. E. Hewitt, and S. F. Thrush. 2008. Biogenic disturbance determines invasion success in a subtidal soft-sediment system. *Ecology* 89(5): 1299–1307.
- Lores, E. M., J. M. Patrick, and J. K. Summers. 1993. Humic acid effects on uptake of hexachlorobenzene and hexachlorobiphenyl by sheepshead minnows in static sediment/water systems. *Environ Toxicol and Chem* 12(3): 541–550.

- Lotufo, G. R., J. D. Farrar, and T. S. Bridges. 2000. Effects of exposure source, worm density, and sex on DDT bioaccumulation and toxicity in the marine polychaete *Neanthes arenaceodentata*. *Environ Toxicol Chem* 19(2): 472–484.
- Lotufo, G. R., P. F. Landrum, and M. L. Gedeon. 2001. Toxicity and bioaccumulation of DDT in freshwater amphipods in exposures to spiked sediments. *Environ Toxicol Chem* 20(4): 810–825.
- Lotufo, G. R., A. J. Kennedy, J. G. Coleman, L. A. Fernandez, R. M. Burgess, and T. S. Bridges. Comparative bioaccumulation kinetics of sediment-associated PCBs in four marine infaunal invertebrates belonging to different functional groups. *Environ Toxicol Chem*, in prep.
- Lu, X., A. Skwarski, B. Drake, and D. D. Reible. 2011. Predicting bioavailability of PAHs and PCBs with porewater concentrations measured by solid-phase microextraction fibers. *Environ Toxicol Chem* 30(5): 1109–1116.
- Mackay, D., and A. Fraser. 2000. Bioaccumulation of persistent organic chemicals: Mechanisms and models. *Environ Pollut* 110(3): 375–391.
- Magnusson, K., R. Ekelund, R. Grabic, and P. A. Bergqvist. 2006. Bioaccumulation of PCB congeners in marine benthic infauna. *Mar Environ Res* 61(4):379–395.
- Maire, O., P. Lecroart, F. Meysman, R. Rosenberg, J. C. Duchêne, and A. Grémare. 2008. Quantification of sediment reworking rates in bioturbation research: A review. *Aquatic Biology* 2: 219–238.
- Manyin, T., and C. Rowe. 2006. Chronic exposure of *Leptocheirus plumulosus* to Baltimore Harbor sediment: Bioenergetic and population-level effects. *Marine Environmental Research*. 62(2): 116–130.
- Matisoff, G., and X. Wang. 2000. Particle mixing by freshwater bioirrigators- midges (Chironomidae: Diptera) and mayflies (Ephemeroidea: Ephemeroptera). *Jour. Great Lakes Res.* 26(2): 174–182.
- Matisoff, G., and X. Wang. 1998. Solute transport in sediments by freshwater infaunal bioirrigators. *Limnol. Oceanogr.* 43(7): 1487–1499.
- Matisoff, G., X. Wang, and P. L. McCall. 1999. Biological redistribution of lake sediments by tubificid oligochaetes: *Branchiura sowerbyi* and *Limnodrilus hoffmeisteri*/Tubifex tubifex. *Jour. Great Lakes Res.* 25(1): 205–219.
- Matisoff, G., and X. Wang. 2000. Particle mixing by freshwater infaunal bioirrigators: midges (chironomidea: Diptera) and mayflies (ephemeridae: Ephemeroptera). *Journal of Great Lakes Research* 26(2) 174–182.
- Mayer, P., W. H. J. Vaes, F. Wijnker, K. C. H. M Legierse, R. H. Kraaij, J. Tolls, and J. L. M. Hermens. 2000. Sensing dissolved sediment porewater concentrations of persistent and bioaccumulative pollutants using disposable solid-phase microextraction fibers. *Environ Sci Technol* 34(24): 5177–5183.

- McCaffrey, R. J., A. C. Myers, E. Davey, G. Morrison, M. Bender, N. Luedtke, D. Cullen, P. Froelich, and G. Klinkhammer. 1980. The relation between porewater chemistry and benthic fluxes of nutrients and manganese in Narragansett Bay, Rhode Island. *Limnology and Oceanography* 25(1):31–44.
- McCall, P. 1977. Community patterns and adaptive strategies of infaunal benthos of central Long Island Sound. *J. of Mar. Res.* 35(2): 221–266
- McCall, P. L., and M. J. S. Tevesz. 1982. Animal-sediment relations. The biogenic alteration of sediments. New York, New York: Plenum Press.
- McCall, P., and F. M. Soster. 1990. Benthos response to disturbance in western Lake Erie: regional faunal surveys. *Can. J. Fish. Aquatic Sci.* 47: 1996–2009
- McCall, P. L., M. J. S. Tevesz, X. Wang, and J. R. Jackson. 1995. Particle mixing rates of freshwater bivalves: *Anodonta grandis* (Unionidae) and *Sphaerium striatinum* (Pisidiidae). *Journal of Great Lakes Research* 21(3): 333–339.
- McGee, B. L., and M. Spencer. 2001. A field-based population model for the sediment toxicity test organism *Leptocheirus plumulosus*: II. Model application. *Mar Environ Res* 51:347–363.
- McGroddy, S. E., and J. W. Farrington. 1995. Sediment porewater partitioning of polycyclic aromatic hydrocarbons in three cores from Boston Harbor, Massachusetts. *Environmental Science and Technology* 29(6): 1542–1550.
- McMurty, G. M., R. C. Schneider, P. L. Colin, R. W. Buddemeir, and T. M. Suchanek. 1986. Vertical distribution of fallout radionuclides in Enewetak lagoon sediments: effects of burial and bioturbation on the radionuclide inventory. *Bull. Marine Science* 38(1): 35–55.
- Meador, J. P., N. G. Adams, E. Casillas, and J. L. Bolton. 1997. Comparative bioaccumulation of chlorinated hydrocarbons from sediment by two infaunal invertebrates. *Archives of Environmental Contamination and Toxicology* 33(4): 388–400.
- Means, J. C., and A. E. McElroy. 1997. Bioaccumulation of tetrachlorobiphenyl and hexachlorobiphenyl congeners by *Yolida limatula* and *Nephtys incisa* from bedded sediments: Effects of Sediment- and animal- related parameters. *Environ Toxicol Chem* 16(6): 1277–1286.
- Meyer, P., W. J. Vaes, F. Wijnker, K. Legierse, R. Kraaij, J. Tolls, and J. M. Hermens. 2000. Sensing dissolved sediment porewater concentrations of persistent and bioaccumulative pollutants using disposable solid-phase microextraction fibers. *Environ Sci Technol* 34(24): 5177–5183.
- Millward, R. N., K. R. Carman, J. W. Fleeger, R. P. Gambrell, R. T. Powell, and M. A. Rouse. 2001. Linking ecological impact to metal concentrations and speciation: a microcosm experiment using a salt marsh meiofaunal community. *Environ Toxicol Chem.* 20(9): 2029–2037.
- Millward, R. N., T. S. Bridges, U. Ghosh, J. R. Zimmerman, and R. G. Luthy. 2005. Addition of activated carbon to sediments to reduce PCB bioaccumulation by a polychaete (*Neanthes arenaceodentata*) and an Amphipod (*Leptocheirus plumulosus*). *Environmental Science & Technology* 39(8): 2880–2887.

- Mitra, S., R. M. Dickhut, S. A. Kuehl, and K. L. Kimbrough. 1999. Polycyclic aromatic hydrocarbon (PAH) source, sediment deposition patterns, and particle geochemistry as factors influencing PAH distribution coefficients in sediments of the Elizabeth River, VA, USA. *Marine Chemistry* 66(1-2): 113–127.
- Mobile, M. A. 2008. RECOVERY-RD: The development of a biotransformation model for sediment systems contaminated with PCBs. MS Thesis, Virginia Polytechnic Institute and State University, Blacksburg, Virginia.
- Morrison, H. A., F. A. P. C. Gobas, R. Lazar, and G. D. Haffner. 1996. Development and verification of a bioaccumulation model for organic contaminants in benthic invertebrates. *Environ. Sci. Technol.* 30(11): 3377–3384.
- Mount, D. R., T. D. Dawson, and L. P. Burkhard. 1999. Implications of gut purging for tissue residues determined in bioaccumulation testing of sediment with *Lumbriculus variegatus*. *Environ Toxicol Chem* 18(6): 1244–1249.
- Murdoch, A., and S. D. MacKnight. 1991. Handbook of techniques for aquatic sediments sampling. Boca Raton, FL: CRC Press, Inc.
- Muslow, S., P. F. Landrum, and J. A. Robbins. 2002. Biological mixing responses to sublethal concentrations of DDT in sediments by *Heteromastus filiformis* using a ¹³⁷Cs marker layer technique. *Marine Ecology Progress Series* 239: 181–191.
- Nakaoka, M. 2010. Spatial and seasonal variation in growth rate and secondary production of *Yoldia notabilis* in Otsuchi Bay, Japan, with reference to the influence of food supply from the water column. *Marine Ecology-Progress Series* 88: 215–223.
- National Research Council (NRC). 2003. Bioavailability of contaminants in soils and sediments. Washington, DC: The National Academies Press.
- Nichols, F. 1979. Natural and Anthropogenic Influences on Benthic Community Structure in San Francisco Bay. In *San Francisco Bay, The Urbanized Estuary: Investigations into the Natural History of San Francisco Bay and Delta With Reference to the Influence of Man*. California Academy of Sciences, ed. T. J. Conomos, 409–426.
- Norkko, A., R. Rosenberg, S. F. Thrush, and R. B. Whitlatch. 2006. Scale- and intensity-dependent disturbance determines the magnitude of opportunistic response. *Journal of Experimental Marine Biology and Ecology* 330(1):195–207.
- Oen, A. M. P., E. M. L. Janssen, G. Cornelissen, G. D. Breedveld, E. Eek, and R. G. Luthy. 2011. In Situ measurement of PCB pore water concentration profiles in activated carbon-amended sediment using passive samplers. *Environ Sci Technol* 45(9): 4053–4059.
- Ozretich, R. J., S. P. Ferraro, J. O. Lamberson, and F. A. Cole. 2000. Test of Σ polycyclic aromatic hydrocarbon model at a creosote-contaminated site, Elliott Bay, Washington, USA. *Environ Toxicol Chem* 19(9): 2378–2389.
- Pablo, F. and R. V. Hyne. 2009. Endosulfan application to a stream mesocosm: Studies on fate, uptake into passive samplers and caged toxicity test with the fish *M.ambigua*. *Arch Environ Contam Toxicol* 56(3): 525–535.

- Pearson, T. H. 2001. Functional group ecology in soft-sediment marine benthos: the role of bioturbation. *Oceanogr. Mar. Biol. Ann. Rev.* 39: 233–267
- Pearson, T. H., and R. Rosenberg. 1978. Macrobenthic succession in relation to organic enrichment and pollution of the marine environment. *Oceanogr. Mar. Biol. Ann. Rev.* 16: 229–311.
- Persson, N. J., O. Gustafsson, T. D. Bucheli, R. Ishaq, K. Næs, and D. Broman. 2002. Soot-carbon influenced distribution of PCDD/F in the marine environment of The Grenlandsfjords. *Norway. Environ. Sci. Technol.* 36(23): 4968–4974.
- Postma, J. F., S. de Valk, M. Dubbeldam, J. L. Maas, M. Tonkes, C. A. Schipper, and B. J. Kater. 2002. Confounding factors in bioassays with freshwater and marine organisms. *Ecotoxicology and Environmental Safety* 53(2): 226–237.
- Pruell, R. J., J. L. Lake, W. R. Davis, and J. G. Quinn. 1986. Uptake and depuration of organic contaminants by blue mussels (*Mytilus edulis*) exposed to environmentally contaminated sediment. *Marine Biology* 91(4): 497–507.
- Pruell, R. J., C. B. Norwood, R. D. Bowen, W. S. Boothman, P. F. Rogerson, M. Hackett, and B. C. Butterworth. 1990. Geochemical study of sediment contamination in New Bedford Harbor, Massachusetts. *Marine Environmental Research* 29(2): 77–101
- Qin, X., H. Sun, C. Wang, Y. Yu, and T. Sun. 2010. Impacts of crab bioturbation on the fate of polycyclic aromatic hydrocarbons in sediment from the Beitang estuary of Tianjin, China. *Environ Toxicol and Chem* 29(6): 1248–1255.
- Quintana, C. O., M. Tang, and E. Kristensen. 2007. Simultaneous study of particle reworking, irrigation transport and reaction rates in sediment bioturbated by the polychaetes *Heteromastus* and *Marenzelleria*. *Journal of Experimental Marine Biology and Ecology* 352(2): 392–406.
- Rhoads, D. C., P. L. McCall, and J. Y. Yingst. 1978. Disturbance and production on the estuarine seafloor. *American Scientist*. 66(5): 577–586.
- Rhoads, D. C., and J. D. Germano. 1986. Interpreting long-term changes in benthic community structure: a new protocol. *Hydrobiologia* 142(1): 291–308
- Risk, M. J., and J. S. Moffat. 1977. Sedimentological significance of fecal pellets of *Macoma balthica* in the Minas basin Bay of Fundy. *Journal of Sedimentary Petrology* 47(4): 1425–1436.
- Ruiz, C. E., N.M. Aziz, and P.R. Schroeder. 2001. RECOVERY: A contaminated sediment-water interaction model. *Environmental Modeling & Assessment* 6(3): 151–158.
- Ruiz, C. E., and T. K. Gerald. 2001. *RECOVERY Version 2.0: A mathematical model to predict the temporal response of surface water to contaminated sediments*. ERDC/EL TR 01-3. Vicksburg, MS: U.S. Army Engineer Research and Development Center.

- Ruiz, C. E., P. R. Schroeder, M. S. Dortch, and T. K. Gerald. 2007. RECOVERY: A Contaminated Sediment-Water Interaction Model. In *Proceedings, Battelle 4th International Conference on Remediation of Contaminated Sediments, 22–25 January, Savannah, GA*.
- Rust, A. J., R. M. Burgess, B. J. Brownawell, and A. E. McElroy. 2004. Relationship between metabolism and bioaccumulation of benzo[a]pyrene in benthic invertebrates. *Environ Toxicol Chem* 23(11): 2587–2593.
- Rust, A. J., R. M. Burgess, A. E. McElroy, M. G. Cantwell, and B. J. Brownawell. 2004. Influence of soot carbon on the bioaccumulation of sediment-bound polycyclic aromatic hydrocarbons by marine invertebrates: An interspecies comparison. *Environ Toxicol Chem* 23(11):2594–2603.
- Santschi, P. H., U. P. Nyffeler, P. Ohara, M. Bucholtz, and W. S. Broecker. 1984. Radiotracer uptake on the sea floor: results from the MANOP chamber deployments in the eastern Pacific. *Deep Sea Res.* 31(5): 451–468.
- Scott, K. 1989. Effects of contaminated sediments on marine benthic biota and communities. In *Committee on Contaminated Marine Sediments, National Research Council, Contaminated Marine Sediments: Assessment and Remediation 508*, 132–154. Washington, DC: National Academy Press.
- SERDP. 2008. Bioavailability of contaminants in soils and sediments. In *Proceedings, SERDP and ESTCP Expert Panel Workshop on Research & Development Needs for Understanding and Assessing the Bioavailability of Contaminants in Soils and Sediments, 20–21 August, Annapolis, MD*. Accessed at: <http://docs.serdp-estcp.org/index.cfm>
- Smedes, F., R. W. Geertsma, T. Van der Zande, and K. Booij. 2009. Polymer-water partition coefficients of hydrophobic compounds for passive sampling: Application of cosolvent models for validation. *Environ. Sci. Technol.* 43(18): 7047–7054.
- Smith, K. E. C., N. Dom, R. Blust, and P. Mayer. 2010. Controlling and maintaining exposure of hydrophobic organic compounds in aquatic toxicity tests by passive dosing. *Aquatic Toxicology* 98(1): 15–24.
- Solan, M., B. D. Wigham, I. R. Hudson, R. Kennedy, C. H. Coulon, K. Norling, H. C. Nilsson, and R. Rosenberg. 2004. In situ quantification of bioturbation using time-lapse fluorescent sediment profile imaging (f-SPI), luminophore tracers and model simulation. *Marine Ecology Progress Series* 271: 1–12.
- Sormunen, A. J., M. T. Leppanen, and J. V. Kukkonen. 2008. Influence of sediment ingestion and exposure concentration on the bioavailable fraction of sediment-associated tetrachlorobiphenyl in oligochaetes. *Environ Toxicol Chem* 27(4): 854–863.
- Soster, F., G. Matisoff, P. L. McCall, and J. A. Robbins. 2001. In situ effects of organisms on porewater geochemistry in Great Lakes sediments. In *Organism sediment interactions*, 279–295. Columbia, SC: University of South Carolina Press.

- Sun, X., D. Werner, and U. Ghosh. 2009. Modeling PCB mass transfer and bioaccumulation in a freshwater Oligochaete before and after amendment of sediment with activated carbon. *Environ Sci Technol* 43(4): 1115–1121.
- Swartz, R. C., D. W. Schults, R. J. Ozretich, J. O. Lamberson, F. A. Cole, S. P. Ferraro, T. H. Dewitt, and M. S. Redmond. 1995. ΣPAH: A model to predict the toxicity of polynuclear aromatic hydrocarbon mixtures in field-collected sediments. *Environ Toxicol Chem* 14(11):1977–1987.
- Swartz, R. C., D. W. Schults, T. H. DeWitt, G. R. Ditsworth, and J. O. Lamberson. 1990. Toxicity of fluoranthene in sediment to marine amphipods: A test of the equilibrium partitioning approach to sediment quality criteria. *Environ Toxicol Chem* 9(8):1071–1080.
- Thorsson, M. H., J. E. Hedman, C. Bradshaw, J. S. Gunnarsson, and M. Gilek. 2008. Effects of settling organic matter on the bioaccumulation of cadmium and BDE-99 by Baltic Sea benthic invertebrates. *Mar Environ Res* 65(3): 264–281.
- U.S. Environmental Protection Agency (U.S. EPA). 1994. *Methods for assessing the toxicity of sediment-associated contaminants with estuarine and marine amphipods*. EPA/600/R-94/025. Washington, D.C.: U.S. Environmental Protection Agency.
- U.S. Environmental Protection Agency. 2000. Bioaccumulation testing and interpretation for the purpose of sediment quality assessment: Status and needs. EPA-823-R-00-001. Washington, D.C.: Office of Water.
- U.S. Environmental Protection Agency. 2001. *Method for assessing the chronic toxicity of marine and estuarine sediment-associated contaminants with the amphipod *Leptocheirus plumulosus**. First edition. EPA 600/R-01/020. Washington, DC: U.S. Environmental Protection Agency, Office of Research and Development.
- U.S. Environmental Protection Agency (EPA). 2007. *Sediment toxicity identification evaluation: Phases I, II, and III guidance document*. EPA/600/R-07/080. Washington, D.C.: U.S. Environmental Protection Agency, Office of Research and Development.
- U.S. Environmental Protection Agency (U.S. EPA)/U.S. Army Corps of Engineers (USACE). 1998. *Evaluation of material proposed for discharge to waters of the US – Testing manual (Inland Testing Manual)*. EPA/823/B-98/004. Washington, D.C.: U.S. Environmental Protection Agency.
- Van Handel, E. 1985. Rapid determination of total lipids in mosquitoes. *Journal of the American Mosquito Control Association* 1(3): 302–304.
- Vinturella, A. E., R. M. Burgess, B. A. Coull, K. M. Thompson, and J. P. Shine. 2004. Use of passive samplers to mimic uptake of polycyclic aromatic hydrocarbons by benthic polychaetes. *Environ Sci Technol* 38(4): 1154–1160.
- Wang, X., and G. Mafisoff. 1997. Solute transport in sediments by a large freshwater Oligochaete, *Branchiura sowerbyi*. *Environ Sci Technol* 31(7): 1926–1933.

- Wheatcroft, R. A., P. A. Jumars, C. R. Smith, and R. M. Nowell. 1990. A mechanistic view of the particulate biodiffusion coefficient: Step lengths, rest periods and transport directions. *Journal of Marine Research* 48(1): 177–207.
- Widdowson, M. A. 2002. SEAM3D – *A numerical model for three-dimensional solute transport coupled to sequential electron acceptor-based biological reactions in groundwater*. Blacksburg, VA: The VA Department of Civil and Environmental Engineering, Virginia Polytechnic Institute and State University.
- Witt, G., G. A. Liehr, D. Borck, and P. Mayer. 2009. Matrix solid-phase microextraction for measuring freely dissolved concentrations and chemical activities of PAHs in sediment cores from the western Baltic Sea. *Chemosphere* 74(4): 522–529.
- Yang, Z. Y., E. Y. Zeng, H. Xia, J. Z. Wang, B. X. Mai, and K. A. Maruya. 2006. Application of a static solid-phase microextraction procedure combined with liquid-liquid extraction to determine poly(dimethyl)siloxane-water partition coefficients for selected polychlorinated biphenyls. *Journal of Chromatography A* 1116(1-2): 240–247.
- You, J., P. F. Landrum, T. A. Trimble, and M. J. Lydy. 2007. Availability of polychlorinated biphenyls in field-contaminated sediment. *Environ Toxicol Chem* 26(9): 1940–1948.
- You, J., P. F. Landrum, and M. J. Lydy. 2006. Comparison of chemical approaches for assessing bioavailability of sediment-associated contaminants. *Environ Sci Technol* 40(20): 6348–6353.

Appendix A: Supporting Data

Table S1. Summary of analytical methods used.

Analysis	Matrix	Analytical method	Reporting limits
PCB congeners	Sediment	EPA Method 3545 Accelerated Solvent Extraction	0.2 µg/kg
PCB congeners	Water	EPA Method 3510 Separatory Funnel Extraction	0.002 µg/kg
PCB congeners	Tissue	EPA Method 3550 Ultrasonic Extraction modified	1 µg/kg
PCB congeners	Extract cleanup	EPA Method 3630 Silica Gel or 3665 Sulfuric Acid modified	1 ng
		Method 8082 – GC w/ECD using dual column detection	
PCB congeners	Polyethylene devices	extracted by soaking in solvent then analyzed by 8082	Not applicable
TOC	Sediment	EPA Method 9060 or Lloyd Kahn	1300 mg/kg
Grain size	Sediment	ASTM Method D422	Not applicable

A.1 Supporting information for Section 11. Partition coefficients for octanol-water (K_{OW}), polyethylene-water (K_{PEW}) and polydimethylsiloxane (K_f)

Log K_{PEW} were calculated from log K_{OW} , using a regression described in Fernandez et al (2012) referencing data from the following studies: Adams et al (2007), Booij et al (2003), Cornelissen et al (2008), Fernandez et al (2009), Hale et al (2009), and Smedes et al (2009). K_f for the polydimethylsiloxane used in the SPME came from Yang et al (2006). Log K_{OW} were taken from the SPARC model (Hilal et al 2003) or Hawker and Connell (1989).

PCB Congener	Log K _{ow}	Log K _{PEW} (L/Kg)	Log K _f (L/L)
PCB6	5.06	4.60	4.75
PCB8	5.07	4.90	4.76
PCB12/13	5.00	4.90	4.70
PCB15	5.10	5.09	4.78
PCB17	5.20	5.00	4.86
PCB18	5.32	5.03	4.96
PCB22	5.33	5.30	4.97
PCB25	5.30	5.30	4.94
PCB26	5.26	5.30	4.91
PCB27	5.36	5.30	4.99
PCB28/31	5.30	5.45	4.94
PCB32	5.36	5.50	4.99
PCB33	5.30	5.50	4.94
PCB34	5.30	5.50	4.94
PCB35	5.30	5.60	4.94
PCB40/71	5.82	5.50	5.37
PCB42	5.79	5.50	5.34
PCB44	5.75	5.50	5.31
PCB45	5.83	5.50	5.38
PCB46	5.84	5.50	5.39
PCB47	5.77	5.60	5.33
PCB48	5.70	5.56	5.27
PCB49	5.73	5.63	5.30
PCB51	5.81	5.50	5.36
PCB52	5.68	5.62	5.25
PCB53	5.70	5.60	5.27
PCB56	5.76	5.90	5.32
PCB60	5.81	5.90	5.36
PCB63	5.78	5.90	5.34
PCB66	5.71	6.00	5.28
PCB70	5.67	6.00	5.25
PCB74	5.75	6.00	5.31
PCB77	5.69	6.10	5.26
PCB82	6.31	6.10	5.77
PCB83	6.26	6.10	5.73
PCB84	6.20	6.10	5.68

PCB Congener	Log K _{OW}	Log K _{PEW} (L/Kg)	Log K _f (L/L)
PCB85	6.28	6.10	5.75
PCB87	6.22	6.10	5.70
PCB90/101	6.17	6.10	5.66
PCB91	6.25	6.30	5.72
PCB92	6.20	6.40	5.68
PCB95	6.20	6.30	5.68
PCB97	6.25	6.30	5.72
PCB99	6.23	6.40	5.70
PCB100	6.29	6.40	5.75
PCB103	6.23	6.10	5.70
PCB107	6.20	6.40	5.68
PCB117	6.20	6.40	5.68
PCB118	6.17	6.50	5.66
PCB119	6.25	6.30	5.72
PCB122	6.20	6.50	5.68
PCB123/131	6.20	6.50	5.68
PCB124	6.20	6.50	5.68
PCB128	6.78	6.50	6.15
PCB130	6.70	6.50	6.09
PCB131	6.70	6.50	6.09
PCB132	6.74	6.50	6.12
PCB134	6.77	6.50	6.15
PCB135	6.72	6.50	6.10
PCB136	6.72	6.50	6.10
PCB137	6.79	6.60	6.16
PCB138/163	6.73	6.60	6.11
PCB141	6.74	6.60	6.12
PCB144	6.80	6.30	6.17
PCB146	6.68	6.30	6.07
PCB147	6.70	6.30	6.09
PCB149	6.70	6.40	6.09
PCB151	6.69	6.40	6.08
PCB153	6.68	6.70	6.07
PCB154	6.74	6.40	6.12
PCB156	6.74	6.90	6.12
PCB157	6.71	6.90	6.10

PCB Congener	Log K _{ow}	Log K _{PEW} (L/Kg)	Log K _f (L/L)
PCB158	6.76	6.80	6.14
PCB164	6.67	6.80	6.06
PCB167	6.66	7.00	6.06
PCB170	7.30	7.00	6.58
PCB171	7.31	7.00	6.59
PCB174	7.27	7.00	6.55
PCB178	7.21	7.00	6.51
PCB179	7.20	6.90	6.50
PCB180	7.25	7.10	6.54
PCB183	7.25	6.90	6.54
PCB190	7.30	7.30	6.58

A.2 Supporting Tables for Section 8

Table S2. Summary of initial laboratory observational experiments in control sediment.

Organism	Survival	Burrow Depth (cm)	Whole tissue mass (g)	Wet individual tissue mass (mg)	Minimum # for analytical (50 mg wet)	Shell height (mm, if applicable)	Lipid content (% mass)	Comments / behavior
<i>Eohaustorius estuarius</i>	53 ± 6 ⁴	0.8 – 1.5	NA	4.4	11-20	NA	2.8	No organisms observed above sediment until day 5 (10 – 30% of organism observed above sediment under light conditions)
<i>Yoldia limatula</i>	100 ± 0	3 - 11	1020 ± 408	416 ± 148	1	11 ± 0.6	1.3 ± 0.2	Overlying water extremely turbid. No organisms observed above sediment; siphons occasionally observed ejected sediment flumes during dark conditions
<i>Ampelisca abdita</i>	88 ± 13	1 – 3.5	NA	1.2 ± 0.3	42-83	NA	2.0 ± 0.3	No organisms observed on sediment surface in light or dark
<i>Mercenaria mercenaria</i>	100 ± 0	0 – 3.0	3274 ± 896	396 ± 173	1	19 ± 1	Pending	No organisms observed on sediment surface in light or dark; siphons observed
<i>Neanthes arenaceodentata</i>	87 ± 12	0.5 – 11.5 ⁵	NA	2·10 ⁶	5-10	NA	2.6 ± 0.3 ⁷	Organisms observed above sediment under dark conditions but below sediment surface under dark conditions. Burrow depth exceeded 3 cm.

⁴ May have been a temperature and salinity (10 ppt) acclimation issue⁵ Burrows superficially observed to bottom of chamber (12.5 cm)⁶ Kennedy et al (2009)⁷ Kennedy et al (unpublished, ESTCP)

Organism	Survival	Burrow Depth (cm)	Whole tissue mass (g)	Wet individual tissue mass (mg)	Minimum # for analytical (50 mg wet)	Shell height (mm, if applicable)	Lipid content (% mass)	Comments / behavior
<i>Streblospio</i>	87 ± 6	0 - 0.5	NA	0.355 (0.225 dry)	141	NA	NA	Tube observed at substrate surface (ant farm sediment and sand control); 0 - 0.25 cm: black layer; 0.25 - 0.5 cm: disturbance. Despite good overall survival, very difficult to locate in sediment (more so in sand). Breakdown over 2 days, 1-1.5. man hours per beaker.
<i>Leptocheirus plumulosus</i>	75% (1 ant farm)	0 - 2	NA	2.0	25	NA	NA	Organisms observed often on top of sediment.

NA = not applicable.

Table S3. Organism field and extrapolated maximum loading densities for exposure chambers.

Organism	Test initiation	Test termination	Duration (days)	Suppl. food?	Survival	Burrow Depth (cm)	Initial Condition	28d in sand	Comments / behavior
<i>Yoldia limatula</i>	31 March 2010	28 April 2010	28	No	93 ± 12	4 (bottom)	Tissue: 41.4 ± 4.1% Lipid: 1.3 ± 0.2%	Tissue: 30.9 ± 5.9% Lipid: 0.7 ± 0.1 ⁸	Burrowed and came to surface throughout exposure. Siphons observed periodically
<i>Mercenaria mercenaria</i>	31 March 2010	28 April 2010	28	No	100 ± 0	4 (bottom)	Tissue: 11.8 ± 2.0% Lipid: 1.1 ± 0.3%	Tissue: 10.4 ± 1.4% Lipid: 0.6 ± 0.1% ⁸	Burrowed throughout exposure. Siphons initially observed but not seen after 5–6 days.
<i>Streblospio benedicti</i>	2 April 2010	22 April 2010	20	½ 28-d Leptocheirus ration (MWF)	85 ± 7	0	NA ⁹	NA ⁹	Shallow if any burrowing. Tubes observed on sand surface.
<i>Neanthes arenaceodentata</i>	6 April 2010	4 May 2010	28	½ 28-d Leptocheirus ration (MWF)	87 ± 12	0.25 – 1.0	2.6		Burrows clearly observed from 0.5 to 1 cm.
<i>Leptocheirus plumulosus</i>	8 April 2010	6 May 2010	28	½ 28-d Leptocheirus ration (MWF)	72 ± 3	Unk	1.2 - 1.5		Several amphipods typically observed on surface (but most were burrowed) at any given time.

⁸ Organisms not fed⁹ Insufficient tissue

Organism	Test initiation	Test termination	Duration (days)	Suppl. food?	Survival	Burrow Depth (cm)	Initial Condition	28d in sand	Comments / behavior
<i>Eohaustorius estuarius</i>	16 April 2010	14 May 2010	28	½ 28-d Leptocheirus ration (MWF)		Unk	2.8		No organisms observed at surface. Burrowed very rapidly upon loading.
<i>Ampelisca abdita</i>	16 April 2010	14 May 2010	28	½ 28-d Leptocheirus ration (MWF)		Unk	2.0 ± 0.3		Tubes observed. Anoxic (black) regions also present, especially in Rep A.

Table S4. Organism field and extrapolated maximum loading densities for exposure chambers.

Organism	Field Density (m ²)	Reference	75% Maximum density (m ²)	1 L Beaker (d = 0.1 m ²) (0.0079 m ²)	Subchamber (0.04 x 0.10 cm) (0.004 m ²)	Number required for analytical
<i>Leptocheirus</i>	190 – 29,217	McGee et al (2001) Mar Environ Res 51: 347-63	21,912	173 (1 – 173)	87 (1 – 87)	25
<i>Ampelisca</i>	10,000 – 100,000	Dr. Peter McCall, Case Western University personal communication	75,000	592 (79 – 790)	300 (40 – 400)	42-83
<i>Macoma balthica</i>	143 – 2,142 1000 ¹⁰	Risk and Moffat (1977) J Sed Petr 47: 1425-36	1,607	12 (1 – 16)	6 (0.6 – 8)	1
<i>Yoldia limatula</i>	1.141 – 216 2.50 – 100	1. Nakaoka (1992) Mar Ecol Prog Ser 88: 215-23 ¹¹ 2. McCaffrey et al (1980) 25: 31-44	162	1.3 (1.1 – 1.7)	0.6 (0.6 – 0.9)	1
<i>Streblosbio</i>	5,000 – 400,000	Dr. Peter McCall, personal communication	300,000	592 (79 – 790)	300 (40 – 400)	141
<i>Mercenaria</i>	100–1,200 ¹²	Bricelj (1993)	900	7 (1 – 9)	3 (0 – 5)	1
<i>Eohaustorius</i>	3,500	Kravitz et al (1999) ETC 18: 1232-5	2,625	20 (27)	10 (14)	20
<i>Neanthes</i>	350 (84 – 1,059)	Bridges et al (1996) J Exp Mar Biol Ecol 195: 221-35	794	6 (1 – 8)	3 (0 – 4)	5-10

¹⁰ Density effect reported by Olafsson (1989) Mar Ecol Prog Series. 55 171-179.¹¹ For *Yoldia notabilis*¹² Juveniles

A.3 Supporting information for Section 13

Three stainless steel mesh envelopes containing four SPME fibers each were added to the three replicated in-place pore water PICs in the *Mercenaria mercenaria* tank and sampled weekly following initial sediment addition to the system. Data indicate a time dependent increase in select congener concentrations indicating PCBs were moving into the chambers.

Figure S1. Pre-exposure confirmation of PCB diffusion into the pore water PICs using SPME fibers in the NBH experiment.

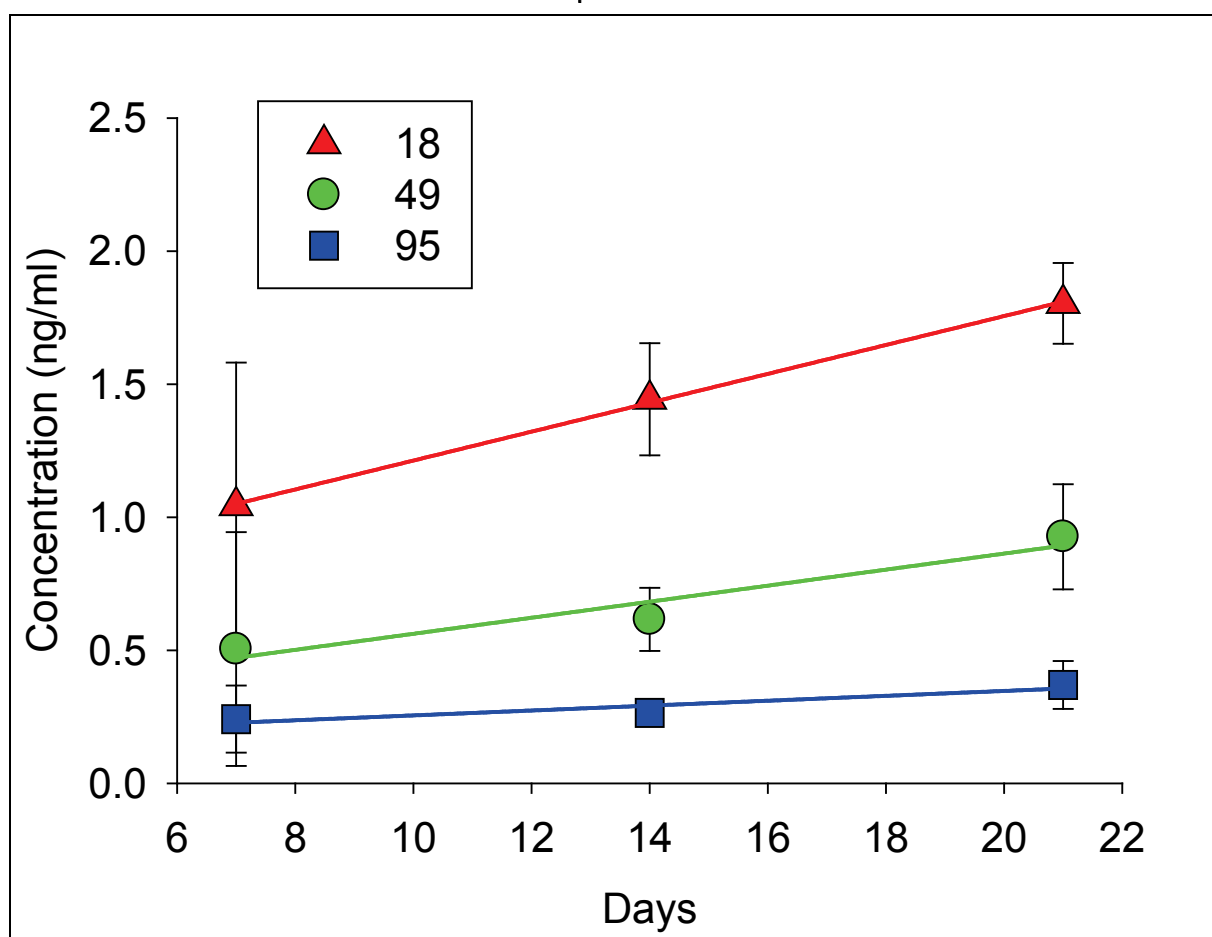


Figure S2. Photograph of in-use exposure system. Panel (a) exposure system. The reactor, which contains the solid phase membrane device (SPMD), is the silver box shown in the lower right-hand image. Panel (b) PICs.

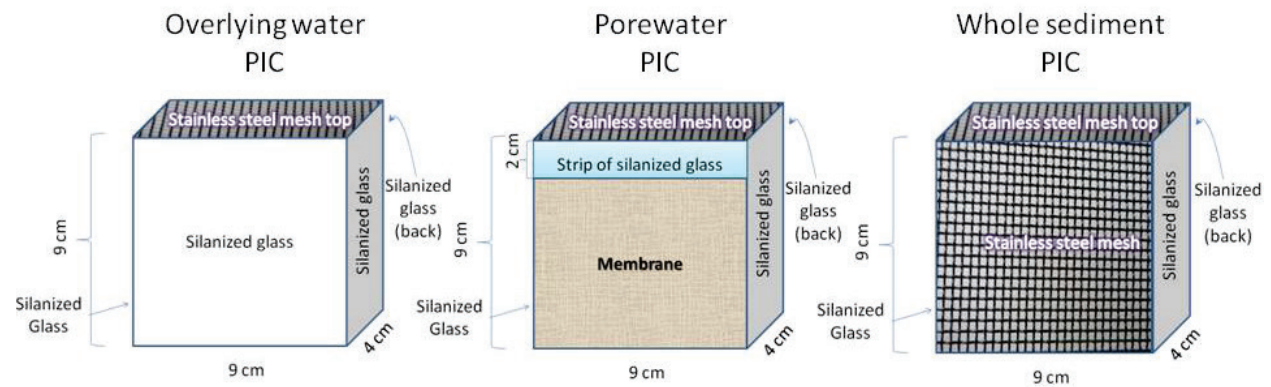
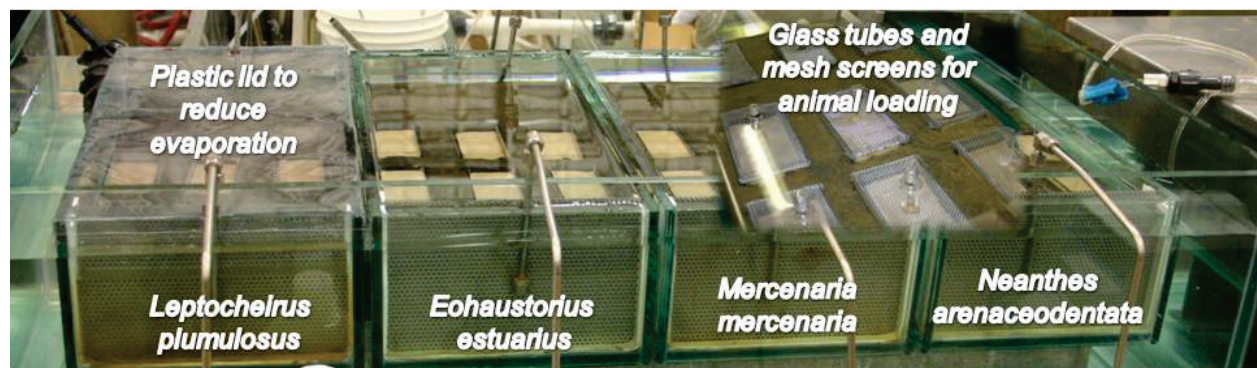


Figure S3. Summary of PCB congener distribution for the two test sediments. Congeners not shown were below analytical reporting limits ($< 2 \mu\text{g/kg}$).

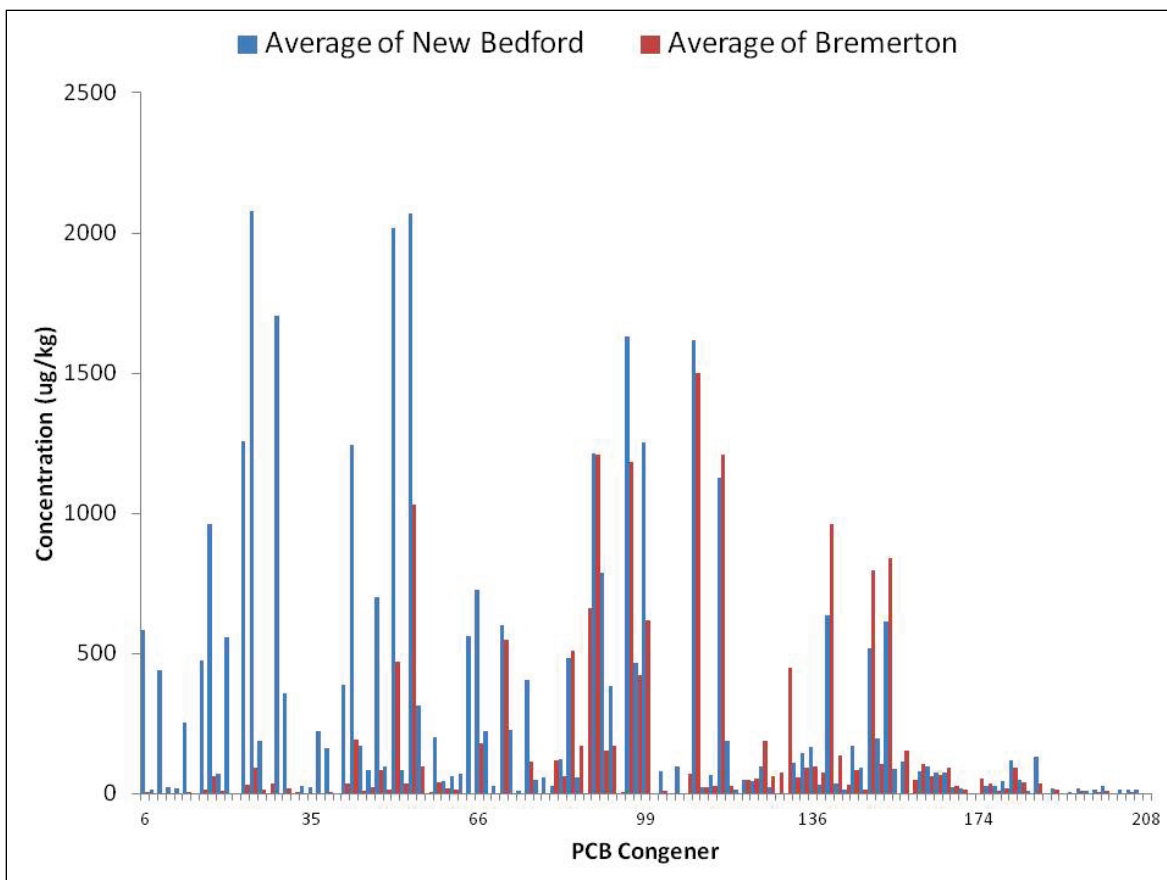


Table S5. List of PCB congeners and concentrations ($\mu\text{g/kg}$) in the project sediments.

Congener	Sum of New Bedford	Sum of Bremerton
6	585.6	6.0
7	13.6	0.0
8	439.9	2.1
9	24.3	0.0
10	18.1	0.0
12	254.6	6.1
15	0.0	3.1
17	477.1	17.2
18	961.3	64.2
19	71.9	13.3
22	558.2	0.0
24	0.0	0.0

Congener	Sum of New Bedford	Sum of Bremerton
25	1258.0	34.6
26	2078.1	92.0
27	188.3	16.1
28	0.0	36.8
31	1703.4	
32	357.8	19.0
33	0.0	8.3
34	26.8	0.0
35	26.3	0.0
37	225.4	
40	162.8	8.9
41	0.0	0.7
42	391.2	35.7
44	1243.1	193.6
45	170.7	11.2
46	86.7	25.5
47	703.7	83.6
48	97.0	15.0
49	2019.6	471.0
51	84.1	37.5
52	2068.7	1030.0
53	317.1	97.3
54	0.0	4.9
56	201.7	41.5
59	47.6	18.2
60	64.3	14.5
63	70.1	0.0
64	562.7	
66	727.8	180.2
67	226.0	
69	29.3	0.0
70	603.2	550.0
71	228.1	
73	12.9	0.0

Congener	Sum of New Bedford	Sum of Bremerton
74	406.5	114.6
75	50.0	
77	60.7	3.3
82	28.0	121.5
83	125.5	61.8
84	482.8	511.0
85	57.9	172.5
87	0.0	662.0
90	1212.8	1210.0
91	788.9	154.9
92	382.6	172.3
93	0.0	7.3
95	1632.3	1184.0
97	467.5	424.0
99	1254.7	618.0
100	0.0	4.0
103	81.6	9.6
104	0.0	0.0
105	96.7	
107	0.0	73.2
110	1617.3	1499.0
114	22.4	25.5
117	69.4	29.6
118	1126.4	1210.0
119	188.9	27.5
122	13.6	0.0
123	52.4	48.8
124	44.9	54.2
128	96.6	191.3
129	22.5	64.5
130	0.0	74.6
132	0.0	451.0
134	109.6	59.2
135	145.3	92.9

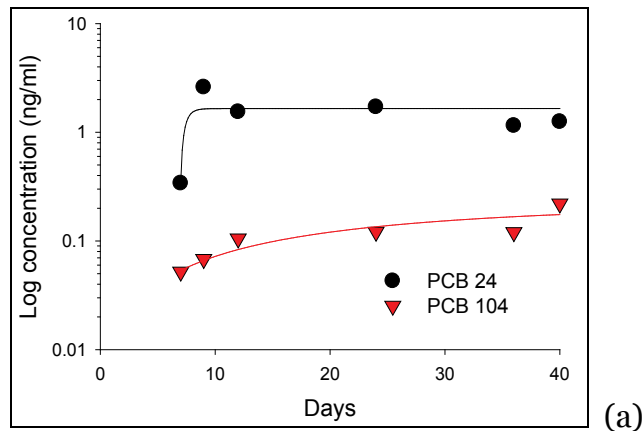
Congener	Sum of New Bedford	Sum of Bremerton
136	167.9	99.2
137	32.2	77.0
138	634.8	964.0
141	38.9	135.5
144	15.2	35.1
146	173.2	83.9
147	92.6	17.6
149	517.9	796.0
151	198.5	107.4
153	615.7	839.0
154	91.6	0.0
156	113.5	156.5
157	0.0	48.3
158	82.5	106.7
164	98.3	62.5
167	77.3	67.8
170	77.6	93.8
171	24.9	30.0
172	20.4	14.9
173	0.0	4.2
174	0.0	55.8
177	29.9	35.6
178	27.4	9.7
179	48.2	19.9
180	121.9	94.6
183	49.1	40.9
185	9.8	0.0
187	134.0	35.3
189	0.0	4.5
190	19.4	16.2
191	4.4	4.6
193	8.7	4.1
194	21.9	11.0
195	12.0	4.4

Congener	Sum of New Bedford	Sum of Bremerton
196	13.8	5.0
199	27.0	9.3
201	4.5	0.0
202	13.8	0.0
203	16.0	6.5
206	13.5	0.0
208	4.0	1.4
Sum congeners	33677.0	16568.3

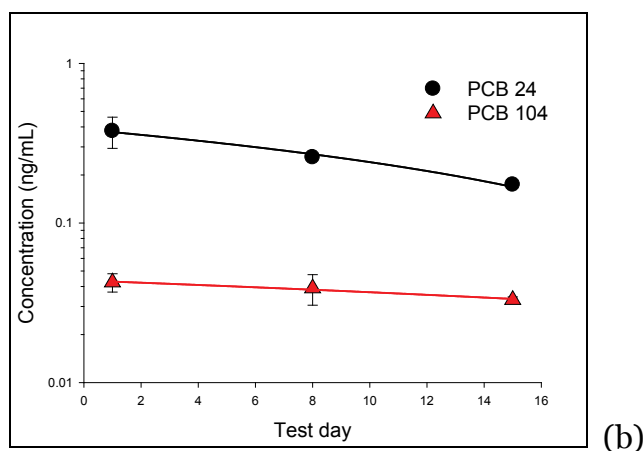
Table S6. Survival of *Eohaustorius estuarius* at termination of the uptake exposure.

Days exposed	Replicate	Number organisms added	Number organisms recovered	% Survival
4	1	35	30	86
4	2	35	33	94
4	3	35	30	86
7	1	35	23	66
7	2	35	20	57
7	3	35	20	57
9	1	35	15	43
9	2	35	15	43
9	3	35	19	54
11	1	35	17	49
11	2	35	13	37
11	3	35	22	63
14	1	35	16	46
14	2	35	15	43
14	3	35	31	89

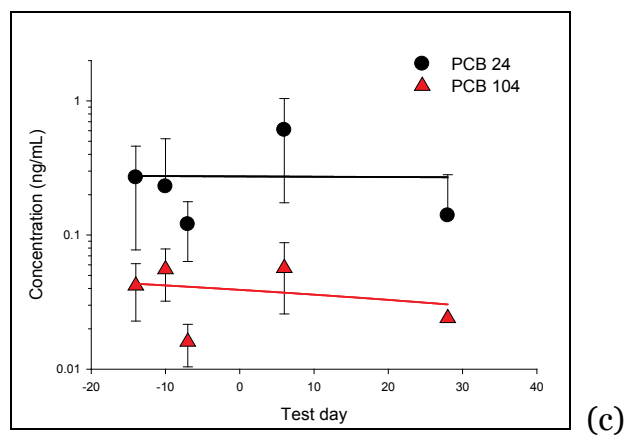
Figure S4. Overlying water concentrations of PCB congeners 24 and 104 in a preliminary water-only experiment (a) and during the NBH (b) and BNC (c) sediment exposures.



(a)

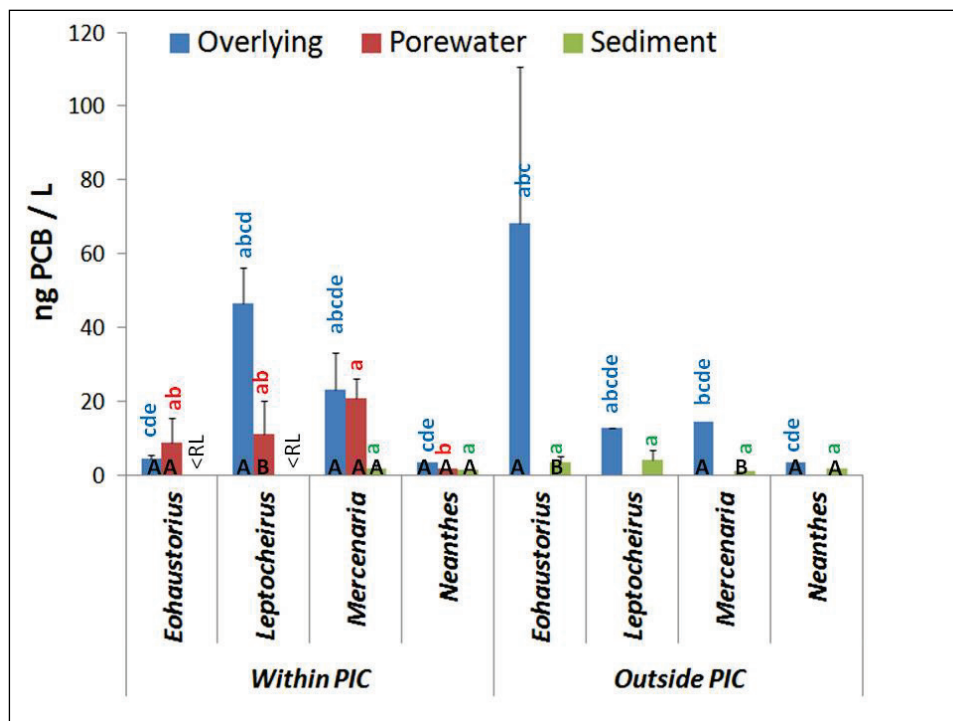


(b)

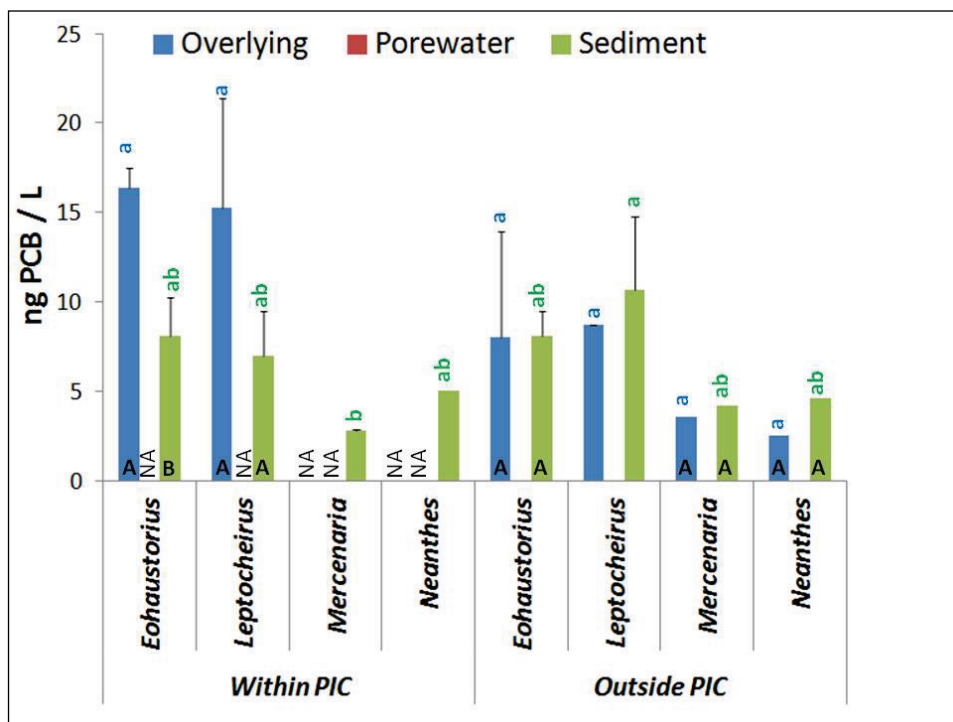


(c)

Figure S5. Estimated dissolved concentrations in the Bremerton sediment exposure using polyethylene devices (PEDs) for (a) PCB24 and (b) PCB104.



(a)



(b)

Figure S6. Bioaccumulated PCB homolog groups in test organisms exposed to the NBH sediment in PICs. Results are presented as (a) bulk tissue residues and (b) lipid-normalized tissue residues. No data were reported for the overlying water pathway for *Neanthes arenaceodentata* due to the lack of sufficient tissue mass being recovered from that treatment.

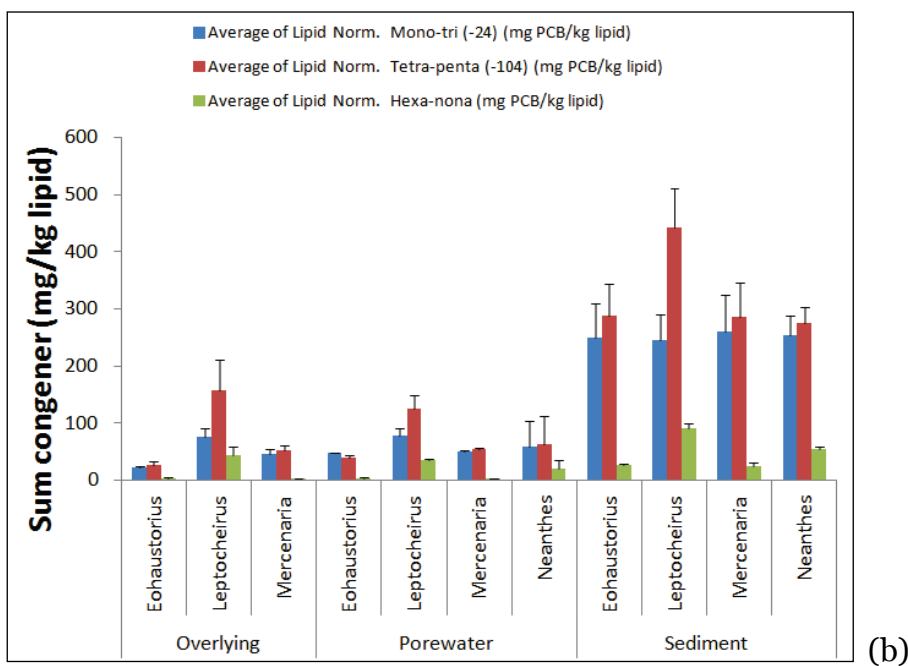
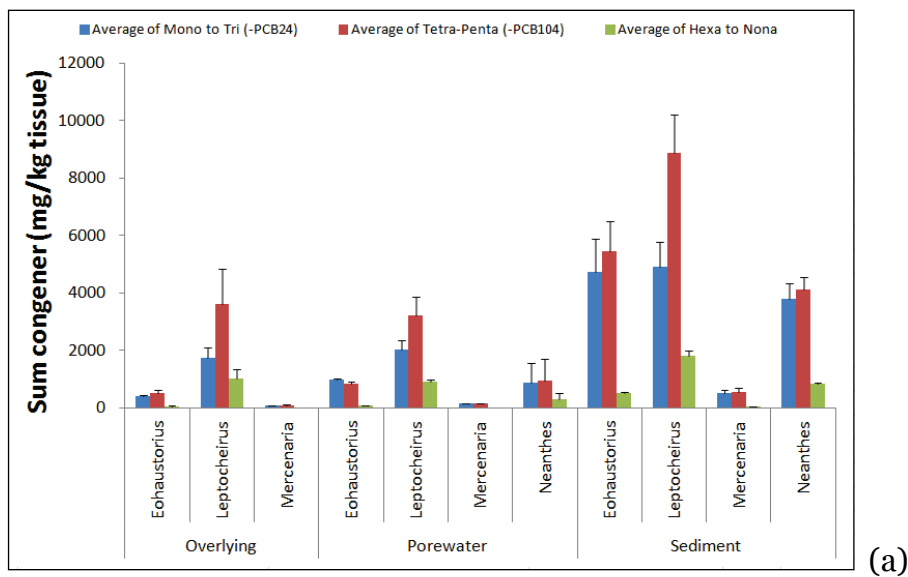
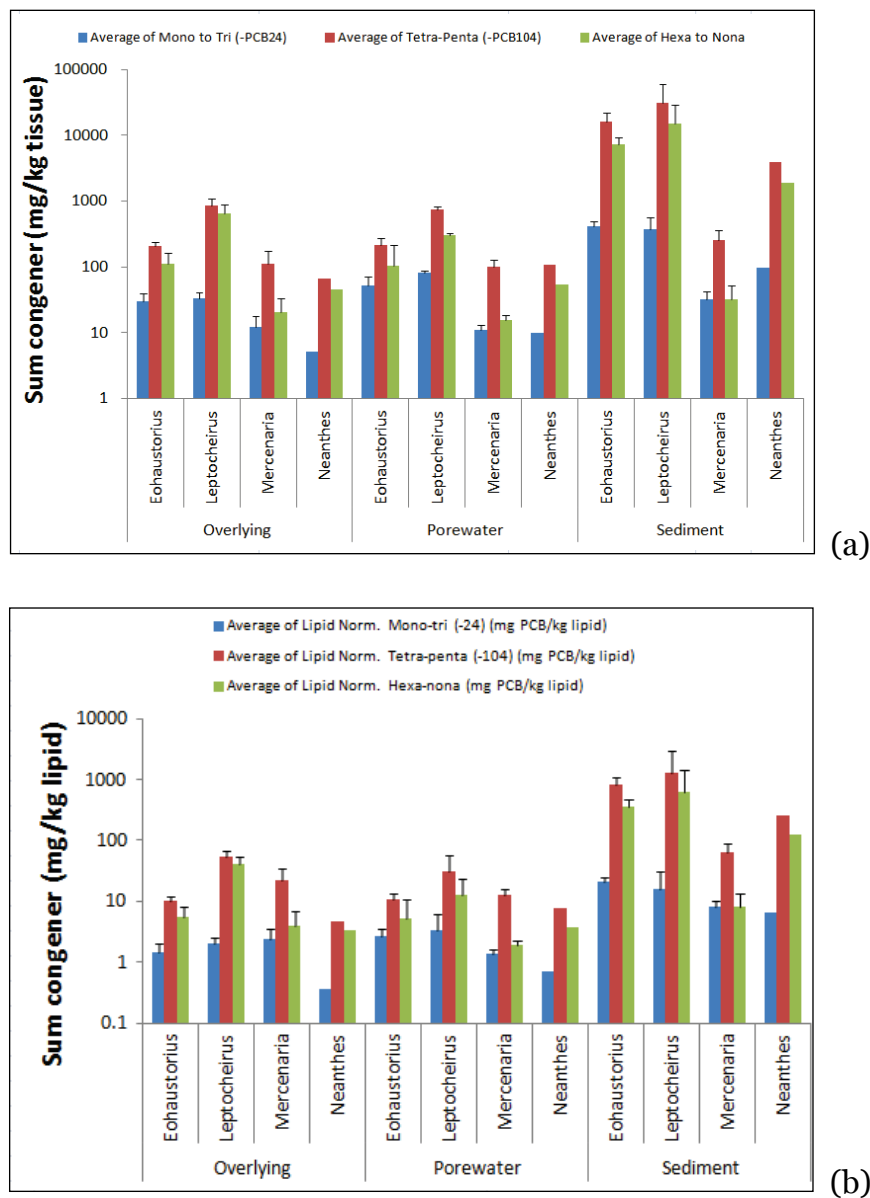


Figure S7. Bioaccumulated PCB homolog groups in test organisms exposed to the BNC sediment in PICs. Results are presented as (a) bulk tissue residues and (b) lipid-normalized tissue residues.



REPORT DOCUMENTATION PAGE				Form Approved OMB No. 0704-0188	
<p>The public reporting burden for this collection of information is estimated to average 1 hour per response, including the time for reviewing instructions, searching existing data sources, gathering and maintaining the data needed, and completing and reviewing the collection of information. Send comments regarding this burden estimate or any other aspect of this collection of information, including suggestions for reducing the burden, to Department of Defense, Washington Headquarters Services, Directorate for Information Operations and Reports (0704-0188), 1215 Jefferson Davis Highway, Suite 1204, Arlington, VA 22202-4302. Respondents should be aware that notwithstanding any other provision of law, no person shall be subject to any penalty for failing to comply with a collection of information if it does not display a currently valid OMB control number.</p> <p>PLEASE DO NOT RETURN YOUR FORM TO THE ABOVE ADDRESS.</p>					
1. REPORT DATE (DD-MM-YYYY) January 2017		2. REPORT TYPE Technical Report: final		3. DATES COVERED (From - To) 1 Jan 2013 - 1 Jan 2015	
4. TITLE AND SUBTITLE The Biology of Bioavailability: The Role of Functional Ecology in Exposure Processes: SERDP ER-1750				5a. CONTRACT NUMBER NA	
				5b. GRANT NUMBER SERDP ER-1750	
				5c. PROGRAM ELEMENT NUMBER SERDP ER-1750	
6. AUTHOR(S) Todd S. Bridges, Alan. J Kennedy, Guilherme R. Lotufo, Jessica G. Coleman, Carlos E. Ruiz, James H. Lindsay, Jeffery A. Steevens, Allyson Wooley				5d. PROJECT NUMBER SERDP ER-1750	
				5e. TASK NUMBER SERDP ER-1750	
				5f. WORK UNIT NUMBER SERDP ER-1750	
7. PERFORMING ORGANIZATION NAME(S) AND ADDRESS(ES) Engineer Research and Development Center, Environmental Laboratory, 3909 Halls Ferry Rd, Vicksburg, MS 39180; Case Western Reserve University, Cleveland, OH; Northeastern University, Boston, MA; US Environmental Protection Agency, Narragansett,				8. PERFORMING ORGANIZATION REPORT NUMBER ERDC/EL TR-17-2	
9. SPONSORING/MONITORING AGENCY NAME(S) AND ADDRESS(ES) Strategic Environmental Research and Development Program (SERDP)				10. SPONSOR/MONITOR'S ACRONYM(S) SERDP	
				11. SPONSOR/MONITOR'S REPORT NUMBER(S) SERDP ER-1750	
12. DISTRIBUTION/AVAILABILITY STATEMENT Approved for public release; distribution is unlimited.					
13. SUPPLEMENTARY NOTES					
14. ABSTRACT <p>The research objective was to improve accuracy of sediment exposure assessments by considering the functional ecology of benthic organisms and different exposure routes (sediment particles, pore water, overlying water). Laboratory experiments were conducted using four marine invertebrates (a worm, two amphipods, and a clam). Organisms were exposed to two different contaminated sediments within mesocosms designed to assess polychlorinated biphenyl (PCB) exposure from overlying water and whole sediment using pathway isolation chambers. The impacts of two sediment remediation methods were also tested: (1) a 2 cm sand cap; and (2) activated carbon (AC) that was not aggressively mixed with sediment prior to organism testing to simulate a field deployment. Porewater concentrations were assessed using polyethylene devices (PEDs) and provided a reasonable indicator of organism exposure but did not account for organisms with connections to the overlying water and direct particle ingestion. The sand cap significantly reduced PCB exposure for all the species except the clam while non-equilibrated AC did not result in significant reductions in bioaccumulation. These results can be used to design functional bioavailability assessments and provide basis for future guidance. Data were used to enhance the capability and predictive reliability of an existing modeling framework (RECOVERY).</p>					
15. SUBJECT TERMS <p>Sediment, Bioaccumulation, Passive samplers, Amphipod, Polychaete, Bioavailability, Benthos, Aquatic ecology, Aquatic organisms-- Effect of contaminated sediments on, Contaminated sediments, Environmental risk assessment, Environmental management</p>					
16. SECURITY CLASSIFICATION OF:			17. LIMITATION OF ABSTRACT	18. NUMBER OF PAGES 246	19a. NAME OF RESPONSIBLE PERSON Alan J Kennedy
a. REPORT	b. ABSTRACT	c. THIS PAGE			19b. TELEPHONE NUMBER (Include area code) 601-634-3344
UU	UU	UU	UU		